

AD-A145 583

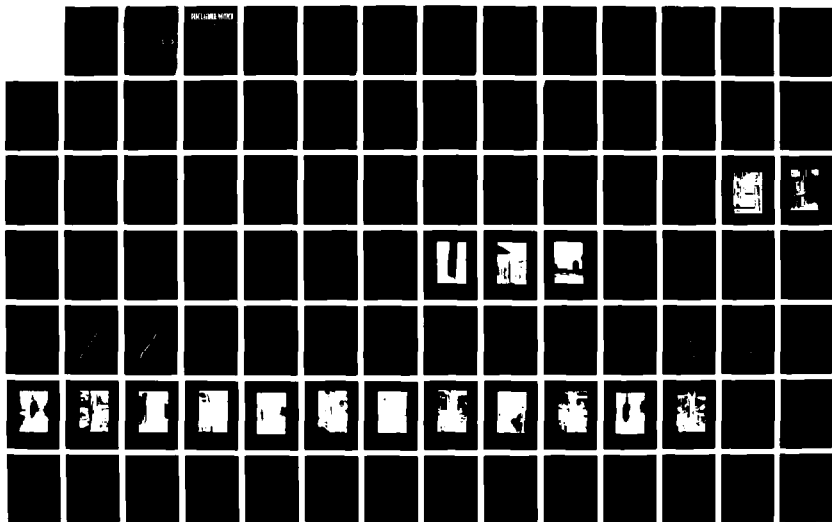
AN EXPERIMENTAL STUDY OF JET IMPINGEMENT ON A CIRCULAR
CYLINDER(U) AIR FORCE INST OF TECH WRIGHT-PATTERSON AFB
OH D W POTTS AUG 84 AFIT/CI/NR-84-50T

173

UNCLASSIFIED

F/G 20/4

NL



UNCLASS

SECURITY CLASSIFICATION OF THIS PAGE (When Data Entered)

REPORT DOCUMENTATION PAGE		READ INSTRUCTIONS BEFORE COMPLETING FORM
1. REPORT NUMBER AFIT/CI/NR 84-50T	2. GOVT ACCESSION NO.	3. RECIPIENT'S CATALOG NUMBER
4. TITLE (and Subtitle) An Experimental Study of Jet Impingement on a Circular Cylinder		5. TYPE OF REPORT & PERIOD COVERED THESIS/DOCUMENTATION
7. AUTHOR(s) Dennis W. Potts		6. PERFORMING ORG. REPORT NUMBER
8. CONTRACT OR GRANT NUMBER(s)		
9. PERFORMING ORGANIZATION NAME AND ADDRESS AFIT STUDENT AT: Texas A&M University		10. PROGRAM ELEMENT, PROJECT, TASK AREA & WORK UNIT NUMBERS
11. CONTROLLING OFFICE NAME AND ADDRESS AFIT/NR WPAFB OH 45433		12. REPORT DATE 1984
4. MONITORING AGENCY NAME & ADDRESS (if different from Controlling Office)		13. NUMBER OF PAGES 192
		15. SECURITY CLASS. (of this report) UNCLASS
		15a. DECLASSIFICATION/DOWNGRADING SCHEDULE
16. DISTRIBUTION STATEMENT (of this Report) APPROVED FOR PUBLIC RELEASE; DISTRIBUTION UNLIMITED		
17. DISTRIBUTION STATEMENT (of the abstract entered in Block 20, if different from Report) B		
18. SUPPLEMENTARY NOTES APPROVED FOR PUBLIC RELEASE: IAW AFR 190-1 5-Sep-84 LYNN E. WOLAVER Dean for Research and Professional Development AFIT, Wright-Patterson AFB OH		
19. KEY WORDS (Continue on reverse side if necessary and identify by block number)		
20. ABSTRACT (Continue on reverse side if necessary and identify by block number) ATTACHED		

DD FORM 1 JAN 73 1473

EDITION OF 1 NOV 65 IS OBSOLETE

UNCLASS

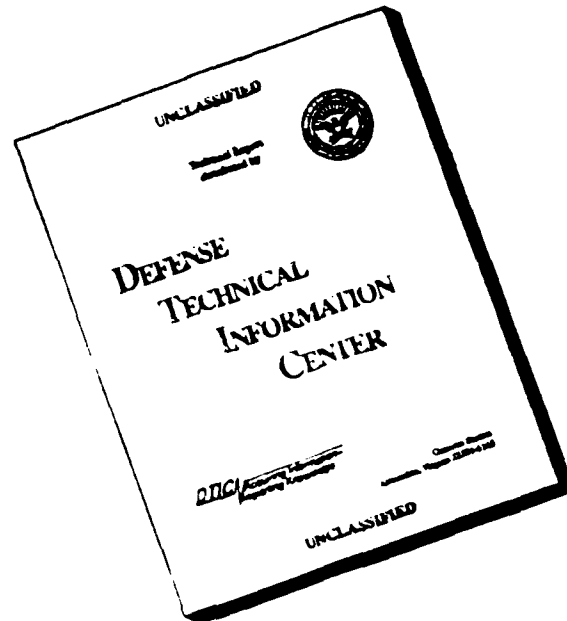
SECURITY CLASSIFICATION OF THIS PAGE (When Data Entered)

84 09 13 012

AD-A145 583

DTIC FILE COPY

DISCLAIMER NOTICE



THIS DOCUMENT IS BEST QUALITY AVAILABLE. THE COPY FURNISHED TO DTIC CONTAINED A SIGNIFICANT NUMBER OF PAGES WHICH DO NOT REPRODUCE LEGIBLY.

ERRATA

AD-A 145 583

Page 152 , Figure 106 is missing - never included in document.

Will ship-later.

ABSTRACT

An Experimental Study of Jet Impingement on a Circular Cylinder. (August 1984)

Dennis Wayne Potts, B.S., Texas A&M University

Chairman of Advisory Committee: Dr. Jose L.F. Porteiro

→ A round turbulent jet was impinged normally upon a circular cylinder and the resulting flow field was studied. The investigation was conducted using a jet which issued from a nozzle with an $11/16$ inch diameter. The cylinder had a diameter of $6\frac{5}{8}$ inches. The jet ⁹was impinged upon the cylinder at nozzle distances of 7, 15, and 30 nozzle diameters, and at velocities of 400 and 500 ft/s. The free jet was studied and found to be ^{typical} by comparing it to earlier studies done with round turbulent jets. Surface flow visualization tests were performed to determine the direction of the flow. The wall jet about the cylinder, resulting from the impinging jet, was studied. Measurements of the velocity profiles and turbulence intensities were made. These results were compared to the same information obtained for flat plates and found to be similar for the nozzle distance of 7 diameters. At nozzle distances of 15 and 30 diameters the data was no longer similar. From ^{the} velocity measurements, the spread rates and decay rates of the wall jet were determined. These results were compared

Cont

to similar studies done for flat plates. ^g The decay rates were found to be less than that of flat plates and the spread rates were greater than that of flat plates, especially about the circumference of the cylinder. An attempt was made to nondimensionalize the wall jet velocity profiles with the same similarity parameters used for flat plates which proved to be unsuccessful. The wall jet was found to separate from the cylinder at about 120 to 160 degrees from the stagnation point. The relationship between the radius of the cylinder and the radius of the nozzle was found to be a very significant parameter.

Accession For	
1. IS GRA&I	<input checked="checked" type="checkbox"/>
2. IT TAB	<input type="checkbox"/>
3. Unpublished	<input type="checkbox"/>
4. Collection	
By	
Distribution/	
Availability Codes	
Avail and/or	
Dist	Special
A-1	



AFIT RESEARCH ASSESSMENT

The purpose of this questionnaire is to ascertain the value and/or contribution of research accomplished by students or faculty of the Air Force Institute of Technology (AU). It would be greatly appreciated if you would complete the following questionnaire and return it to:

AFIT/NR
Wright-Patterson AFB OH 45433

RESEARCH TITLE: An Experimental Study of Jet Impingement on a Circular Cylinder

AUTHOR: Dennis W. Potts

RESEARCH ASSESSMENT QUESTIONS:

1. Did this research contribute to a current Air Force project?

☐ a. YES

☐ b. NO

2. Do you believe this research topic is significant enough that it would have been researched (or contracted) by your organization or another agency if AFIT had not?

☐ a. YES

☐ b. NO

3. The benefits of AFIT research can often be expressed by the equivalent value that your agency achieved/received by virtue of AFIT performing the research. Can you estimate what this research would have cost if it had been accomplished under contract or if it had been done in-house in terms of manpower and/or dollars?

☐ a. MAN-YEARS _____

☐ b. \$ _____

4. Often it is not possible to attach equivalent dollar values to research, although the results of the research may, in fact, be important. Whether or not you were able to establish an equivalent value for this research (3. above), what is your estimate of its significance?

☐ a. HIGHLY
SIGNIFICANT

☐ b. SIGNIFICANT

☐ c. SLIGHTLY
SIGNIFICANT

☐ d. OF NO
SIGNIFICANCE

5. AFIT welcomes any further comments you may have on the above questions, or any additional details concerning the current application, future potential, or other value of this research. Please use the bottom part of this questionnaire for your statement(s).

NAME _____

GRADE _____

POSITION _____

ORGANIZATION _____

LOCATION _____

STATEMENT(s):

AN EXPERIMENTAL STUDY OF JET IMPINGEMENT ON A
CIRCULAR CYLINDER

A Thesis

by

DENNIS WAYNE POTTS

Submitted to the Graduate College of
Texas A&M University
in partial fulfillment of the requirements for the degree of
MASTER OF SCIENCE

August 1984

Major Subject: Aerospace Engineering

84 09 13 012


AN EXPERIMENTAL STUDY OF JET IMPINGEMENT ON A
CIRCULAR CYLINDER


A Thesis

by


DENNIS WAYNE POTTS

Approved as to style and content by:


Jose L. F. Porteiro
(Chairman of Committee)


Cyrus Ostowari
(Member)


Thomas C. Pollock
(Member)


Ernest J. Cross, Jr.
(Head of Department)

August 1984

ABSTRACT

An Experimental Study of Jet Impingement on a
Circular Cylinder. (August 1984)

Dennis Wayne Potts, B.S., Texas A&M University

Chairman of Advisory Committee: Dr. Jose L.F. Porteiro

A round turbulent jet was impinged normally upon a circular cylinder and the resulting flow field was studied. The investigation was conducted using a jet which issued from a nozzle with an 11/16 inch diameter. The cylinder had a diameter of 6 5/8 inches. The jet was impinged upon the cylinder at nozzle distances of 7, 15, and 30 nozzle diameters, and at velocities of 400 and 500 ft/s. The free jet was studied and found to be "typical" by comparing it to earlier studies done with round turbulent jets. Surface flow visualization tests were performed to determine the direction of the flow. The wall jet about the cylinder, resulting from the impinging jet, was studied. Measurements of the velocity profiles and turbulence intensities were made. These results were compared to the same information obtained for flat plates and found to be similar for the nozzle distance of 7 diameters. At nozzle distances of 15 and 30 diameters the data was no longer similar. From the velocity measurements, the spread rates and decay rates of the wall jet were determined. These results were compared

to similar studies done for flat plates. The decay rates were found to be less than that of flat plates and the spread rates were greater than that of flat plates, especially about the circumference of the cylinder. An attempt was made to nondimensionalize the wall jet velocity profiles with the same similarity parameters used for flat plates which proved to be unsuccessful. The wall jet was found to separate from the cylinder at about 120 to 160 degrees from the stagnation point. The relationship between the radius of the cylinder and the radius of the nozzle was found to be a very significant parameter.

· ACKNOWLEDGMENTS

The author would like to express his sincere appreciation to Dr. Jose L.F. Porteiro for acting as chairman of his advisory committee, whose help and guidance proved invaluable during this research. His advice and friendship will always be valued.

Thanks are also expressed to Dr. Cryus Ostowari and Dr. Thomas C. Pollock for serving as members of the author's advisory committee. Their support was greatly appreciated.

The author would like to thank Mr. John Grillo for his help in acquiring the necessary equipment.

Also, to Miss Barbara Hunger, thanks are given for her help in the early stages of this research.

Finally, the author would like to express his heartfelt gratitude to his wife, Eleanor. Her patience, understanding, and support made the work much easier.

TABLE OF CONTENTS

	Page
ABSTRACT	iii
ACKNOWLEDGEMENTS	v
TABLE OF CONTENTS	vi
LIST OF FIGURES	viii
NOMENCLATURE	xviii
CHAPTER I. INTRODUCTION	1
CHAPTER II. LITERATURE REVIEW	5
A. The Turbulent Free Jet	5
B. The Impinging Jet	7
C. The Wall Jet	7
CHAPTER III. PROPOSED RESEARCH	9
CHAPTER IV. EXPERIMENTAL APPARATUS	11
CHAPTER V. EXPERIMENTAL PROCEDURE	18
A. Phase One -- Free Jet Studies	18
B. Phase Two -- Surface Flow Visualization .	19
C. Phase Three -- Wall Jet Studies	21
D. Data Acquisition and Reduction	26
E. Accuracy of Experimental Procedures	27

	Page
CHAPTER VI. EXPERIMENTAL RESULTS	29
A. Phase One -- Free Jet Studies	29
B. Phase Two -- Surface Flow Visualization .	43
C. Phase Three -- Wall Jet Studies	43
CHAPTER VII. CONCLUSIONS AND RECOMMENDATIONS	76
REFERENCES	80
APPENDIX FIGURES 39 THROUGH 126	84
VITA	173

LIST OF FIGURES

Figure		Page
1	Nozzle geometry	13
2	Photograph of the nozzle set-up	14
3	Photograph of nozzle positioning apparatus	15
4	Instrumentation schematic	17
5	Cylindrical surface coordinate system	22
6	Photograph of the cylinder with "grid"	23
7	Photograph of the wall jet traversing apparatus	24
8	Orientation of the hot film sensor	25
9	Free jet geometry and parameters	30
10	Velocity distribution in the free jet with comparisons to Tollmien and Goertler-type solutions, $U_0 = 400$ ft/s	31
11	Velocity distribution in the free jet with comparisons to Tollmien and Goertler-type solutions, $U_0 = 550$ ft/s	32
12	Axial velocity decay of the free jet	34
13	Velocity scale for free jets	37
14	Rate of spread of circular jets	39
15	Turbulence profiles of the free jet, $U_0 = 400$ ft/s	41

Figure		Page
16	Turbulence profiles of the free jet, $U_o = 550$ ft/s	42
17	Flow visualization for $x/d = 7$, $U_o = 400$ ft/s (front)	44
18	Flow visualization for $x/d = 7$, $U_o = 400$ ft/s (back)	45
19	Flow visualization for $x/d = 15$, $U_o = 400$ ft/s (front)	46
20	Flow visualization for $x/d = 15$, $U_o = 400$ ft/s (back)	47
21	Flow visualization for $x/d = 30$, $U_o = 400$ ft/s (front)	48
22	Flow visualization for $x/d = 30$, $U_o = 400$ ft/s (back)	49
23	Flow visualization for $x/d = 7$, $U_o = 550$ ft/s (front)	50
24	Flow visualization for $x/d = 7$, $U_o = 550$ ft/s (back)	51
25	Flow visualization for $x/d = 15$, $U_o = 550$ ft/s (front)	52
26	Flow visualization for $x/d = 15$, $U_o = 550$ ft/s (back)	53
27	Flow visualization for $x/d = 30$, $U_o = 550$ ft/s (front)	54
28	Flow visualization for $x/d = 30$, $U_o = 550$ ft/s (back)	55

Figure		Page
29	Wall jet geometry and parameters in the axial direction	57
30	Wall jet geometry and parameters in the circumferential direction	58
31	Measurement points about the surface of the cylinder	59
32	Surface flow direction for $U_o = 400$ ft/s, $x/d = 7$	60
33	Surface flow direction for $U_o = 400$ ft/s, $x/d = 15$	61
34	Surface flow direction for $U_o = 400$ ft/s, $x/d = 30$	62
35	Surface flow direction for $U_o = 550$ ft/s, $x/d = 7$	63
36	Surface flow direction for $U_o = 550$ ft/s, $x/d = 15$	64
37	Surface flow direction for $U_o = 550$ ft/s, $x/d = 30$	65
38	Surface direction radials for presenting the wall jet data	67
39	Wall jet velocity profile for $U_o = 400$ ft/s, $x/d = 7$ (circumferential radial)	85
40	Wall jet velocity profile for $U_o = 400$ ft/s, $x/d = 7$ (radial 2)	86
41	Wall jet velocity profile for $U_o = 400$ ft/s, $x/d = 7$ (radial 4)	87

Figure		Page
42	Wall jet velocity profile for $U_o = 400$ ft/s, $x/d = 7$ (axial radial)	88
43	Wall jet velocity profile for $U_o = 550$ ft/s, $x/d = 7$ (circumferential radial)	89
44	Wall jet velocity profile for $U_o = 550$ ft/s, $x/d = 7$ (radial 2)	90
45	Wall jet velocity profile for $U_o = 550$ ft/s, $x/d = 7$ (radial 4)	91
46	Wall jet velocity profile for $U_o = 550$ ft/s, $x/d = 7$ (axial radial)	92
47	Wall jet velocity profile for $U_o = 400$ ft/s, $x/d = 15$ (circumferential radial)	93
48	Wall jet velocity profile for $U_o = 400$ ft/s, $x/d = 15$ (radial 2)	94
49	Wall jet velocity profile for $U_o = 400$ ft/s, $x/d = 15$ (radial 4)	95
50	Wall jet velocity profile for $U_o = 400$ ft/s, $x/d = 15$ (axial radial)	96
51	Wall jet velocity profile for $U_o = 550$ ft/s, $x/d = 15$ (circumferential radial)	97
52	Wall jet velocity profile for $U_o = 550$ ft/s, $x/d = 15$ (radial 2)	98
53	Wall jet velocity profile for $U_o = 550$ ft/s, $x/d = 15$ (radial 4)	99
54	Wall jet velocity profile for $U_o = 550$ ft/s, $x/d = 15$ (axial radial)	100

Figure	Page
55 Wall jet velocity profile for $U_o = 400$ ft/s, $x/d = 30$ (circumferential radial ^o)	101
56 Wall jet velocity profile for $U_o = 400$ ft/s, $x/d = 30$ (radial 2)	102
57 Wall jet velocity profile for $U_o = 400$ ft/s, $x/d = 30$ (radial 4)	103
58 Wall jet velocity profile for $U_o = 400$ ft/s, $x/d = 30$ (axial radial)	104
59 Wall jet velocity profile for $U_o = 550$ ft/s, $x/d = 30$ (circumferential radial ^o)	105
60 Wall jet velocity profile for $U_o = 550$ ft/s, $x/d = 30$ (radial 2)	106
61 Wall jet velocity profile for $U_o = 550$ ft/s, $x/d = 30$ (radial 4)	107
62 Wall jet velocity profile for $U_o = 550$ ft/s, $x/d = 30$ (axial radial)	108
63 Wall jet turbulence profile for $U_o = 400$ ft/s, $x/d = 7$ (circumferential radial)	109
64 Wall jet turbulence profile for $U_o = 400$ ft/s, $x/d = 7$ (radial 2)	110
65 Wall jet turbulence profile for $U_o = 400$ ft/s, $x/d = 7$ (radial 4)	111
66 Wall jet turbulence profile for $U_o = 400$ ft/s, $x/d = 7$ (axial radial)	112

Figure	Page
67 Wall jet turbulence profile for $U_o = 550$ ft/s, $x/d = 7$ (circumferential radial)	113
68 Wall jet turbulence profile for $U_o = 550$ ft/s, $x/d = 7$ (radial 2)	114
69 Wall jet turbulence profile for $U_o = 550$ ft/s, $x/d = 7$ (radial 4)	115
70 Wall jet turbulence profile for $U_o = 550$ ft/s, $x/d = 7$ (axial radial)	116
71 Wall jet turbulence profile for $U_o = 400$ ft/s, $x/d = 15$ (circumferential radial)	117
72 Wall jet turbulence profile for $U_o = 400$ ft/s, $x/d = 15$ (radial 2)	118
73 Wall jet turbulence profile for $U_o = 400$ ft/s, $x/d = 15$ (radial 4)	119
74 Wall jet turbulence profile for $U_o = 400$ ft/s, $x/d = 15$ (axial radial)	120
75 Wall jet turbulence profile for $U_o = 550$ ft/s, $x/d = 15$ (circumferential radial)	121
76 Wall jet turbulence profile for $U_o = 550$ ft/s, $x/d = 15$ (radial 2)	122
77 Wall jet turbulence profile for $U_o = 550$ ft/s, $x/d = 15$ (radial 4)	123
78 Wall jet turbulence profile for $U_o = 550$ ft/s, $x/d = 15$ (axial radial)	124

Figure	Page
79 Wall jet turbulence profile for $U_o = 400$ ft/s, $x/d = 30$ (circumferential radial)	125
80 Wall jet turbulence profile for $U_o = 400$ ft/s, $x/d = 30$ (radial 2)	126
81 Wall jet turbulence profile for $U_o = 400$ ft/s, $x/d = 30$ (radial 4)	127
82 Wall jet turbulence profile for $U_o = 400$ ft/s, $x/d = 30$ (axial radial)	128
83 Wall jet turbulence profile for $U_o = 550$ ft/s, $x/d = 30$ (circumferential radial)	129
84 Wall jet turbulence profile for $U_o = 550$ ft/s, $x/d = 30$ (radial 2)	130
85 Wall jet turbulence profile for $U_o = 550$ ft/s, $x/d = 30$ (radial 4)	131
86 Wall jet turbulence profile for $U_o = 550$ ft/s, $x/d = 30$ (axial radial)	132
87 Spread rate of the wall jet along the axis of the cylinder as compared to a flat plate	133
88 Spread rate of the wall jet for $U_o = 400$ ft/s, $x/d = 7$	134
89 Spread rate of the wall jet for $U_o = 400$ ft/s, $x/d = 15$	135
90 Spread rate of the wall jet for $U_o = 400$ ft/s, $x/d = 30$	136

Figure	Page
91 Spread rate of the wall jet for $U_o = 550 \text{ ft/s}$, $x/d = 7$	137
92 Spread rate of the wall jet for $U_o = 550 \text{ ft/s}$, $x/d = 15$	138
93 Spread rate of the wall jet for $U_o = 550 \text{ ft/s}$, $x/d = 30$	139
94 Velocity scale of the wall jet along the axis of the cylinder a compared to a flat plate	140
95 Velocity scale of the wall jet for $U_o = 400 \text{ ft/s}$, $x/d = 7$	141
96 Velocity scale of the wall jet for $U_o = 400 \text{ ft/s}$, $x/d = 15$	142
97 Velocity scale of the wall jet for $U_o = 400 \text{ ft/s}$, $x/d = 30$	143
98 Velocity scale of the wall jet for $U_o = 550 \text{ ft/s}$, $x/d = 7$	144
99 Velocity scale of the wall jet for $U_o = 550 \text{ ft/s}$, $x/d = 15$	145
100 Velocity scale of the wall jet for $U_o = 550 \text{ ft/s}$, $x/d = 30$	146
101 Nondimensional velocity profiles of the wall jet for $U_o = 400 \text{ ft/s}$, $x/d = 7$ (circum- ferential radial)	147
102 Nondimensional velocity profiles of the wall jet for $U_o = 400 \text{ ft/s}$, $x/d = 7$ (radial 2)	148
103 Nondimensional velocity profiles of the wall jet for $U_o = 400 \text{ ft/s}$, $x/d = 7$ (radial 4)	149

Figure	Page
104 Nondimensional velocity profiles of the wall jet for $U_0 = 400$ ft/s, $x/d = 7$ (axial radial) .	150
105 Nondimensional velocity profiles of the wall jet for $U_0 = 550$ ft/s, $x/d = 7$ (circum- ferential radial)	151
106 Nondimensional velocity profiles of the wall jet for $U_0 = 550$ ft/s, $x/d = 7$ (radial 2)	152
107 Nondimensional velocity profiles of the wall jet for $U_0 = 550$ ft/s, $x/d = 7$ (radial 4)	153
108 Nondimensional velocity profiles of the wall jet for $U_0 = 550$ ft/s, $x/d = 7$ (axial radial) .	154
109 Nondimensional velocity profiles of the wall jet for $U_0 = 400$ ft/s, $x/d = 15$ (circum- ferential radial)	155
110 Nondimensional velocity profiles of the wall jet for $U_0 = 400$ ft/s, $x/d = 15$ (radial 2)	156
111 Nondimensional velocity profiles of the wall jet for $U_0 = 400$ ft/s, $x/d = 15$ (radial 4)	157
112 Nondimensional velocity profiles of the wall jet for $U_0 = 400$ ft/s, $x/d = 15$ (axial radial)	158
113 Nondimensional velocity profiles of the wall jet for $U_0 = 550$ ft/s, $x/d = 15$ (circum- ferential radial)	159
114 Nondimensional velocity profiles of the wall jet for $U_0 = 550$ ft/s, $x/d = 15$ (radial 2)	160
115 Nondimensional velocity profiles of the wall jet for $U_0 = 550$ ft/s, $x/d = 15$ (radial 4)	161

Figure		Page
116	Nondimensional velocity profiles of the wall jet for $U_0 = 550$ ft/s, $x/d = 15$ (axial radial)	162
117	Nondimensional velocity profiles of the wall jet for $U_0 = 400$ ft/s, $x/d = 30$ (circumferential radial)	163
118	Nondimensional velocity profiles of the wall jet for $U_0 = 400$ ft/s, $x/d = 30$ (radial 2)	164
119	Nondimensional velocity profiles of the wall jet for $U_0 = 400$ ft/s, $x/d = 30$ (radial 4)	165
120	Nondimensional velocity profiles of the wall jet for $U_0 = 400$ ft/s, $x/d = 30$ (axial radial)	166
121	Nondimensional velocity profiles of the wall jet for $U_0 = 550$ ft/s, $x/d = 30$ (circumferential radial)	167
122	Nondimensional velocity profiles of the wall jet for $U_0 = 550$ ft/s, $x/d = 30$ (radial 2)	168
123	Nondimensional velocity profiles of the wall jet for $U_0 = 550$ ft/s, $x/d = 30$ (radial 4)	169
124	Nondimensional velocity profiles of the wall jet for $U_0 = 550$ ft/s, $x/d = 30$ (axial radial)	170
125	Possible areas where the wall jet separates from the surface of the cylinder for $U_0 = 400$ ft/s	171
126	Possible areas where the wall jet separates from the surface of the cylinder for $U_0 = 550$ ft/s	172

NOMENCLATURE

Symbols	Meaning
x	distance from nozzle along axis of jet, Fig. 9
d	nozzle diameter, Fig. 9
r	radial distance from center of jet, Fig. 9
b	radial distance from center of jet to point where the velocity is 1/2 the maximum velocity at the jet center, Fig. 9
R	radial distance from surface of cylinder, Figs. 29 and 30
B	radial distance from surface of cylinder to point where velocity of wall jet is 1/2 the maximum velocity, Figs. 29 and 30
Z	distance parallel the axis of cylinder from the stagnation point of the impinging jet, Fig. 29
S	distance along cylinder surface in the circumferential direction from the stagnation point of the impinging jet, Fig. 30
θ	angle in circumferential direction from the impingement point relative to the cylinder's surface (i.e. $\theta = S/R_{cyl}$), Fig. 30
U	local mean velocity in the direction of flow, Figs. 9, 29 and 30
U_o	exit velocity of jet from nozzle, Fig. 9
U_m	reference velocity (i.e. the maximum velocity of either the impinging jet or the wall jet), Figs. 9, 29 and 30

Symbols	Meaning
u'	the root-mean-square of the perturbation velocity
R'	the radial distance outward from impingement point along the surface of the cylinder, Fig. 38

CHAPTER I

INTRODUCTION

The study of free jets and jet impingement has been going on for many years. This research dates back to the fundamentals and theory presented by Torricelli in his "De Motu Gravium Naturaliter Accelerato", in 1643 and Bernoulli's "Hydrodynamica", in 1738. In fact, there are hundreds of reports and studies into the theory and applications of jets and the task of preparing a complete list of examples is of itself a major undertaking. For a brief review of some of the more prominent studies, the reader is referred to Krzywoblocki [1].

Interest in free jets, jet impingement, and the resulting wall jet has been motivated by a number of engineering problems. Jets issuing from hydraulic outlet works, weirs, verticle take-off aircraft, various spraying devices, and the cooling of turbine blades are examples of such problems. It should be noted, however, that none of these studies look into the phenomnom of a jet impinging on a circular cylinder. There are two basic reasons for this apparent lack of interest. First, the absence of complete symmetry and the highly three-dimensional nature of the

The AIAA Journal is the model for this thesis.

wall jet makes data taking tedious and theoretical analysis almost impossible. Secondly, there has been no apparent need for such a study.

Recent problems discovered during the launch of the Space Shuttle have made it necessary to explore the phenomena of jet impingement upon cylinders. An integral part of the Space Shuttle is the External Tank (ET). This large cylindrical tank holds the liquid fuels used to power the orbiter's main engines and these fuels are cryogenic. Several hours prior to launch, these fuels are loaded into the ET. Ice forms on the surface of the ET and, as a result of the violent vibration which occurs during the launch, the ice breaks off and has been known to damage the Thermal Protection System tiles on the orbiter. These fragile tiles are necessary to the safe return of the orbiter and their possible damage is a primary concern. In order to prevent this problem; NASA, in conjunction with the U. S. Air Force, has proposed a system to prevent the ice formation by using the exhausts of turbojet engines mounted in the proximity of the ET surface [2]. The jet exhausts would be arranged in such a way that they would generate a temperature and velocity field, about the surface of the ET, which would produce a heat transfer coefficient adequate enough to prevent the ice from forming. At the present time, there is no comprehensive flow field or heat

transfer data on jet impingement on circular cylinders.

The rate of heat transfer depends upon the heat transfer coefficient, and this coefficient is affected by the characteristics of the flow field in which the heat flux is taking place. To provide an accurate estimate of this coefficient, some basic properties of the flow field must be known. Very little of the properties or characteristics of the flow field generated by a jet impinging upon a cylinder is known, hence very little is known about the resulting heat transfer coefficient.

It is the purpose of this research to study, experimentally, the effects of a turbulent jet impinging normally on a circular cylinder in order to provide the basis upon which future studies into the heat transfer resulting from this impingement can be made. This information could aid in making decisions concerning the ice suppression system for the Space Shuttle. The characteristics of the impinging jet will be presented in this monograph and will include the velocity profiles and turbulence intensities of the free jet. In order to insure that the jet itself behaves as expected, it will be compared to data based upon the work done previously in the area of free jets.

Other possible applications of this research include using jets to cool reactor cores, to transfer heat to or from cylindrical cooling or heating elements, and to initi-

ate research into the area of jet impingement upon non-symmetrical bodies.

CHAPTER II

LITERATURE REVIEW

In order to accurately describe the flow field of an impinging turbulent jet it can be divided into several zones as proposed by Poreh, et al. [3,4]. In general, the literature about jets which is relevant to this research can be divided into three areas: First, studies of the free jet; second, studies of the impinging jet; and third, studies of the wall jet. Obviously, these areas overlap greatly and many reports cover all three. The review of literature in this report will be divided, as much as possible, into these three areas.

A. The Turbulent Free Jet

The turbulent free jet has been extensively studied and there are numerous cases from which comparisons of experimental data can be made. Since a circular jet was used in this research project, this review will be limited to jets of that nature. Numerous experimental studies of the characteristics of circular or axially symmetric jets have been made. Albertson et al. [5] provide an excellent study of the diffusion of jets. This study includes detailed discussions by Holdhusen, Citrini, Corrsin, Baines, Streiff, Henry, Albertson, Dai, Jensen, and Rouse.

Wyganski and Fielder [6], using hot wire probes, investigated the self-preserving nature of the free jet. Sami et al. [7], using a ceramic piezo-electric tube as well as hot wires, studied the diffusion of the jet including measurements of radial velocities and pressure fluctuations. Gibson [8] studied the turbulent energy of a round free jet. The static pressure distribution was investigated by Miller and Comings [9]. Measurements of entrainment were made by Ricou and Spalding [10]. Also, an extensive report by Love et al. [11] makes several comparisons between experimental and theoretical studies of the axisymmetrical free jet. Donaldson et al. [12,13] made some excellent studies into the structure of the turbulent axially symmetric free jet. These papers provide excellent sources of data for comparative purposes. Rajaratnam [14] provides an excellent comparison of some of the above studies as well as many others. In the above reports, the experimental results are generally compared to the predictions made by theory. For theoretical considerations the reader is referred to Abramovich [15] and Pai [16]. Hinze [17] and Schlichting [18] present excellent summaries of several theoretical analyses. In most cases, Tollmien's [19] solution is used as a comparison. However, Kueth [20] has extended the solution to include the velocity distribution near the nozzle of an axially symmetrical jet and for plane

jets in a moving stream.

B. The Impinging Jet

As stated earlier, there have been no definitive studies into the area of jet impingements on a circular cylinder. However, extensive studies have been performed in the area of jet impingements on flat plates. Donaldson and Snedeker [12] have studied this as well as briefly discussing other shapes such as hemispheres and cylindrical cups. Similarly, several experimental studies on circular impinging jets have been performed by Poreh and Cermak [3], Tani and Komatsu [21], Poreh et al. [4], Beltaos and Rajaratnam [22], Donaldson et al. [13], and Bradshaw and Love [23]. Again, the reader is referred to Rajaratnam [24] for a detailed comparison of some of these reports. Generally, the characteristics of the resulting wall jet are compared to the predictions made by Glauert [25]. In all of the above studies, flat or symmetrical shapes are used and no consideration is given to circumstances where the jet may separate from the wall.

C. The Wall Jet

Finally, the last zone of consideration is the wall jet. Glauert [25] has presented the theoretical considerations against which most experimental data is compared.

Poreh et al. [4] and Bakke [26] present thorough studies of radial wall jets. In fact, this is the area of research which presents the most difficulty in obtaining data which can be compared to the wall jet on the cylinder. All experimental data to date deals with either radial or two-dimensional jets. The wall jet resulting from jet impingement on a cylinder is neither two dimensional nor purely radial, and there is the problem of adverse pressure gradients and jet separation from the wall. Although Gartshore and Newman [27] treat the problem of pressure gradient and separation, their experiments were performed with a two dimensional jet in a nonquiescent medium. The theory cannot be of real use to the problem studied in this research. Dvorak [28] has made some analysis of a wall jet over curved surfaces but this information is also limited to two-dimensional wall jets.

CHAPTER III

PROPOSED RESEARCH

From the previous chapters it is obvious that a potential area for research exists. The development of the Ice Suppression System for the Space Shuttle poses the unique problem of a jet impinging on a circular cylinder. As indicated in Chapter II, no known literature exists which describes any facet of this phenomenon, hence no previous information on this subject is available. In this research, basic data about the flow field which develops as a result of the impinging jet was gathered and presented. To gather this information, a round turbulent jet was impinged normally on a circular cylinder and the characteristics of the resulting wall jet were measured. The research was divided into three areas or phases of study.

Phase One was a study of the characteristics of the free jet. Since so many studies into the nature of free jets have been done, and since axially symmetric jets have been well documented, no new studies were performed here. The characteristics of the jet used in this study, however, were measured and compared to those studies already done. This was necessary in order to validate the jet and detect any unusual characteristics.

Phase Two dealt with surface flow visualization.

Unlike jets impinging on flat plates or symmetric objects, the usual assumptions about the symmetry of the wall jet cannot be made and some indication of the surface flow direction must be known. The flow visualization should give a better understanding of how the jet progresses about the cylinder. This phase is also intended to provide information which will aid in the positioning of the hot film sensor used in the final phase of study.

In Phase Three, the characteristics of the wall jet were measured to include velocity profiles and turbulence levels. As shown, no known information, theoretical or experimental, is available. Therefore, only comparisons to existing results of the work done previously can be made. It is hoped that this information can provide the basis for further studies into deriving some possible models to describe this flow field.

CHAPTER IV

EXPERIMENTAL APPARATUS

Previous experimental studies of the Ice Suppression System (ISS) have been performed using a two percent model of the Space Shuttle and its launch complex [2]. To make the information obtained for this report compatible with the work already accomplished, it was decided to use an experimental set up which would represent a two percent model of the ET. Therefore, a five foot section of PVC pipe with an outer diameter of 6 5/8 inches was used to simulate the ET. To insure minimum effects on the wall jet due to the cylinder surface, the PVC pipe was sanded to a smooth, uniform surface. This surface was then painted with several coats of white lacquer. The lacquer was chosen because of the glossy smooth finish it supplies and to contrast the flow visualization method used.

The nozzle was manufactured from a 5 inch section of brass rod. The solid rod was drilled out along its axis using an 11/16 inch (0.69 inch) bit. To create a favorable pressure gradient, the opening was gradually widened so that the upstream diameter was 0.89 inch. This end was then threaded, in turn, into a bell reducer and a 1.4 inch diameter pipe. The transition from the 1.4 inch pipe through the bell reducer to the nozzle was made as smooth

as possible so that the overall effect was that of a converging nozzle. To align the flow in the nozzle and to minimize undesired effects a four foot section of straight pipe immediately preceded the nozzle. This section of pipe shall be referred to as the aligning pipe. Fig. 1 shows a schematic of the nozzle and aligning pipe. Fig. 2 is a photograph of the nozzle set-up. This size (11/16 inches) constitutes a two percent model of the actual nozzle proposed for the ISS.

The nozzle assembly was attached to a traveling mount so that the nozzle could be moved to the desired distance from the cylinder. The range of movement for the nozzle was from seven nozzle diameters to 40 nozzle diameters from the surface of the cylinder (see Fig. 3).

The working medium was air which was supplied from a very large tank. Using a compressor, the tank could be repressurized to 100 psi as necessary. Because of the supply tank's large size, it provided a sufficient mass flow and maintained very stable flow conditions.

Velocities were monitored by a total pressure probe mounted in the aligning pipe at the end farthest from the nozzle and were controlled by a pressure regulator mounted upstream from the aligning pipe. The total pressure was measured using a Validyne pressure transducer rated at five

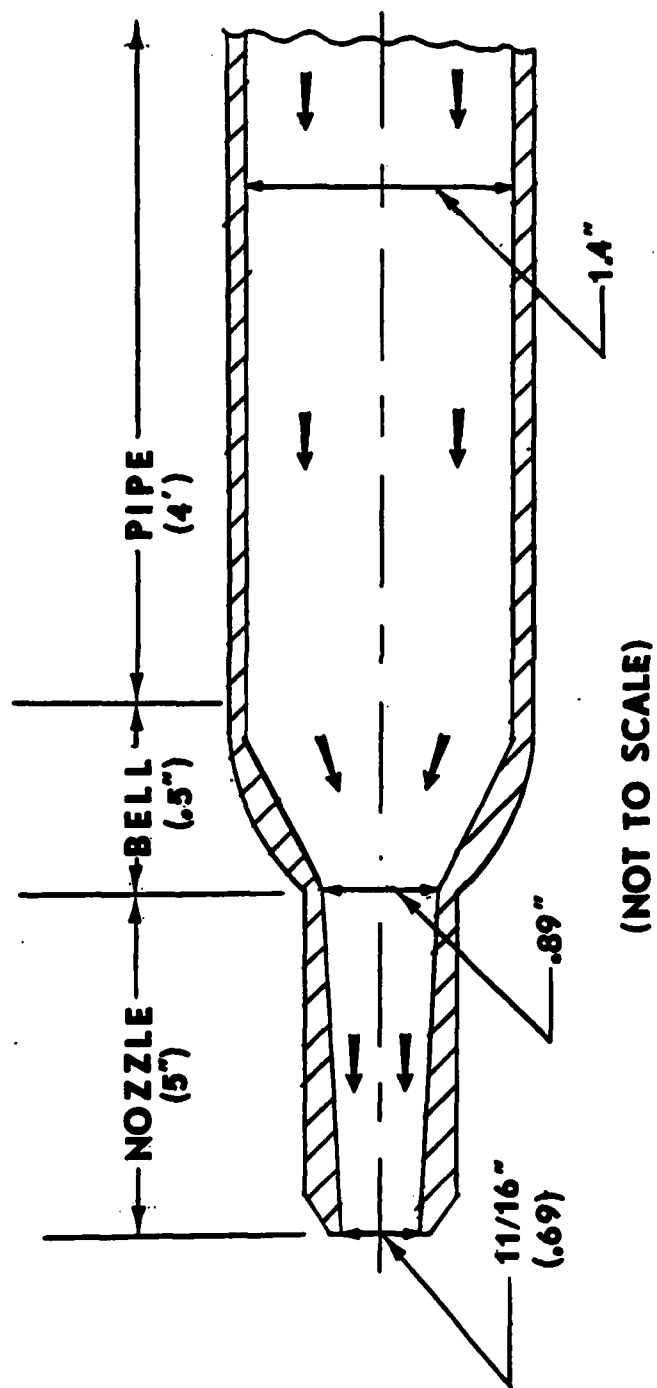


Fig. 1 Nozzle geometry.



Fig. 2 Photograph of the nozzle set-up.

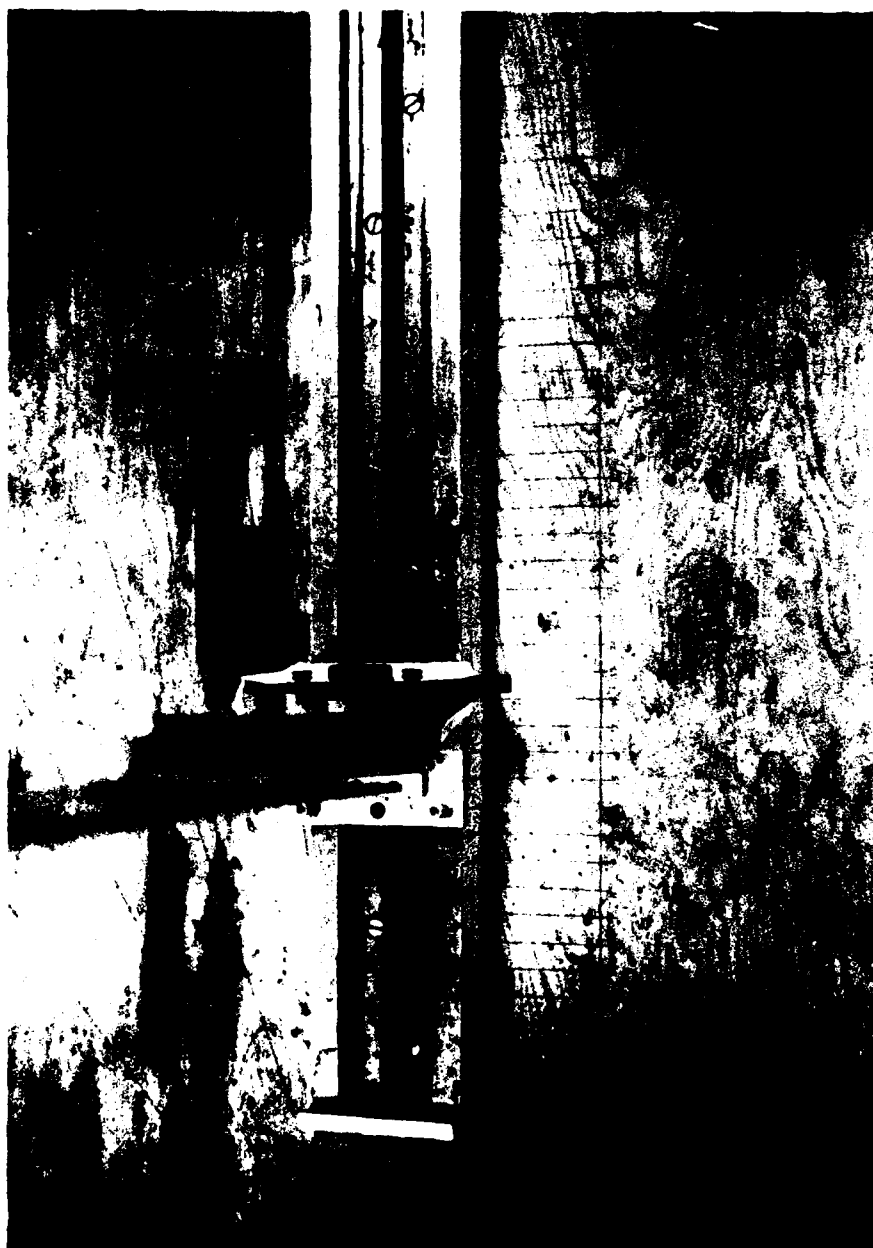


Fig. 3 Photograph of nozzle positioning apparatus.

psi. The transducer was calibrated to give the velocity of the flow at the nozzle. During the tests the output of this transducer was continuously monitored to insure a constant nozzle velocity. The velocities in the free jet and in the wall jet about the cylinder were measured using a Thermal Systems Inc. (TSI) model 1050 constant temperature anemometer with a model 1051 linearizer.

A potentiometer was attached to the traversing mechanism which moved the hot film probe through the free and wall jets. A constant voltage was applied across the potentiometer which was calibrated in such a way that the change in resistance, hence change in voltage, corresponded to the distance moved by the probe. The "zero" voltage was obtained by bringing a sensor in contact with the surface of the cylinder and recording that value. This value was found not to vary perceptably in the circumferential direction about the cylinder. It did vary a maximum of 0.02 inches in the axial direction along the cylinder. This variation could be compensated for by adjusting the input voltage. Allowing for this disparity, errors in distances are within 0.01 inch.

The data was collected and reduced using a microcomputer. Fig. 4 gives a schematic of the instruments used in these tests.

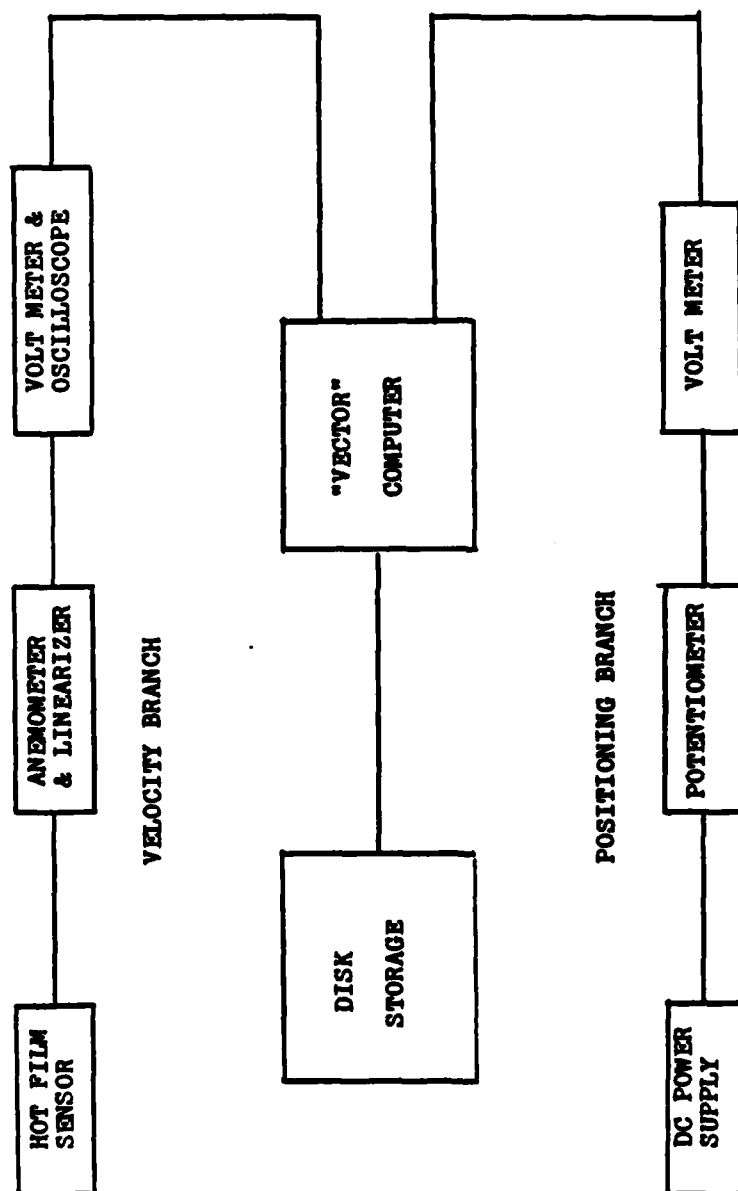


Fig. 4 Instrumentation schematic.

CHAPTER V

EXPERIMENTAL PROCEDURE

A. Phase One -- Free Jet Studies

The mean velocity was measured with a single hot film perpendicular to the axis of the flow. Measurements were taken for two different velocities (400 ft/s and 550 ft/s) and at nozzle distances (x/d) of one diameter spacing from 0 to 7 nozzle diameters and at 10, 15, 20, 25 and 30 diameters. These distances were chosen for several reasons; to establish the potential core region, to provide a uniform spacing of the data points, and to coincide with the projected impingement points used later in the tests.

The turbulence levels were calculated from the root-mean-square (rms) of the perturbation velocity in the axial direction and assuming the flow within the jet to be isotropic. Gibson [8] has shown that this assumption is not unreasonable. His measurements have shown that the radial and circumferential perturbation velocities are very nearly equal to the axial components at least until the mean velocity is half the maximum velocity at the jet center. Beyond that point, the axial component dominates the spectrum and even then the turbulent measurements, although high, will still give a reasonable indication of the turbulence intensity. Miller and Comings [9] also made

similar assumptions in their measurements of a two-dimensional free turbulent jet noting only that measured velocities are in error for low velocity-high turbulence areas (i.e. toward the edge of the jet). Sami et al. [7] also made measurements of a free jet using the same assumptions as previously stated, then compared this data with data taken using an "X" wire probe and also found that the assumptions were valid except at the outer edge of the jet for the same reasons. Wygnanski and Fiedler [6] also compared single hot wire to "X" wire data and found them to be identical for turbulence measurements; but they found the circumferential and radial components to be somewhat less than those of Gibson, although the axial components agreed completely. In any case, the axial component either equals or dominates the radial and circumferential components so that the assumptions made here are within reason.

B. Phase Two -- Surface Flow Visualization

The jet was impinged perpendicularly upon the circular cylinder. In order to measure the resulting wall jet using hot film anemometry, its direction must be known, and this is determined through surface flow visualization. The problem is in finding an adequate substance which will give a good indication of the surface flow patterns without

affecting the flow itself. In earlier studies done on the ISS by Porteiro et al. [2], a combination of kerosene and black tempra paint proved to be very effective. As the flow moves along the surface, the mixture leaves "streaks" parallel to the flow direction. The kerosene then evaporates leaving the tempra powder behind indicating the surface flow patterns. The surface of the cylinder was painted with white lacquer because the lacquer will not react with the kerosene and the white glossy surface provides the best contrast from the black tempra.

In order to recreate the surface flow directions during the wall jet measurement phase and then accurately keep track of the measurements, a surface coordinate system was employed. For each nozzle distance and velocity to be recorded, a flow visualization was performed by "painting" the cylinder with the kerosene-tempra mixture and impinging the jet onto the cylinder until the flow field was well developed and the kerosene had sufficiently evaporated. After the tempra was allowed to dry completely, the cylinder was wrapped in tracing paper which had been marked with a grid representing degrees circumferentially around the cylinder and inches axially along the cylinder. The origin of this coordinate system was designated as the stagnation point of the impinging jet. Fig. 5 indicates

the major points of this coordinate system. Fig. 6 shows the cylinder wrapped with the "grid" paper. Using this coordinate system, the measurements at any point can be reproduced for any nozzle distance at any velocity. From the flow visualization the surface flow direction was marked on the grid every 10° and every $1/2$ inch. From this information, the proper hot film orientation could be maintained.

C. Phase Three -- Wall Jet Studies

Using the grids described, the wall jets were then measured at predetermined points by orienting the hot film probe in the proper direction as indicated by the flow visualization and traversing the wall jet in a radial direction relative to the center on the cylinder. The traversing mechanism was mounted on top of the cylinder in such a way that the axis of the hot film probe remained perpendicular to the cylinder's surface. The entire mechanism could be rotated about the cylinder's axis insuring the hot film traveled in a radial direction relative to the cylinder's axis. Fig. 7 is a photograph of the traversing mechanism and Fig. 8 shows the position of the hot film relative to the cylinder's surface.

Again the mean velocities and turbulence levels were

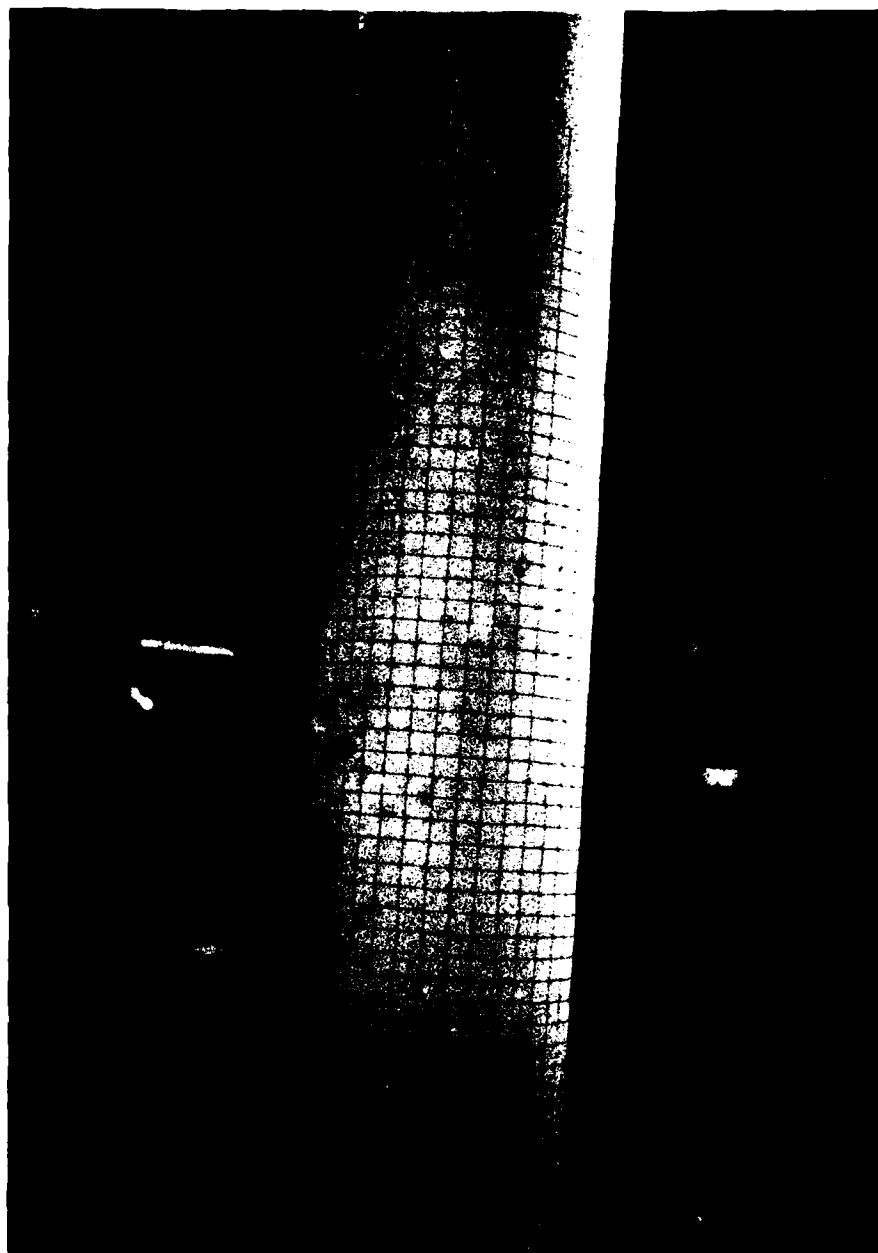


Fig. 6 Photograph of the cylinder with "grid".



Fig. 7 Photograph of the wall jet traversing apparatus.



Fig. 3 Orientation of the hot film sensor.

determined as well as areas where the jet separated from the wall. The turbulence intensities were determined using the same assumptions described for the free jet. The validity of these assumptions as applied to the wall jet will be discussed in Chapter VI. No correction has been made to compensate for the high turbulent levels in the wall jet. The effect of this error depends upon the intensity levels of turbulence. For the mean velocity measurements, errors of about two percent in the mean velocity at a 25 percent turbulence level is generally the considered value. At turbulence levels of 30 percent or higher, the possibility of flow reversal becomes distinct and measurements within these regions should be considered only as indications of the probable flow velocities. The major source of error is in measuring the turbulence intensity itself. The amount of error may be as much as 20 percent at a turbulence intensity of 20 to 25 percent.

These sources of error must be kept in mind when reviewing the data. The mean velocities obtained should be reasonably accurate but the levels of turbulence could have a tendency to be high.

D. Data Acquisition and Reduction

The data was acquired by the Vector Computer using an

analog to digital converter. The computer read 500 voltage outputs from the anemometer over approximately a one-half second period. From these 500 readings a mean voltage and root-mean-square (rms) voltage was calculated. The voltages were then converted to velocities using a calibration equation obtained from the calibration curve for the hot film. This gives a mean velocity (U) and a standard deviation or rms of the perturbation velocities (u'). The turbulence level is simply the ratio of the rms velocity to the mean velocity (u'/U).

The hot film was calibrated at the nozzle exit within the potential core of the jet where turbulence intensities were measured at less than one percent.

E. Accuracy of Experimental Procedures

The accuracy of many of the procedures used in acquiring data have already been indicated. The most significant of these being the errors encountered in making hot film measurements in turbulent flow. Based upon the repeatability of the hot film measurements, errors were less than five percent in both the free jet studies and the wall jet studies.

The instrumentation used is the primary source of error. To prevent errors due to calibration drift, both

the pressure transducer and hot film anemometer were periodically checked. The transducer was not found to vary, although it was recalibrated during the experiments. The accuracy of the transducer was considered to be about five percent for both velocities. During the course of the experiments it was necessary to replace the hot film sensor several times. These replacements required the instrument to be recalibrated each time. The variation between calibrations was less than five percent.

The flow from the nozzle was controlled through a regulator and monitored using the pressure transducer. The flow velocity from the nozzle was not allowed to vary more than five percent from the two established velocities (400 and 550 ft/s). Frequent checks of the pressure transducer showed the velocities to be within five percent of the expected value.

CHAPTER VI

EXPERIMENTAL RESULTS

A. Phase One -- Free Jet Studies

Free jets have been studied extensively and there are many reports which have been rendered on the subject. The purpose of this phase of the research is not to explore any new avenues but to compare the characteristics of the jet used here with those of the numerous studies already done to insure that this jet is similar (i.e. typical). Fig. 9 shows the geometry of the free jet and the different parameters used in describing the jet.

Of primary consideration when analyzing a jet is whether a ¹similarity exists. Nondimensionalizing the velocity (U) against the maximum velocity (U_m), and the radial distance from the jet center (r) against the radius of one-half velocity (b), plots such as Figs. 10 and 11 are obtained. From these plots it can easily be seen that the profiles for areas of fully developed flow are indeed similar.

The velocity distributions in a circular turbulent jet have been calculated by Tollmien [19] and Goertler [29]. It is not the purpose of this report to derive these relationships, only the final results will be presented here. The reader is referred to the individual papers or to

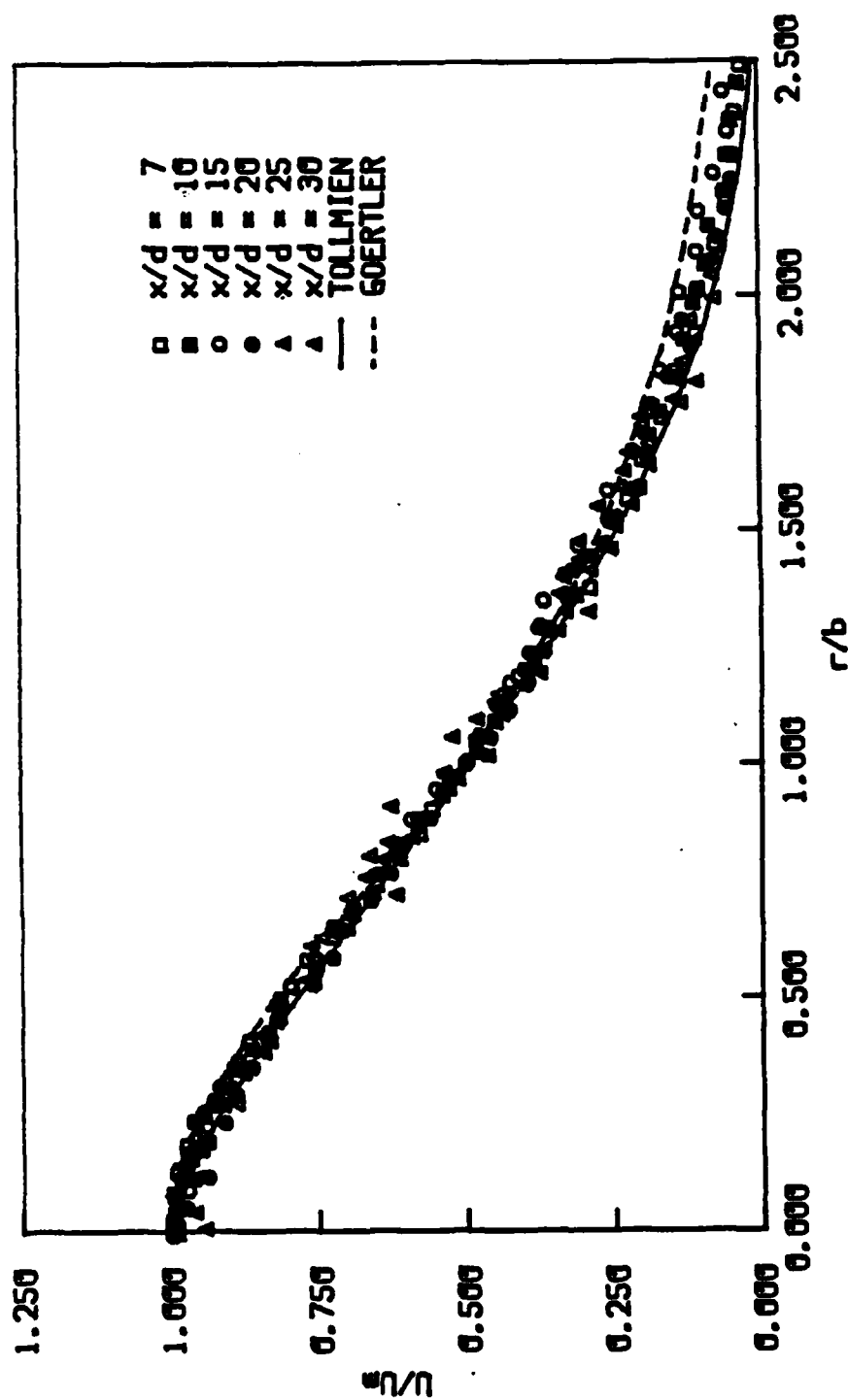


Fig. 10 Velocity distribution in the free jet with comparisons to Tollmien and Goertler-type solutions, $U_0 = 400$ ft/s.

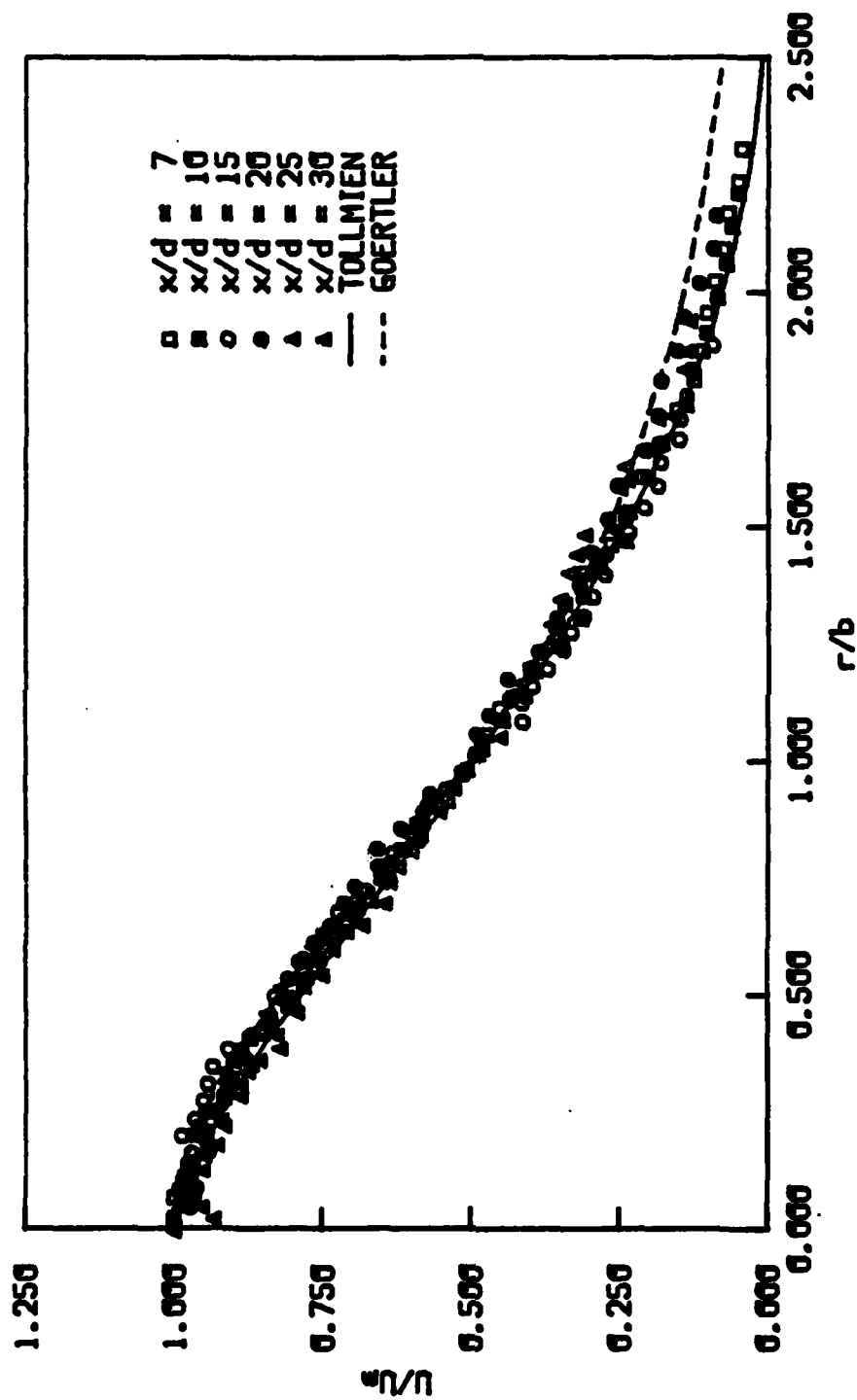


Fig. 11 Velocity distribution in the free jet with comparisons to Tollmien and Goertler-type solutions, $U_0 = 550$ ft/s.

Rajaratnam [14] for a more detailed presentation.

In the past, experimental data has been compared to these predictions and there has been general agreement between the two. In order to validate the jet used in this research, the data obtained from this jet will be compared to these theoretical predictions. If there is substantial agreement between the two, the jet will then be considered "typical". Again the reader is referred to Figs. 10 (p. 31) and 11 (p. 32) which compares the data for both velocities to the Tollmien solution and the Goertler-type solution. In both cases, there is substantial agreement; and, based upon past experimental agreement, the jet is considered to be validated.

Fig. 12 shows the decay characteristics for each of the two velocities. Here, the maximum velocity at the center of the jet (U_m) is normalized against the exit velocity at the nozzle (U_o), and the distance from the nozzle is expressed in terms of nozzle diameters (x/d).

Letting the length of the potential core be defined as the distance (x/d) where the maximum velocity is 95 percent of the velocity at the nozzle, Fig. 12 (p. 34) indicates the length to be about 6.2 diameters from the nozzle. Donaldson and Snedeker [12] suggests lengths of 7.2 to 7.5 diameters at higher velocities. This is consistent with

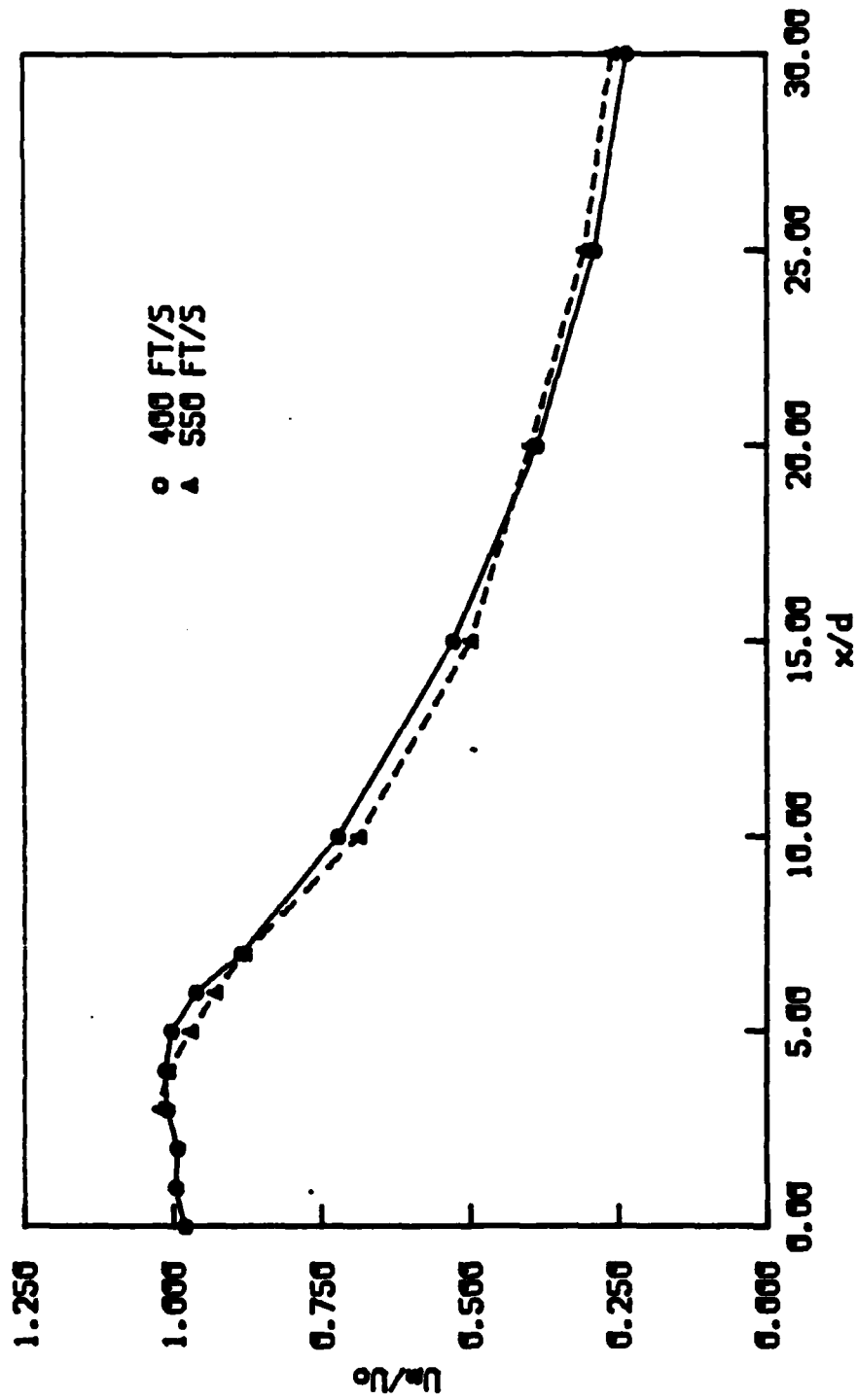


Fig. 12 Axial velocity decay of the free jet.

the existing data.

If the velocity decay is plotted as a velocity scale (i.e. U_o/U_m) it can be compared to the relationships developed by earlier experimenters. Triple (see Abramovich [15]) developed the earliest relationship for the velocity scale where:

$$U_m/U_o = 7.32/(x/d) \quad (1)$$

Reichardt (see Schlichting [18]) developed this velocity scale:

$$U_m/U_o = 5.75/(x/d) \quad (2)$$

Hinze and Zijnen [30] from their experimental observations suggested:

$$U_m/U_o = 6.39/(x^* + 0.6) \quad (3)$$

where x^* is x/d . The virtual origin, for their work, was located $0.6d$ behind the nozzle. Because of the uncertainty involved in predicting this distance, most cases locate the virtual origin at the nozzle itself. From their experiments, Albertson et al. [5] found:

$$U_m/U_o = 6.2/(x/d) \quad (4)$$

These equations for the velocity scale are presented in Fig. 13 as well as the results from this experiment. The current data appears to agree best with the results obtained by Trupel. Rajaratnam [14] pointed out that the results obtained by Hinze and Zijnen [30] and Albertson et al. [5] appear to be between the extreme variations given by Trupel and Reichardt and suggests the following equation to describe the velocity scale:

$$U_m/U_o = 6.3/(x/d) \quad (5)$$

The data obtained in this experiment falls slightly outside the extreme suggested by Trupel but agrees reasonably well with the jet decay observed by Donaldson and Snedeker [12].

The difference between these experimental results can be attributed to secondary effects described by Donaldson and Snedeker [12] who pointed out that because of such secondary effects, a jet issuing from a hole in a plane surface exhibits a higher rate of decay and spread than does one from the end of a long pipe. As noted, the jet

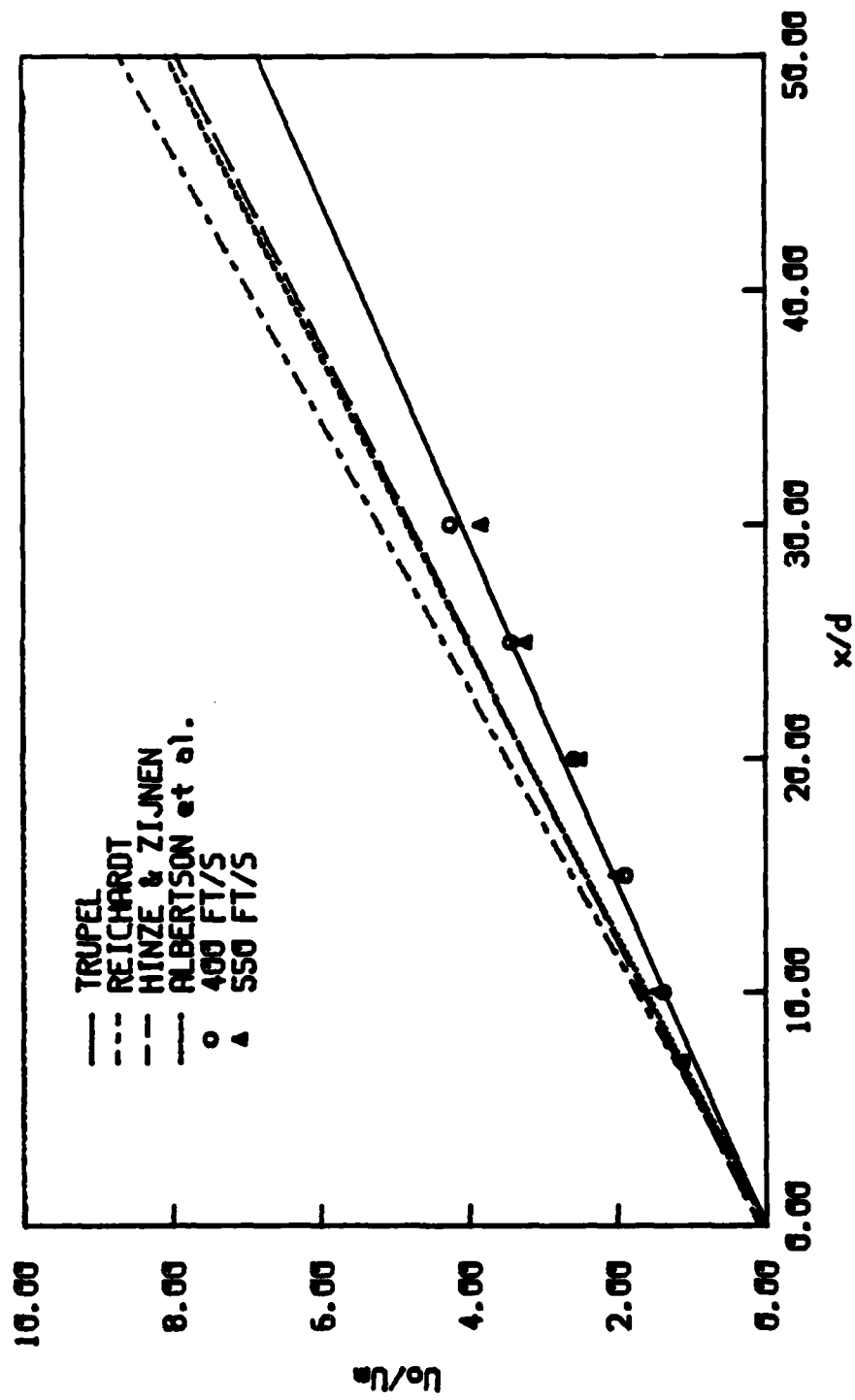


Fig. 13 Velocity scale for free jets.

used in this experiment issued from a long pipe, so slightly lower rates of decay and spread are to be expected. The data seems to bear out this assumption. It can be seen from these varying results that the free jet is very much subject to the secondary influences described by Donaldson and Snedeker [12].

The rate of spread of a jet has also been studied by a number of experts who have suggested several different equations to predict this rate. From dimensional considerations, the solution can have the form:

$$b = C_1 x \quad (6)$$

where C_1 is a constant determined experimentally. Tollmien's [19] solution's suggests $C_1 = 0.082$. The data of Corrsin [31] indicates a value of 0.084 for C_1 . Albertson et al. [5] found a value of 0.0965 worked best and 0.094 for the data of Hinze and Zijnen [30]. Fig. 14 compares these different relationships with the data found in this experiment. The current data shows a spread rate less than those predicted by Alberson et al. [5] and Hinze and Zijnen [30], but agrees well with Tollmien's [19] solution and Corrsin's [31] data. This is as expected, because the jet decay prediction of Trupel (see Fig. 13,

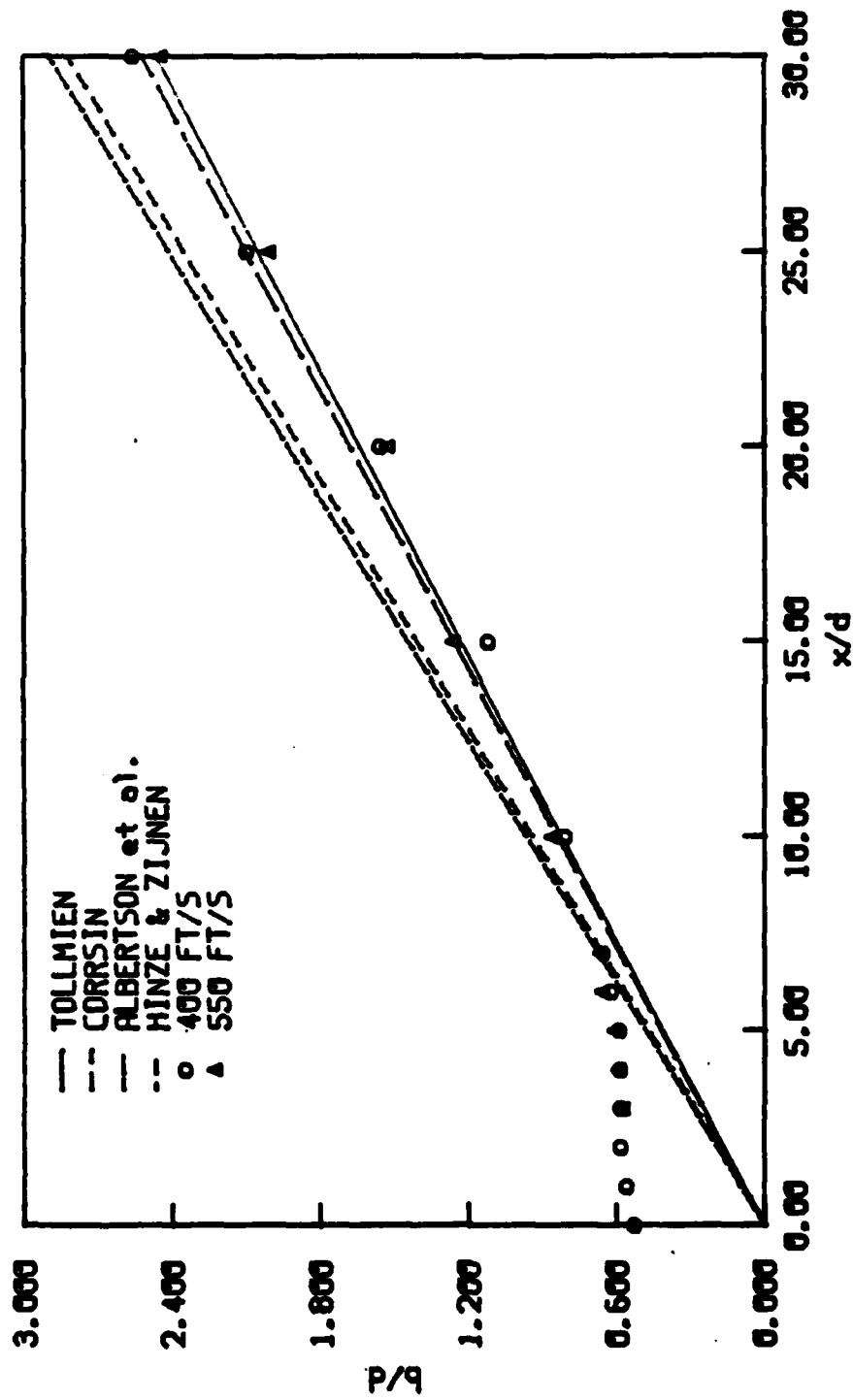


Fig. 14 Rate of spread of circular jets.

p. 37) was based on Tollmien; therefore, data fitting one prediction should be expected to fit the other. This lesser spread rate can also be attributed to the secondary effects described in the preceeding paragraph.

An area of final consideration for the characteristics of the free jet is that of turbulence. The turbulence profiles for each velocity are given in Figs. 15 and 16. Close to the nozzle exit, the turbulence intensities are very low (less than one percent at the nozzle exit) and gradually increase until about 25 nozzle diameters downstream. At this point, the turbulence intensities stabilize at about 25 percent. According to Wygnanski and Fiedler [6], this is an indication that the jet is becoming self-preserving in nature. In fact, the data available for axisymmetric free jets show that for distances from the nozzle of 30 diameters or greater, the turbulence profiles should become similar with axial intensities about 30 percent [6,8,13,29]. The information in Figs. 15 (p. 41) and 16 (p. 42) appears to be a little high when compared to that from Donaldson et al. [13], but this can be attributed to the fact that the data obtained in this study was not corrected for turbulence. For areas of low turbulence (i.e. x/d less than 10), this data agrees well with that obtained by Sami et al. [7].

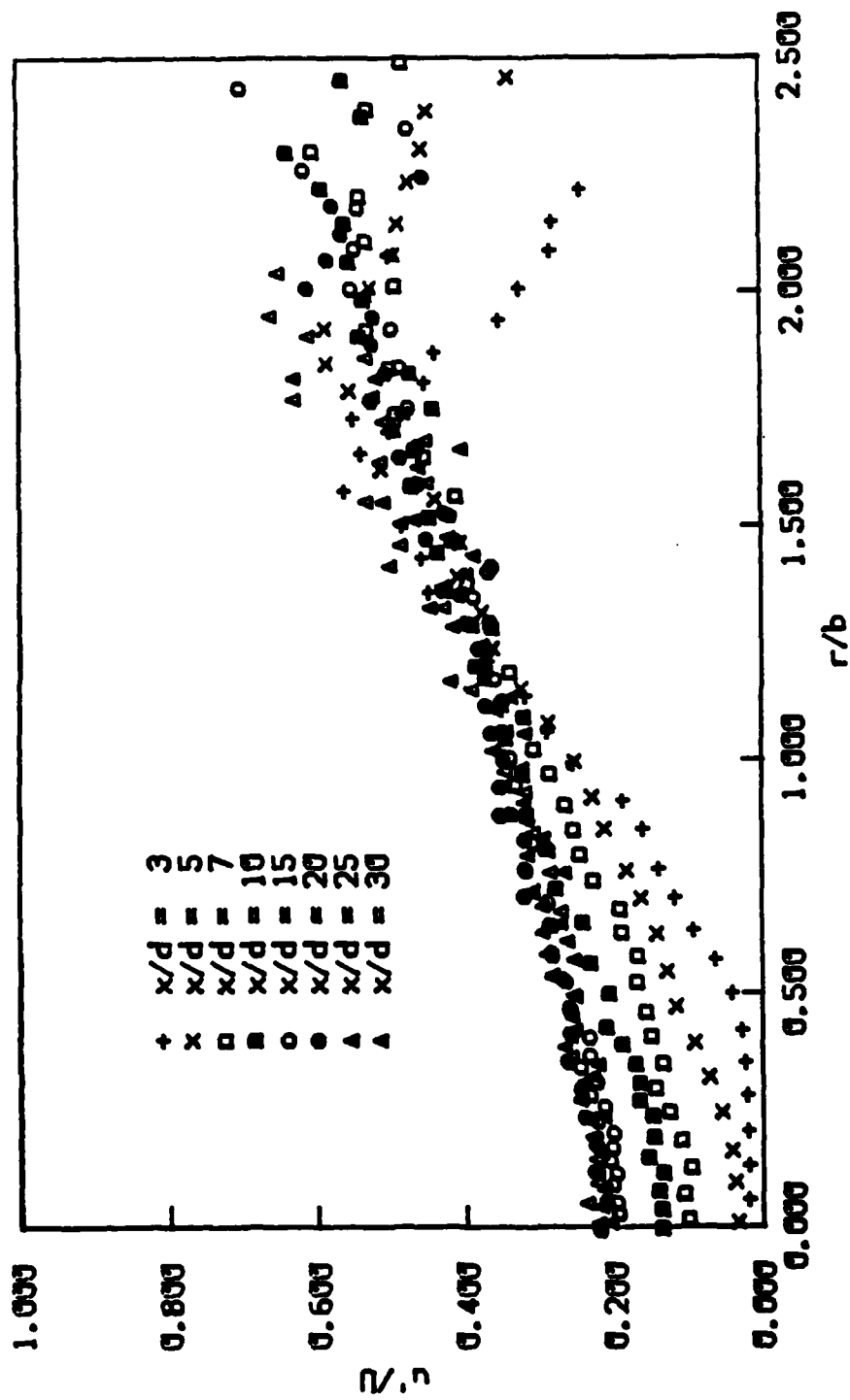


Fig. 15 Turbulence profiles of the free jet, $U_0 = 400$ ft/s.

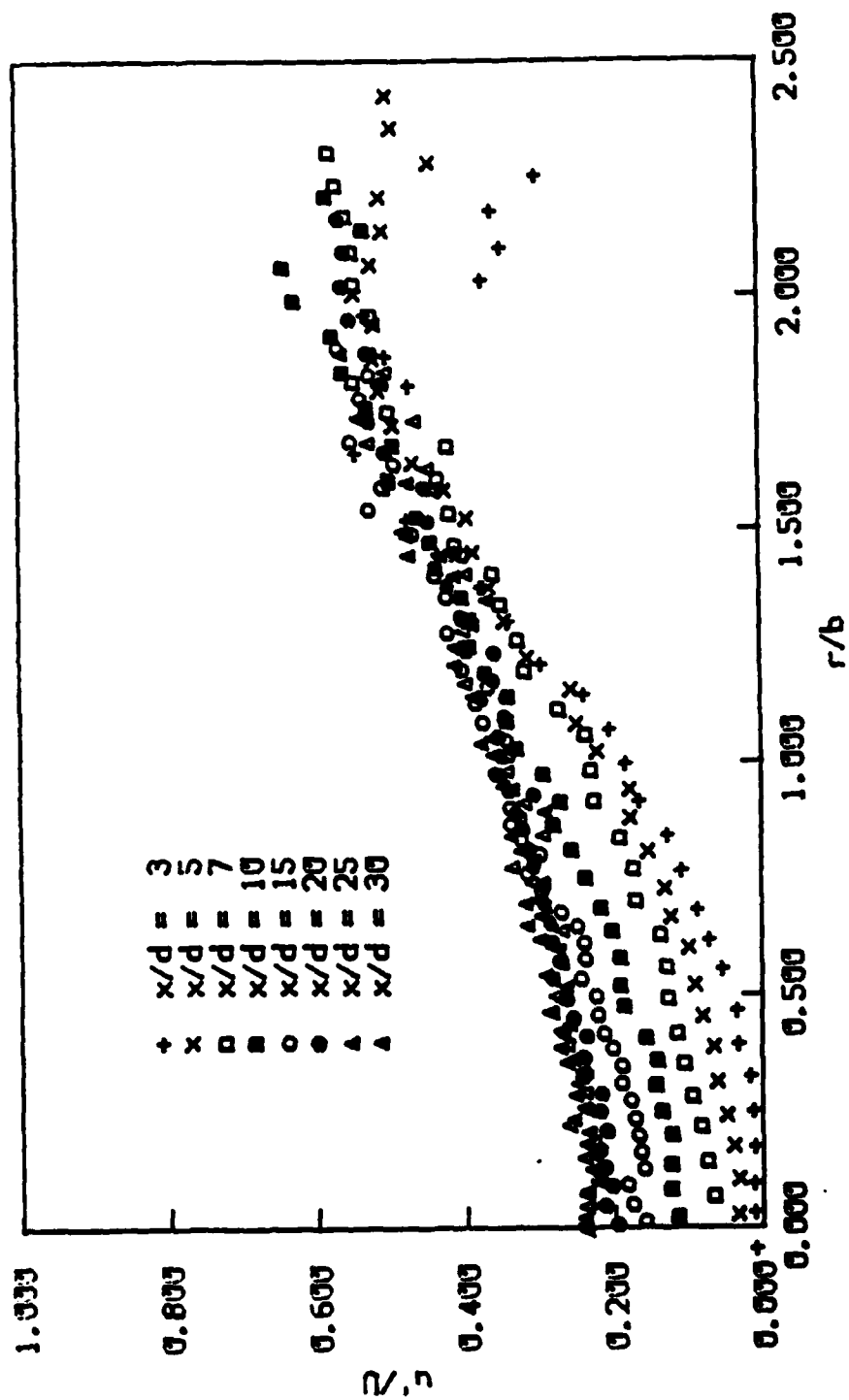


Fig. 16 Turbulence profiles of the free jet, $U_0 = 550$ ft/s.

The overall conclusion based on the results of the above comparisons shows that the jet used in these experiments performs as expected and should produce reliable data in the subsequent tests.

B. Phase Two -- Surface Flow Visualization

Figs. 17 through 28 show the results of the flow visualization tests. Only subtle differences can be seen from the different nozzle distances and at the two velocities. The most noticeable difference is in the streamlines from the stagnation point along the axis of the cylinder (i.e. $\theta = 0$). When the nozzle is close to the cylinder ($x/d = 7$), these streamlines are well developed along the cylinder's axis; but at the further distances ($x/d = 15$ and 30) they are less developed with a tendency to "diverge" from the axis of the cylinder toward the axis of the jet.

C. Phase Three -- Wall Jet Studies

The information available on impinging jets deals, almost exclusively, with flat plates as the object of impingement. Information on other shapes is limited, and nonexistent for impingement upon cylinders. This means the information presented in this chapter is entirely new; to the best of the author's knowledge, there is no other known



Fig. 17 Flow visualization for $x/d = 7$,
 $U_o = 400$ ft/s (front).



Fig. 18 Flow visualization for $x/d = 7$,
 $U_o = 400$ ft/s (back). Showing
areas of flow separation.



Fig. 19 Flow visualization for $x/d = 15$,
 $U_0 = 400$ ft/s (front).



Fig. 20 Flow visualization for $x/d = 15$,
 $U = 400$ ft/s (back). Showing
areas of flow separation.

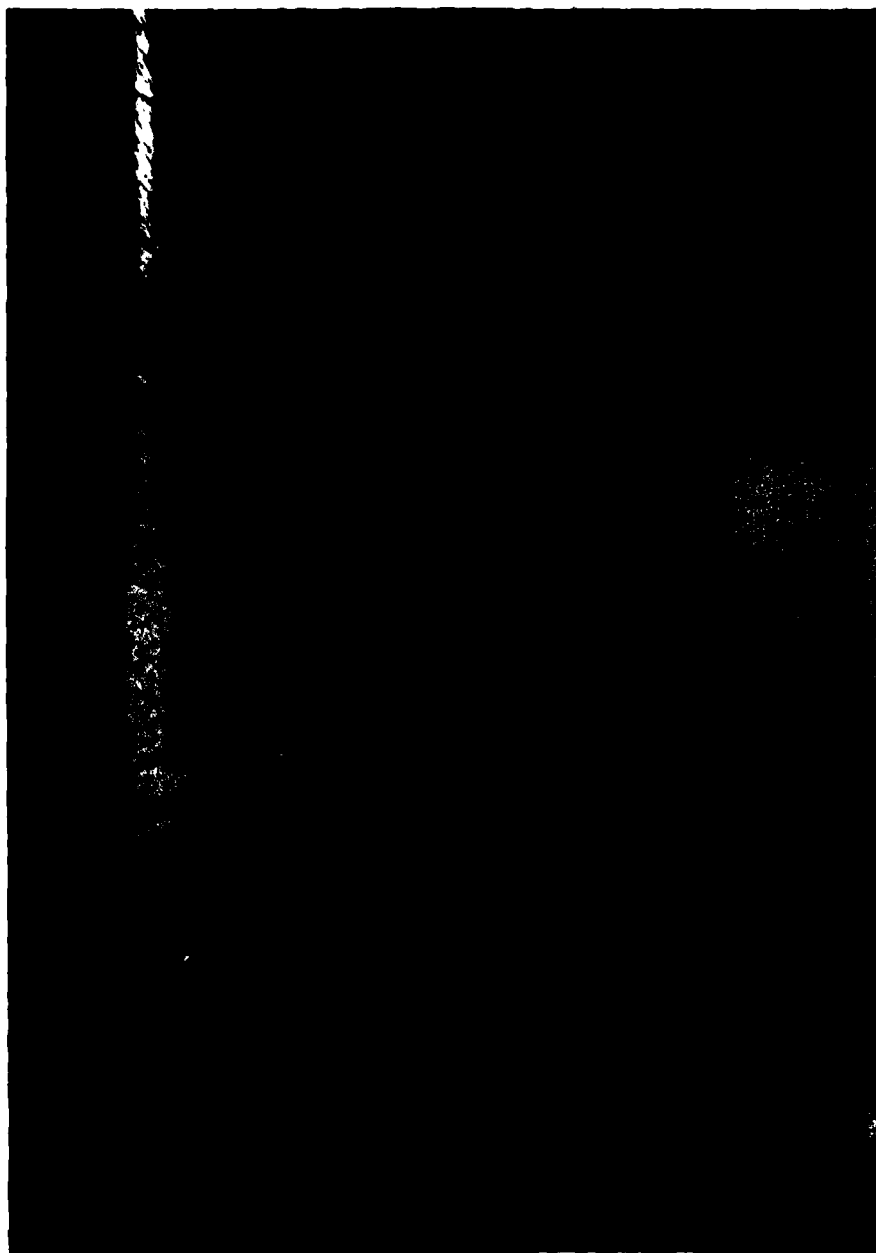


Fig. 21 Flow visualization for $x/d = 30$,
 $U_o = 400$ ft/s (front).



Fig. 22 Flow visualization for $x/d = 30$,
 $U_0 = 400$ ft/s (back). Showing
areas of flow separation.

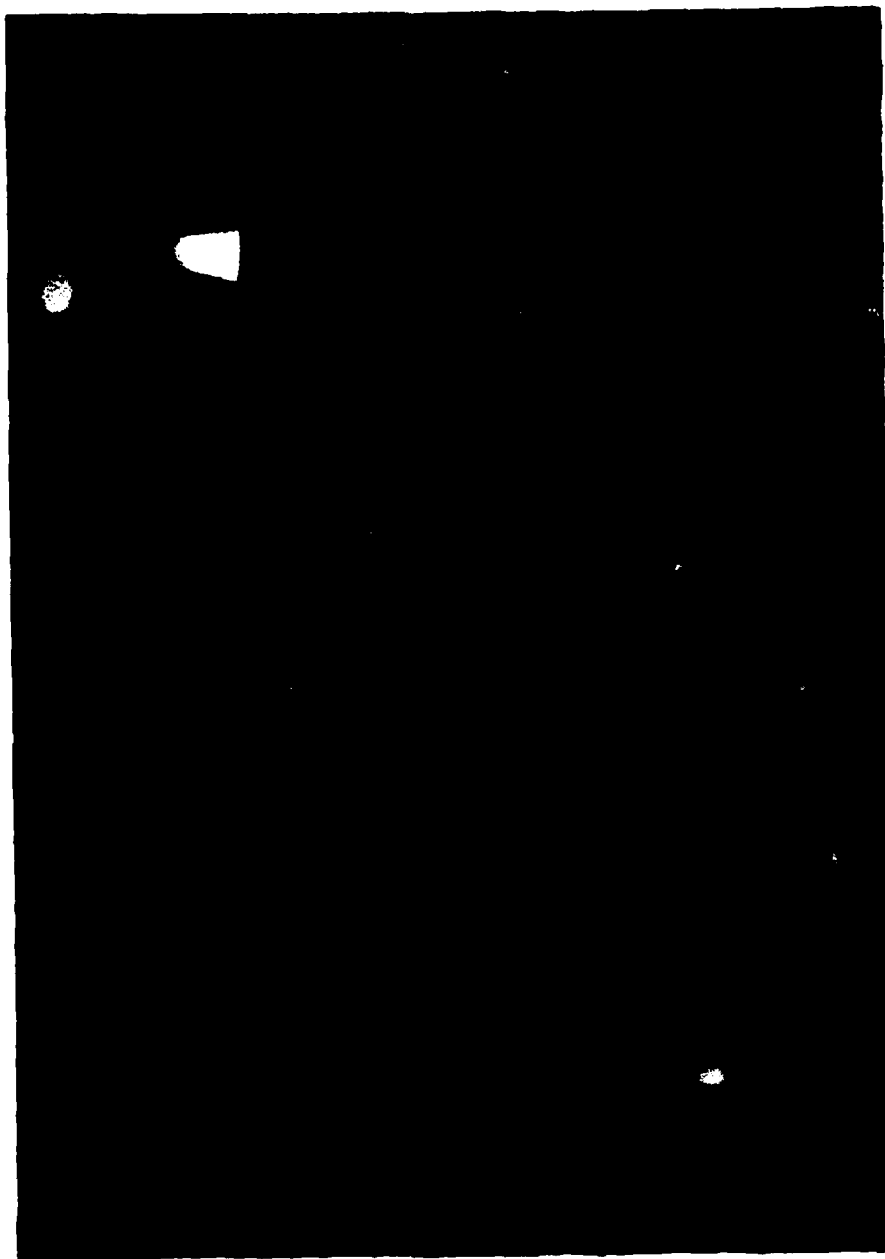


Fig. 23 Flow visualization for $x/d = 7$,
 $U_0 = 550$ ft/s (front).

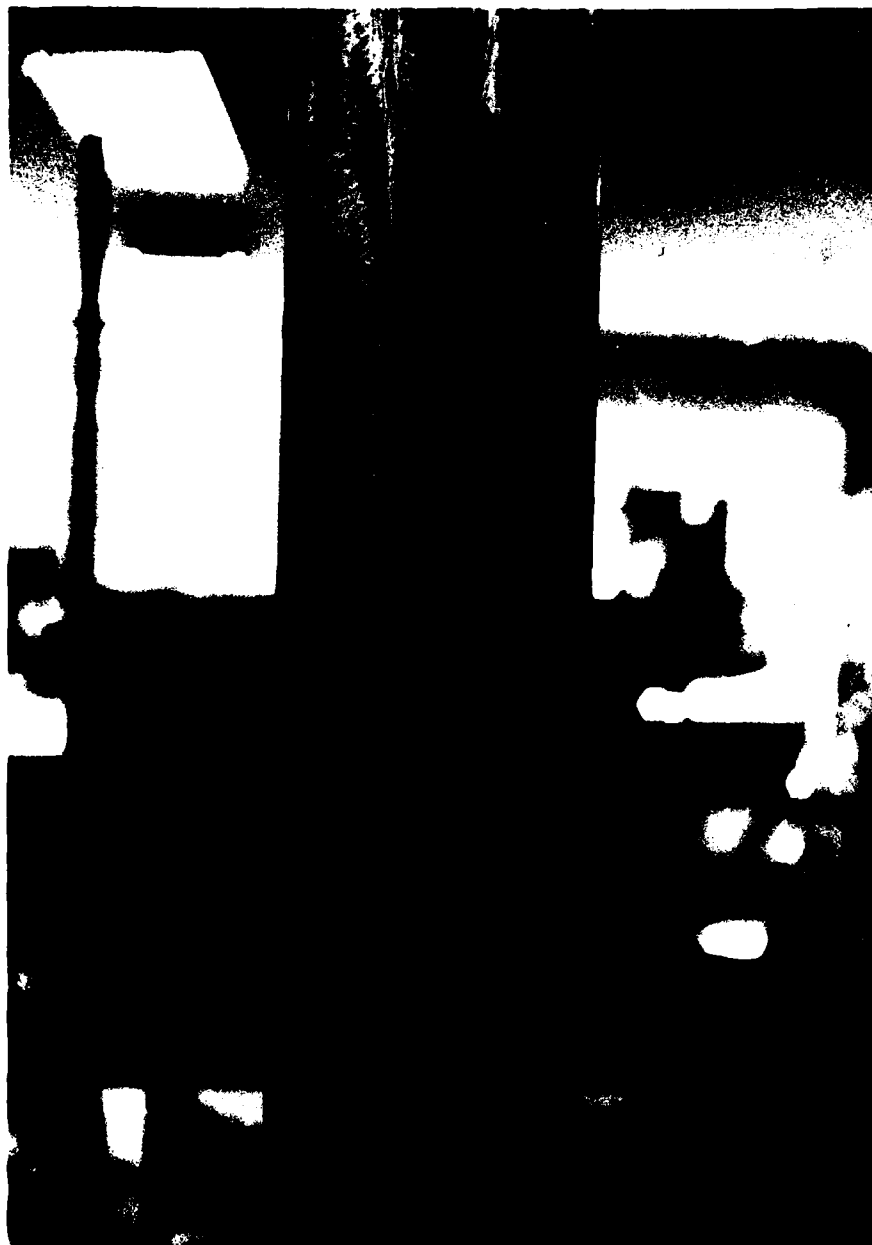


Fig. 24 Flow visualization for $x/d = 7$,
 $U_{\infty} = 550$ ft/s (back). Showing
areas of flow separation.

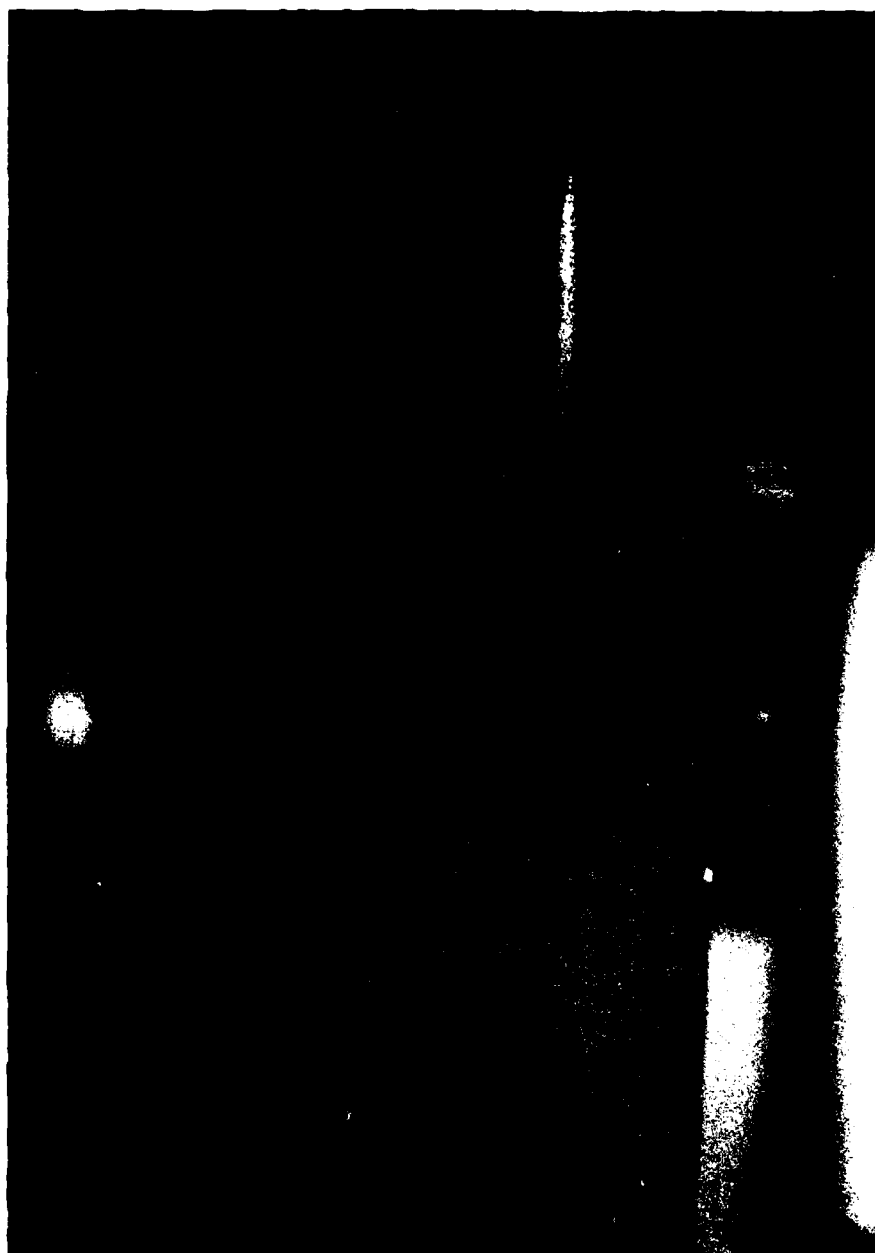


Fig. 25 Flow visualization for $x/d = 15$,
 $U_o = 550$ ft/s (front).



Fig. 26 Flow visualization for $x/d = 15$,
 $U_0 = 550$ ft/s (back). Showing
areas of flow separation.

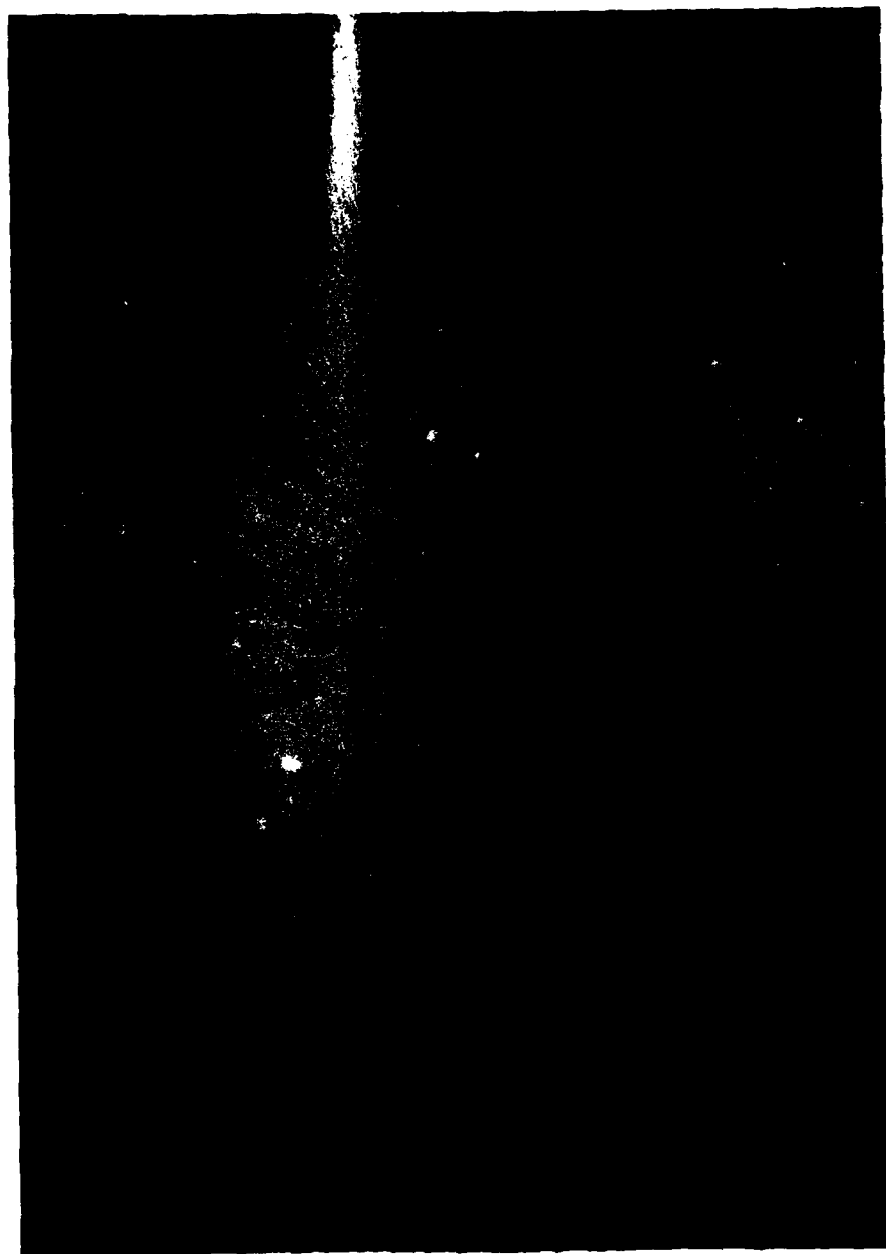


Fig. 27 Flow visualization for $x/d = 30$,
 $U_o = 550$ ft/s (front).



Fig. 28 Flow visualization for $x/d = 30$,
 $U = 550$ ft/s (back). Showing
areas of flow separation.

source of information about this type of flow.

To describe the wall jet, certain parameters must be defined. Fig. 29 shows the geometry of the wall jet along the axis of the cylinder and Fig. 30 shows the geometry about the circumference of the cylinder. A particular problem in this portion of the research is how to present the data in a meaningful manner. Fig. 31 indicates the points where measurements were taken. Presenting each of these points independently would be meaningless and overwhelm the reader with information. If radials are projected outward from the impingement point along the surface of the cylinder, it is possible to study the effects of the wall jet as it progresses along a particular radial. The one limitation in using this method to describe the wall jet lies in the fact that the wall jet is not a truly radial jet. Figs. 32 through 37 show the direction of the flow along the surface of the cylinder as indicated by the flow visualization method previously discussed. From these figures it can be seen that, although the flow may not be radial, it is close enough to at least approximate radial flow.

It should be noted, however, that unlike the radial wall jets produced by a jet impinging on a flat plate, each radial on the cylinder's surface will produce a different wall jet. There is one area of symmetry for the wall jet

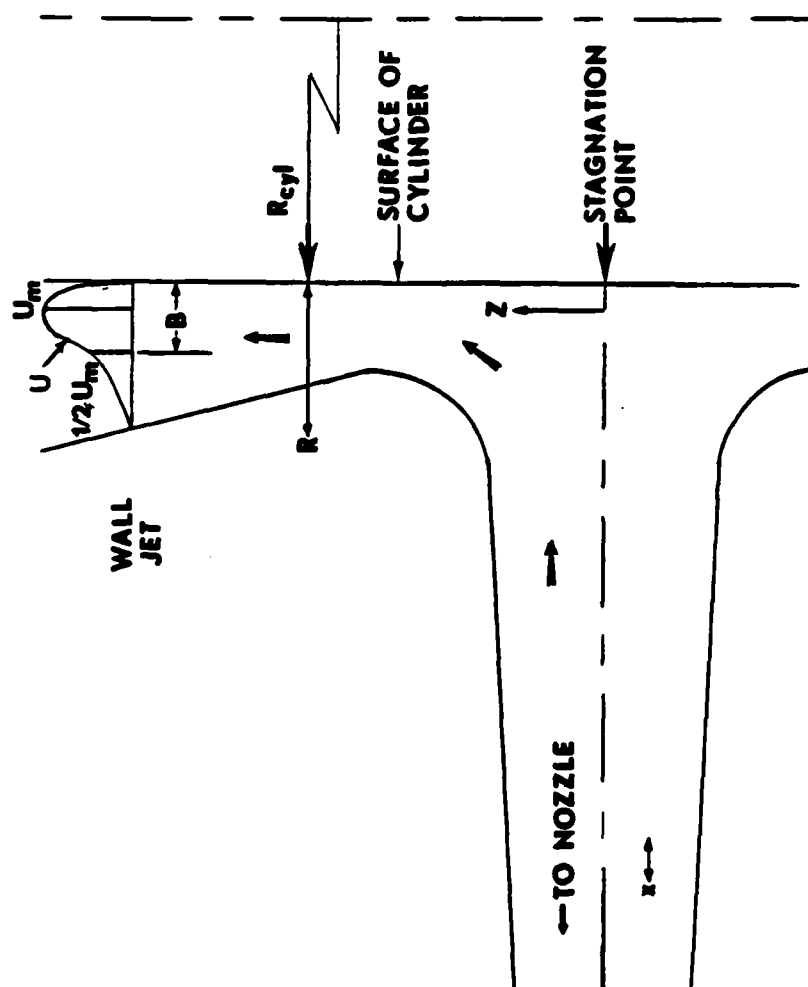


Fig. 29 Wall jet geometry and parameters in the axial direction.

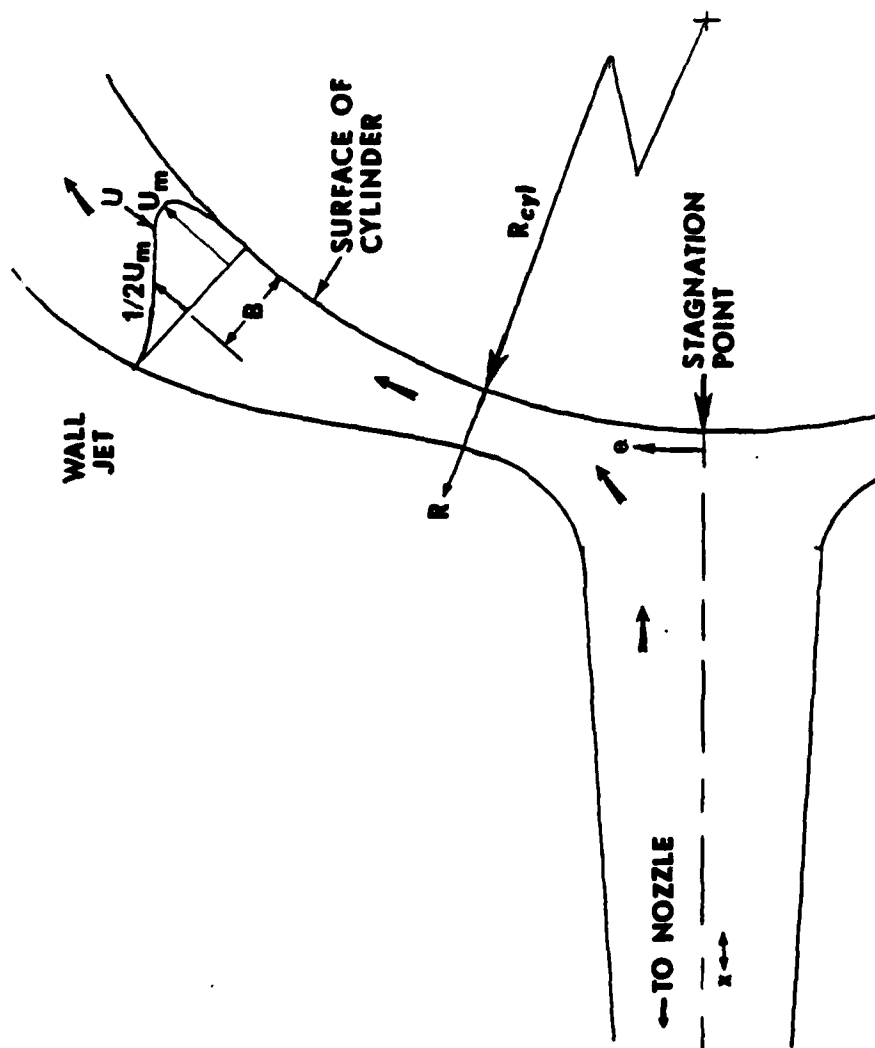


Fig. 30 Wall jet geometry and parameters in the circumferential direction.

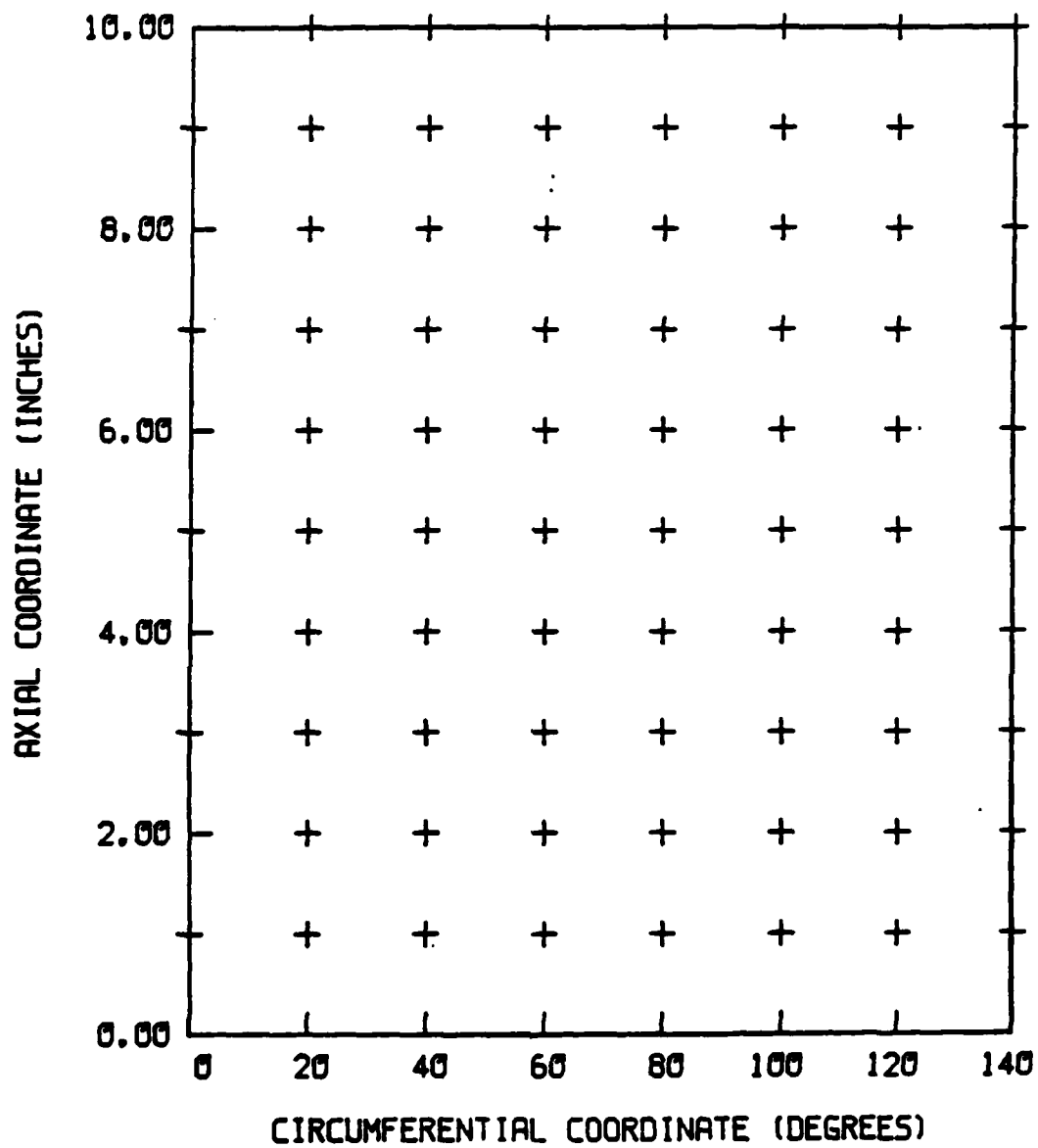


Fig. 31 Measurement points about the surface of the cylinder.

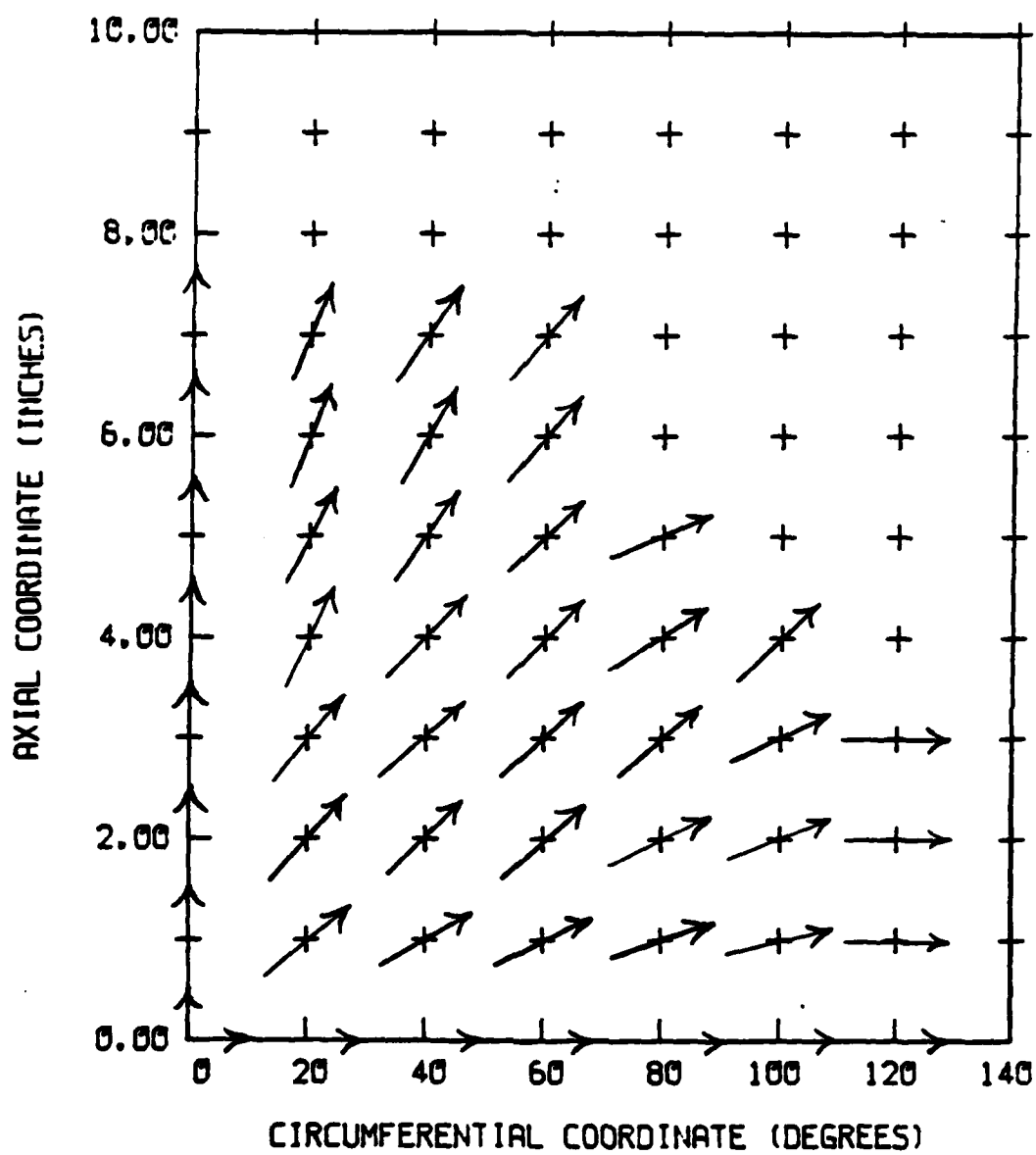


Fig. 32 Surface flow direction for $U_0 = 400$ ft/s,
 $x/d = 7$.

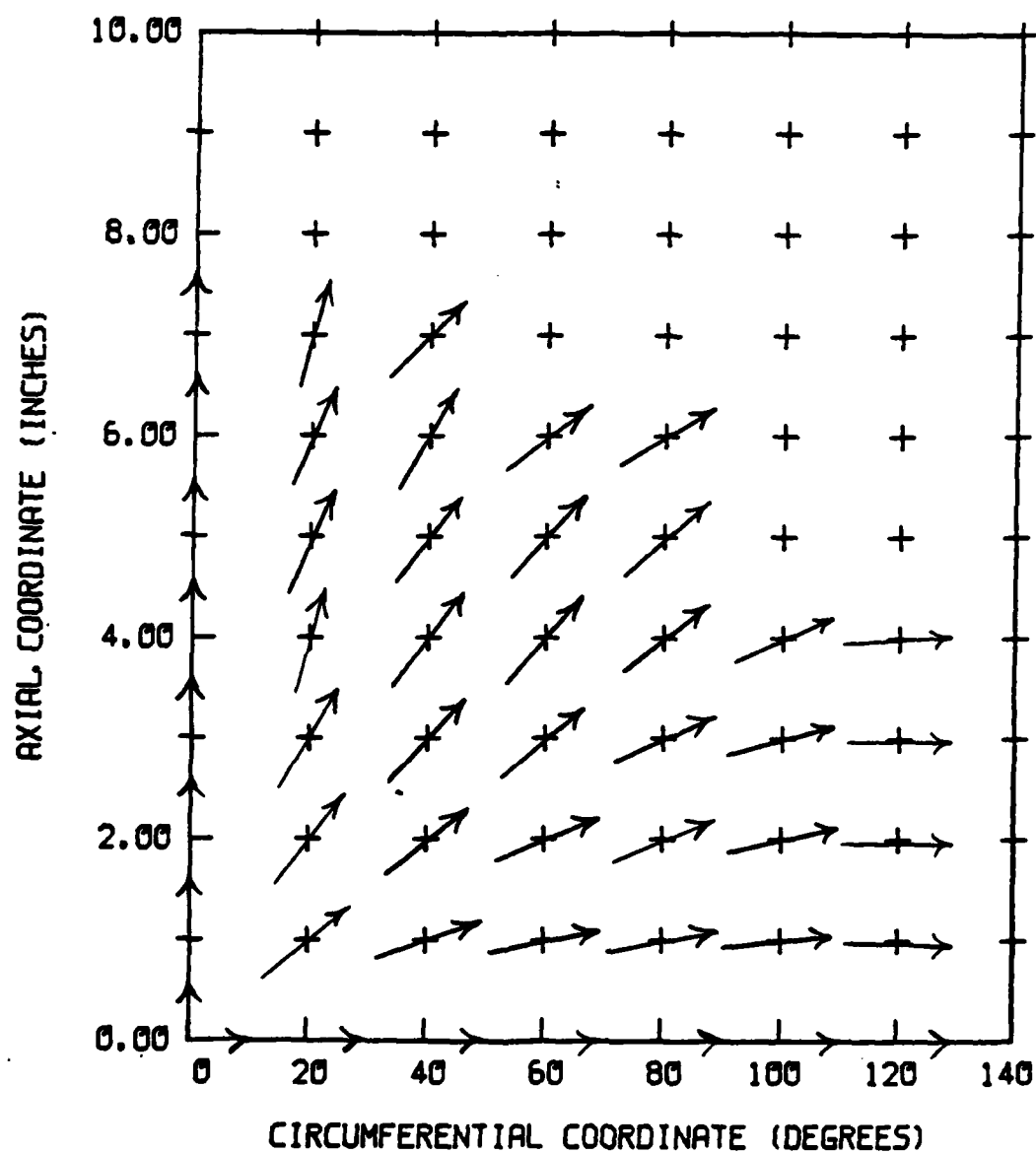


Fig. 33 Surface flow direction for $U_0 = 400$ ft/s,
 $x/d = 15$.

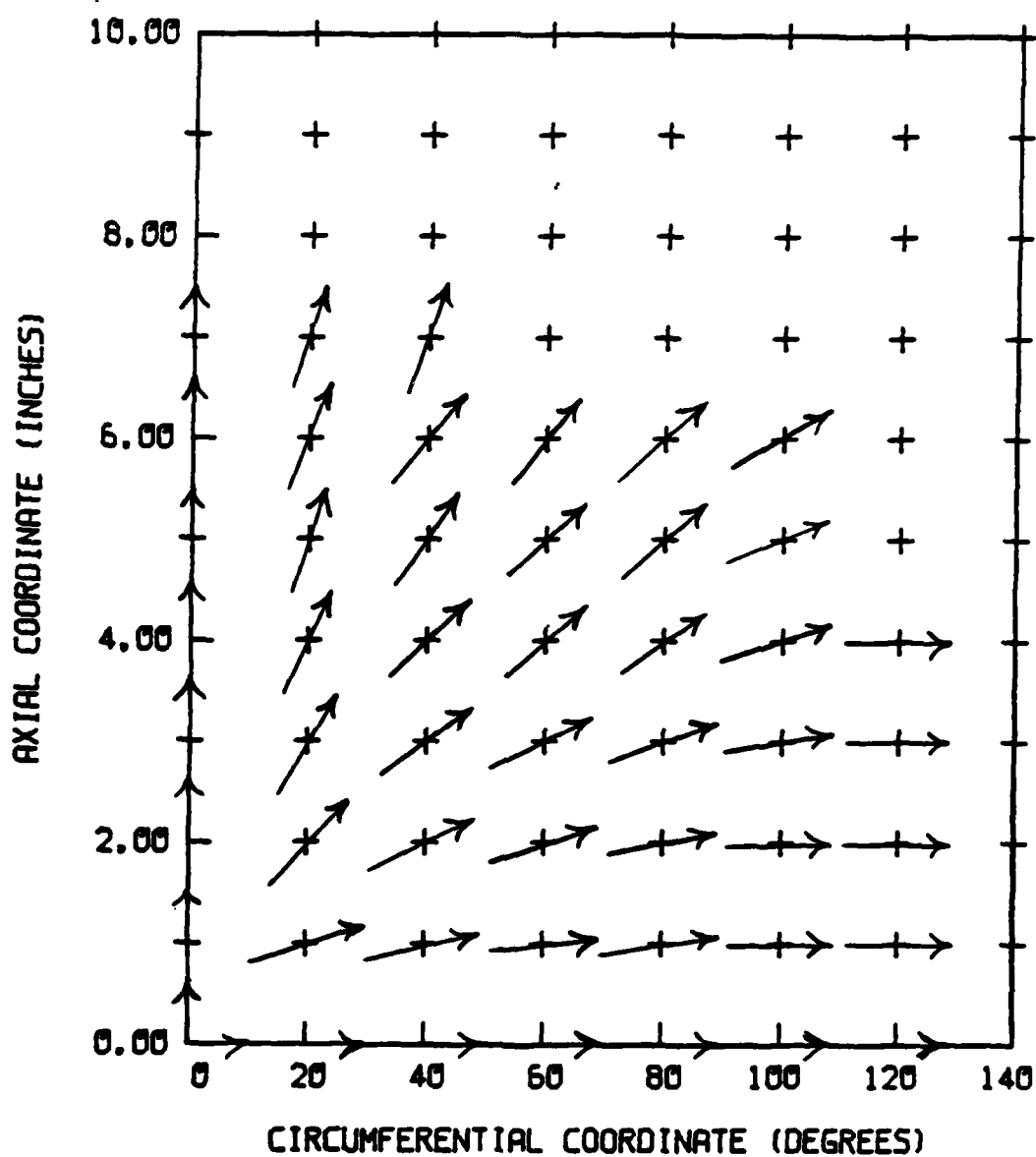


Fig. 34 Surface flow direction for $U_0 = 400$ ft/s,
 $x/d = 30$.

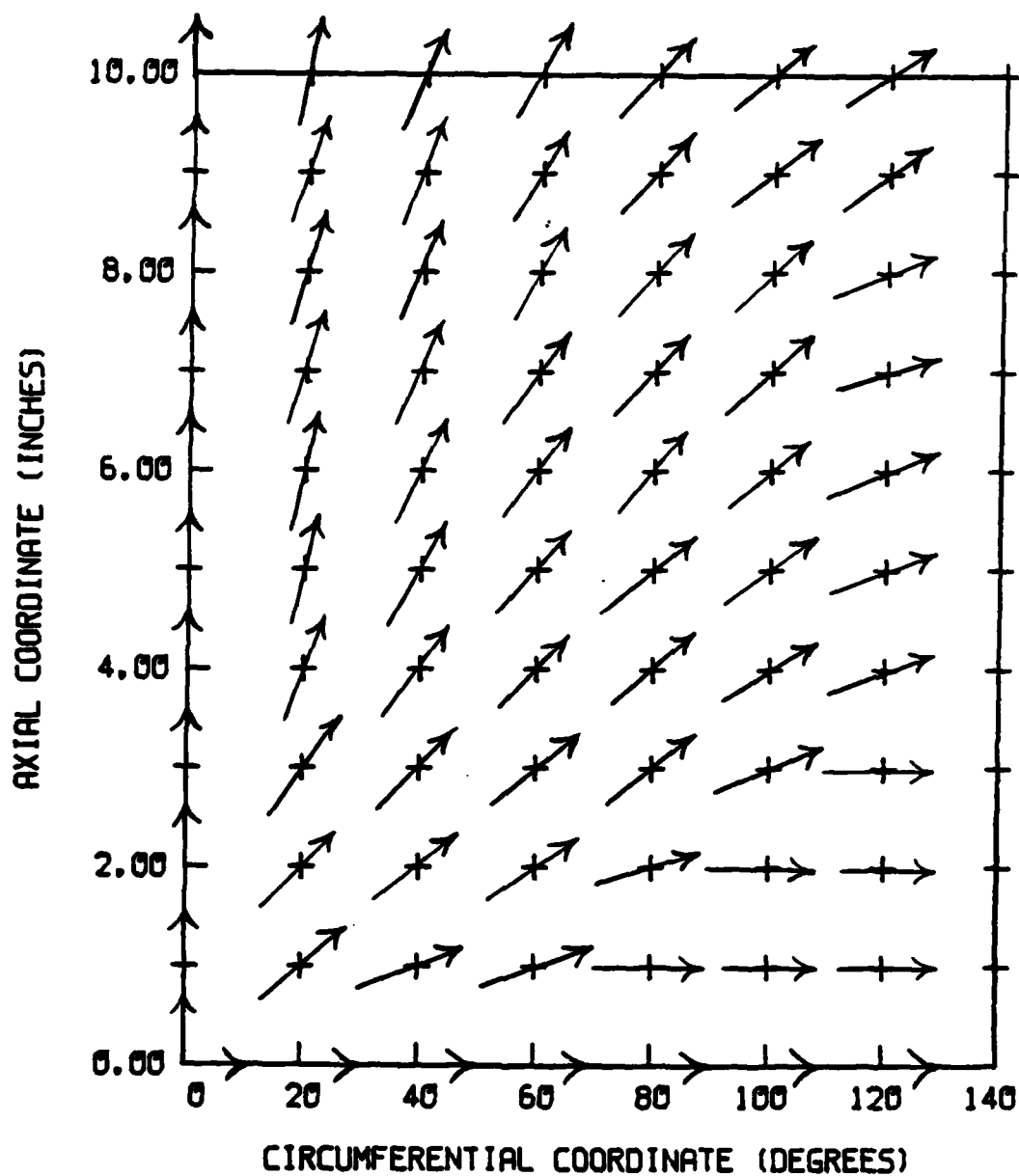


Fig. 35 Surface flow direction for $U_0 = 550$ ft/s,
 $x/d = 7$.

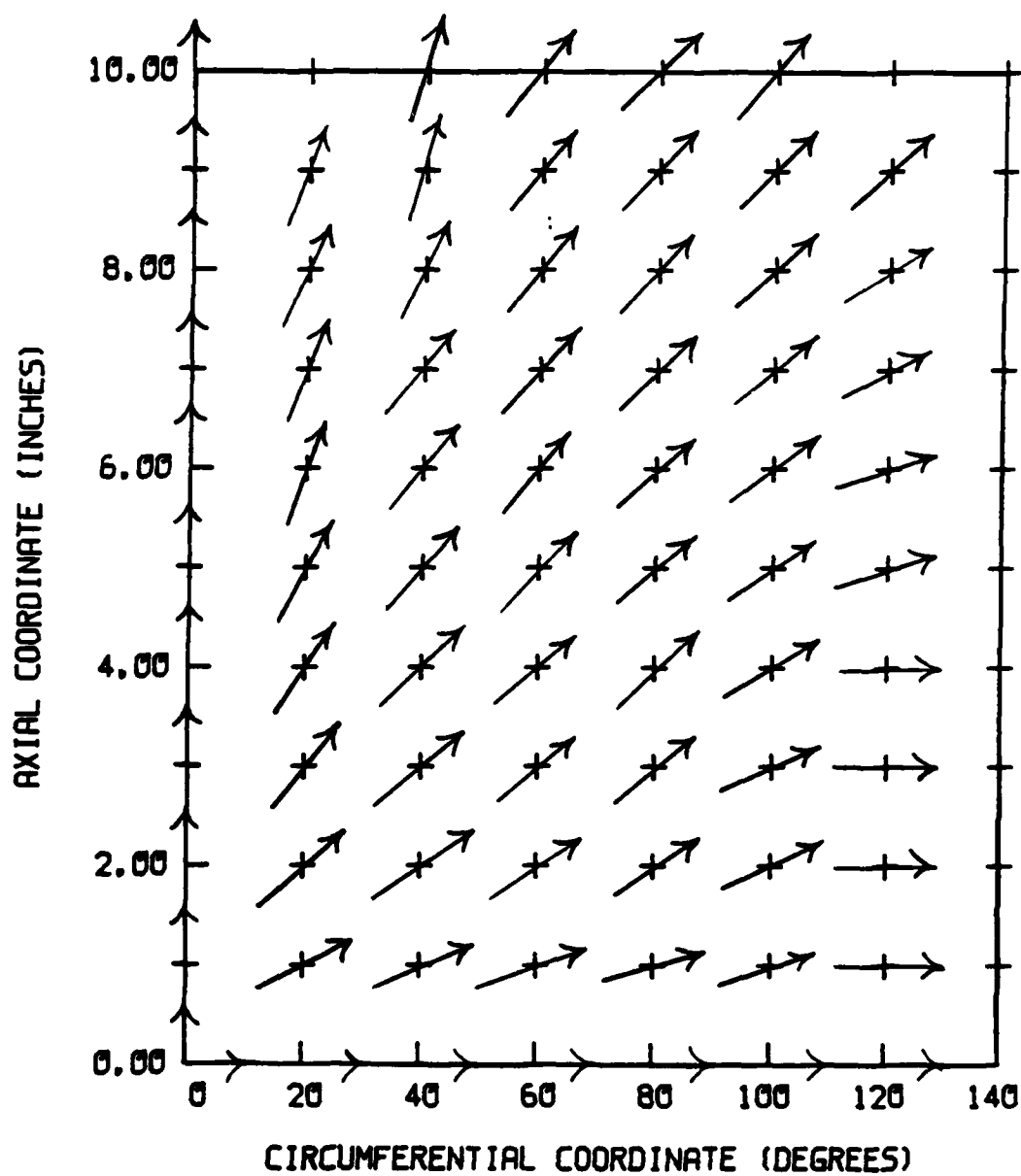


Fig. 36 Surface flow direction for $U_0 = 550$ ft/s,
 $x/d = 15$.

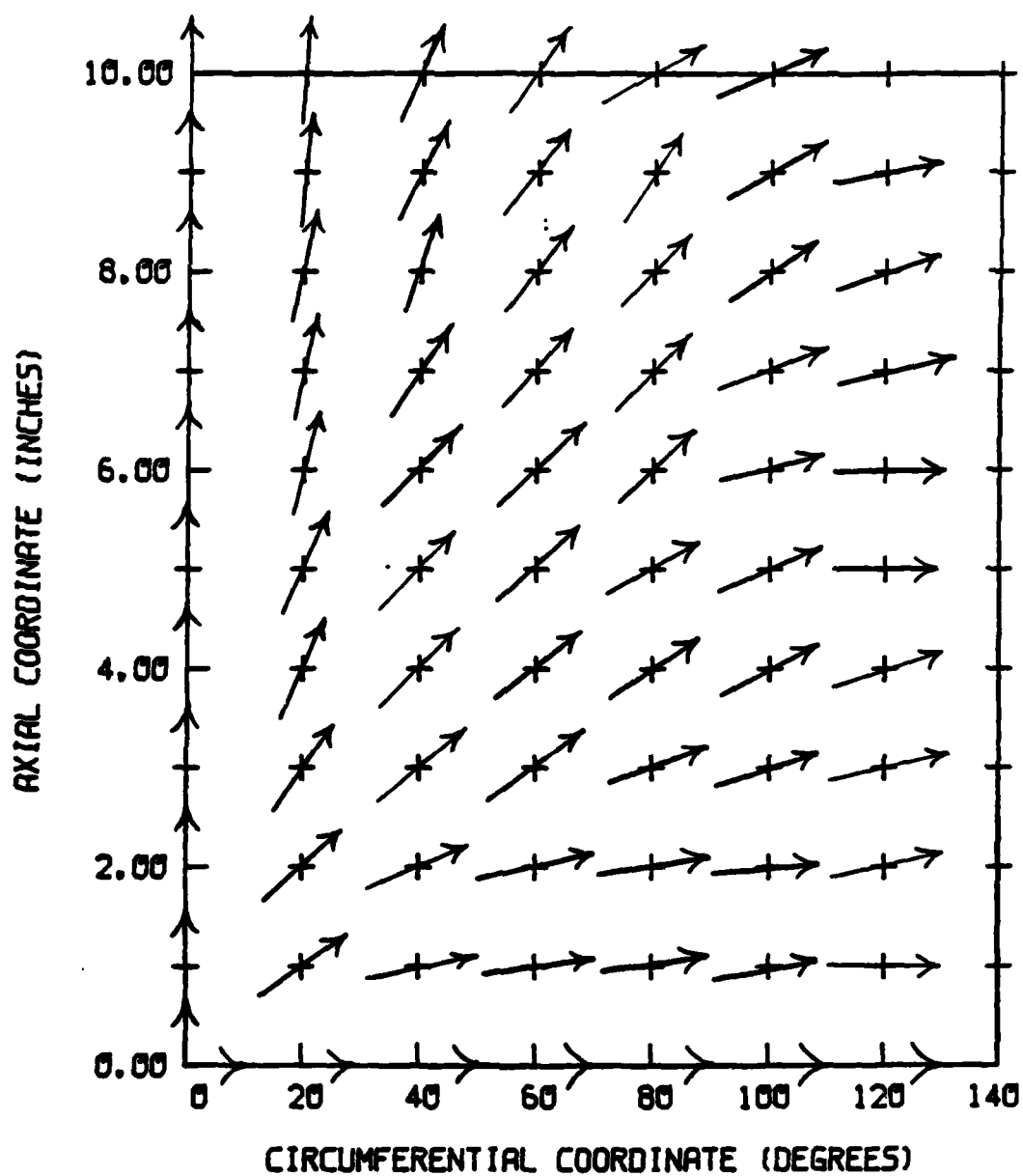


Fig. 37 Surface flow direction for $U_0 = 550$ ft/s,
 $x/d = 30$.

about the cylinder. If the surface of the cylinder is divided into quadrants such that the impingement point is at the intersection of the quadrants, it is necessary only to describe the jet in one of the quadrants, the other three being an image of the first. In other words, the wall jet produced by a normally impinging jet on a cylinder is symmetrical about the axis of the cylinder and about a circumferential line through the impingement point. Based upon this symmetry only the radials in one quadrant will be explored allowing symmetry to account for the remaining quadrants.

Even allowing for the limited symmetry of the wall jet it is still very difficult to completely describe it through radials. Because of the effects of the curvature of the surface it would still take an unlimited number of radials to completely characterize the wall jet. One can, however, give some indications about the nature of the wall jet through a limited number of radials. Based on the previously chosen measurement points (Fig. 31, p. 59) five radials can be projected from the impingement point to intersect them. These radials are shown in Fig. 38. These five radials along with the radials in the direction of the axis of the cylinder (axial radial) and in the direction along the circumferential axis (circumferential radial) provide a total of seven radials in which to present the

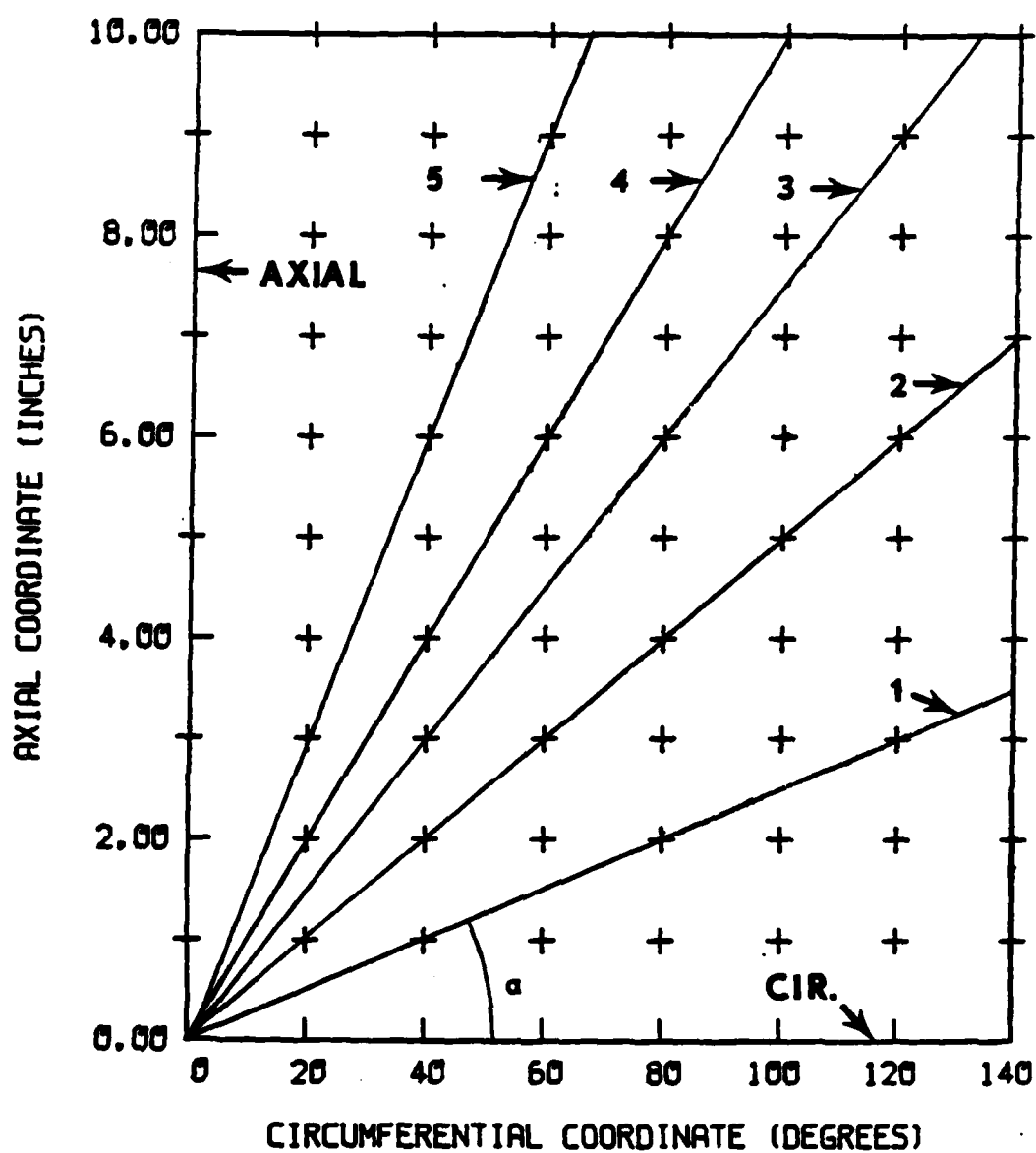


Fig. 38 Surface direction radials for presenting the wall jet data.

flow field data. The distance along each of the radials will be labeled R' . In the subsequent presentation of data, each of the plots will be along a particular radial with each of the points given as both a distance along that radial (R') and as a station number. This station number is merely the coordinates of the point being measured (circumferential coordinate-- θ , degrees/axial coordinate-- Z , inches), as described in Chapter V (see Fig. 6, p. 22). (Note, this station number is not a ratio of the two numbers (θ/Z), it is just a method of determining where on the cylinder's surface the measurement is being taken.)

If the circumferential axis is designated the reference axis for measuring the angle of the radials as well as the flow direction (see Fig. 38, p. 67) the difference between the two angles (radial and flow direction) can easily be shown in Table 1.

The first area of concern in presenting the wall jet is to look at the velocity profiles of the wall jet. Only the circumferential and axial radials, and radials 2 and 4 intersect enough points to make a thorough presentation of the velocity profiles possible. Figs. 39 through 46 (pp. 85-92) show the velocity profiles for the two nozzle exit velocities at a distance of 7 nozzle diameters. Figs. 47 through 54 (pp. 93-100) are for 15 nozzle diameters and Figs. 55 through 62 (pp. 101-108) are for 30 diameters.

Table 1 Flow angles and radial angles relative to the circumferential axis to the nearest 0.5 degree.

		$U_o = 400 \text{ ft/s}$			$U_o = 550 \text{ ft/s}$		
$x/d \rightarrow$		7	15	30	7	15	30
STATION NUMBER \downarrow		α	α	α	α	α	α
40/01		29.5	19.5	13.0	19.5	23.0	12.0
80/02		27.0	22.5	16.0	16.5	33.0	8.0
120/03		25.5	0.0	0.0	0.0	0.0	11.5
20/01		39.0	40.0	17.5	41.0	27.0	34.5
40/02		45.5	38.0	26.0	38.0	34.5	23.0
60/03		43.0	39.0	26.5	39.0	39.0	37.0
80/04		33.5	38.5	35.5	42.0	42.5	33.5
100/05		----	----	22.0	36.5	34.5	22.5
120/06		----	----	0.0	21.5	18.0	0.0
40/03		41.5	48.0	37.0	46.0	38.0	40.0
80/06		----	30.0	41.5	50.0	40.5	44.0
120/09		----	----	----	35.5	41.5	10.0
20/02		48.5	52.5	48.0	45.0	41.5	42.5
40/04		47.5	53.5	45.0	54.5	44.5	46.0
60/06		49.0	37.5	53.0	55.5	51.0	45.0
80/08		----	----	----	48.5	47.0	46.0
100/10		----	----	----	41.0	51.0	----
20/03		51.5	60.0	60.0	54.5	51.5	55.5
40/06		59.5	60.5	52.0	64.5	51.0	46.5
60/09		----	----	----	60.0	50.5	52.5
RADIAL \downarrow							
1		23.5	23.5	23.5	23.5	23.5	23.5
2		41.0	41.0	41.0	41.0	41.0	41.0
3		52.0	52.0	52.0	52.0	52.0	52.0
4		59.5	59.5	59.5	59.5	59.5	59.5
5		68.5	68.5	68.5	68.5	68.5	68.5

The profiles along the axis of the cylinder show the usual characteristics of a wall jet except there is a tendency for the profile to "flatten out" rather quickly. Along the circumference of the cylinder, a well developed wall jet can be detected when the nozzle is close to the cylinder (Figs. 39, p. 85; 43, p. 89; 47, p. 93; and 51, p. 97) but the profiles break down at further distances (Figs. 55, p. 101 and 59, p. 105). The profiles along radials 2 and 4 are variations on the two extremes with radial 2 favoring the circumferential radial and radial 4 favoring the axial radial.

The next area of consideration is the turbulence intensities of the wall jet. Poreh et al. [4] made some studies of the turbulence profiles of a wall jet resulting from a circular jet impinging upon a flat plate. They found intensities (u'/U) near 0.5 close to the surface which decreased to a minimum of about 0.35 within the wall jet near the maximum velocity (U_m) and then increased again as the edge of the jet was approached. These turbulence profiles were independent of the distance from the impingement point.

Figs. 63 through 86 (pp. 109-132) show the turbulence profiles for each of the two velocities and different nozzle distances along each radial. Except in areas where the wall jet is not fully developed (i.e. close to the

impingement point), the turbulence profiles are similar to those shown by Poreh et al. [4]. The profiles in the axial direction appear to agree with that of Poreh et al. [4]. In the circumferential radial the semblance tends to break down, particularly as the nozzle distance is increased. At 7 nozzle diameters, all the radials are in agreement with each other. At 15 diameters the agreement is somewhat less, and at 30 diameters there is significant disagreement. At 30 nozzle diameters the turbulence profiles along the axial radial show an increase in the scatter of the data but the intensities remain about the same. Along the circumferential radial, there is a notable difference when compared to the axial radial. The turbulence intensities are considerably less.

Another area of consideration is the rate of spread of the wall jet. Since the axial radial approximates a flat plate, the rate of spread in the axial direction will be compared to the data available for flat plates. The axial and flat plate spread rates will then be compared to the rate of spread along the remaining radials.

Poreh et al. [4] have shown that the spread of the wall jet along a flat plate is linear and this relationship can be described by the equation:

$$B = 0.087R^*$$

(7)

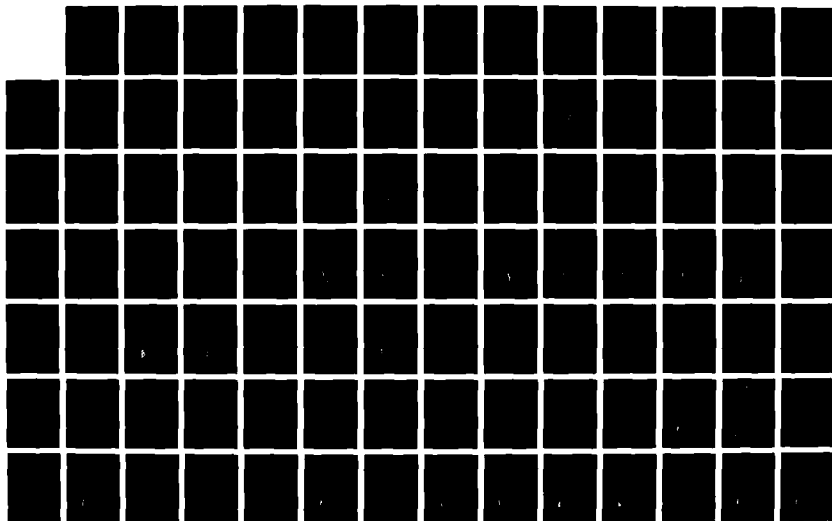
AD-A145 583

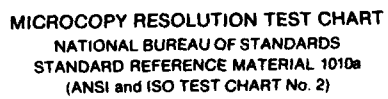
AN EXPERIMENTAL STUDY OF JET IMPINGEMENT ON A CIRCULAR
CYLINDER(U) AIR FORCE INST OF TECH WRIGHT-PATTERSON AFB
OH D W POTTS AUG 84 AFIT/CI/NR-84-50T

UNCLASSIFIED

F/G 20/4

NL





MICROCOPY RESOLUTION TEST CHART
NATIONAL BUREAU OF STANDARDS
STANDARD REFERENCE MATERIAL 1010a
(ANSI and ISO TEST CHART No. 2)

where R^* is the radial distance from the impingement point. Fig. 87 (p. 133) compares the spread rate along the axial radial for each of the runs with the data obtained by Poreh et al. [4]. The obvious conclusion is that the rate of spread along the axis is very similar to that of a flat plate, although the rate is slightly higher.

In Figs. 88 through 93 (pp. 134-139) the spread rates of the remaining radials for each run is compared with that of a flat plate. It can easily be seen that the rate of spread increases as one moves from the axial radial towards the circumferential radial. The differences between the spread rates also increase with increasing nozzle distance. The spread rate being rather substantial in the circumferential direction for $x/d = 30$.

Based on the work done by Poreh et al. [4] and Bradshaw and Love [23], it has been shown that the decay of the wall jet can be expressed linearly, as a velocity scale, by the relationship:

$$U_o/U_m = (R^*/d)/1.03 \quad (8)$$

where R^* is the radial distance from the impingement point.

Fig. 94 (p. 140) compares the velocity scale, along the axial radial, of each of the runs with the relationship

given by Eq. (8). Figs. 95 through 100 (pp. 141-146) then compare the axial radials with the remaining radials. For close nozzle distances ($x/d = 7$) the velocity scale are similar and the wall jet decays uniformly along each of the radials (much like a flat plate). At greater distances ($x/d = 15$ and 30), the similarity breaks down with the jet in the circumferential direction decaying at a much slower rate than in the axial direction.

A final consideration in presenting the wall jet data is to determine if the velocity profiles are similar. The conventional manner to determine similarity is to plot U/U_m versus R/B . Figs. 101 through 124 (pp. 147-170) show the nondimensional plots for each radial and for each run. Except in areas closed to the impingement point, where the wall jet is not yet fully developed, there appears to be a strong indication of similarity. The similarity seems to break down in the circumferential direction at certain distances from the impingement point. This failure of similarity could be used as an indication of flow separation from the wall.

Finding the exact point where the wall jet separates from the surface based upon velocity measurements proved to very difficult. Gartshore and Newman [27] proposed typical velocity profiles for a wall jet in an adverse pressure gradient, but the profiles measured in this

experiment did not, in any way, agree with the ones they proposed. In fact, none of the velocity profiles measured showed the usual indication of separated flow. Even the profiles at 120 degrees from the impingement point where the flow is assumed to have separated showed none of the indications expected. The turbulence profiles were also inconclusive in determining areas where the jet may have separated from the wall. As stated earlier, only the similarity profiles give any indication of possible flow separation and this is based on the, as yet unproven, assumption that deviations from similarity indicate flow separation.

An alternative way of estimating flow separation is through the flow visualization method. Areas of possible flow separation are usually indicated by an accumulation of the substance used in determining the flow visualization (kerosene-tempra mixture in this experiment). The reader is referred to Figs. 17 through 28 (pp. 44-55) where these areas of accumulation can easily be seen.

The flow visualization method indicated areas of separated flow occurring much later than would have been expected. The anticipated area of separation is usually in the vicinity of $\theta = 90$ degrees; about 80 to 100 degrees from the stagnation point. For the impinging jet, however, separation did not occur until 130 to 160 degrees from the

impingement point, depending upon nozzle distance and flow velocity. For $U_o = 400$ ft/s, these areas are indicated in Fig. 125 (p. 171) and for $U_o = 550$ ft/s in Fig. 126 (p. 172).

CHAPTER VII

CONCLUSIONS AND RECOMMENDATIONS

The effects of a round turbulent jet impinging normally on a circular cylinder have been investigated. The experiments were conducted at nozzle exit velocities of 400 and 550 feet per second. The jet was impinged upon the cylinder at distances of 7, 15, and 30 nozzle diameters.

The following are the major results of this experiment:

1. The free jet was validated and found to agree very well with both theoretical predictions and previous experimental work.
2. The velocity profiles about the cylinder were found to be similar to those found on flat plate for nozzle distances close to the cylinder ($x/d = 7$) but became significantly different at farther nozzle distances ($x/d = 15, 30$). At these distances the profiles along the cylinder's axis became very "flat" and in the circumferential direction they showed very little similarity to that of a flat plate.
3. The spread rate of the wall jet about the cylinder was much greater than that found on a flat plate. Increasing both with farther nozzle distances and as the

circumferential axis is approached.

4. The velocity of the wall jet was found to decay much slower than that of a flat plate, particularly about the circumference of the cylinder.

5. The turbulence profiles of the wall jet were found to be similar to those of a wall jet on a flat plate except at $x/d = 30$ where the turbulence in the circumferential direction decreased substantially.

6. An attempt was made to nondimensionalize the wall jet velocity profiles using the standard similarity parameters for a flat plate. The results were inconclusive with the profiles being similar in some cases but varying in others. There is a possibility that the break down of the similarity profiles could be tied to the areas of possible jet separation from the surface of the cylinder.

7. An attempt was also made to determine the areas where the wall jet may have separated from the surface by analyzing the velocity and turbulence profiles of the wall jet. This analysis proved to be inconclusive so flow visualization was used to determine wall jet separation. Based on this data, it was found that the wall jet may have remained attached to the surface until about 120 to 160 degrees from the impingement point, depending upon the

flow velocity and nozzle distance.

From the above results a major conclusion that can be drawn is; there appears to be a significant relationship between the radius of the nozzle and the radius of the cylinder. At the farthest nozzle distance the effective radius of the impinging jet becomes large when compared to the radius of the cylinder. If the effective radius is defined as the radius where the velocity of the jet is one-half that of the maximum velocity, b (see Fig. 9, p. 30), then a comparison between this radius and the cylinder's radius can be made. At seven nozzle diameters the effective radius is 0.45 inches or 14 percent of the cylinder's radius. At 15 nozzle diameters, $b = 0.83$ inches or 25 percent of the cylinder's radius. At 30 nozzle diameters the effective radius becomes $b = 1.75$ inches or 53 percent of the cylinder's radius. At this point, the curvature becomes so great that there is very little surface upon which the wall jet can form.

The following recommendations are suggested:

1. Use a split film sensor or similar method to determine areas of flow reversal, thus locating areas of flow separation.
2. Use a multi-directional sensor (i.e. cross-wire sensor) to determine the turbulence intensities and

velocity components not parallel to the flow. This will have three benefits:

- a. determine if the flow remains in the direction indicated by the surface flow visualization.
- b. enable measurements of the turbulent shear stresses in the flow.
- c. allow for corrections due to the high levels of turbulence.

As with most experimental work, the data raised more questions than it answered. But light has been shed into the nature of this complex and unique flow field.

REFERENCES

1. Krzywoblocki, M.Z., "Jets--Review of Literature," Jet Propulsion, Vol. 26, Sept. 1956, pp. 760-779.
2. Porteiro, J.L.F., Norton, D.J., and Pollock, T.C., "Space Shuttle Ice Suppression System Validation," TEES-TR-4587-82-01, Texas Engineering Experiment Station, Texas A&M University, 1982
3. Poreh, M., and Cermak, J.E., "Flow Characteristics of a Circular Submerged Jet Impinging Normally on a Smooth Boundry," Proceedings of the 6th Midwestern Conference on Fluid Mechanics, University of Texas, Sept. 1959, pp. 198-212.
4. Poreh, M., Tsuei, Y.G., and Cermak, J.E., "Investigation of a Turbulent Radial Wall Jet," Journal of Applied Mechanics, Jun. 1967, pp. 457-463.
5. Albertson, M.L., Dai, Y.B., Jensen, R.A., and Rouse, H., "Diffusion of Submerged Jets," Transactions of the American Society of Civil Engineers, Vol. 115, 1950, pp. 639-697.
6. Wygnanski, I. and Fiedler, H., "Some Measurements in the Self-Preserving Jet," Journal of Fluid Mechanics, Vol. 38, 1969, pp. 577-612.
7. Sami, S., Carmody, T., and Rouse, H., "Jet Diffusion in the Region of Flow Establishment," Journal of Fluid Mechanics, Vol. 27, 1967, pp. 231-252.
8. Gibson, M.M., "Spectra of Turbulance in a Round Jet," Journal of Fluid Mechanics, Vol. 15, 1963, pp. 161-173.
9. Miller, D.R. and Comings, E.W., "Static Pressure Distribution in the Free Jet," Journal of Fluid Mechanics, Vol. 3, 1957, pp. 1-16.

10. Ricou, F.P. and Spalding, D.B., "Measurements of Entrainment by Axisymmetrical Turbulent Jets," Journal of Fluid Mechanics, Vol. 11, 1961, pp. 21-32.
11. Love, E.S., Grigsby, C.E., Lee, L.P., and Woodling, M.J., "Experimental and Theoretical Studies of Axisymmetric Free Jets," NACA TR R-6, 1959.
12. Donaldson, C.DuP. and Snedeker, R.S., "A Study of Free Jet Impingement--Part 1, Mean Properties of Free and Impinging Jets," Journal of Fluid Mechanics, Vol. 45, 1971, pp. 281-319.
13. Donaldson, C.DuP., Snedeker, R.S., and Margolis, D.P., "A Study of Free Jet Impingement--Part 2, Free Jet Turbulent Structure and Impingement Heat Transfer," Journal of Fluid Mechanics, Vol. 45, 1971, pp. 477-512.
14. Rajaratnam, N., "The Circular Turbulent Jet," Developments in Water Science, 5, Turbulent Jets, Elsevier Scientific, New York, 1976, pp. 27-49.
15. Abramovich, G.N., The Theory of Turbulent Jets, M.I.T. Press, Cambridge, Mass., 1963.
16. Pai, S., Fluid Dynamics of Jets, D. Van Nostrand, New York, 1954, pp. 96-138.
17. Hinze, J.O., Turbulence, 2nd ed., McGraw-Hill, New York, 1975, pp. 520-585.
18. Schlichting, H., Boundary Layer Theory, 7th ed., McGraw-Hill, New York, 1979, pp. 729-757.
19. Tollmien, W., "Calculation of Turbulent Expansion Processes," NACA TM No. 1085, 1945.
20. Kuethe, A.M., "Investigations of the Turbulent Mixing Regions Formed by Jets," Journal of Applied Mechanics, 1935, pp. 87-95.

21. Tani, I. and Komatsu, Y., "Impingement of a Round Jet on a Flat Surface," Proceedings of the 11th International Congress of Applied Mechanics, Munich, Germany, 1964, pp. 672-676.
22. Beltaos, S., and Rajaratnam, N., "Impinging Circular Turbulent Jets," Proceedings of the ASCE Journal of Hydraulics Division, Vol. 100, 1974, pp. 1313-1328.
23. Bradshaw, P. and Love, E.M., "The Normal Impingement of a Circular Jet on a Flat Plate," Great Britain Aeronautical Research Council, London, Reports and Memoranda No. 3205, 1964
24. Rajaratnam, N., "Axisymmetric Wall Jets," Developments in Water Science, 5, Turbulent Jets, Elsevier Scientific, New York, 1976, pp. 226-245.
25. Glauert, M.B., "The Wall Jet," Journal of Fluid Mechanics, Vol. 1, 1956, pp. 625-643
26. Bakke, P., "An Experimental Investigation of a Wall Jet," Journal of Fluid Mechanics, Vol. 2, 1957, pp. 467-472.
27. Gartshore, I.S. and Newman, B.G., "The Turbulent Wall Jet in an Arbitrary Pressure Gradient," Aeronautical Quarterly, Vol. 20, Feb. 1969, pp. 25-56.
28. Dvorak, F.A., "Calculation of Turbulent Boundary Layers and Wall Jets Over Curved Surfaces," AIAA Journal, Vol. 11, 1973, pp. 517-524.
29. Goertler, H., "Berechnung von Aufgaben der freien Turbulenz auf Grund eines neuen Nherungsansatzes," Zeitschrift fr Angewandte Mathematik und Mechanik, Vol. 22, 1942, pp. 244-254.
30. Hinze, J.O. and Zijnen, B.G. Van der Hegge, "Transfer of Heat and Matter in the Turbulent Mixing Zone of an Axially Symmetrical Jet," Journal of Applied Scientific Research, Vol. A1, pp. 435-461.

31. Corrsin, S., "Investigation of Flow in an Axially Symmetric Heated Jet of Air," NACA Wartime Report, W-94, 1946.

APPENDIX**FIGURES 39 THROUGH 126**

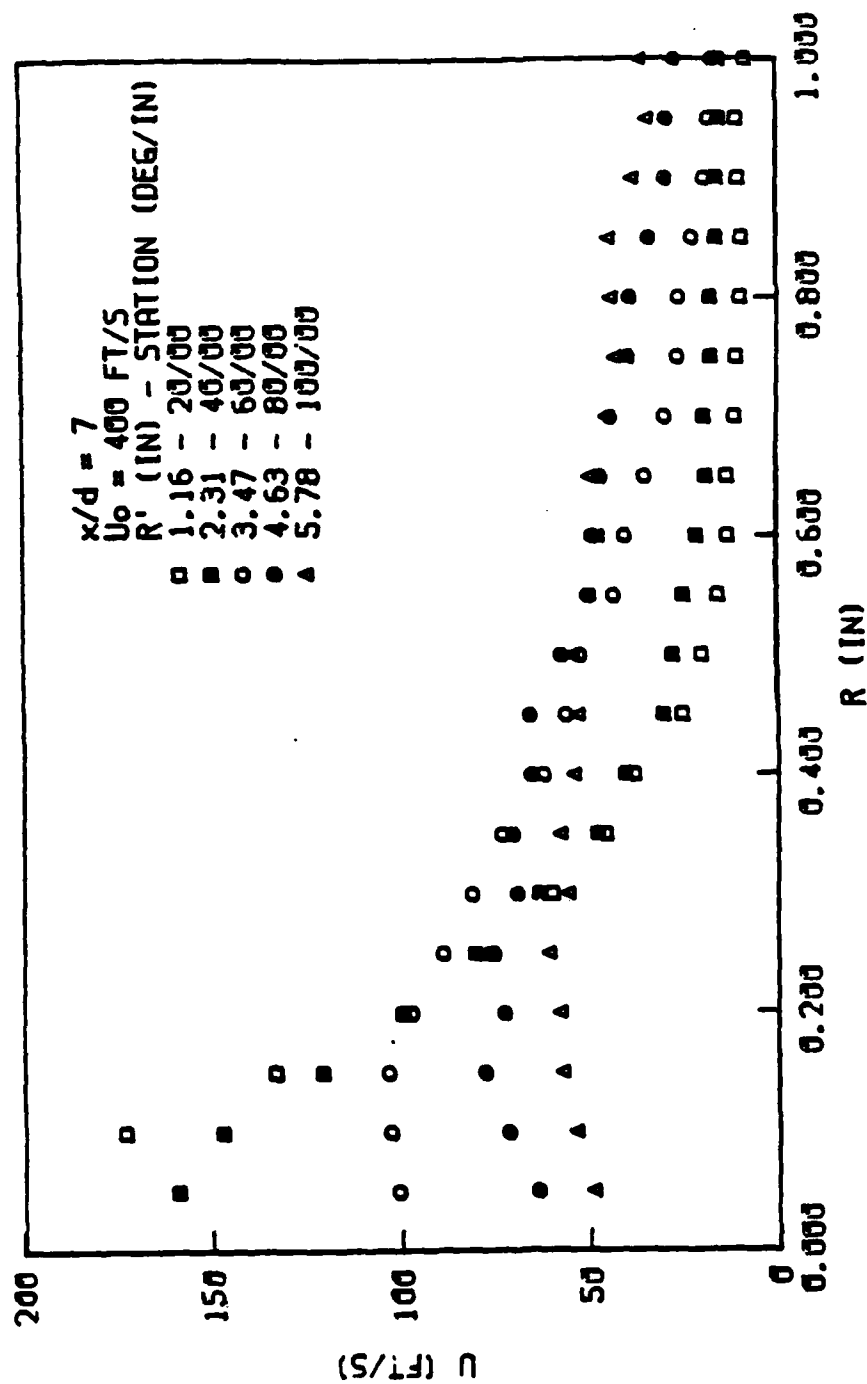


Fig. 39 Wall jet velocity profile for $U_0 = 400 \text{ ft/s}$, $x/d = 7$ (circumferential radial).

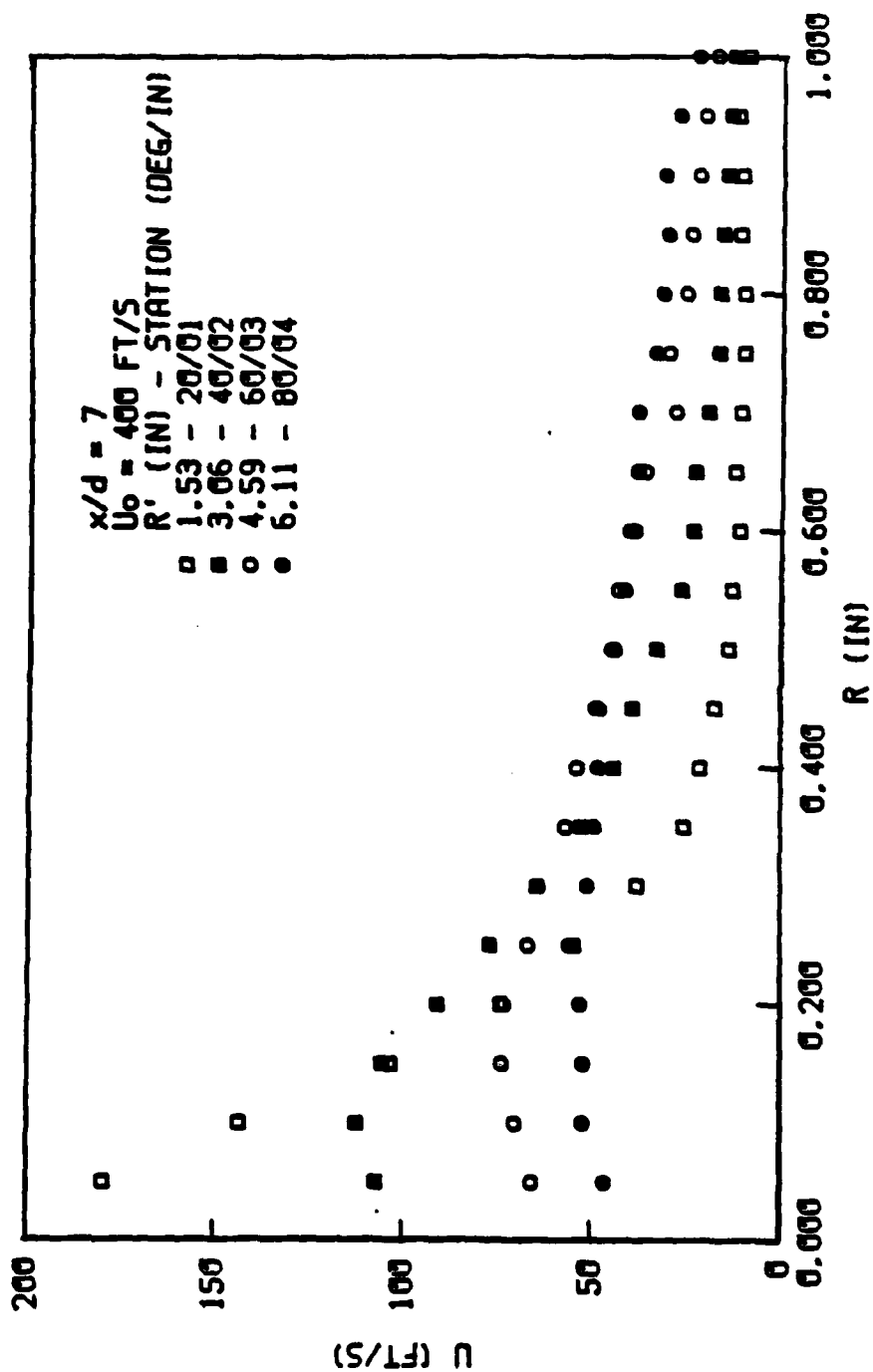


Fig. 40 Wall jet velocity profile for $U_0 = 400 \text{ ft/s}$, $x/d = 7$ (radial 2).

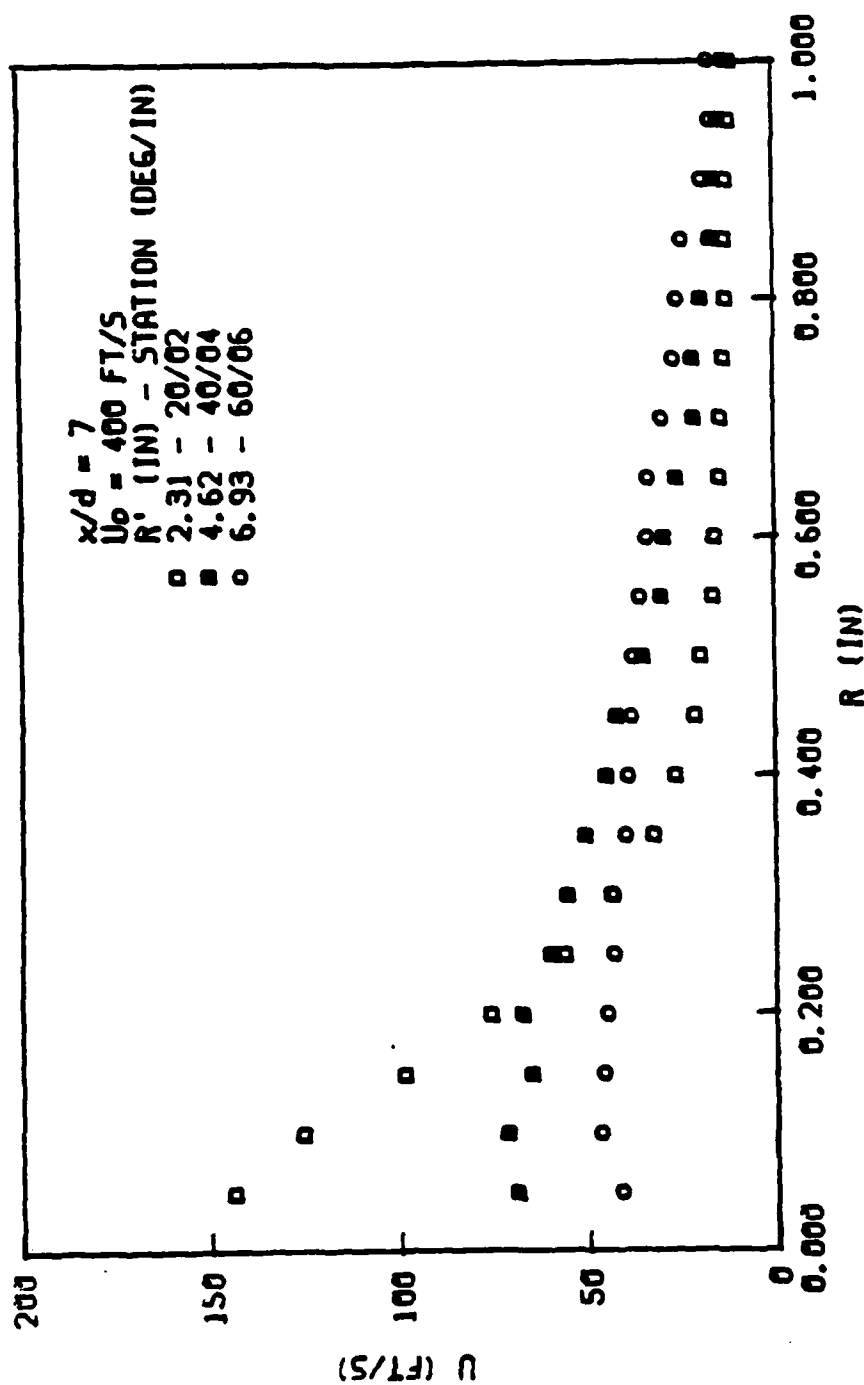


Fig. 41 Wall jet velocity profile for $U_0 = 400 \text{ ft/s}$, $x/d = 7$ (radial 4).

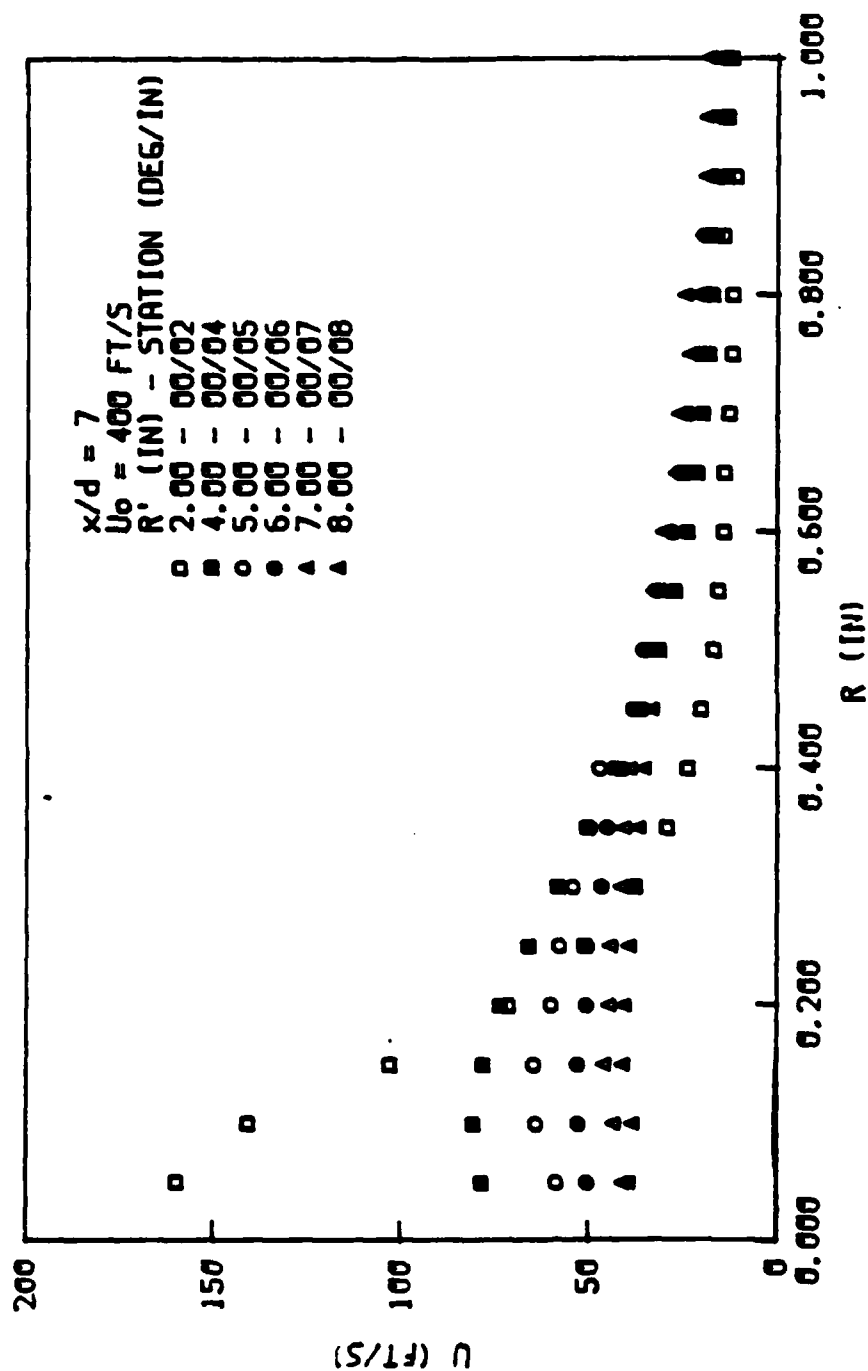


Fig. 42 Wall jet velocity profile for $U_o = 400 \text{ ft/s}$, $x/d = 7$ (axial radial).

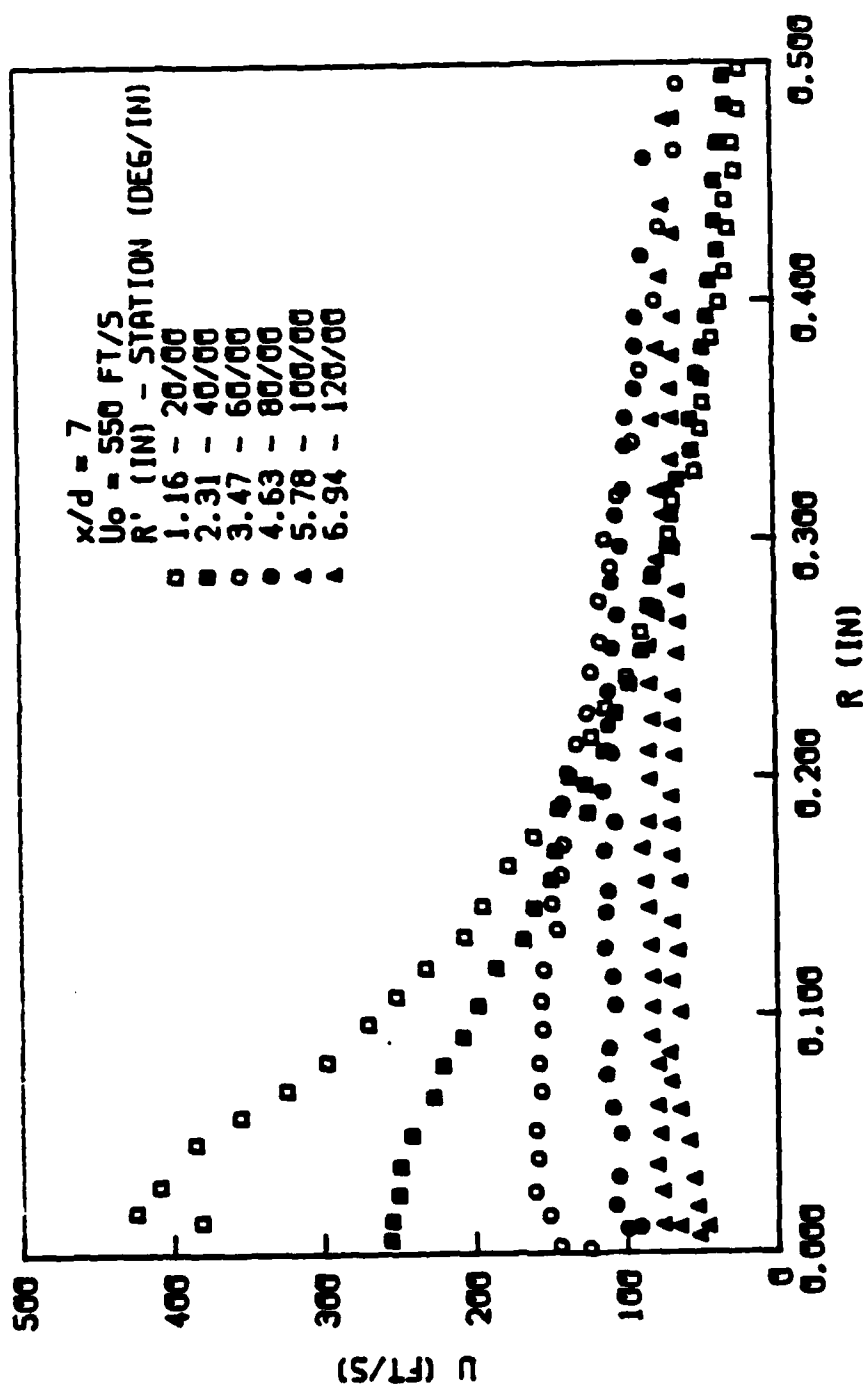


Fig. 43 Wall jet velocity profile for $U_o = 550 \text{ ft/s}$, $x/d = 7$ (circumferential radial).

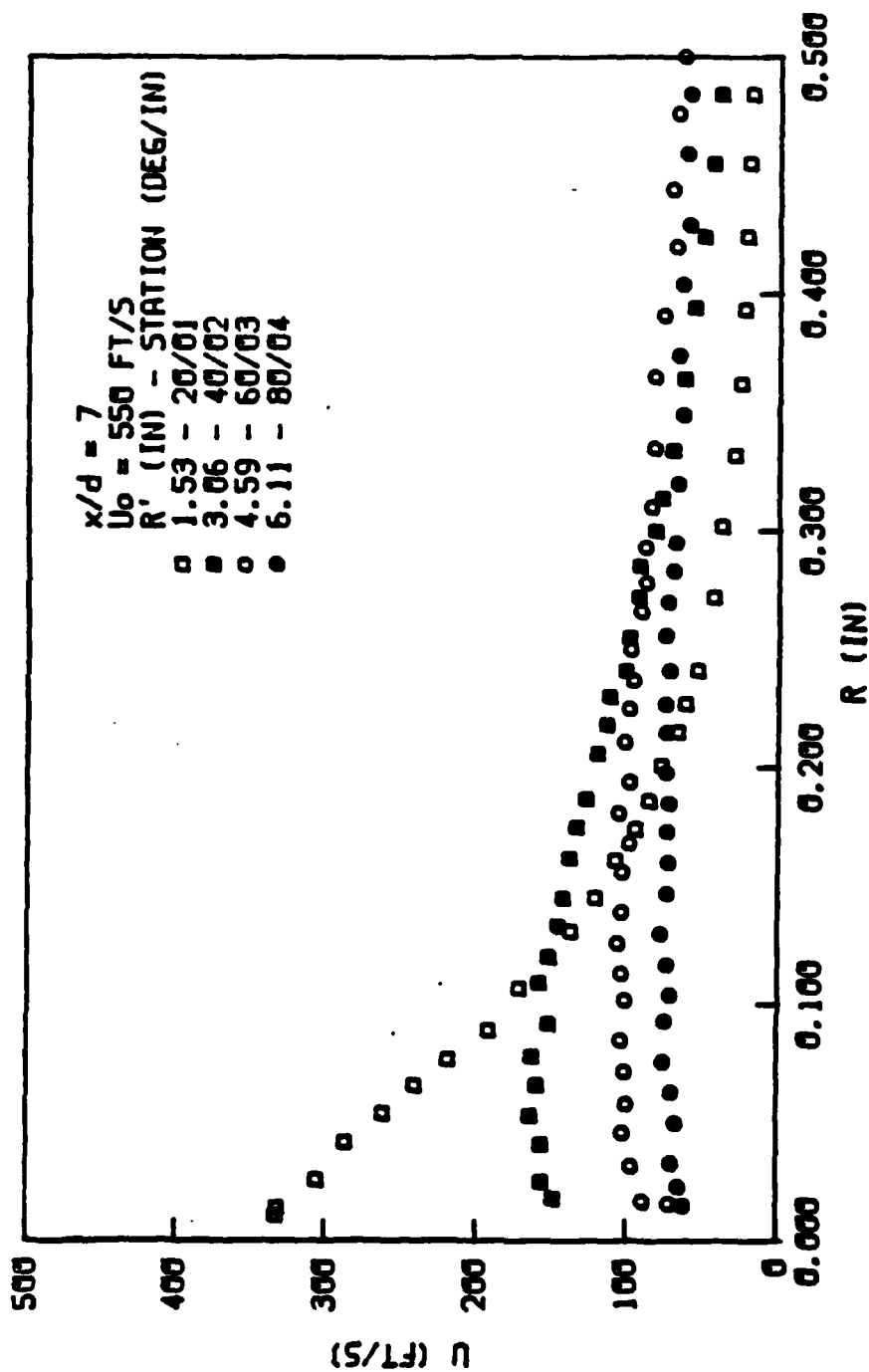


Fig. 44 Wall jet velocity profile for $U_0 = 550 \text{ ft/s}$, $x/d = 7$ (radial 2).

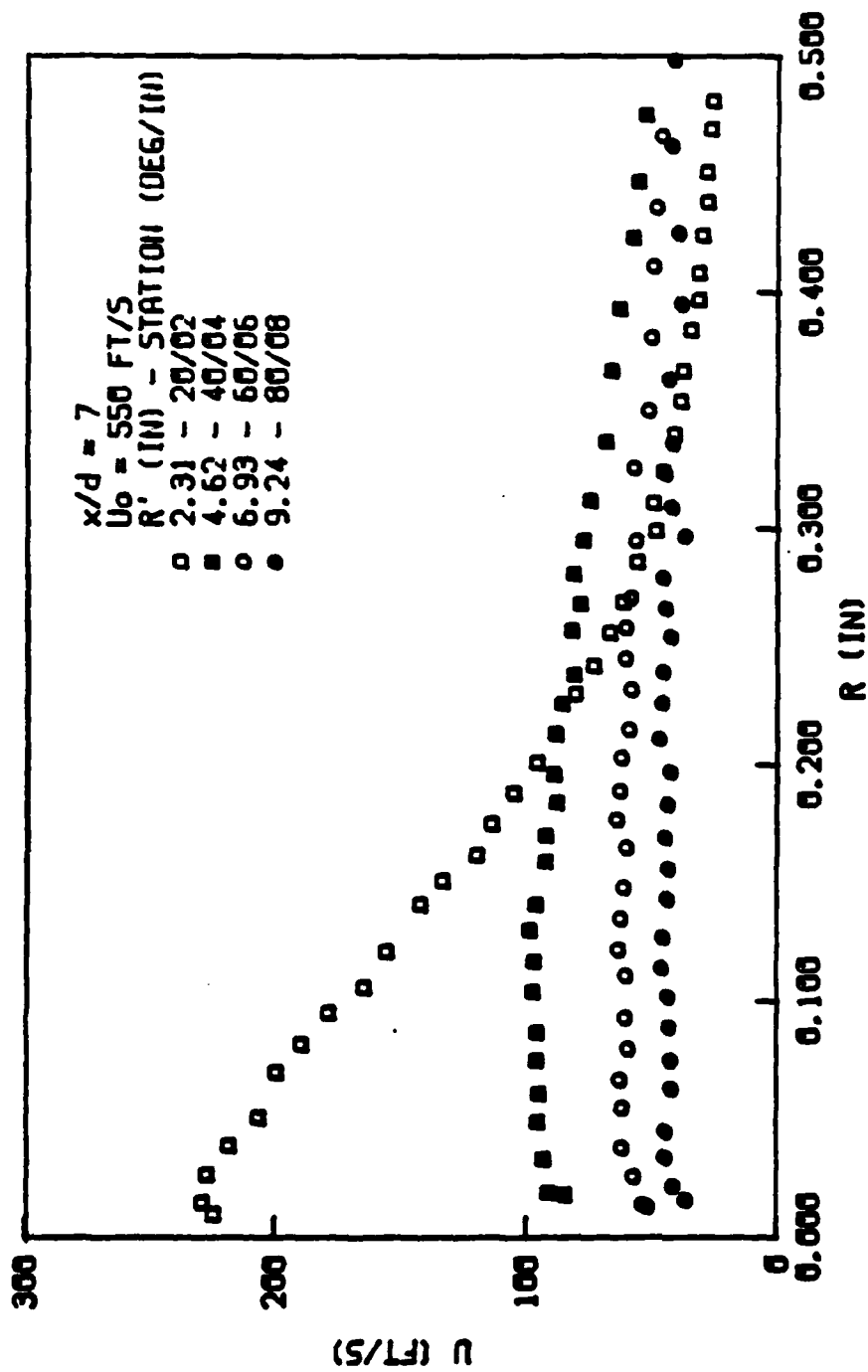


Fig. 45 Wall jet velocity profile for $U_0 = 550 \text{ ft/s}$, $x/d = 7$ (radial 4).

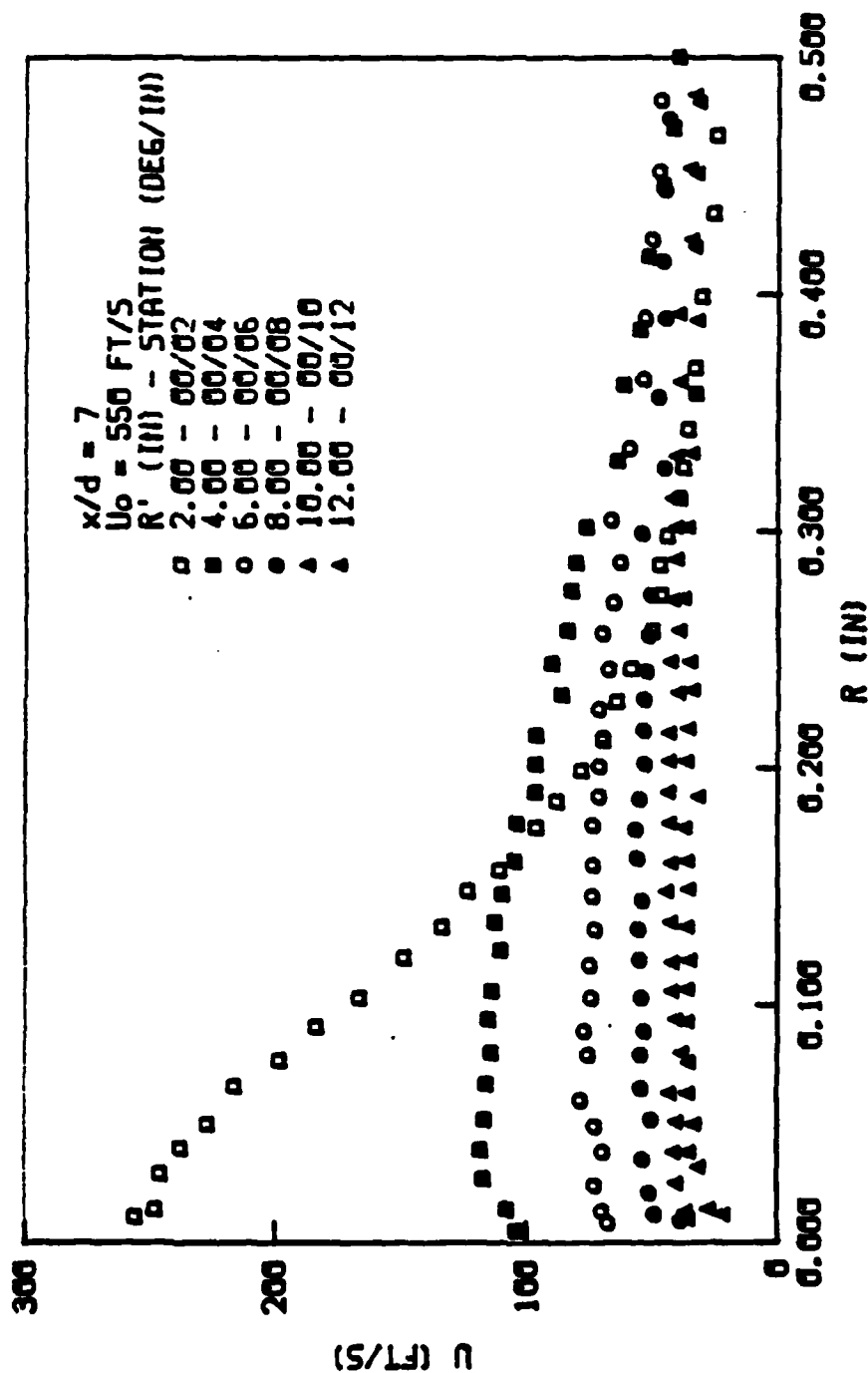


Fig. 46 Wall jet velocity profile for $U_0 = 550 \text{ ft/s}$, $x/d = 7$ (axial radial).

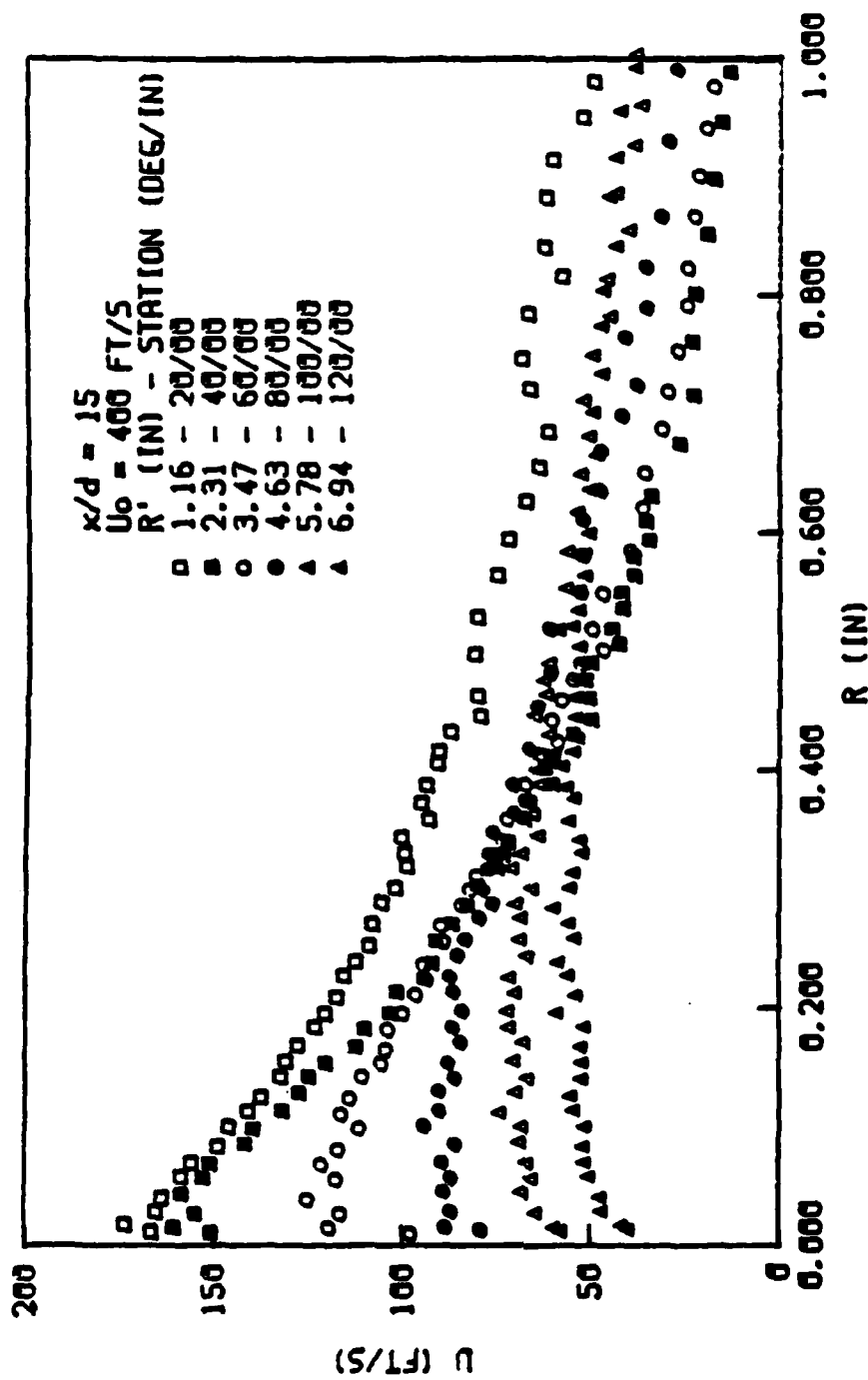


Fig. 47 Wall jet velocity profile for $U_0 = 400 \text{ ft/s}$, $x/d = 15$ (circumferential radial).

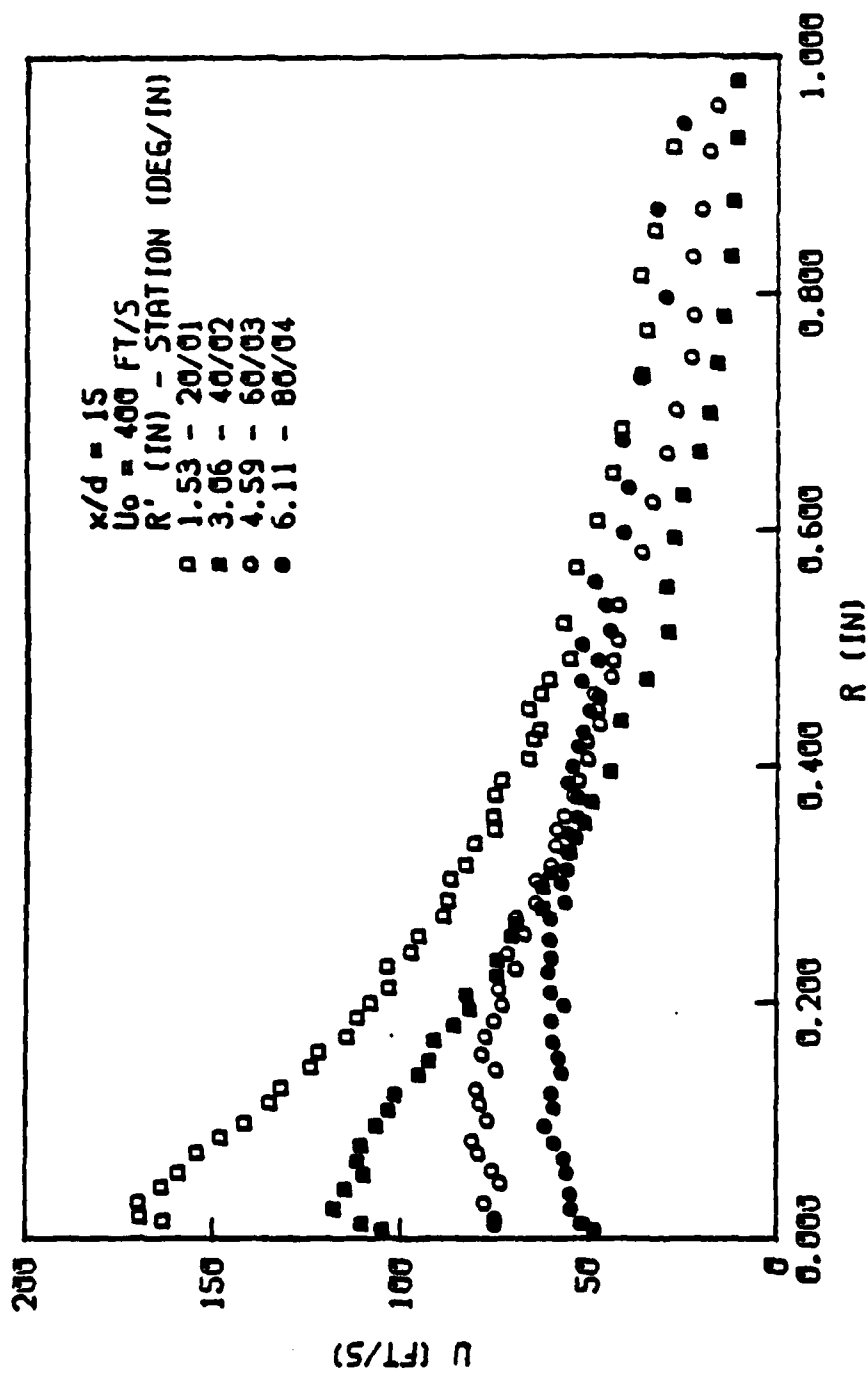


Fig. 48 Wall jet velocity profile for $U_o = 400 \text{ ft/s}$, $x/d = 15$ (radial 2).

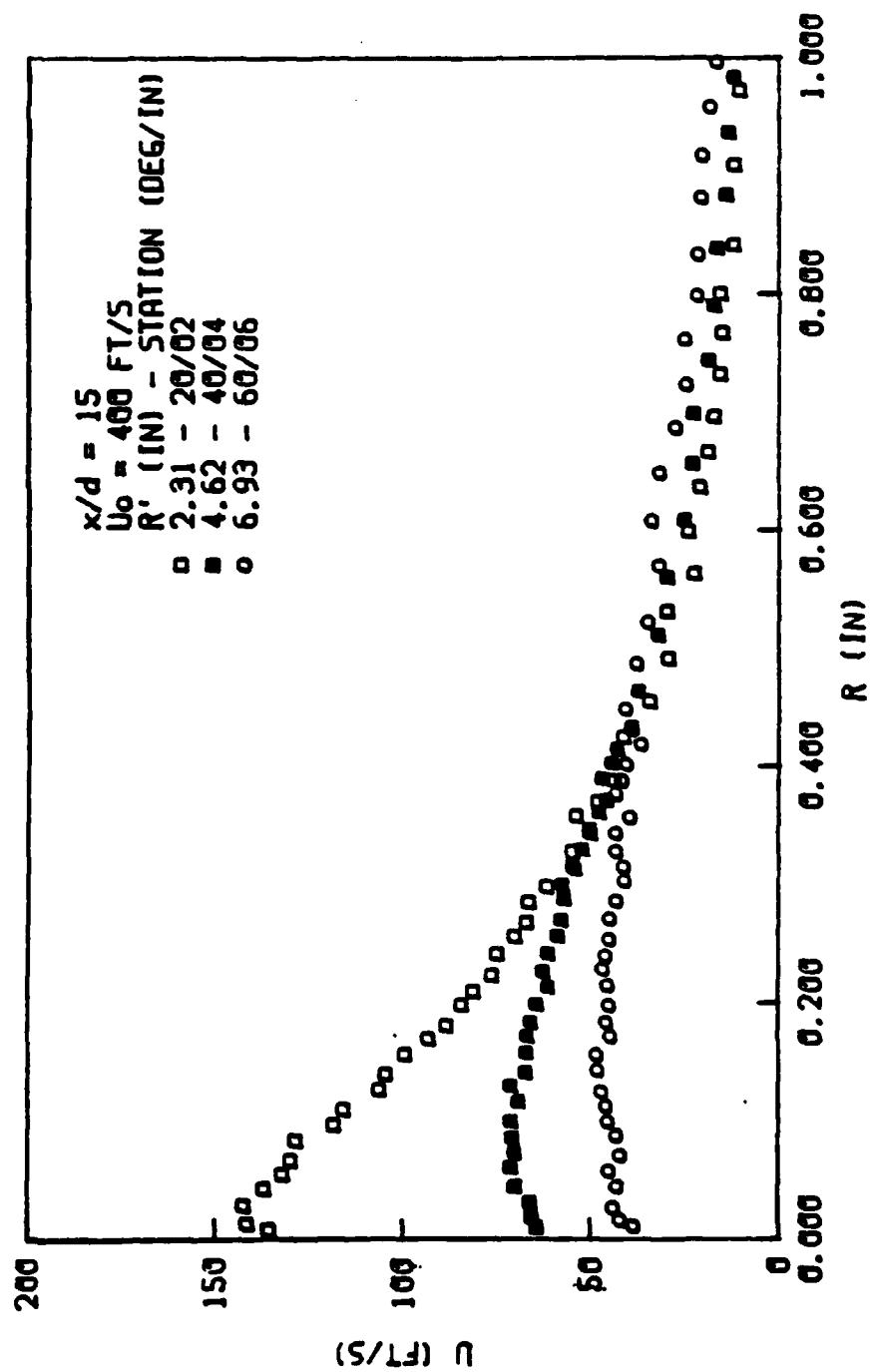


Fig. 49 Wall jet velocity profile for $U_0 = 400 \text{ ft/s}$, $x/d = 15$ (radial 4).

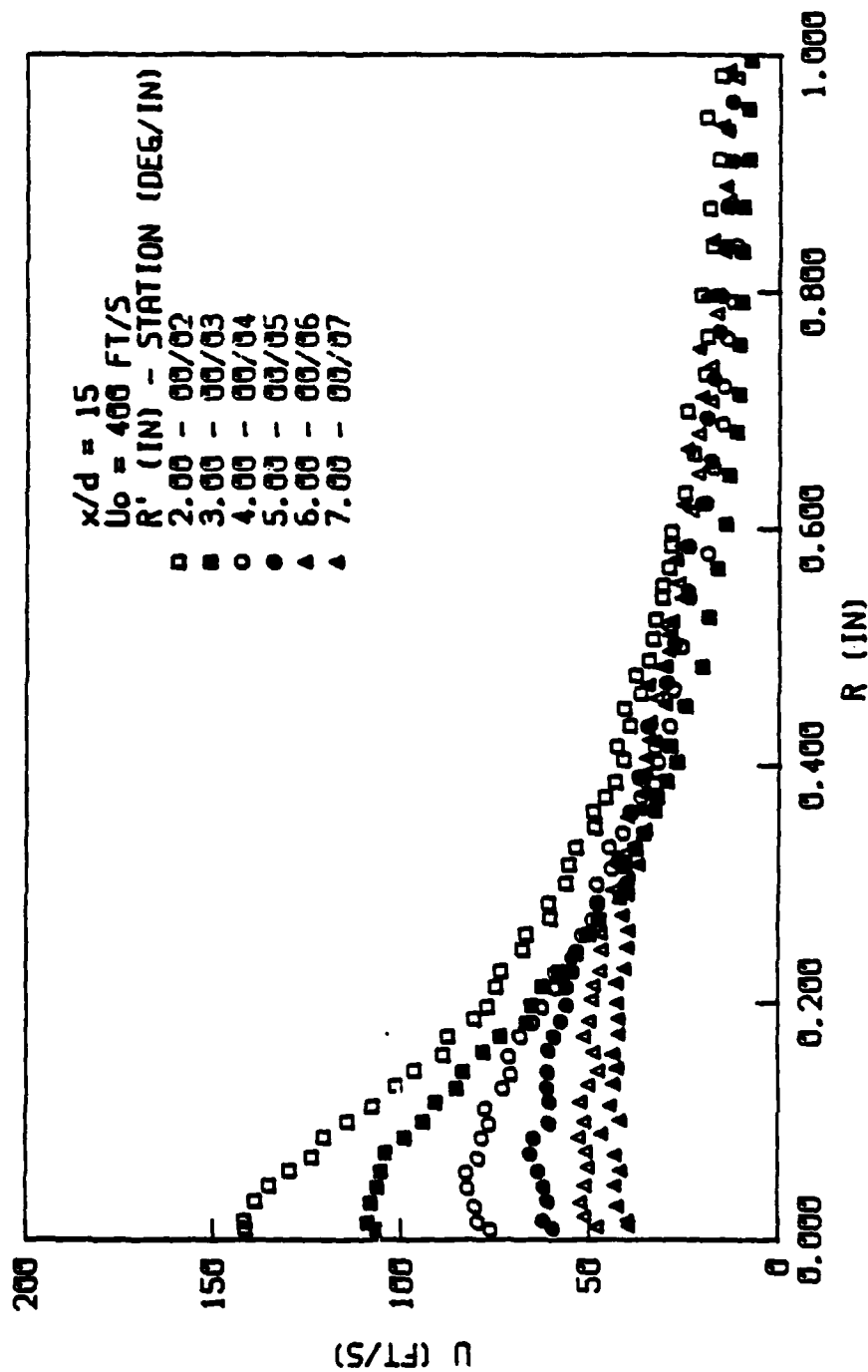


Fig. 50 Wall jet velocity profile for $U_o = 400$ ft/s, $x/d = 15$ (axial radial).

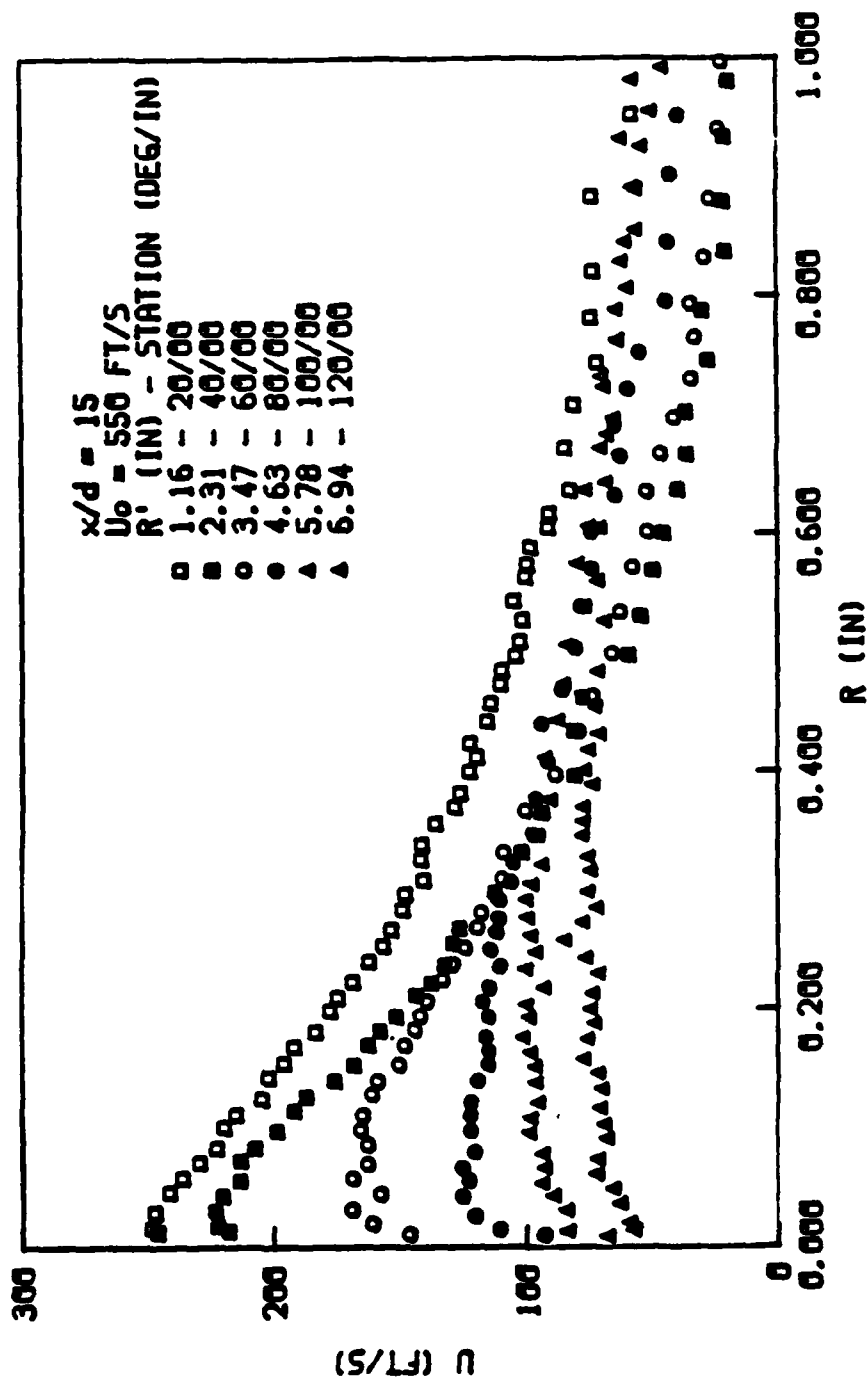


Fig. 51 Wall jet velocity profile for $U_0 = 550 \text{ ft/s}$, $x/d = 15$ (circumferential radial).

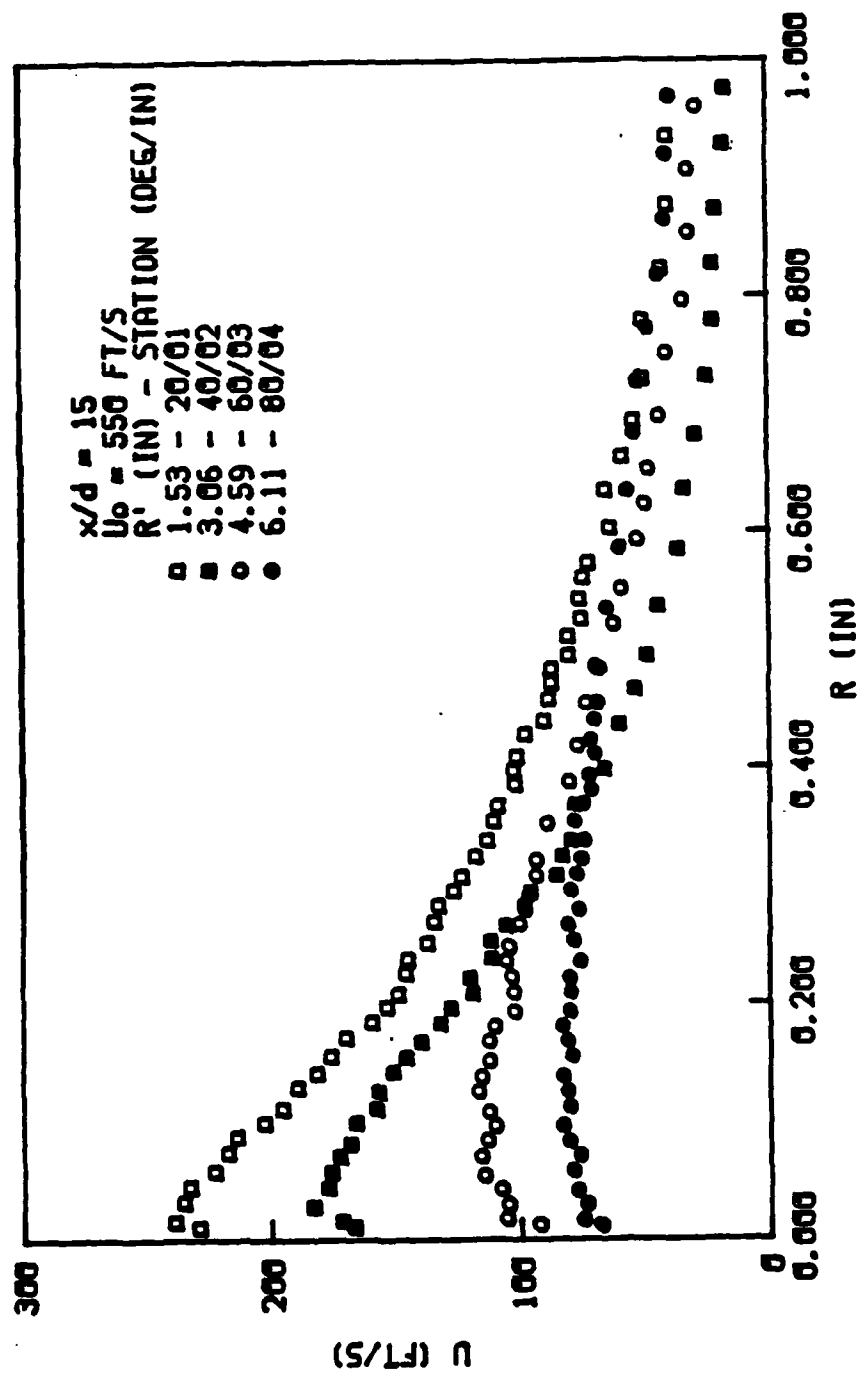


FIG. 52 Wall jet velocity profile for $U_0 = 550 \text{ ft/s}$, $x/d = 15$ (radial 2).

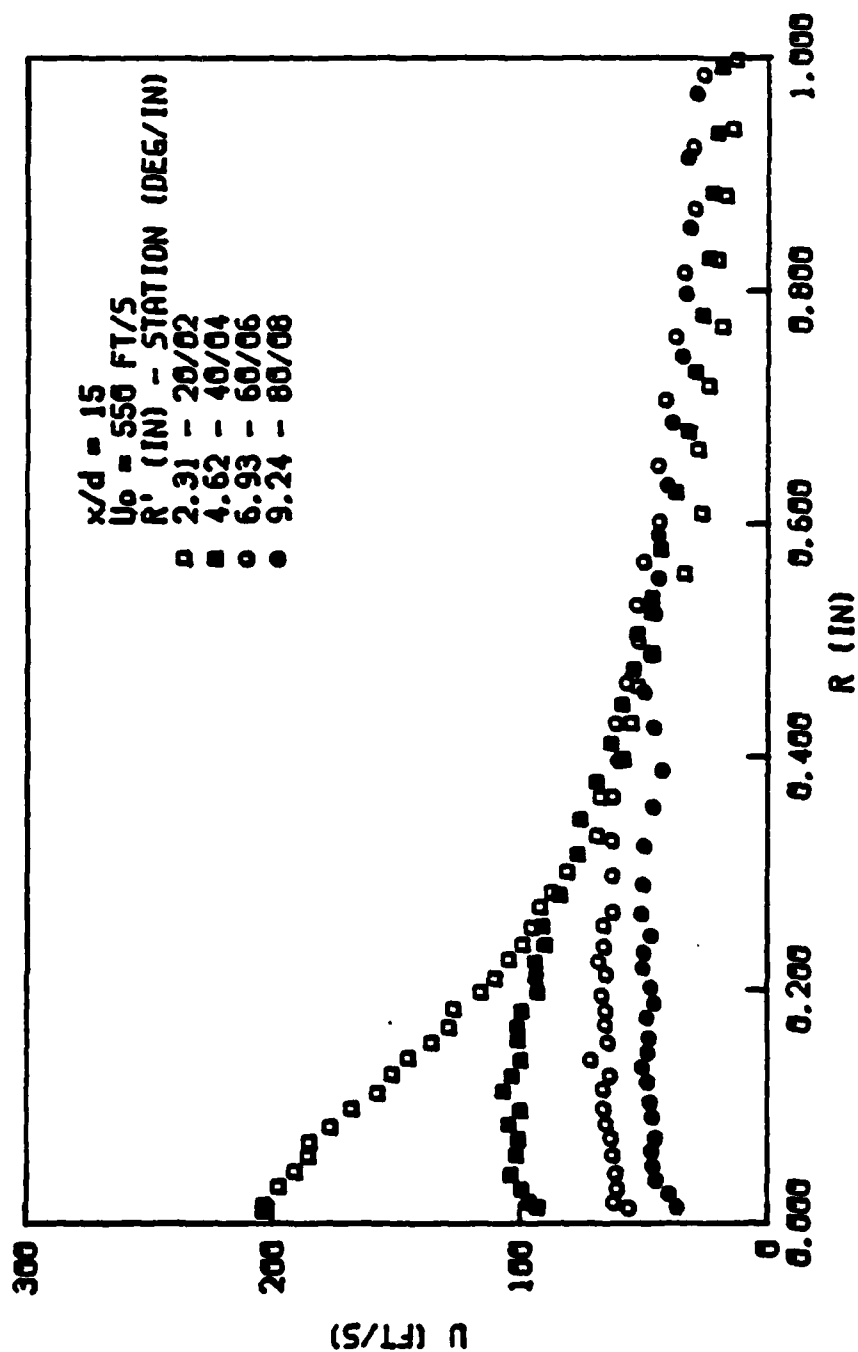


Fig. 53 Wall jet velocity profile for $U_o = 550 \text{ ft/s}$, $x/d = 15$ (radial 4).

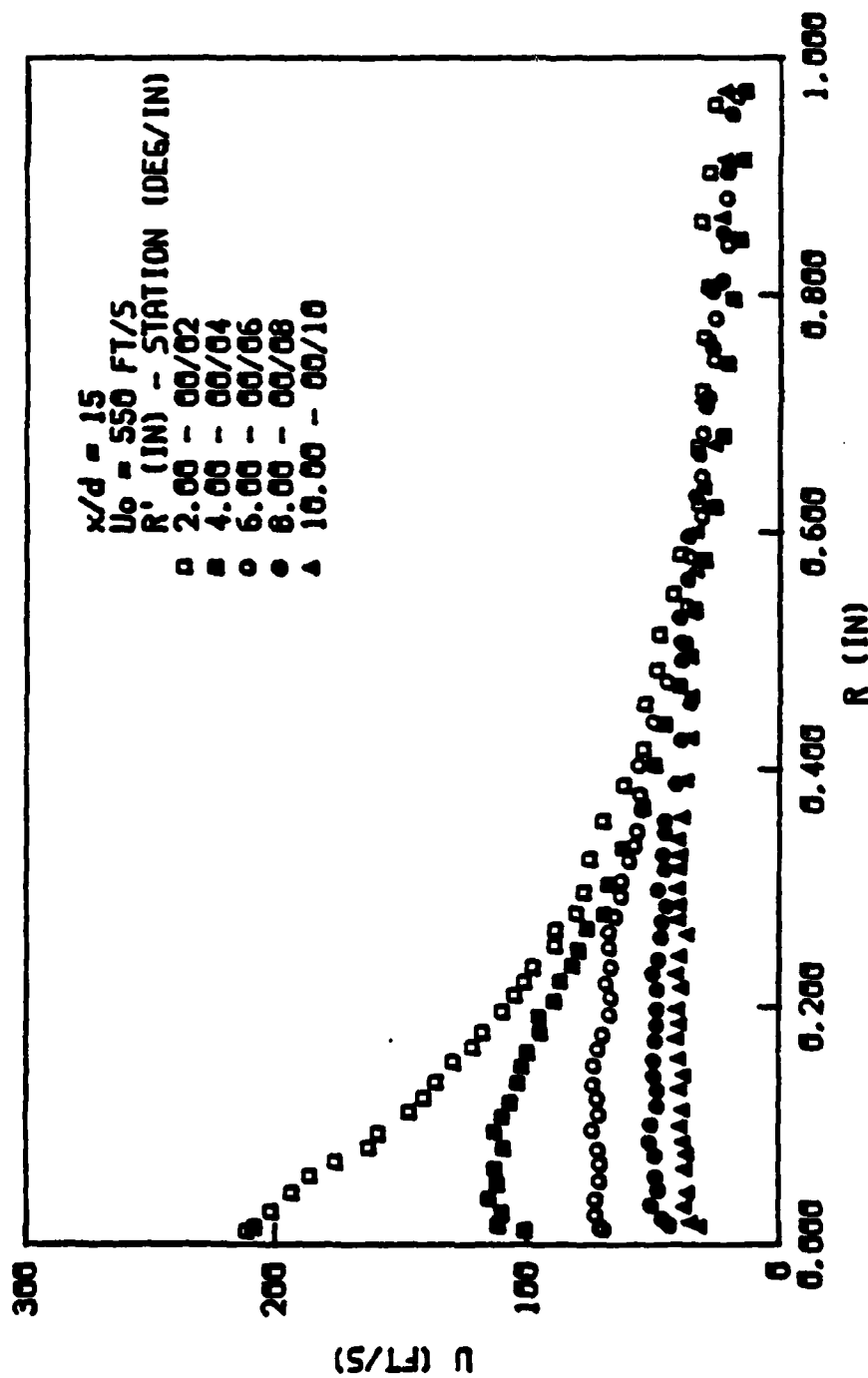


Fig. 54 Wall jet velocity profile for $U_0 = 550 \text{ ft/s}$, $x/d = 15$ (axial radial).

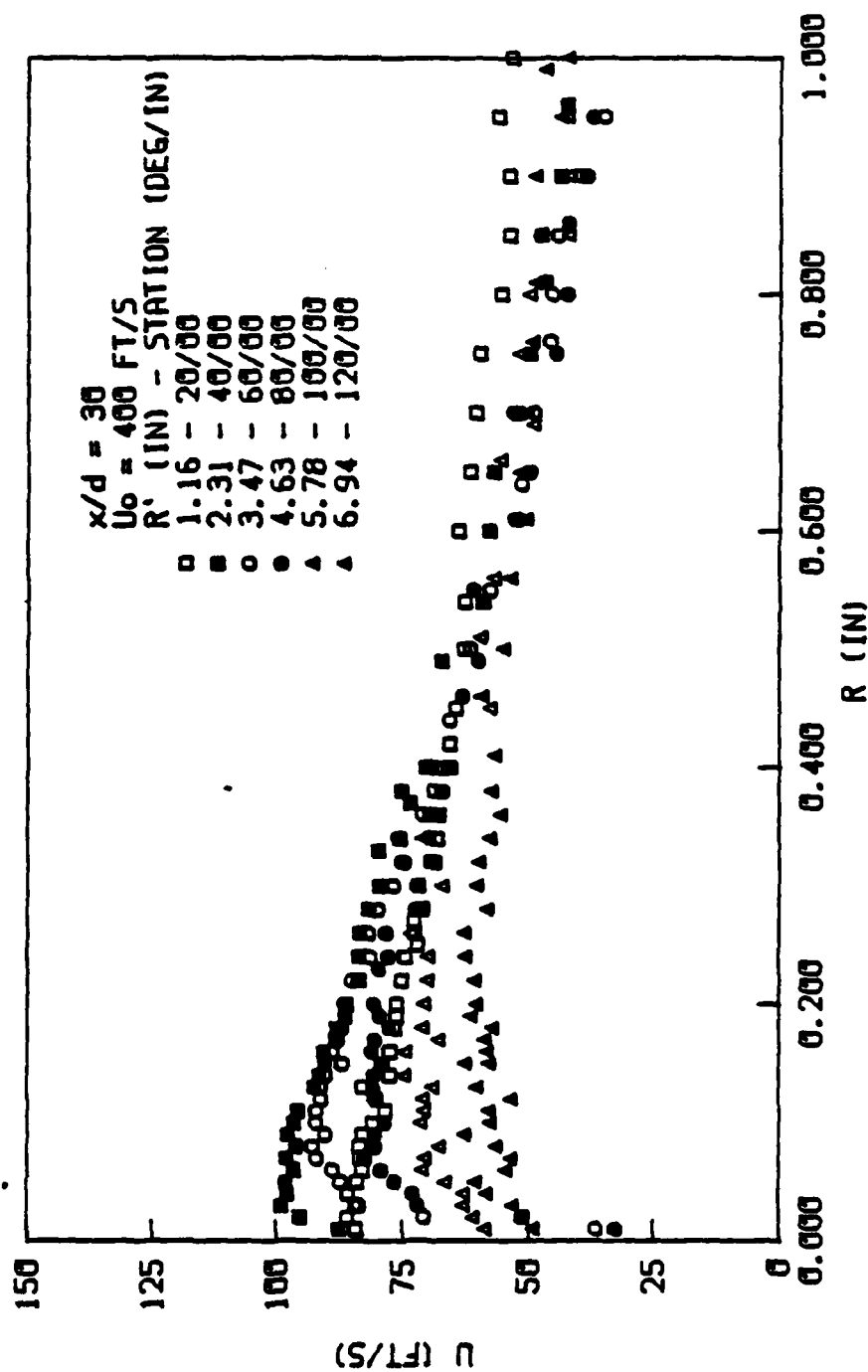


Fig. 55 Wall jet velocity profile for $U_0 = 400 \text{ ft/s}$, $x/d = 30$ (circumferential radial).

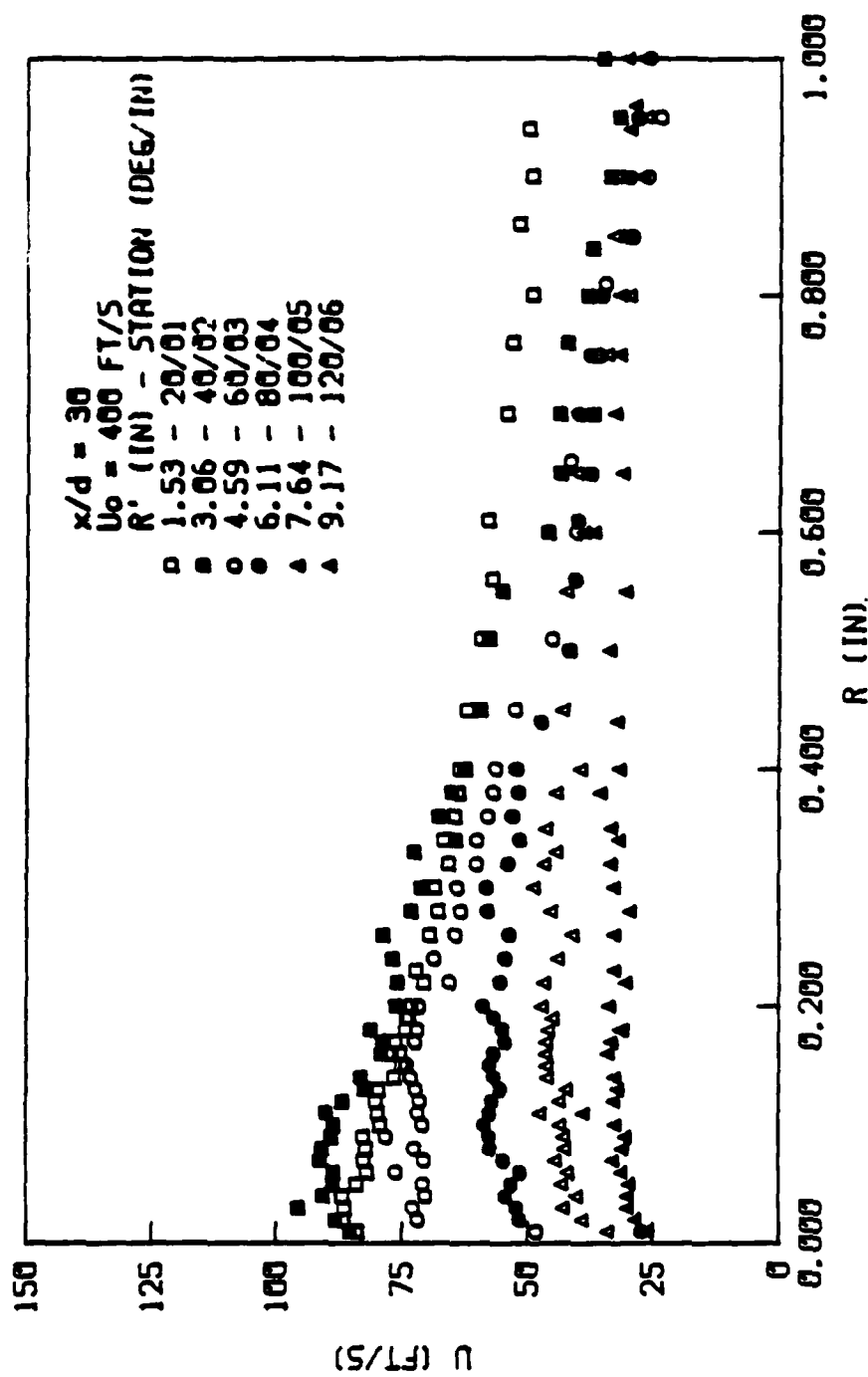


Fig. 56 Wall jet velocity profile for $U_o = 400 \text{ ft/s}$, $x/d = 30$ (radial 2).

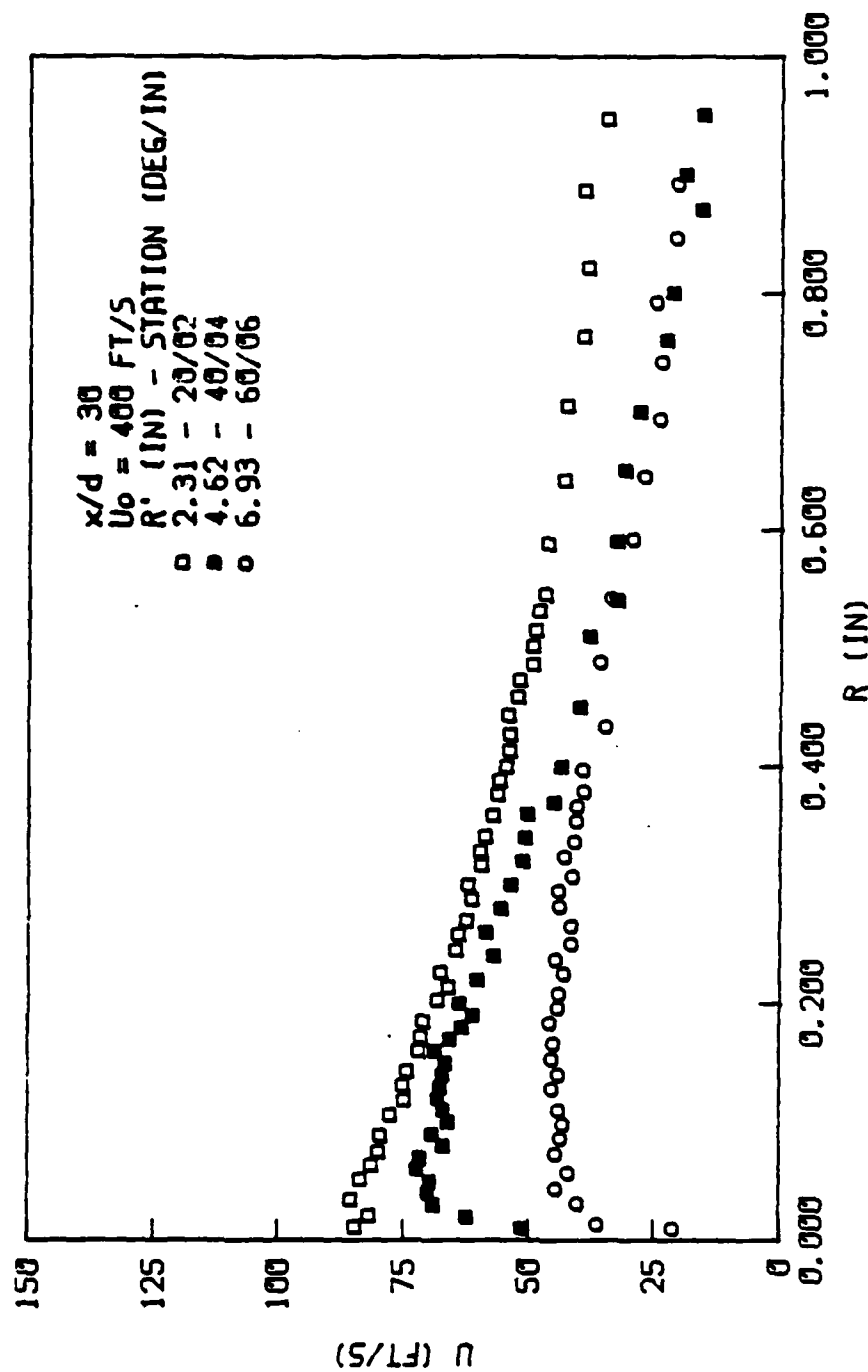


Fig. 57 Wall jet velocity profile for $U_0 = 400 \text{ ft/s}$, $x/d = 30$ (radial 4).

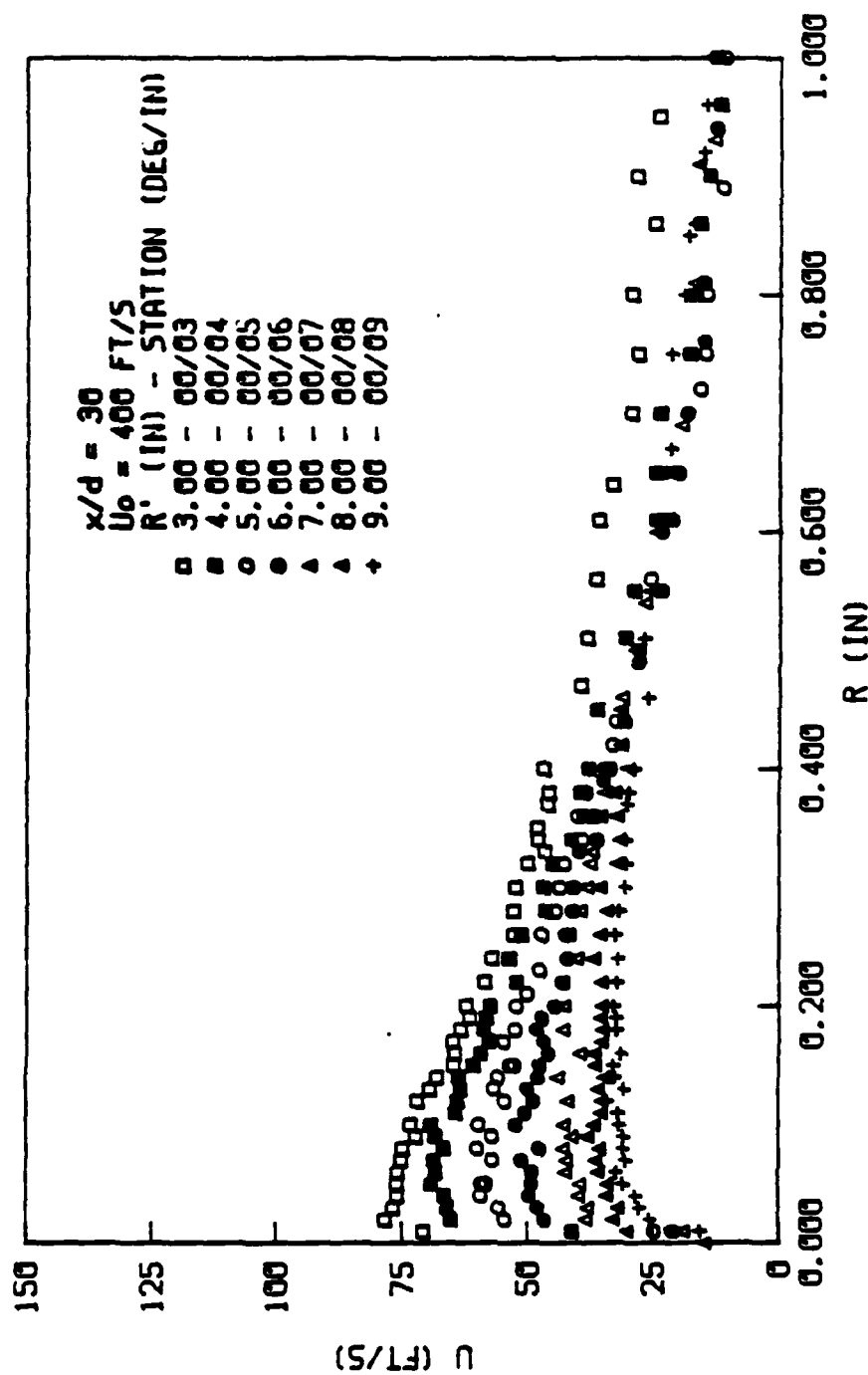


Fig. 53 Wall jet velocity profile for $U_0 = 400 \text{ ft/s}$, $x/d = 30$ (axial radial).

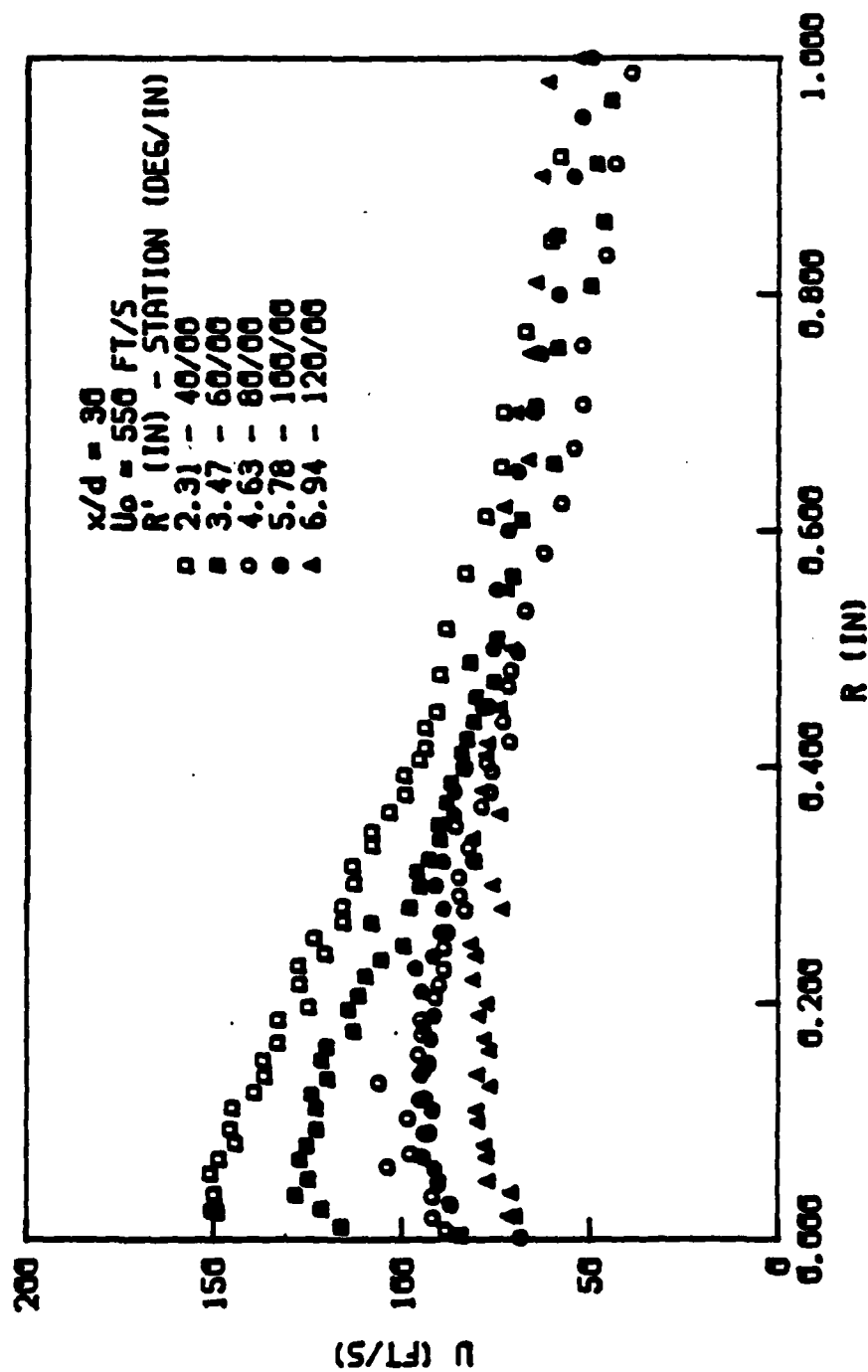


Fig. 59 Wall jet velocity profile for $U_0 = 550 \text{ ft/s}$, $x/d = 30$ (circumferential radial).

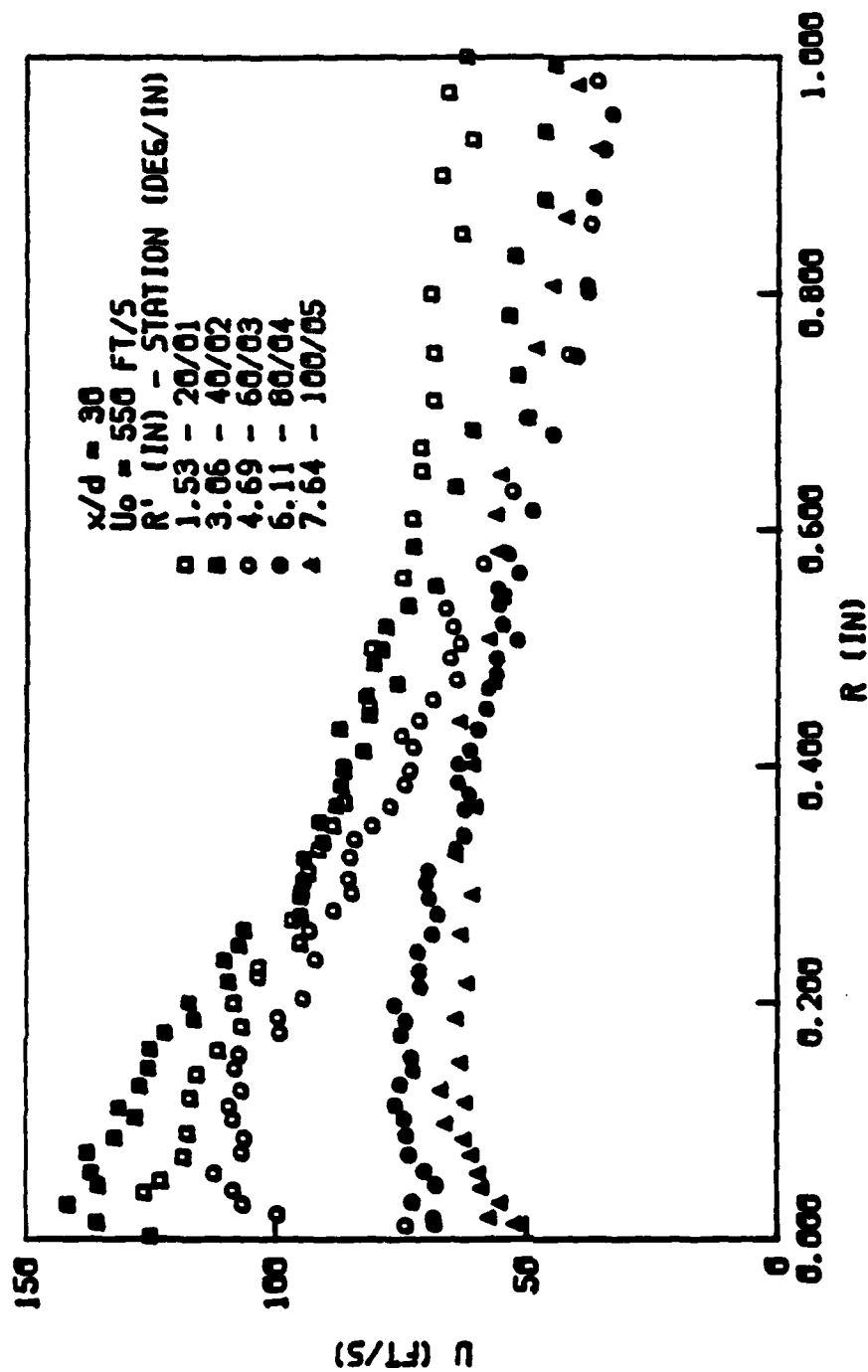


Fig. 60 Wall jet velocity profile for $U_o = 550 \text{ ft/s}$, $x/d = 30$ (radial 2).

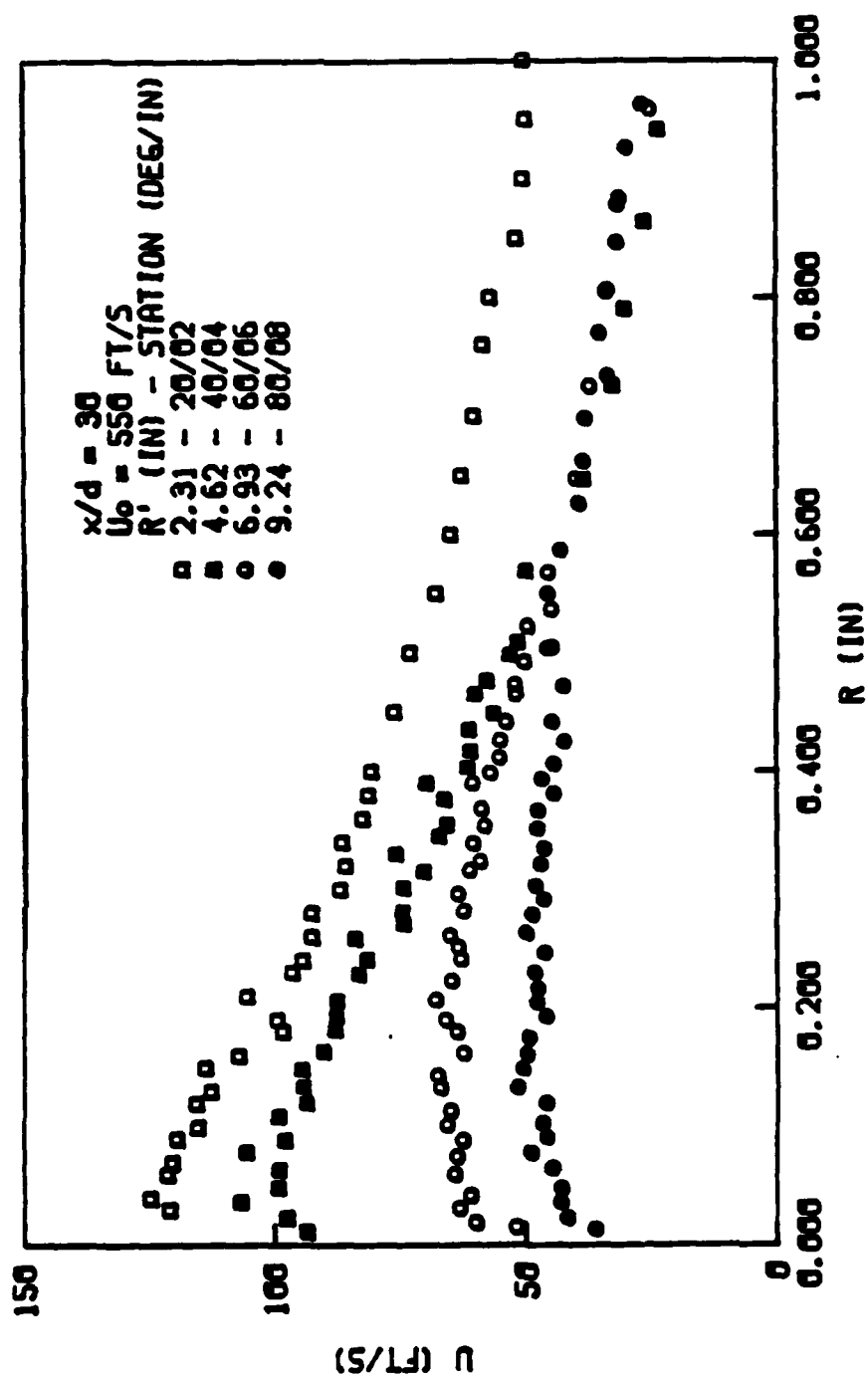


Fig. 61 Wall jet velocity profile for $U_0 = 550 \text{ ft/s}$, $x/d = 30$ (radial 4).

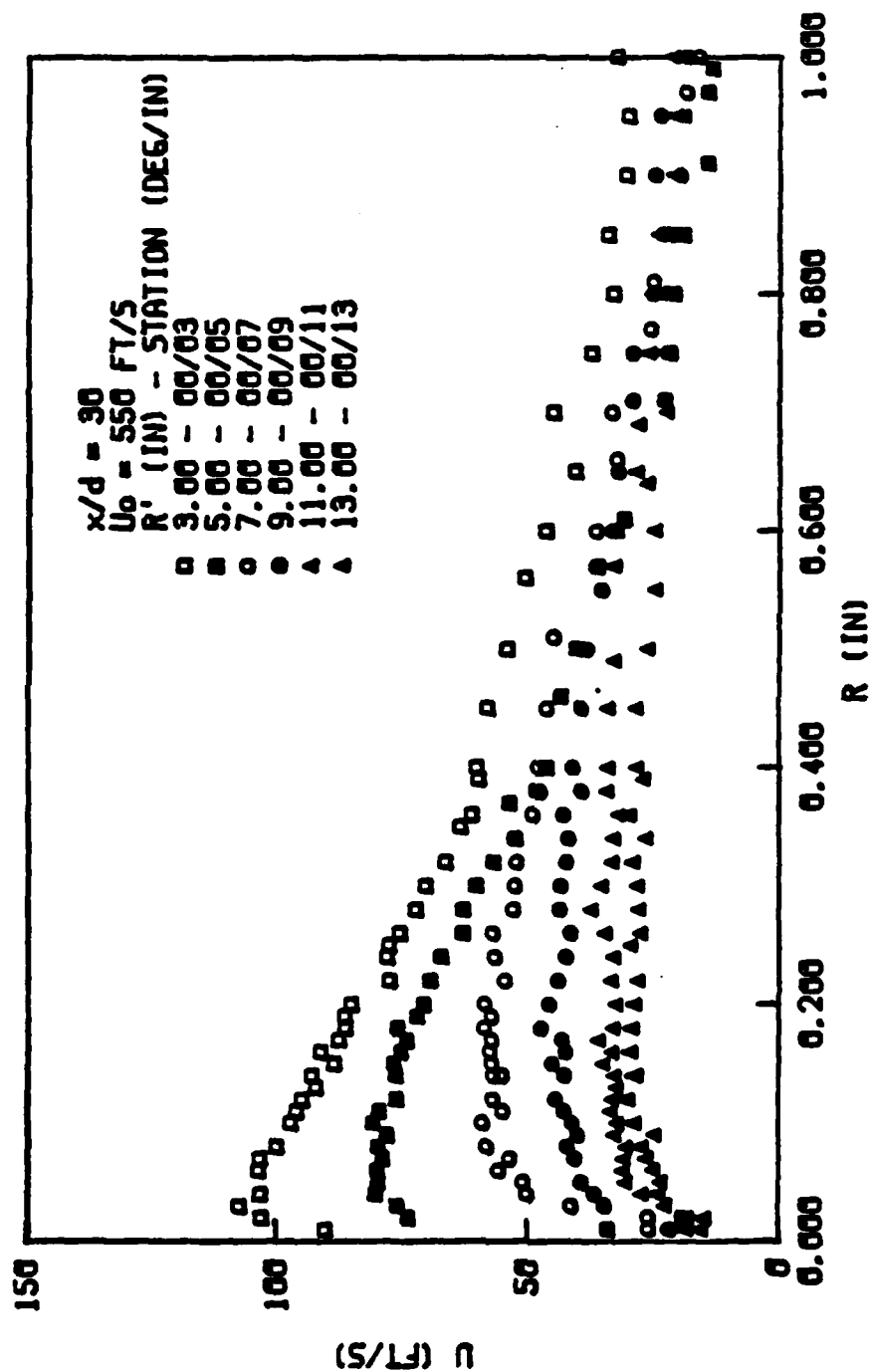


Fig. 62 Wall jet velocity profile for $U_0 = 550 \text{ ft/s}$, $x/d = 30$ (axial radial).

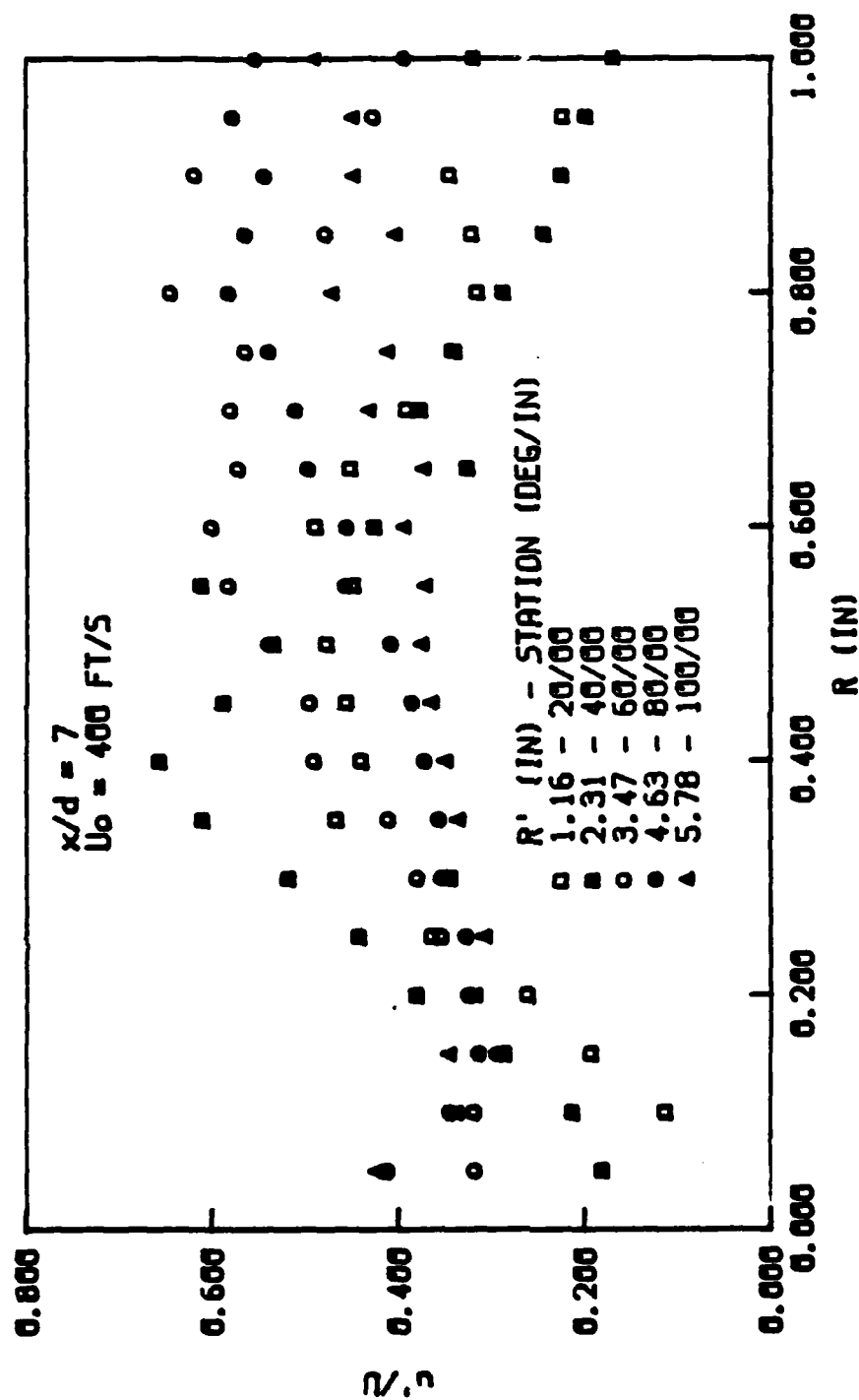


Fig. 63 Wall jet turbulence profile for $U_0 = 400 \text{ ft/s}$, $x/d = 7$ (circumferential radial).

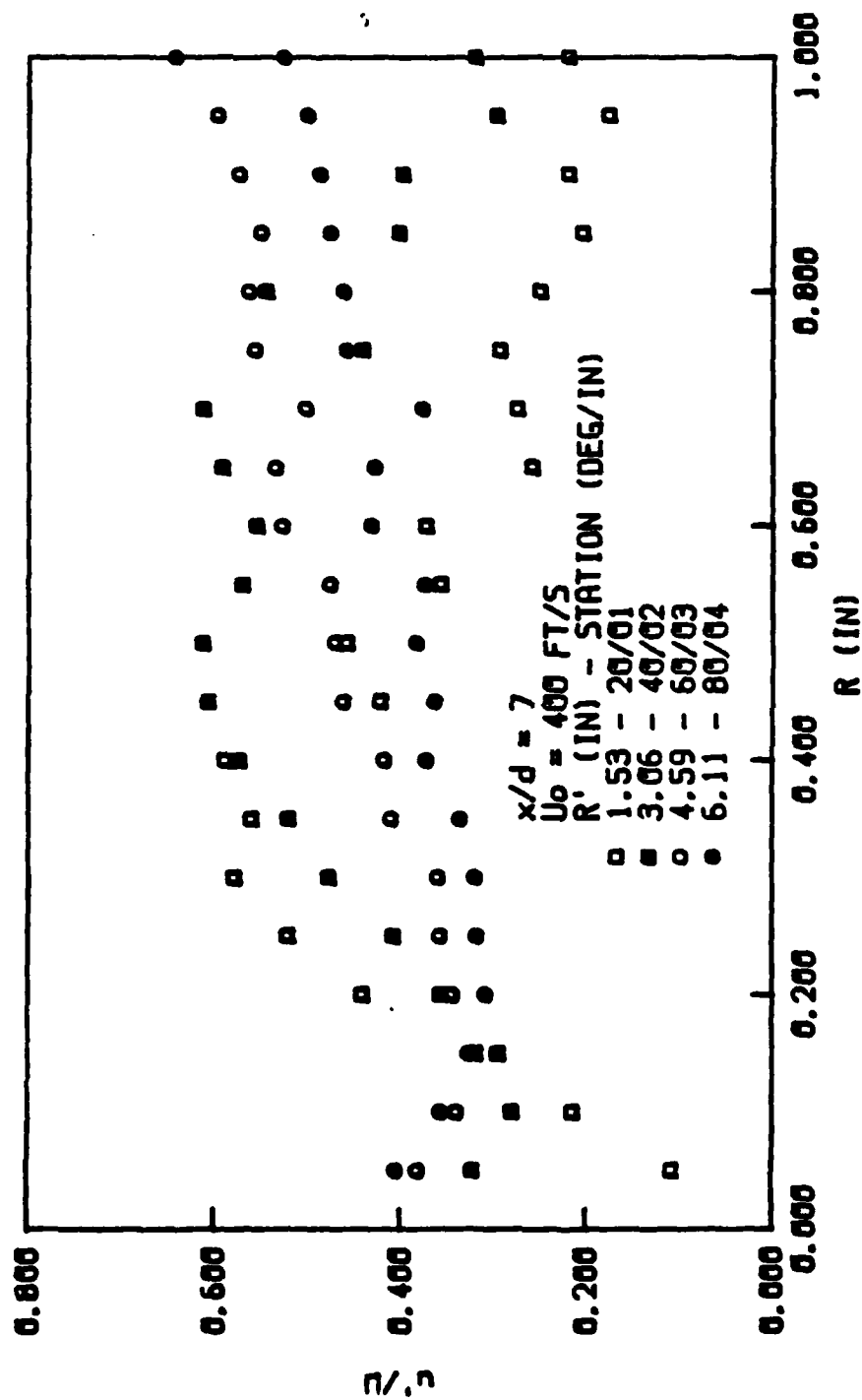


Fig. 64 Wall jet turbulence profile for $U_0 = 400 \text{ ft/s}$, $x/d = 7$ (radial 2).

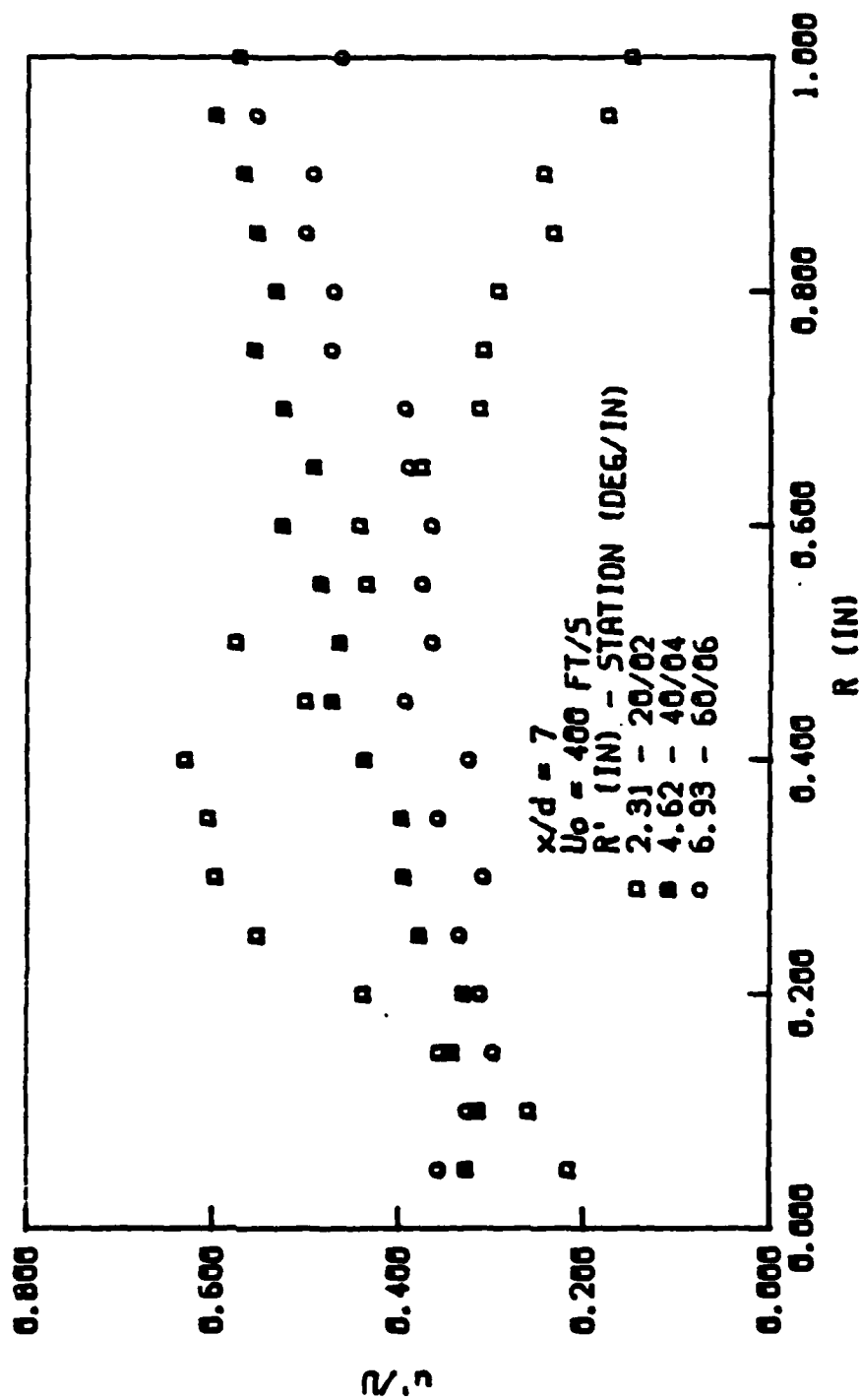


Fig. 65 Wall jet turbulence profile for $U_0 = 400 \text{ ft/s}$, $x/d = 7$ (radial 4).

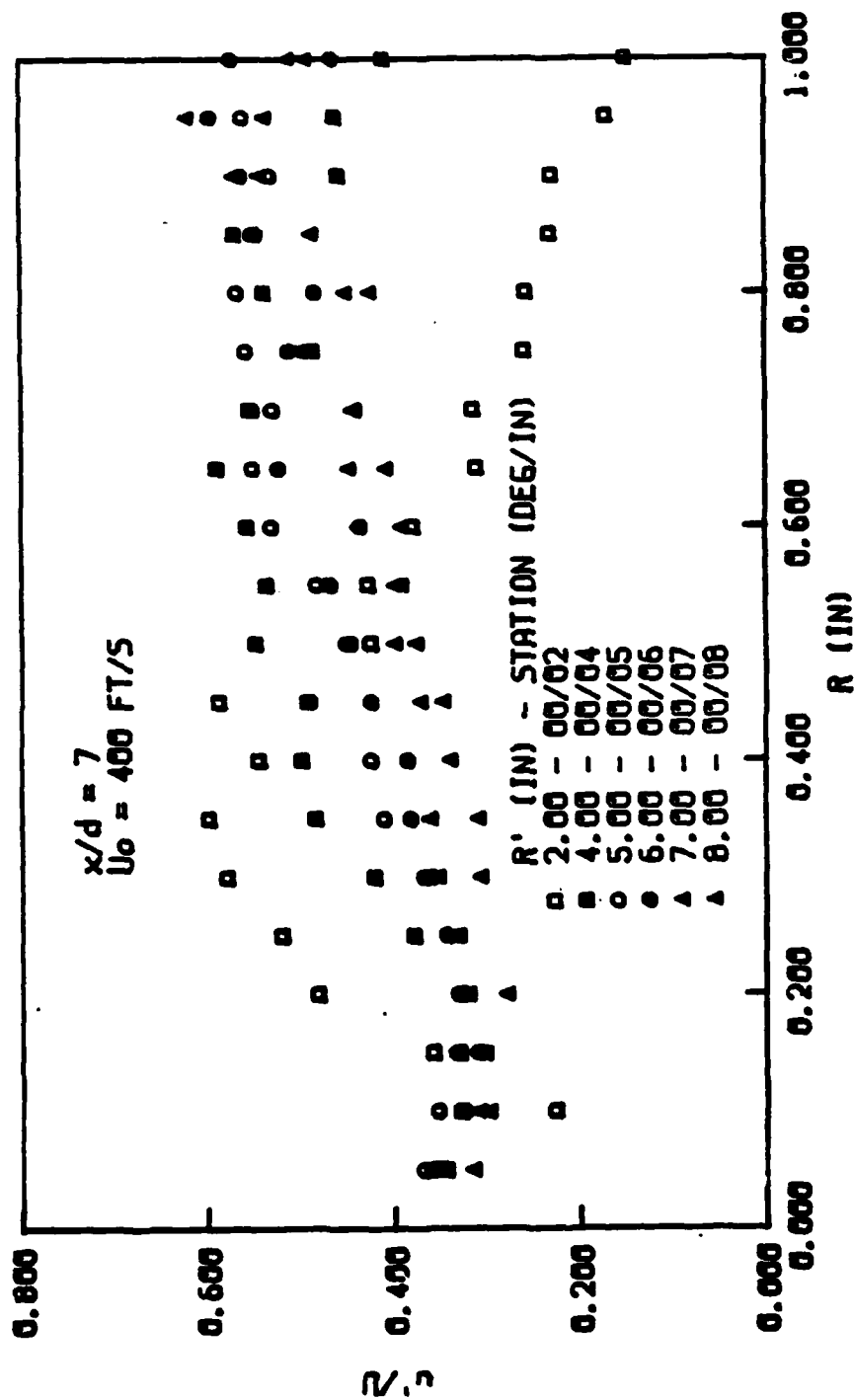


Fig. 66 Wall jet turbulence profile for $U_0 = 400 \text{ ft/s}$, $x/d = 7$ (axial radial).

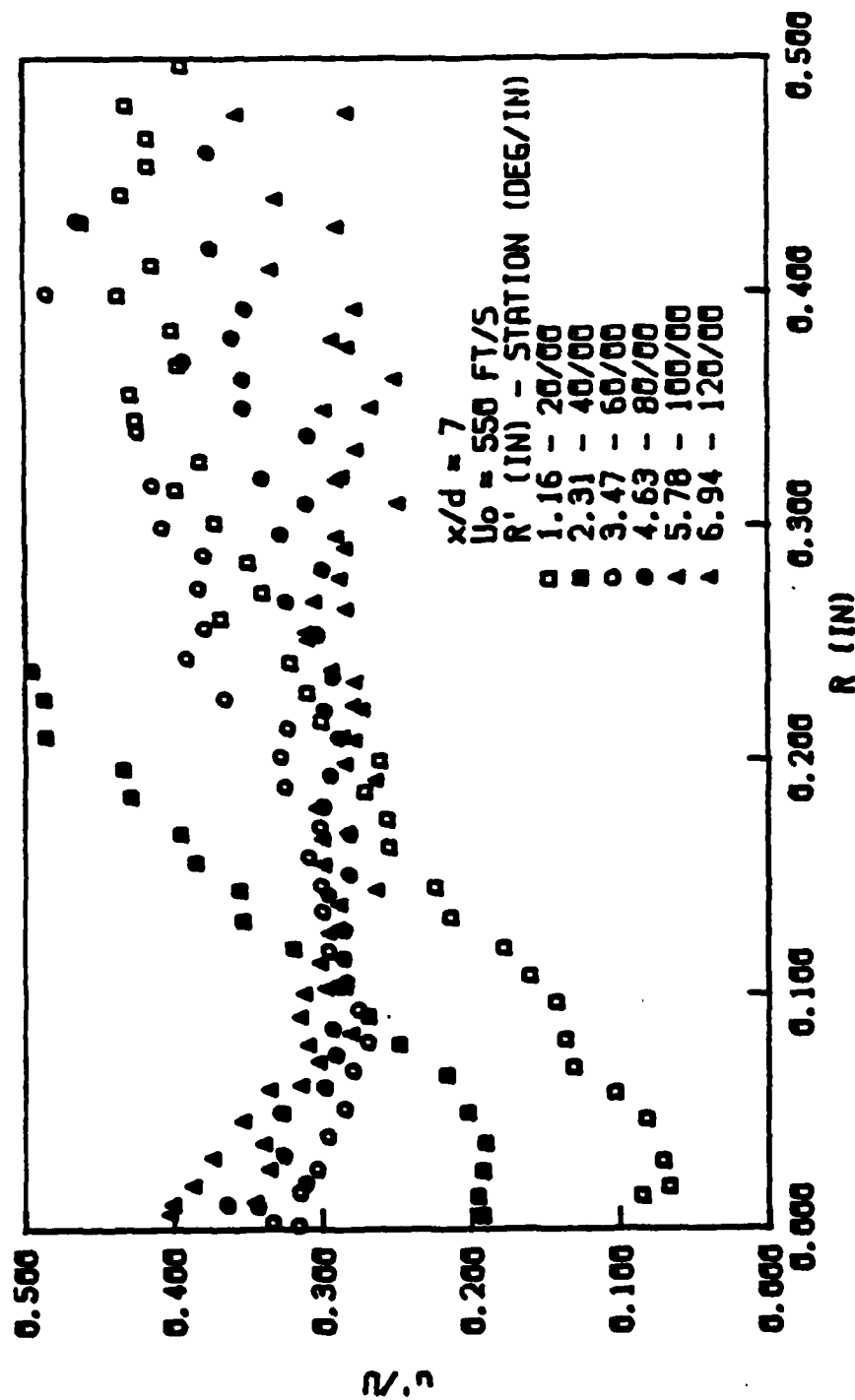


Fig. 67 Wall jet turbulence profile for $U_0 = 550$ ft/s, $x/d = 7$ (circumferential radial).

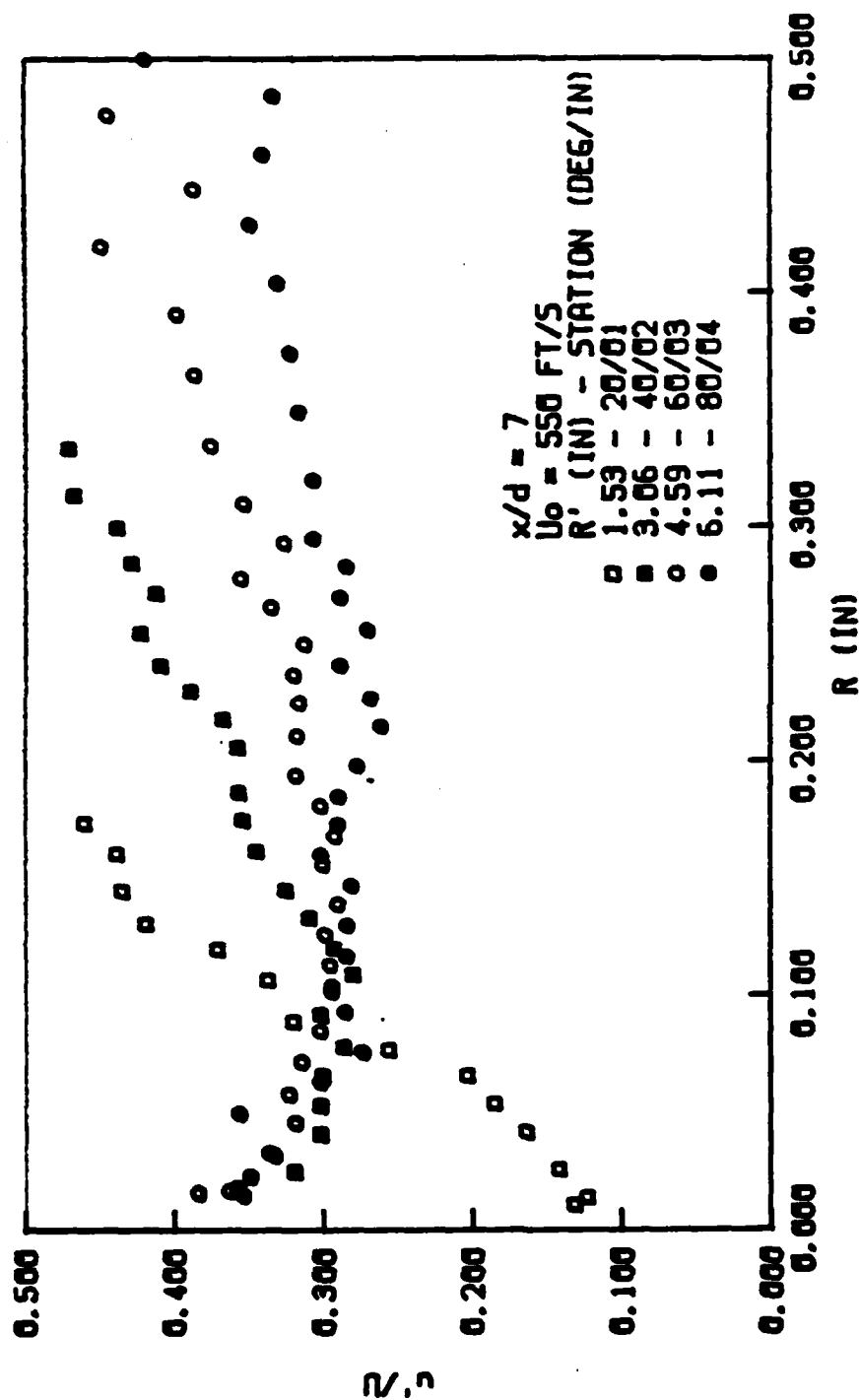


Fig. 63 Wall jet turbulence profile for $U_0 = 550 \text{ ft/s}$, $x/d = 7$ (radial 2).

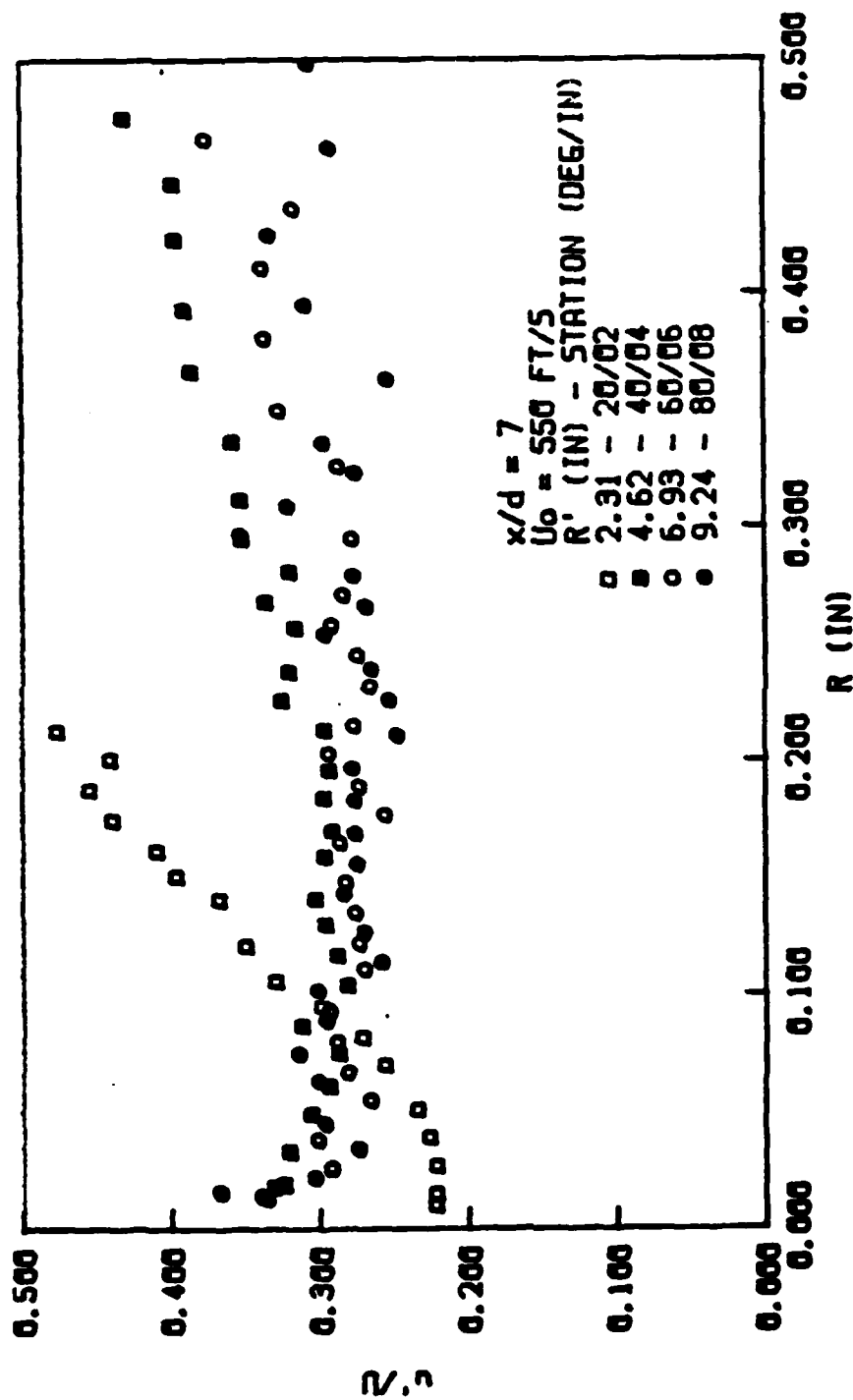


Fig. 69 Wall jet turbulence profile for $U_0 = 550$ ft/s, $x/d = 7$ (radial 4).

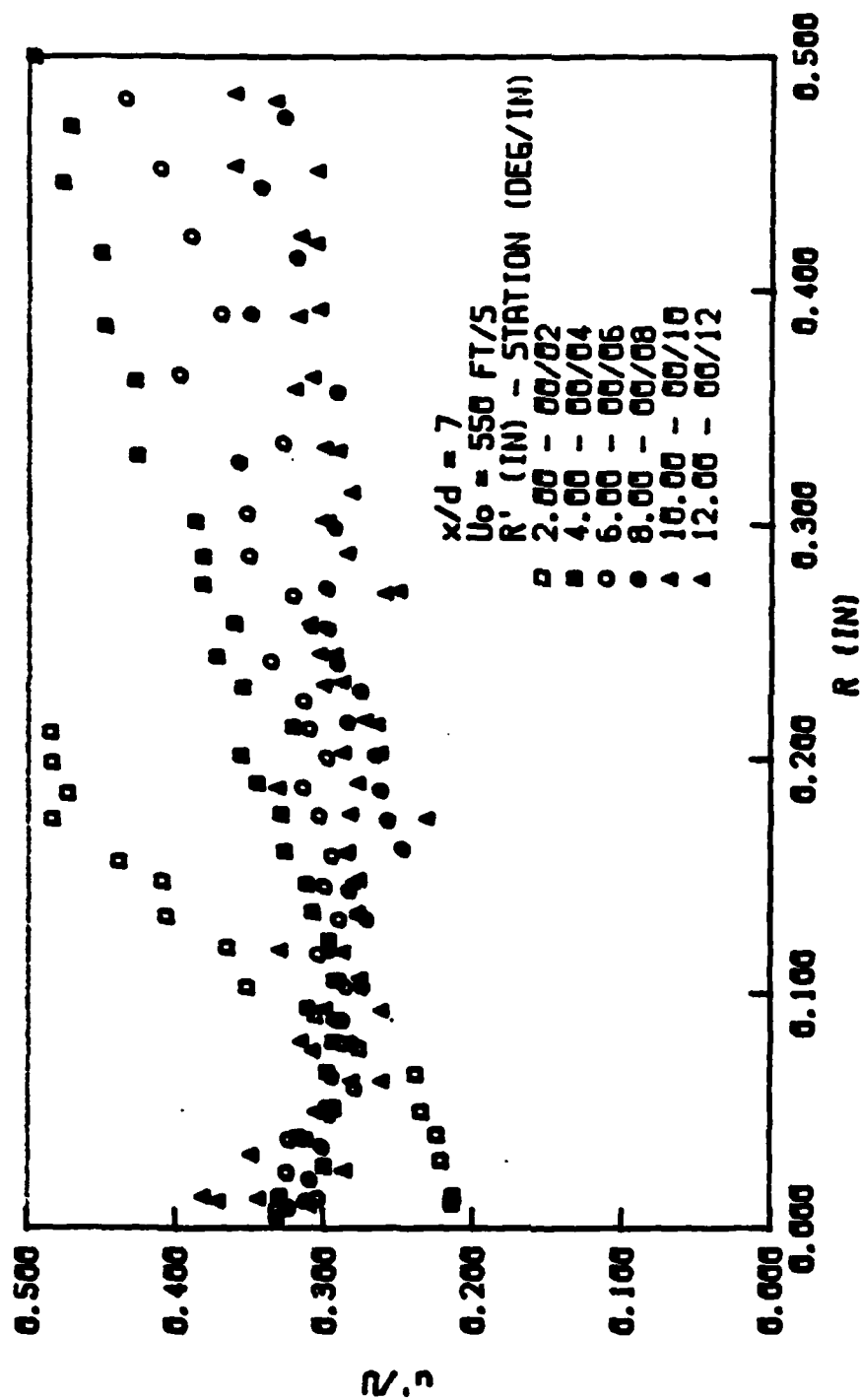


Fig. 70 Wall jet turbulence profile for $U_0 = 550 \text{ ft/s}$, $x/d = 7$ (axial radial).

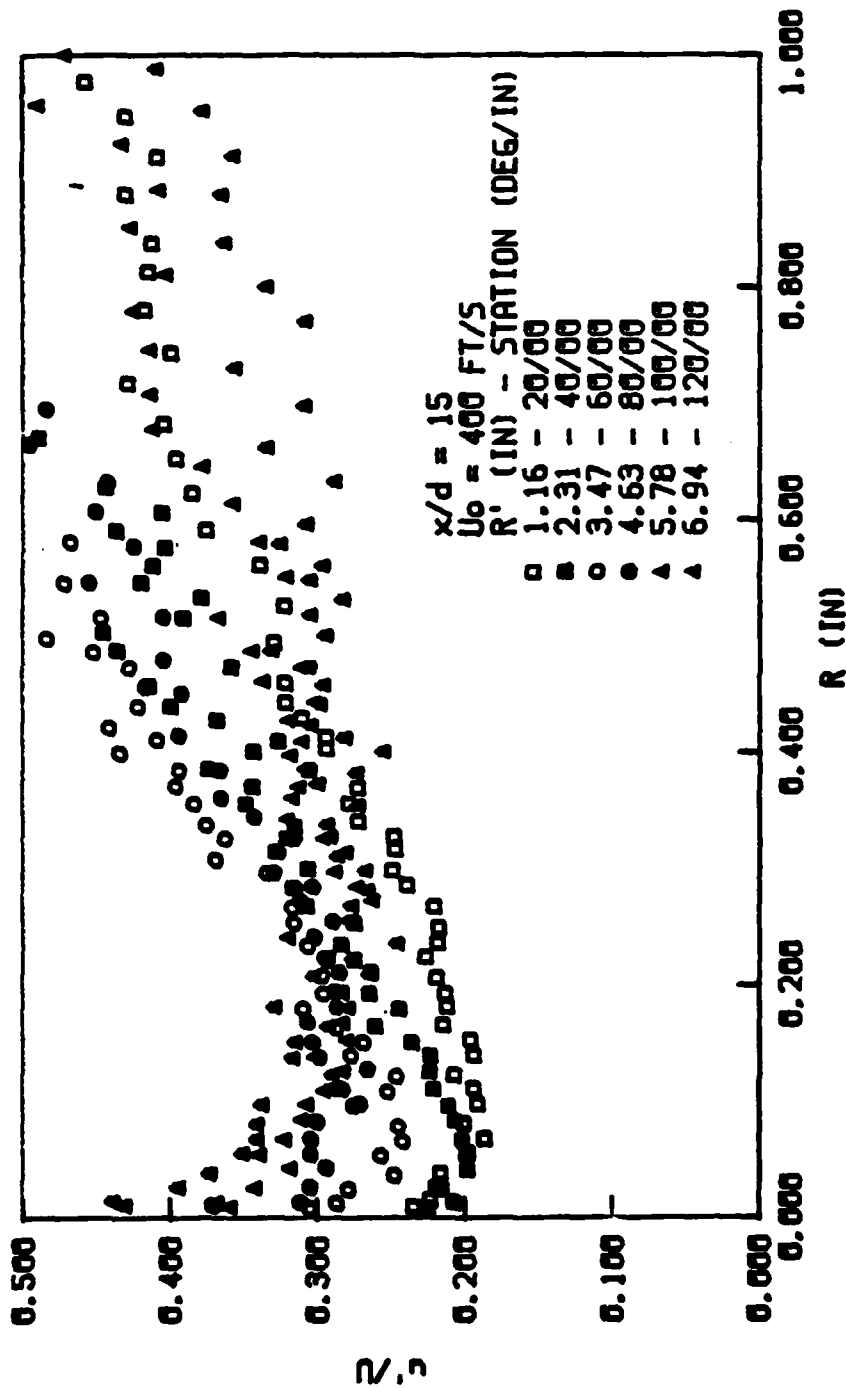


Fig. 71 Wall jet turbulence profile for $U_o = 400 \text{ ft/s}$, $x/d = 15$ (circumferential radial).

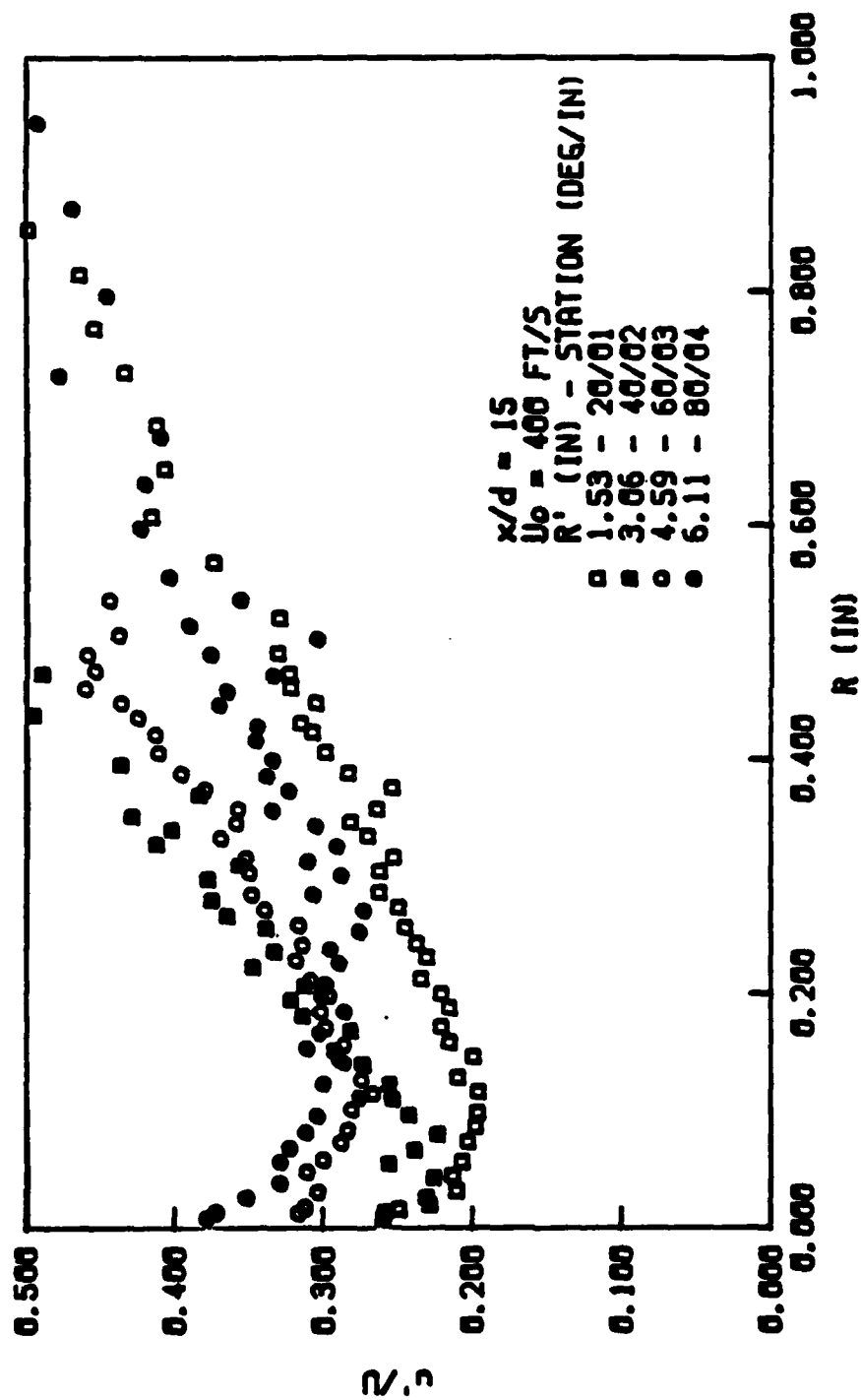


Fig. 72 Wall jet turbulence profile for $U_0 = 400 \text{ ft/s}$, $x/d = 15$ (radial 2).

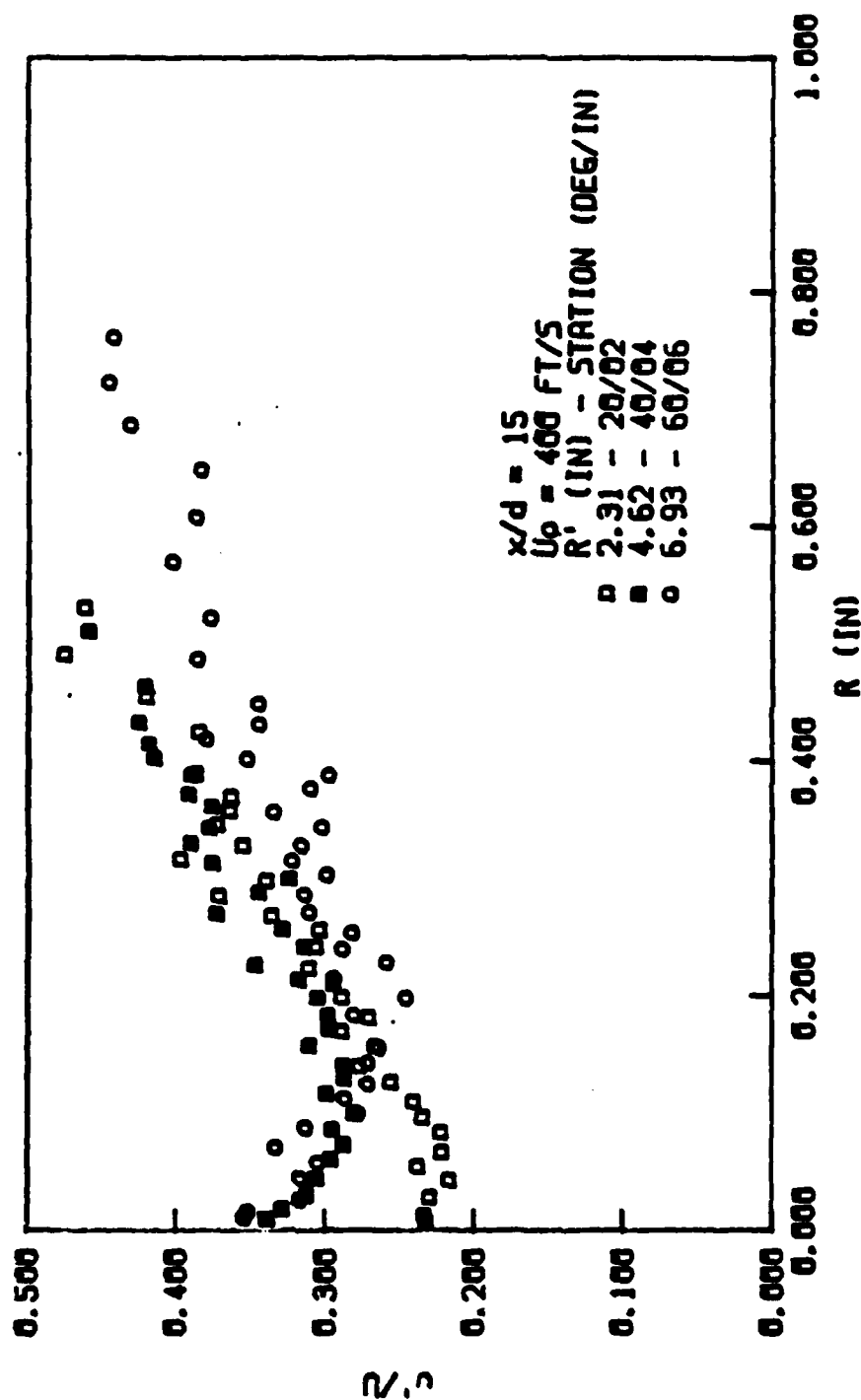


Fig. 73 Wall jet turbulence profile for $U_0 = 400 \text{ ft/s}$, $x/d = 15$ (radial 4).

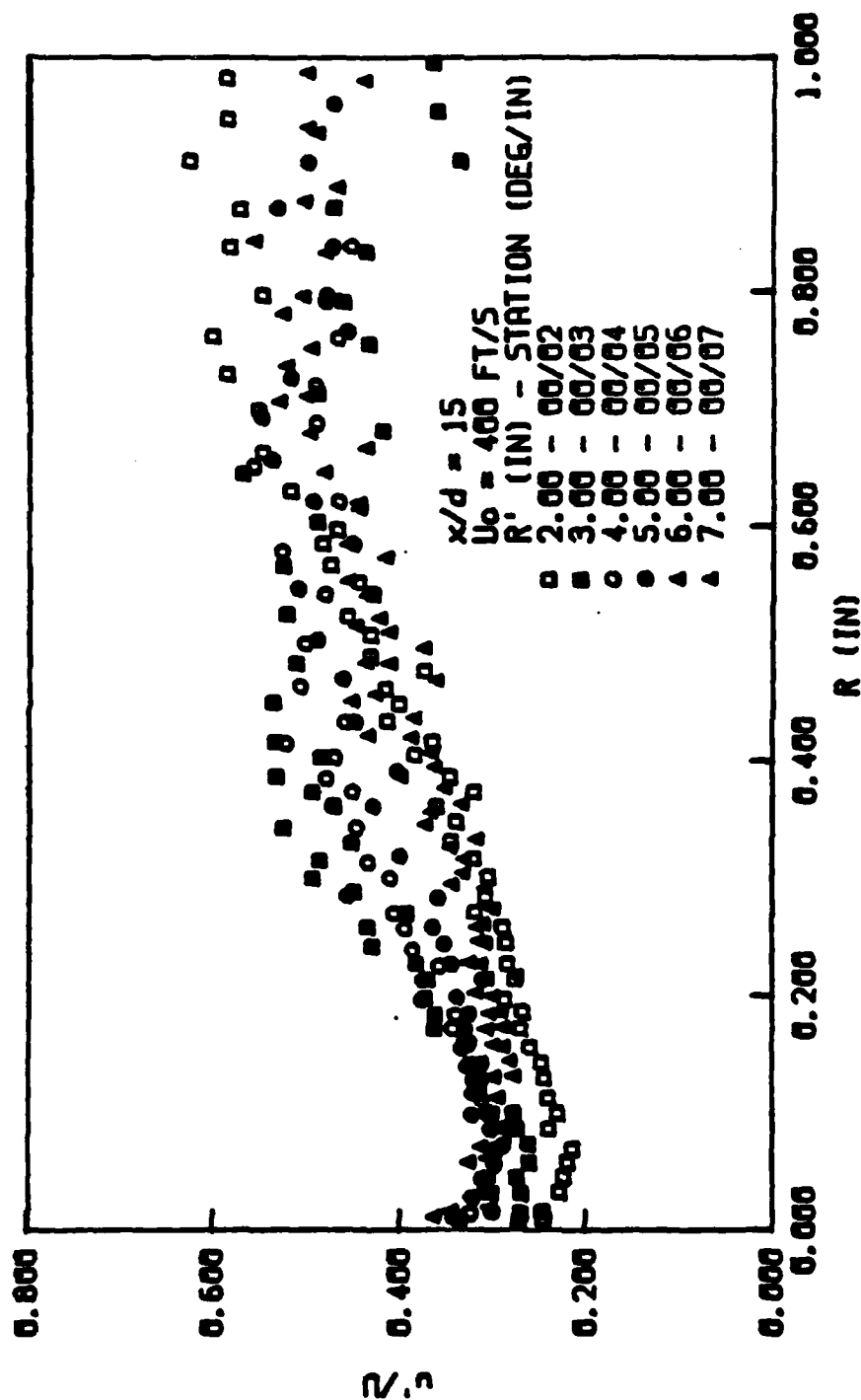


Fig. 74 Wall jet turbulence profile for $U_0 = 400 \text{ ft/s}$, $x/d = 15$ (axial radial).

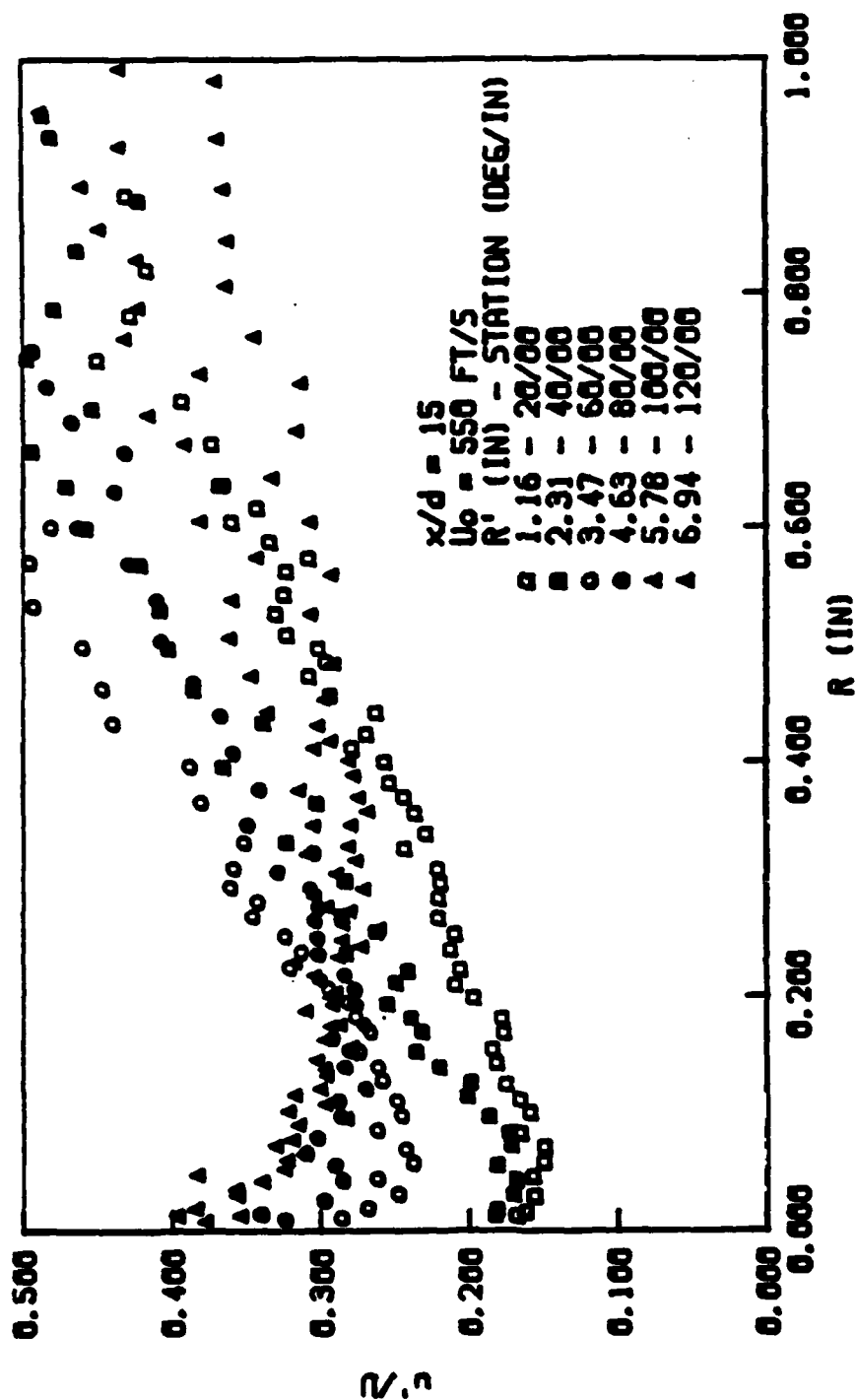


Fig. 75 Wall jet turbulence profile for $U_0 = 550 \text{ ft/s}$, $x/d = 15$ (circumferential radial).

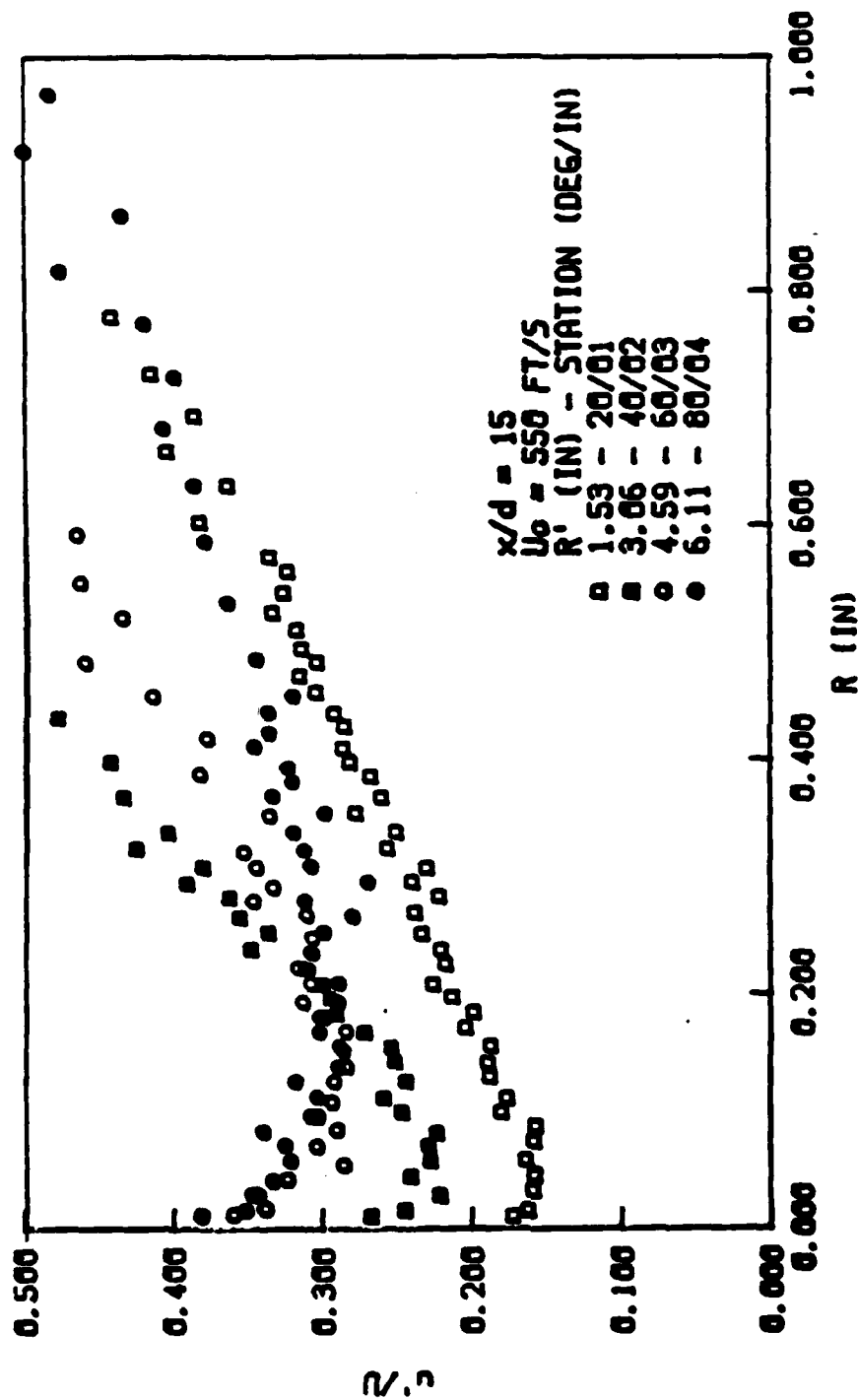


Fig. 76 Wall jet turbulence profile for $U_0 = 550 \text{ ft/s}$, $x/d = 15$ (radial 2).

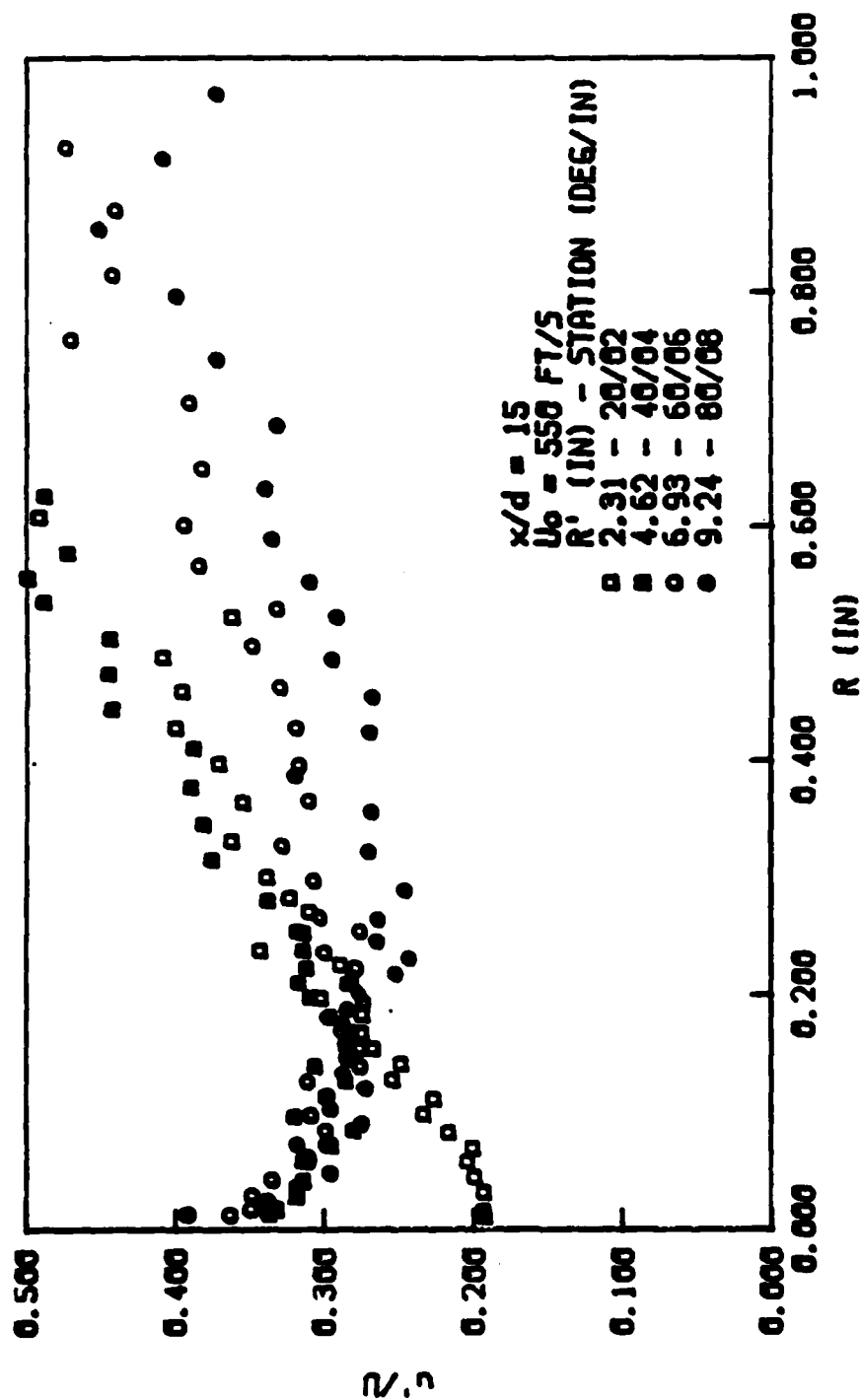


Fig. 77 wall jet turbulence profile for $U_0 = 550 \text{ ft/s}$, $x/d = 15$ (radial 4).

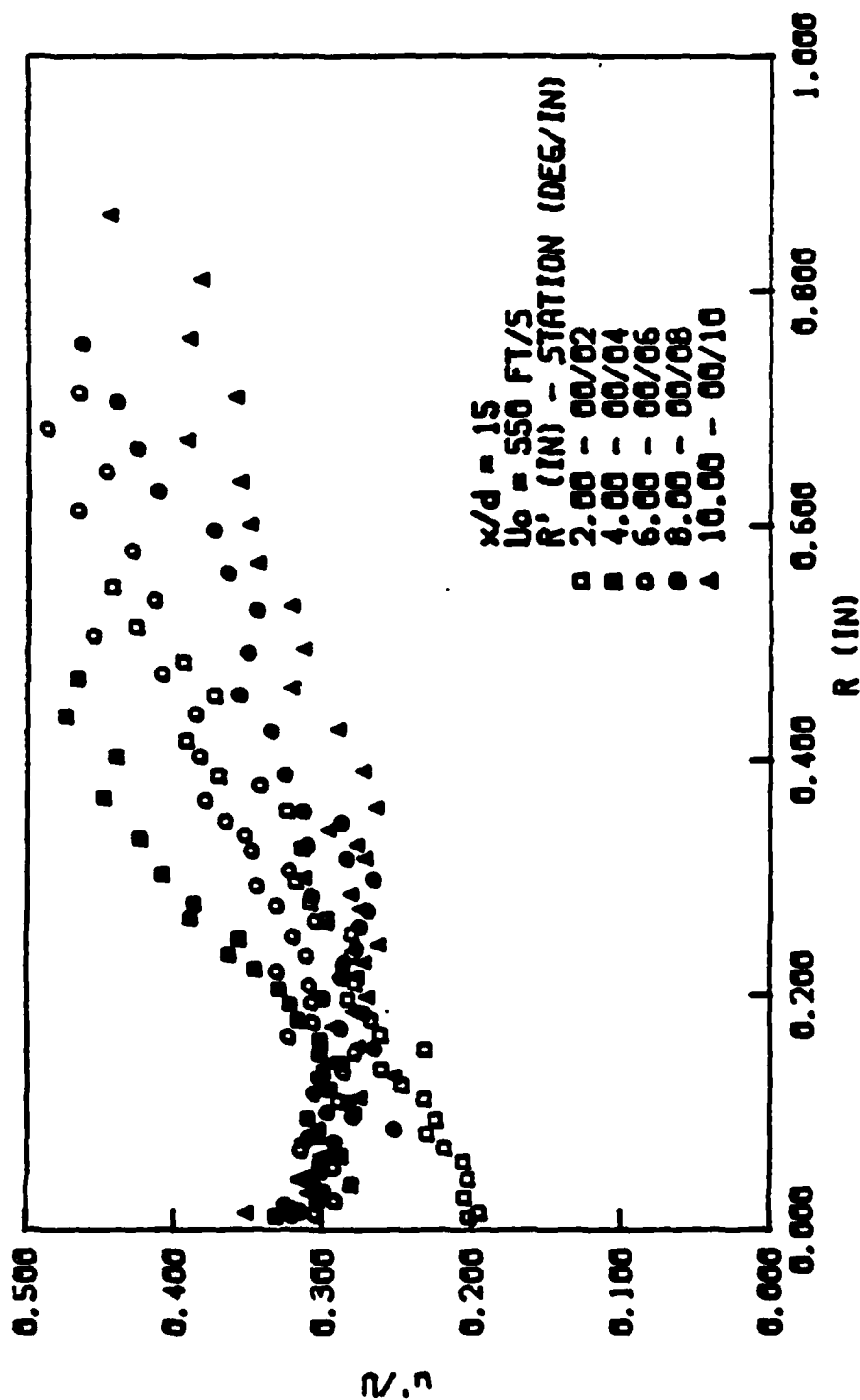


Fig. 78 Wall jet turbulence profile for $U_0 = 550$ ft/s, $x/d = 15$ (axial radial).

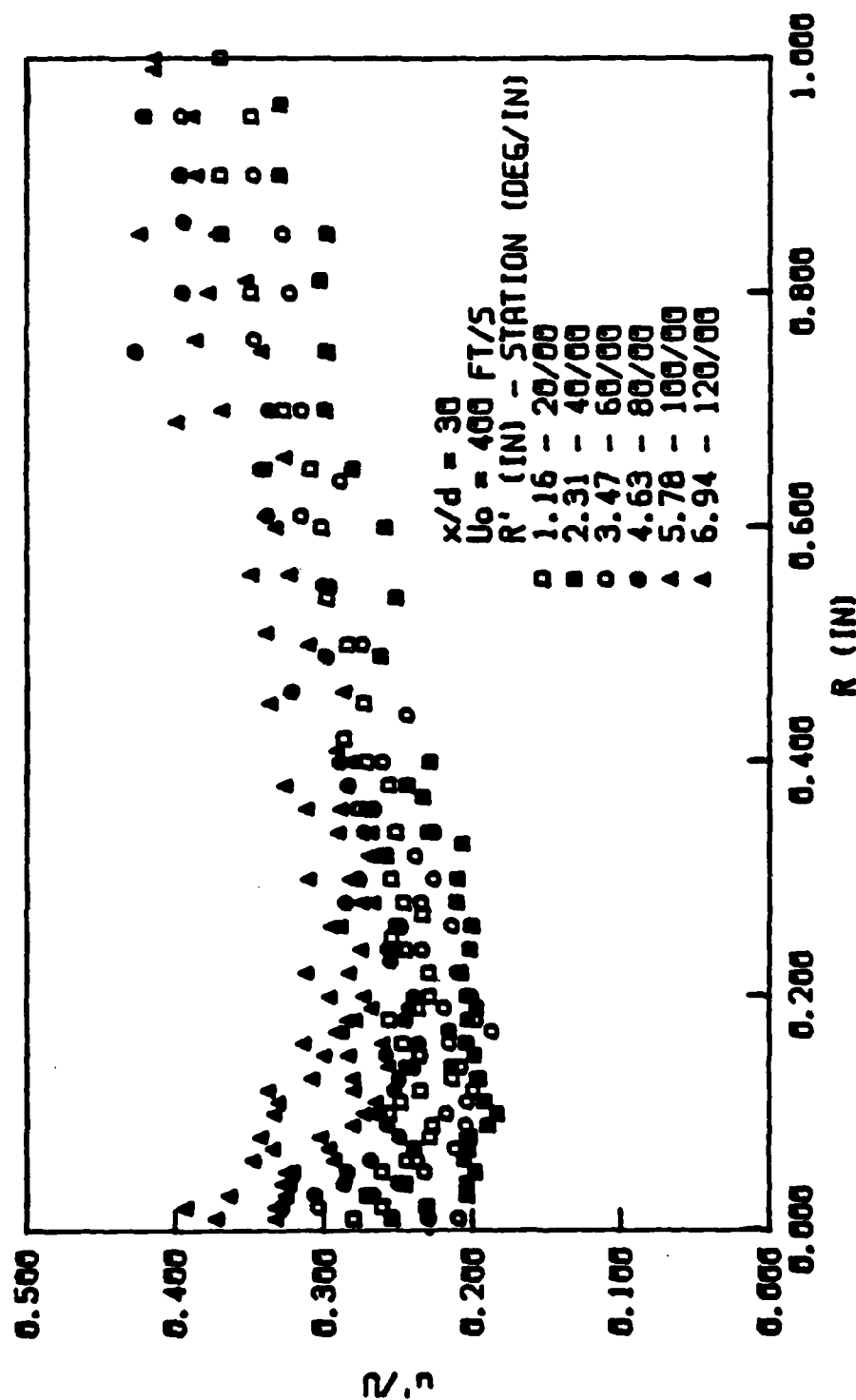


Fig. 79 Wall jet turbulence profile for $U_0 = 400$ ft/s, $x/d = 30$ (circumferential radial).

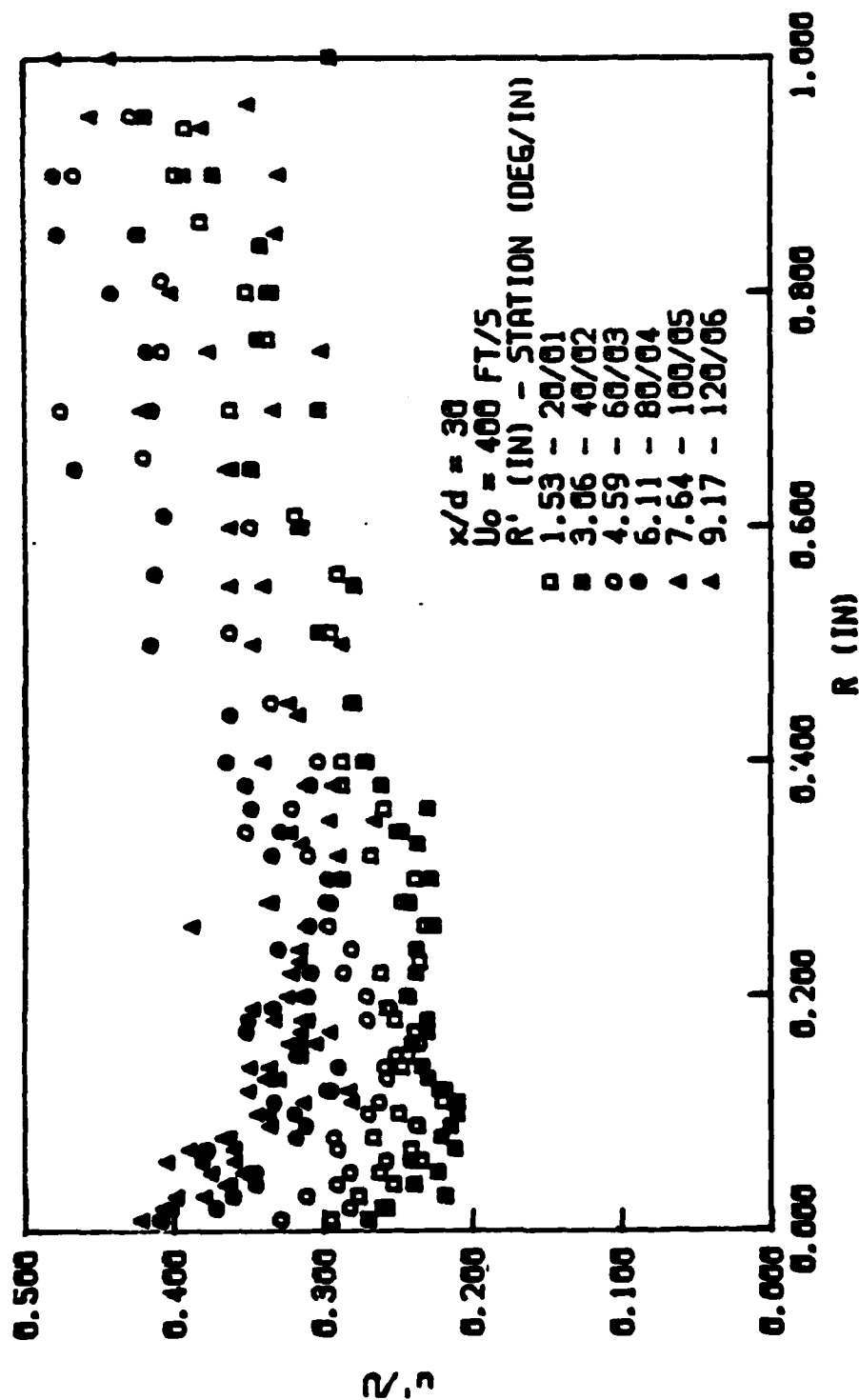


Fig. 80 Wall jet turbulence profile for $U_0 = 400 \text{ ft/s}$, $x/d = 30$ (radial 2).

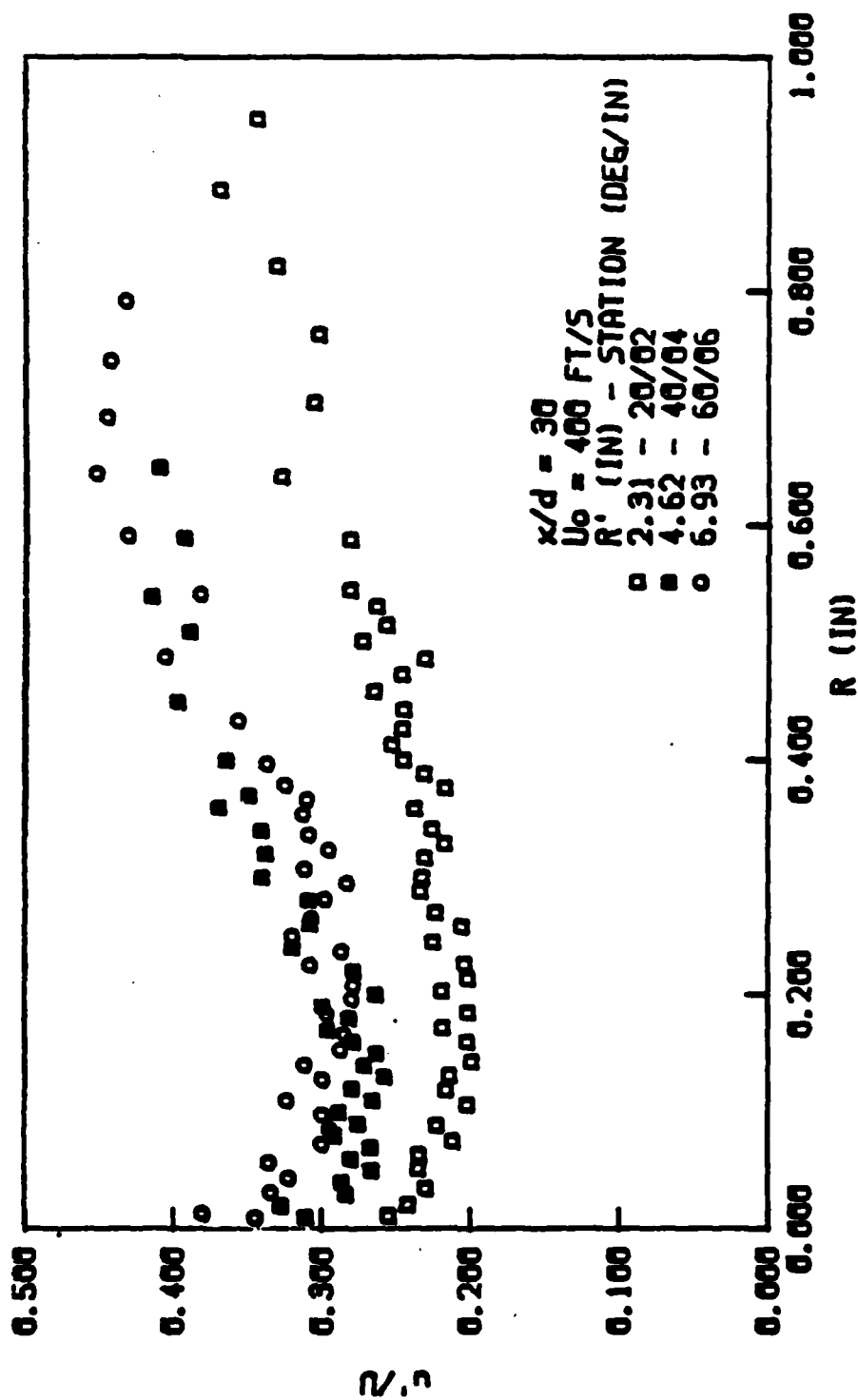


Fig. 81 Wall jet turbulence profile for $U_0 = 400 \text{ ft/s}$, $x/d = 30$ (radial 4).

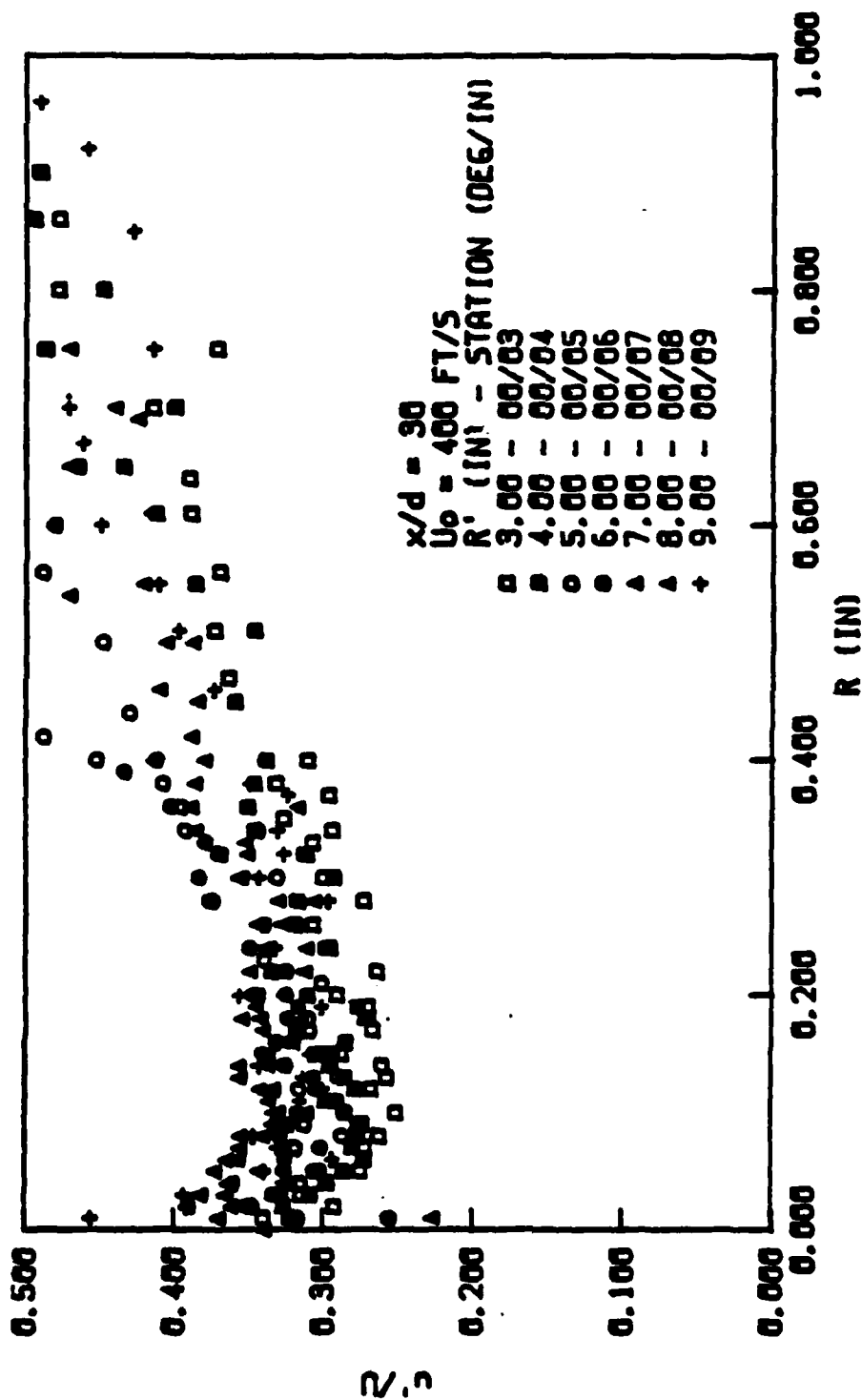


Fig. 82 Wall jet turbulence profile for $U_0 = 400 \text{ ft/s}$, $x/d = 30$ (axial radial).

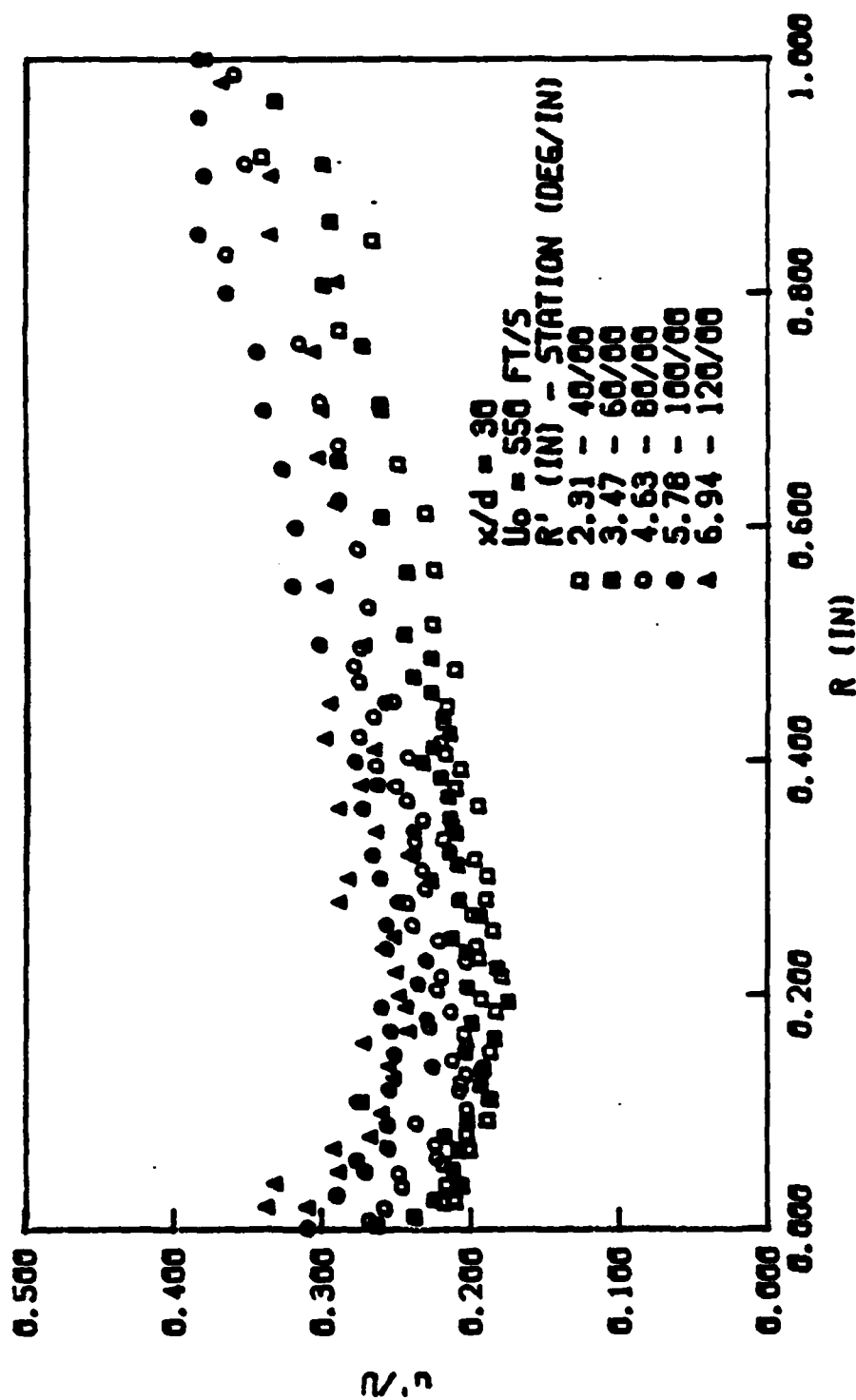


Fig. 83 Wall jet turbulence profile for $U_0 = 550 \text{ ft/s}$, $x/d = 30$ (circumferential radial).

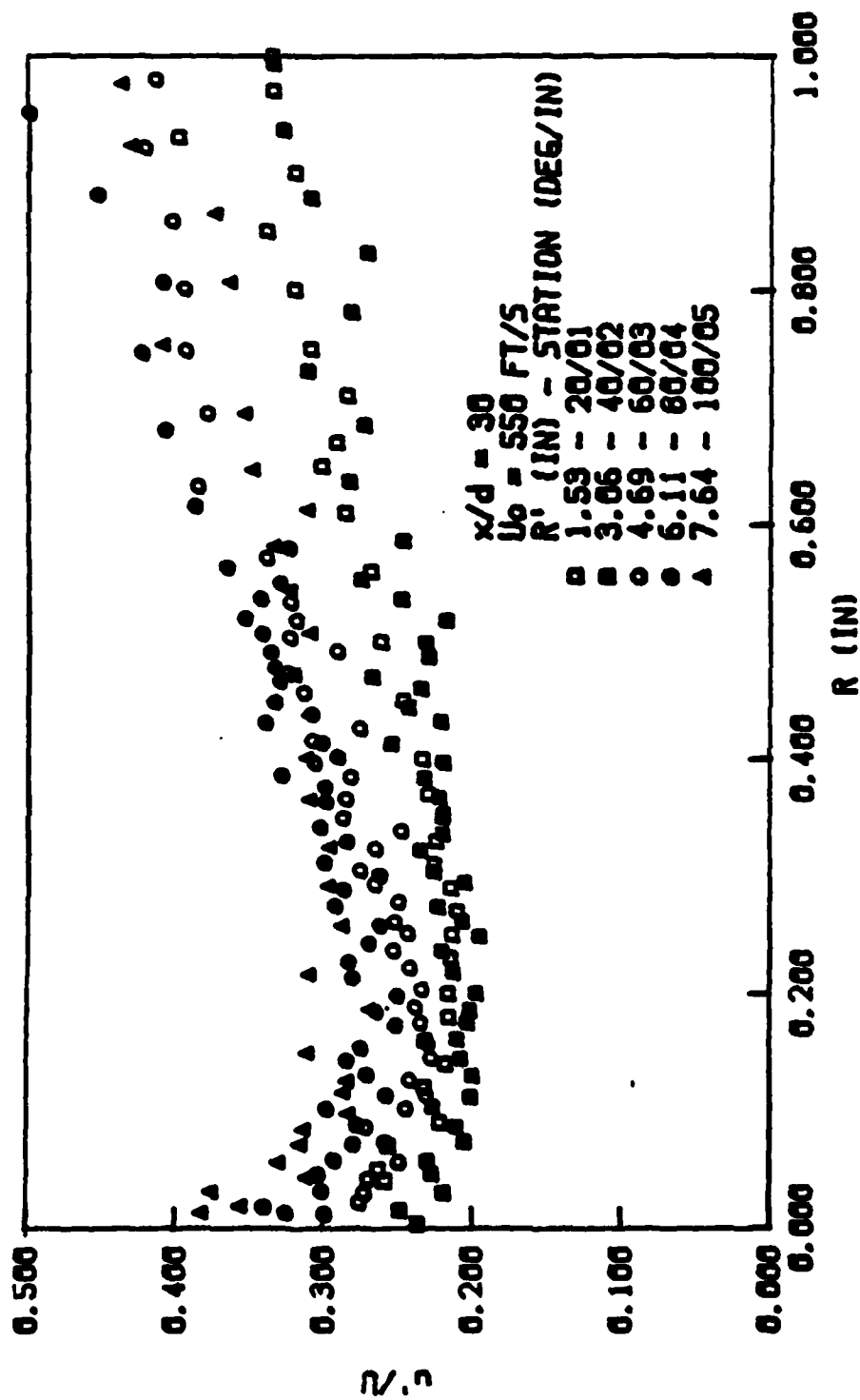


Fig. 84 Wall jet turbulence profile for $U_0 = 550 \text{ ft/s}$, $x/d = 30$ (radial 2).

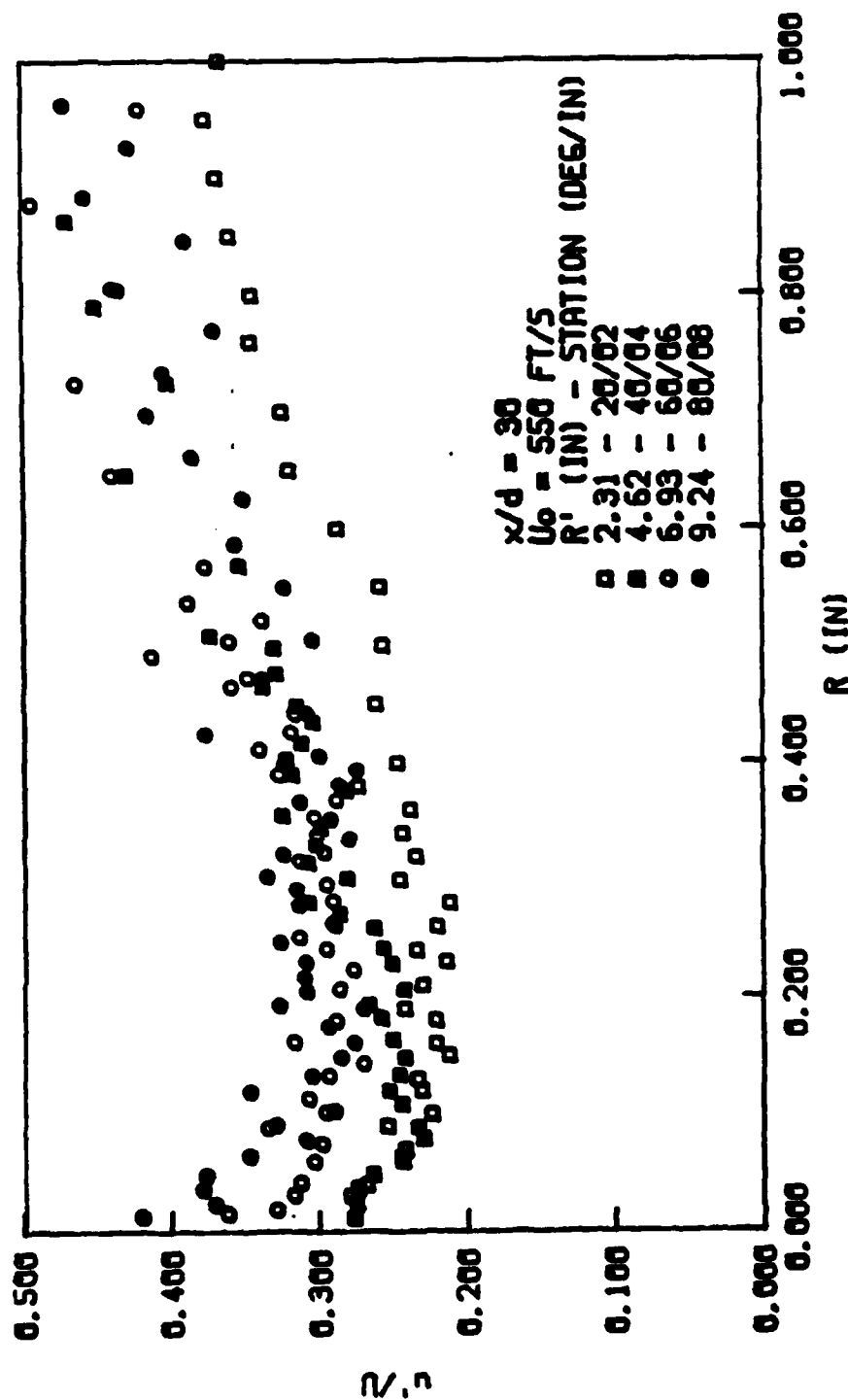


Fig. 85 Wall jet turbulence profile for $U_0 = 550$ ft/s, $x/d = 30$ (radial 4).

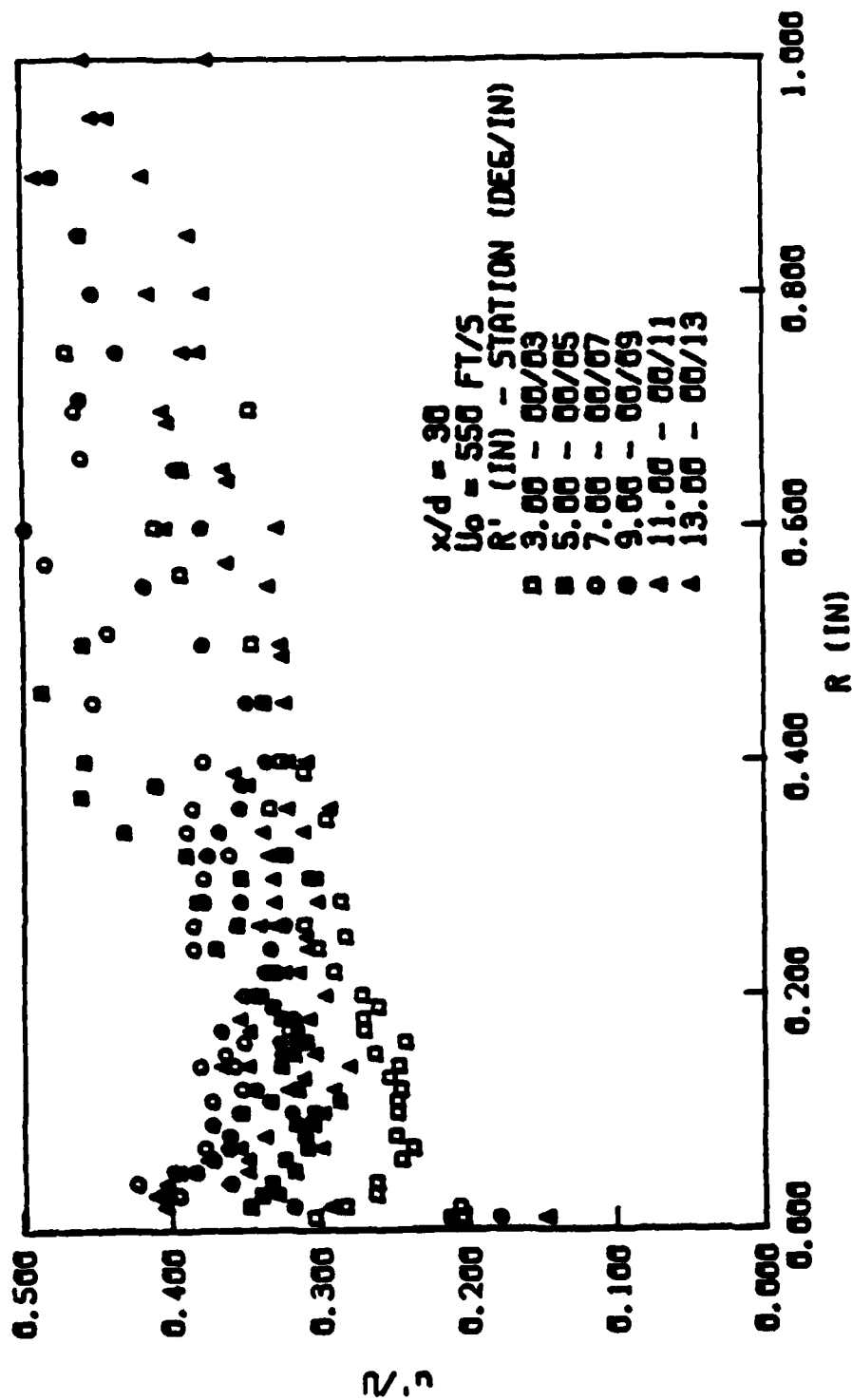


Fig. 86 Wall jet turbulence profile for $U_0 = 550$ ft/s, $x/d = 30$ (axial radial).

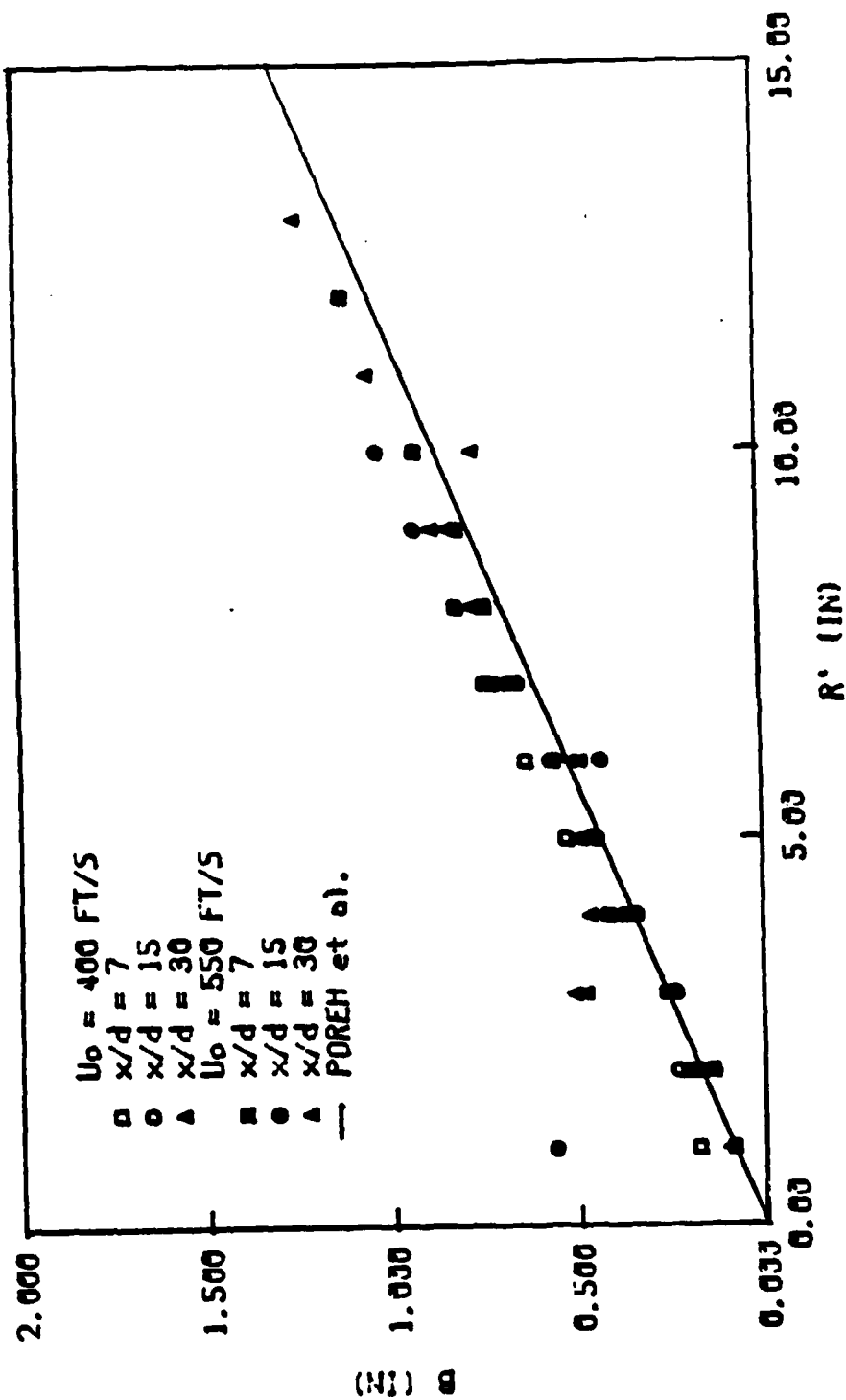


Fig. 87 Spread rate of the wall jet along the axis of the cylinder as compared to a flat plate.

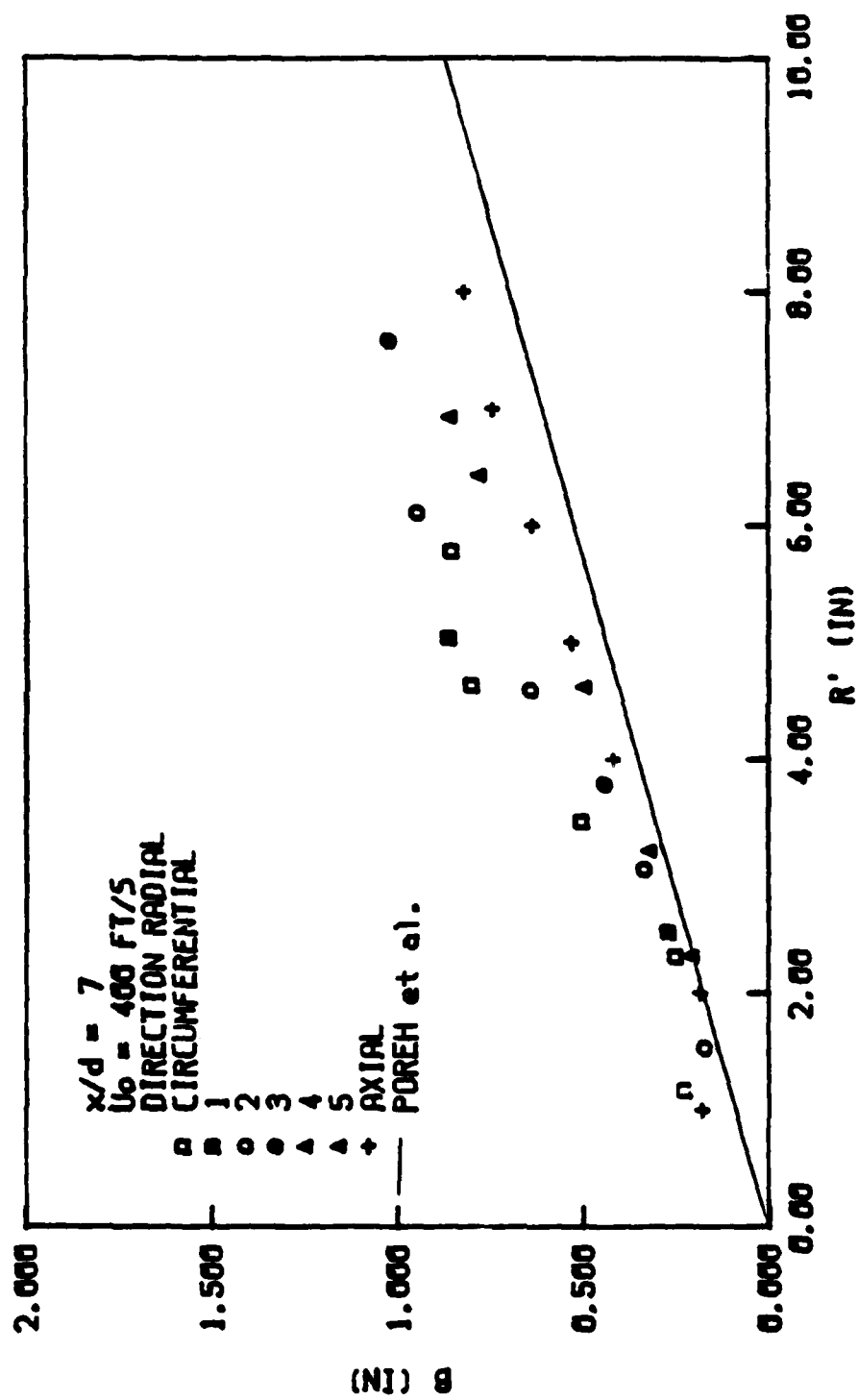


Fig. 88 Spread rate of the wall jet for $U_0 = 400 \text{ ft/s}$, $x/d = 7$.

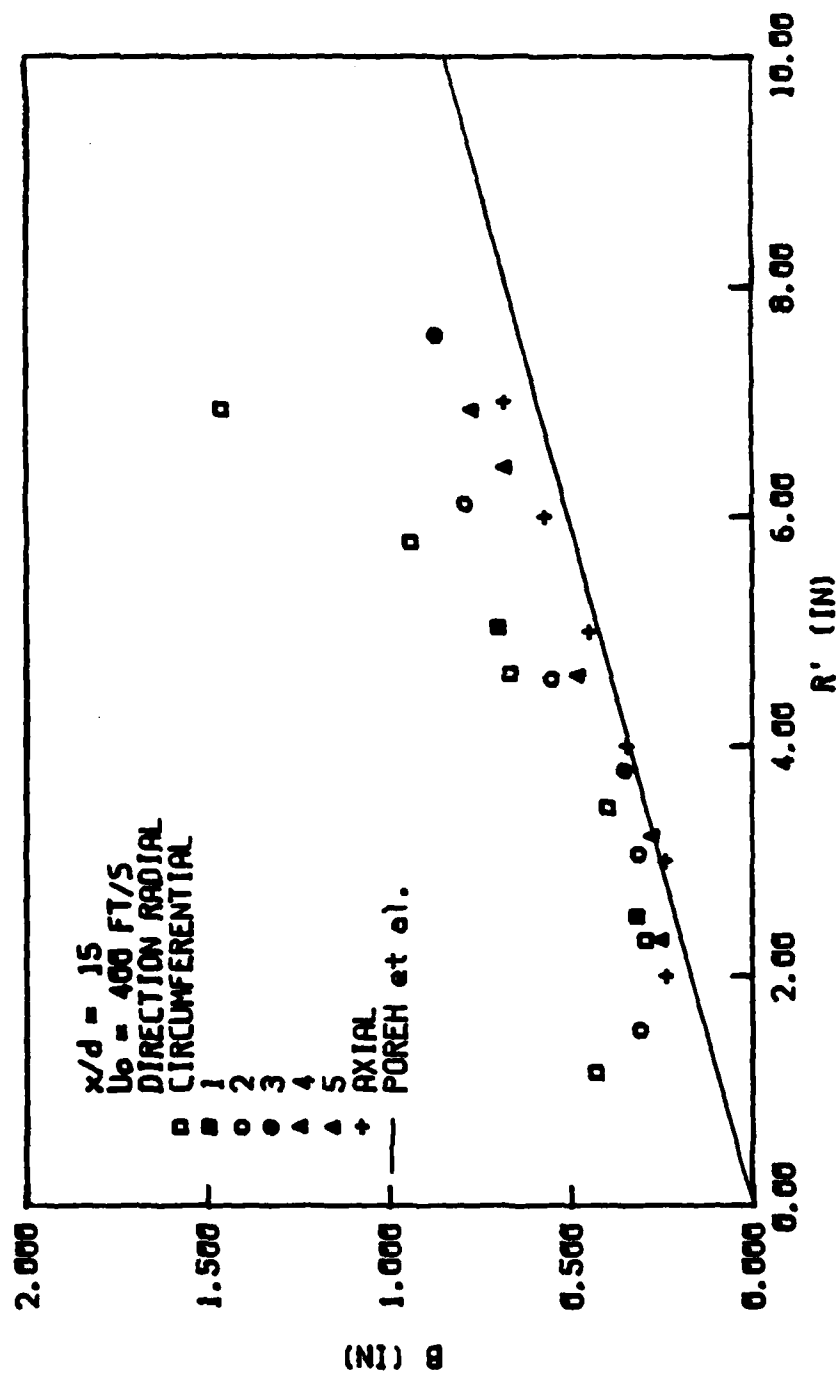


Fig. 89 Spread rate of the wall jet for $U_0 = 400 \text{ ft/s}$, $x/d = 15$.

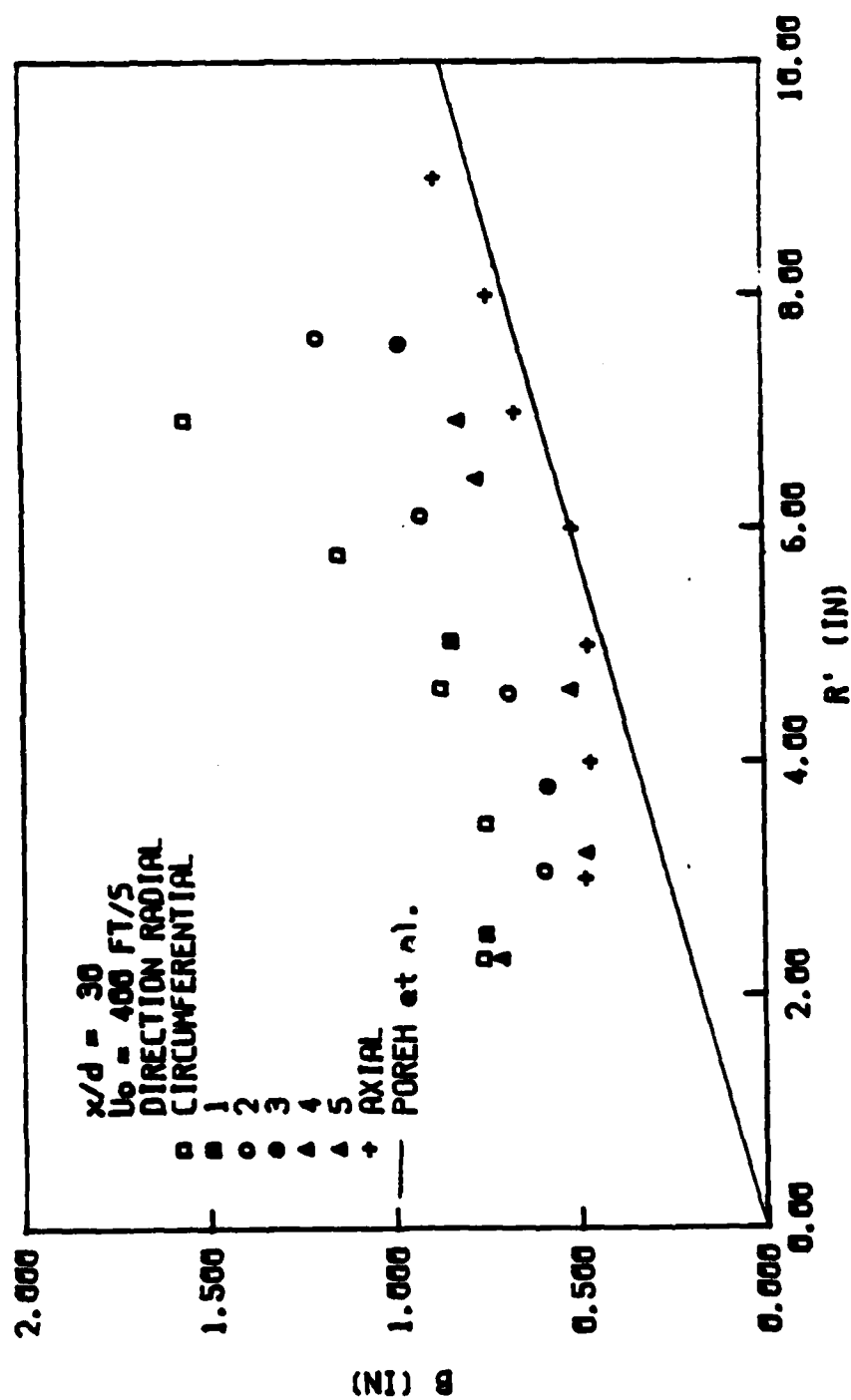


Fig. 90 Spread rate of the wall jet for $U_0 = 400 \text{ ft/s}$, $x/d = 30$.

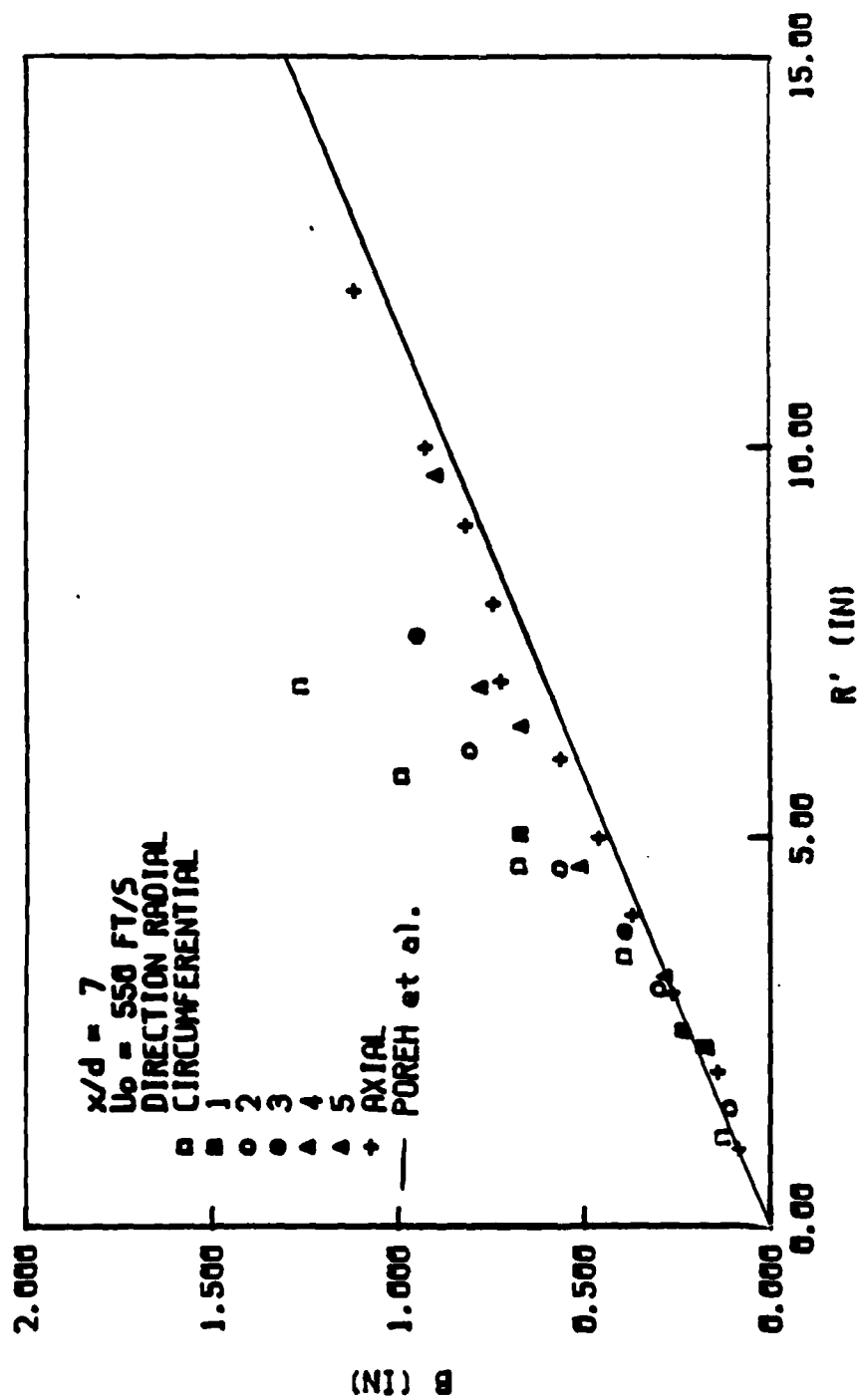


Fig. 91 Spread rate of the wall jet for $U_0 = 550 \text{ ft/s}$, $x/d = 7$.

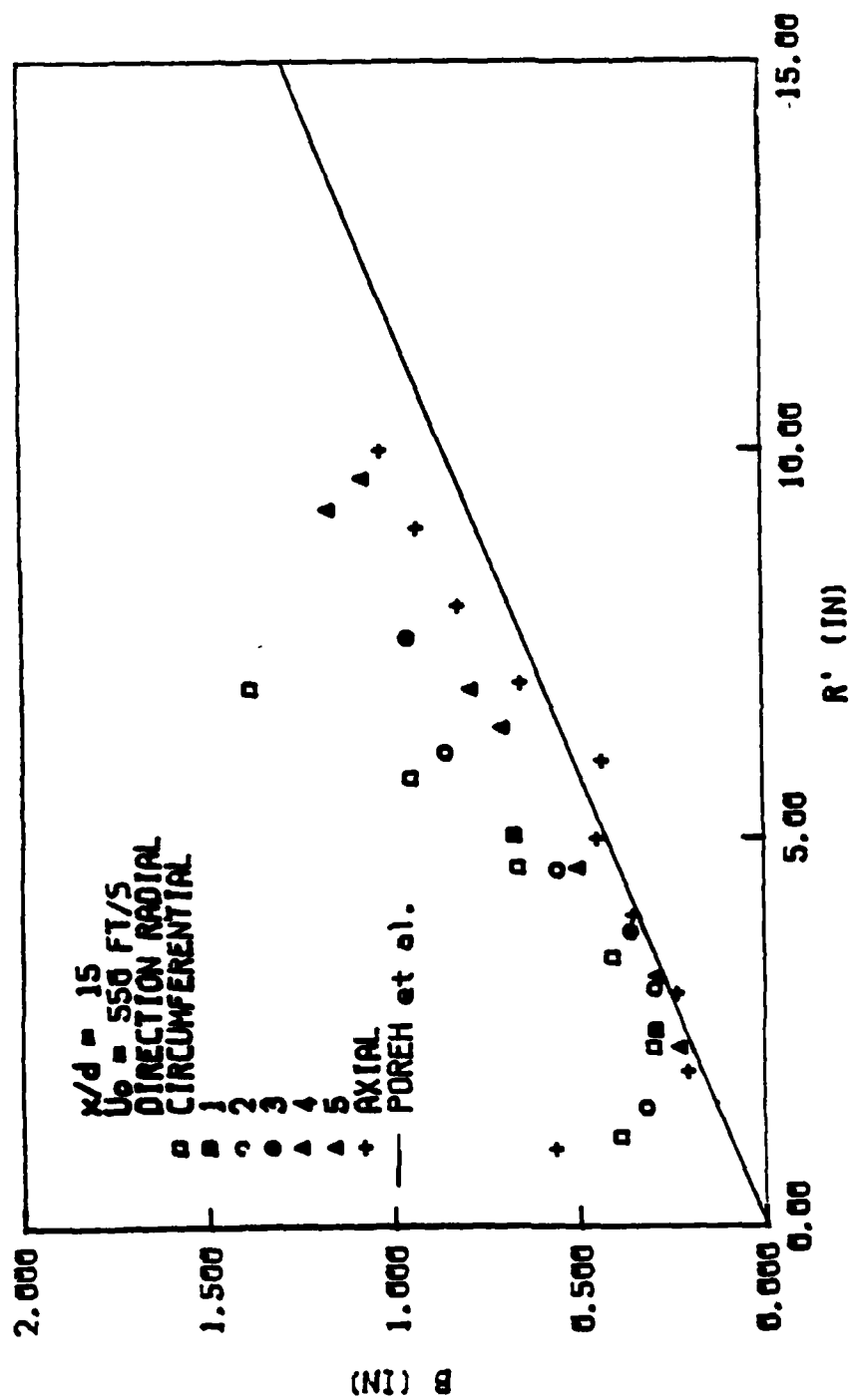


Fig. 92 Spread rate of the wall jet for $U_0 = 550 \text{ ft/s}$, $x/d = 15$.

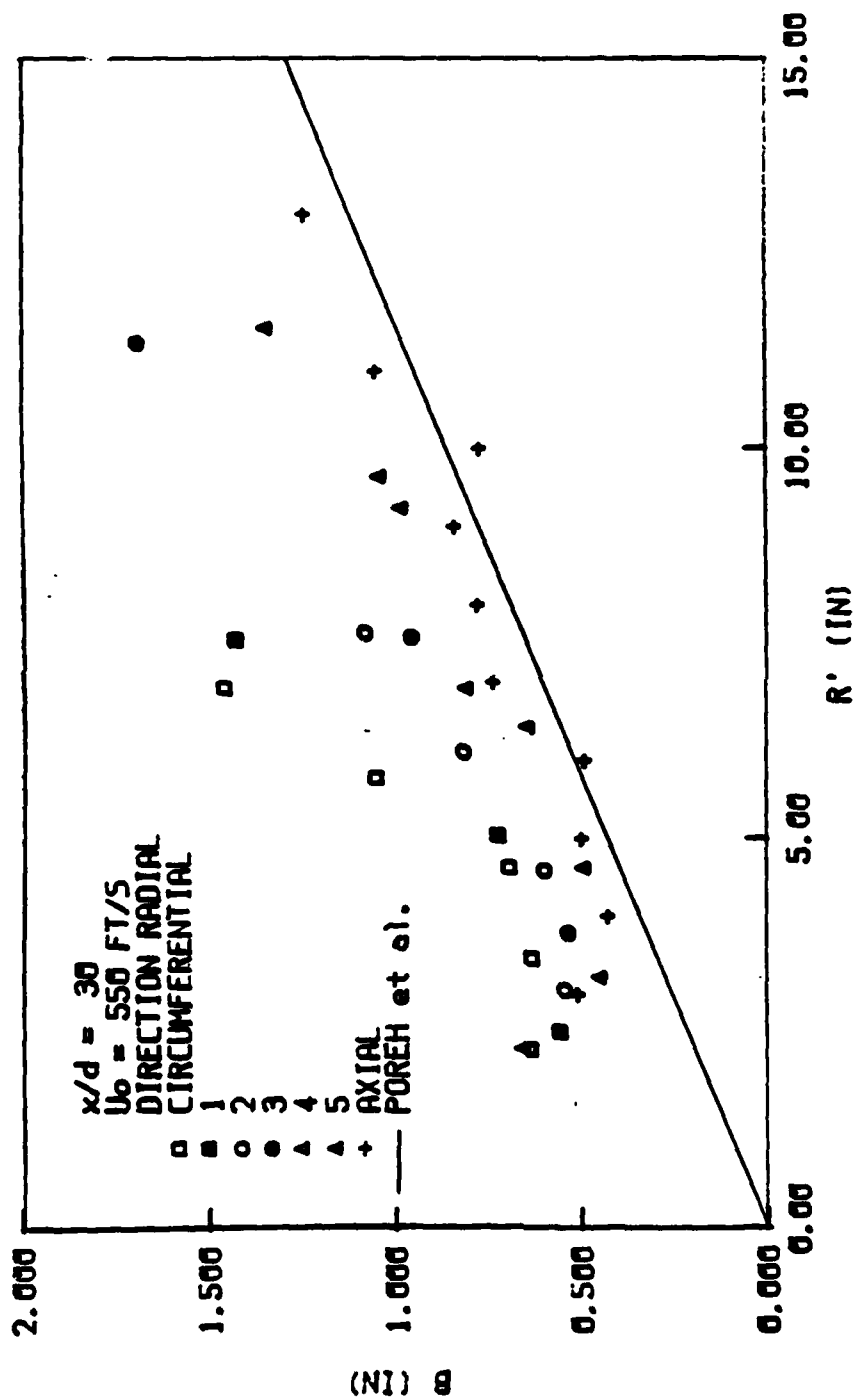


Fig. 93 Spread rate of the wall jet for $U_0 = 550 \text{ ft/s}$, $x/d = 30$.

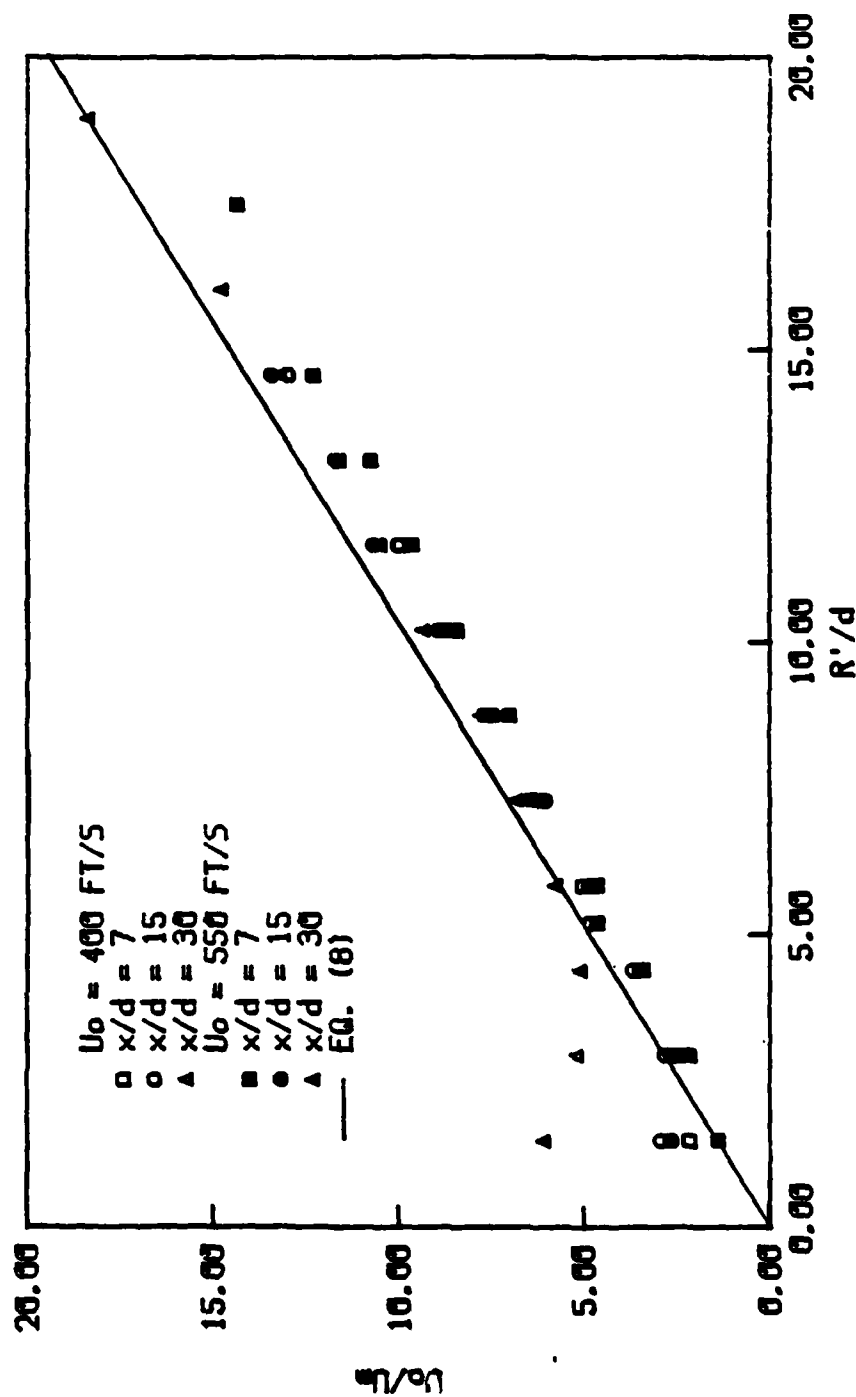


Fig. 94 Velocity scale of the wall jet along the axis of the cylinder as compared to a flat plate.

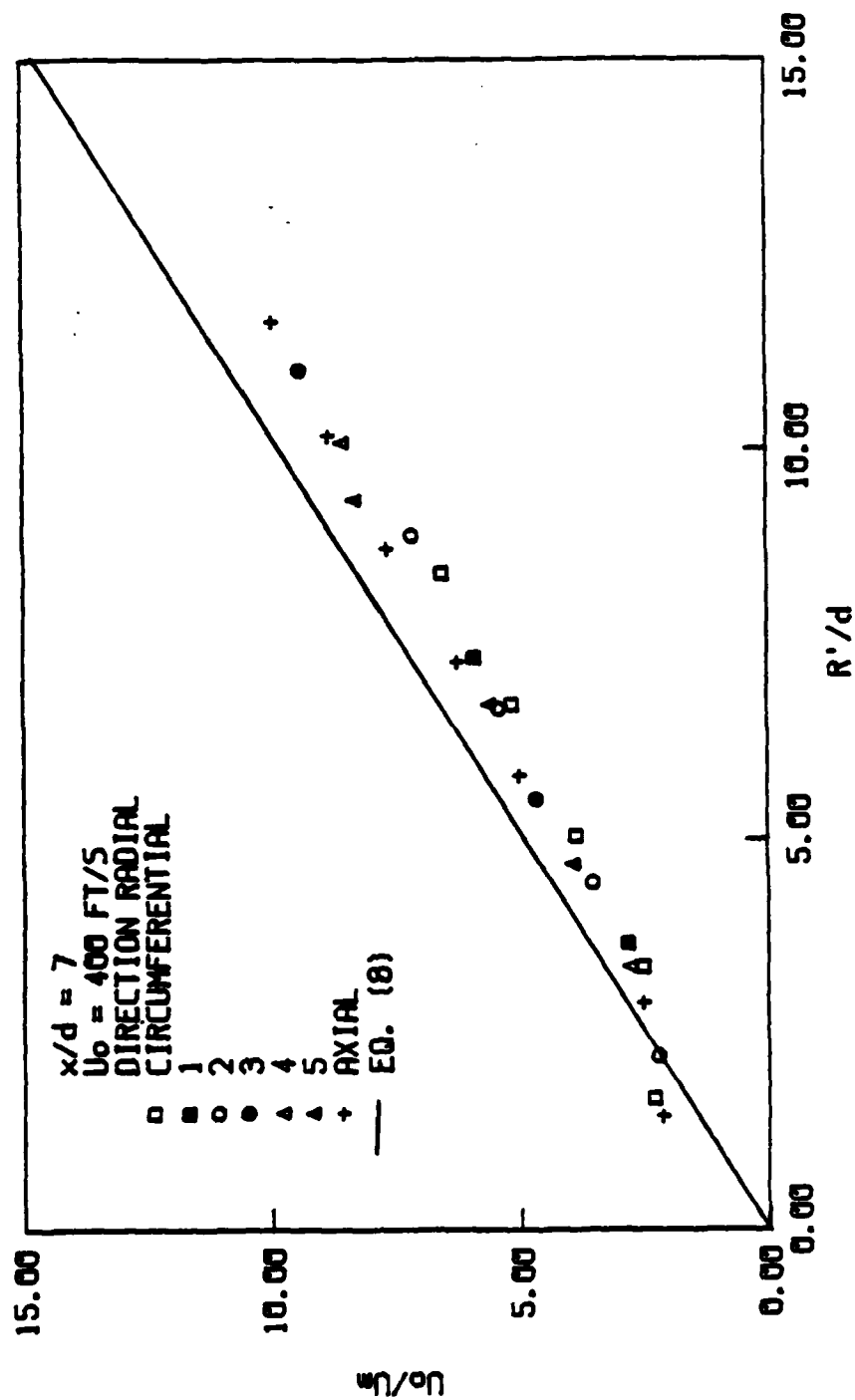


Fig. 95 Velocity scale of the wall jet for $U_0 = 400 \text{ ft/s}$, $x/d = 7$.

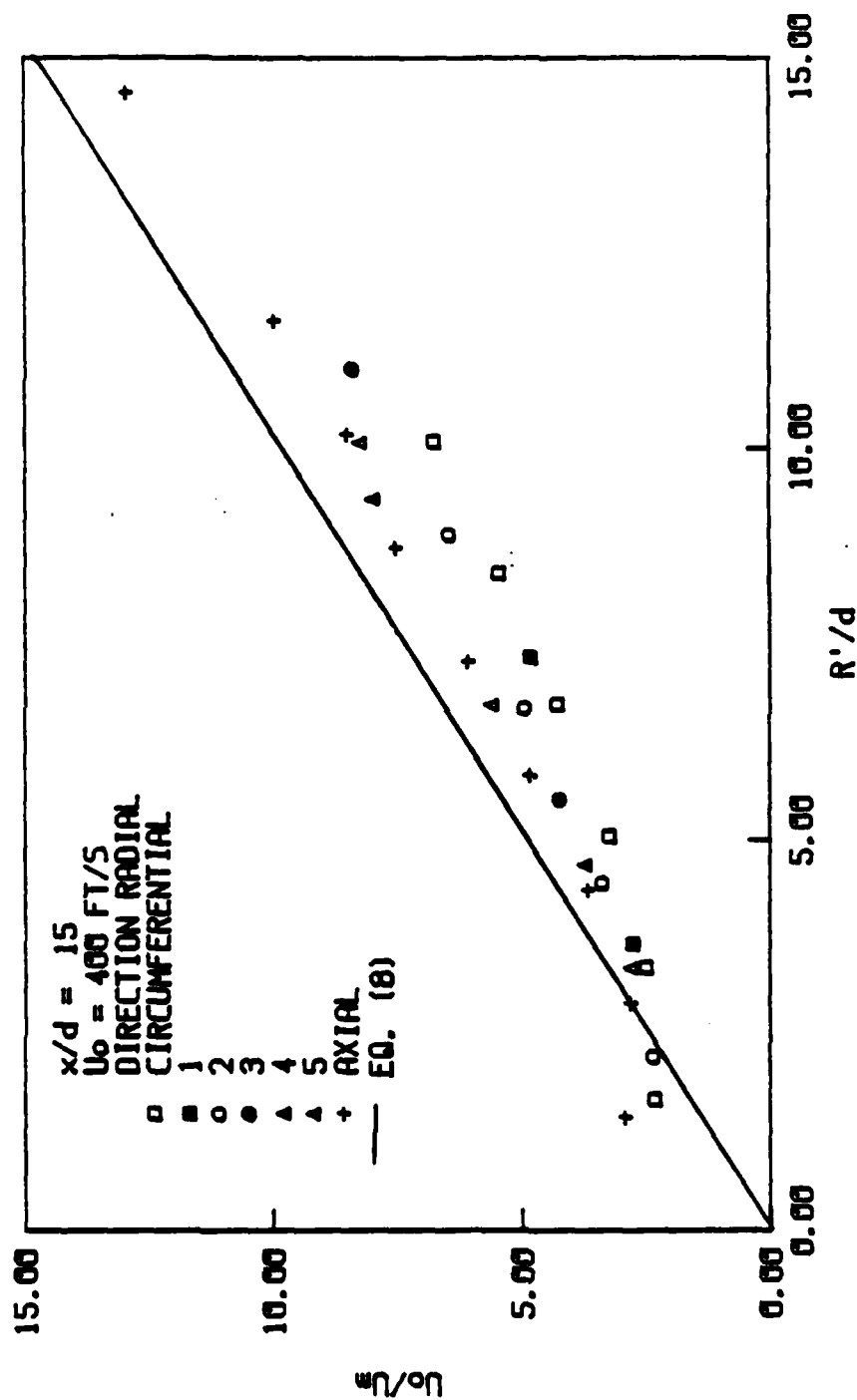


Fig. 96 Velocity scale of the wall jet for $U_0 = 400 \text{ ft/s}$, $x/d = 15$.

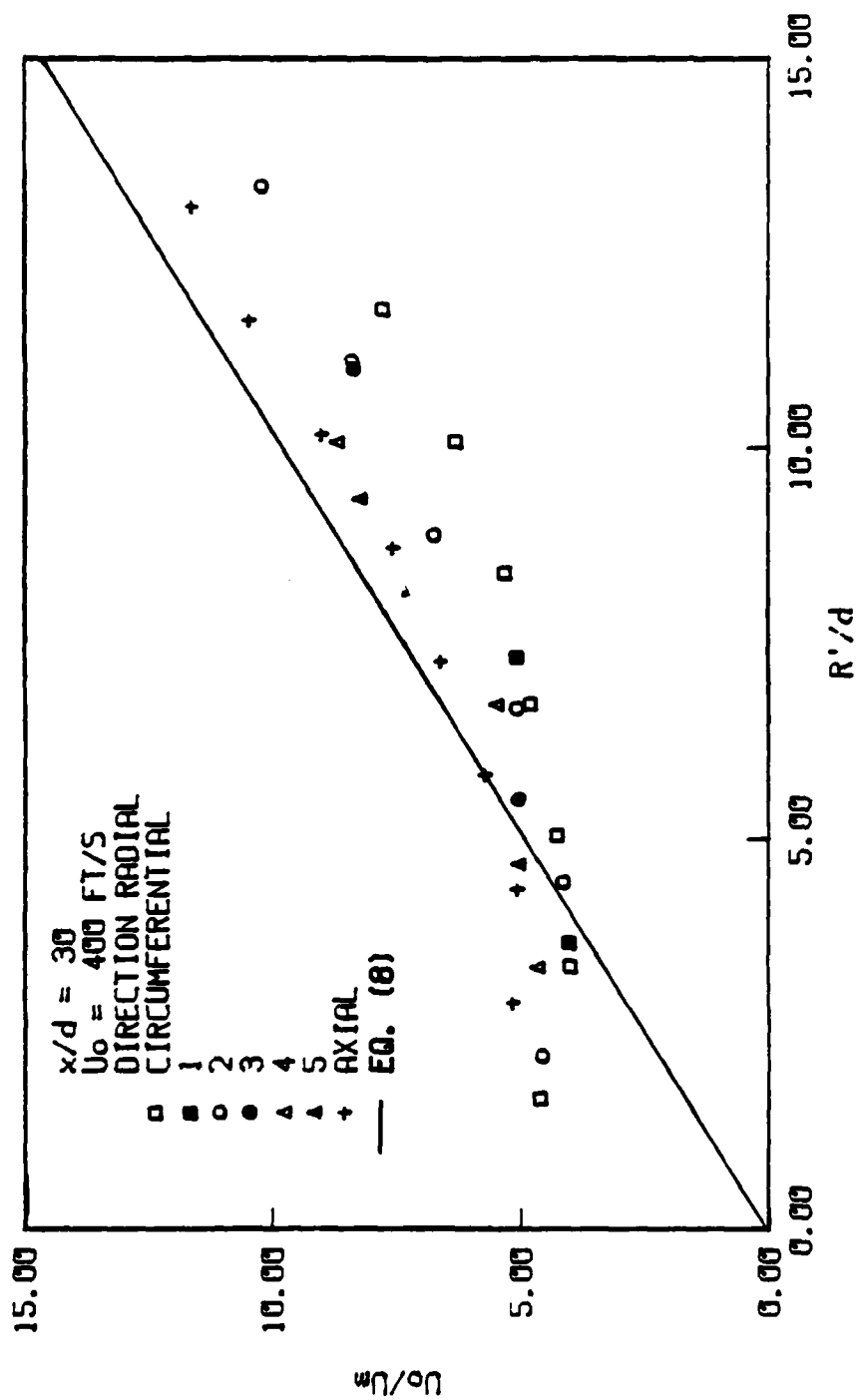


Fig. 97 Velocity scale of the wall jet for $U_o = 400 \text{ ft/s}$, $x/d = 30$.

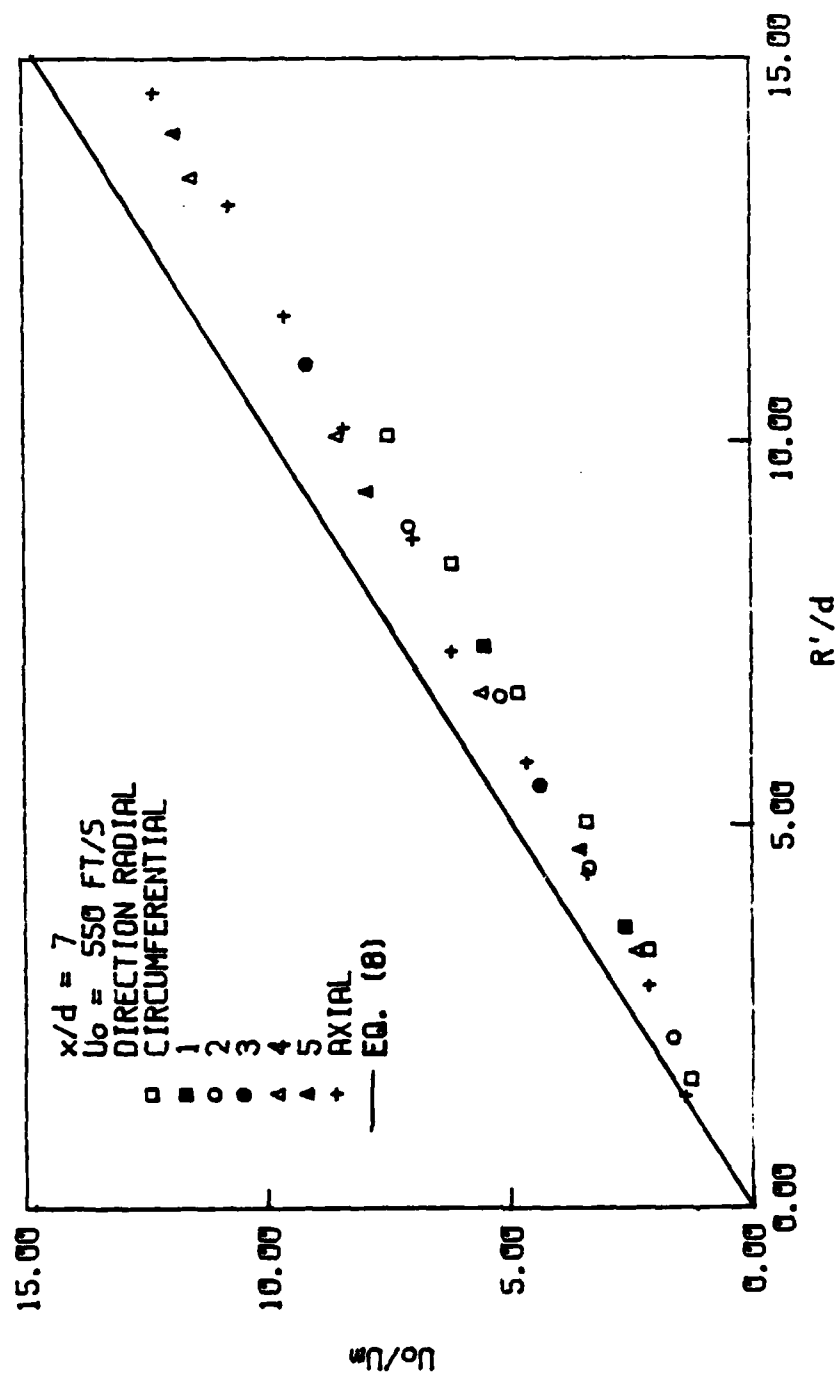


Fig. 98 Velocity scale of the wall jet for $U_0 = 550 \text{ ft/s}$, $x/d = 7$.

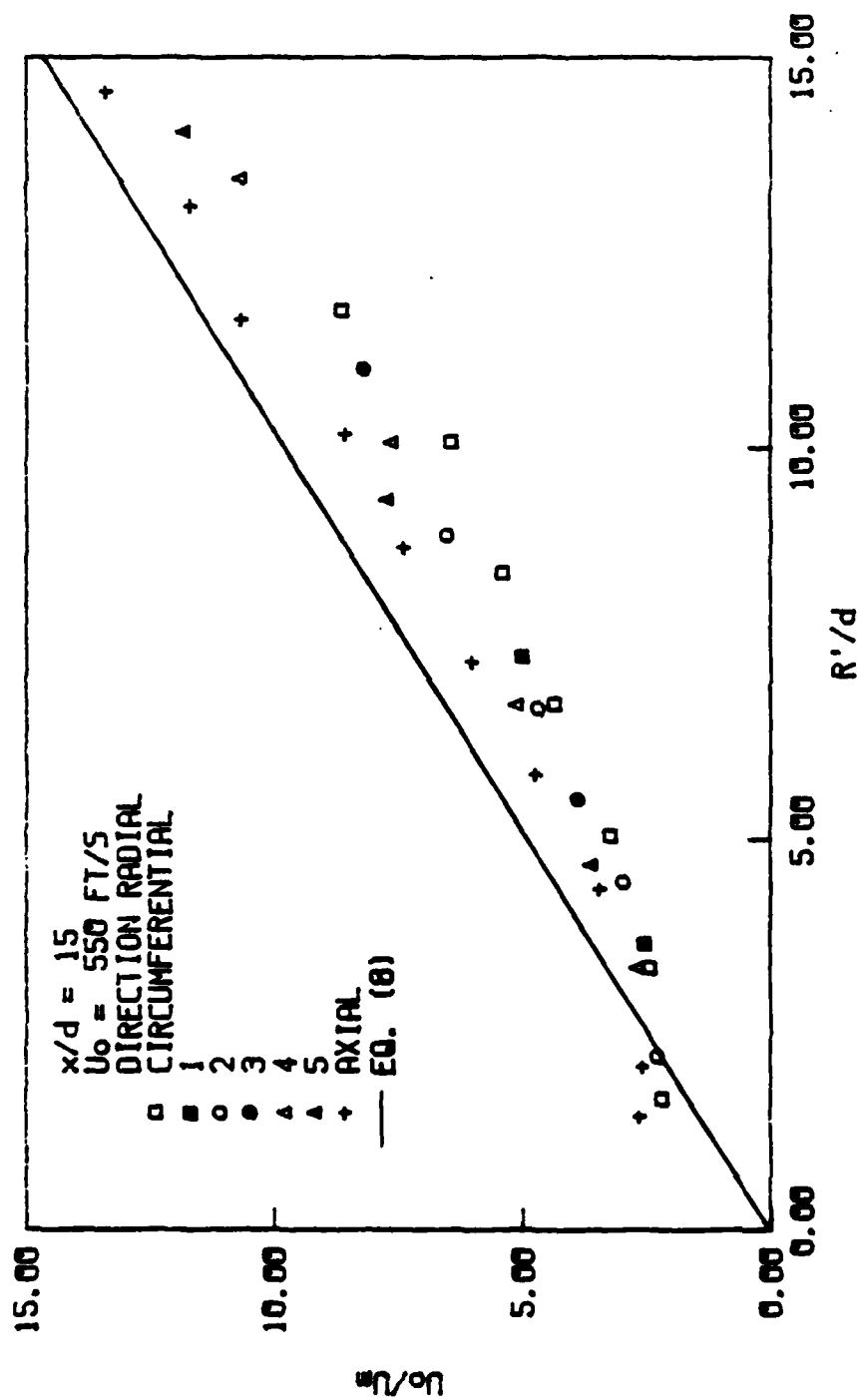


Fig. 99 Velocity scale of the wall jet for $U_o = 550 \text{ ft/s}$, $x/d = 15$.

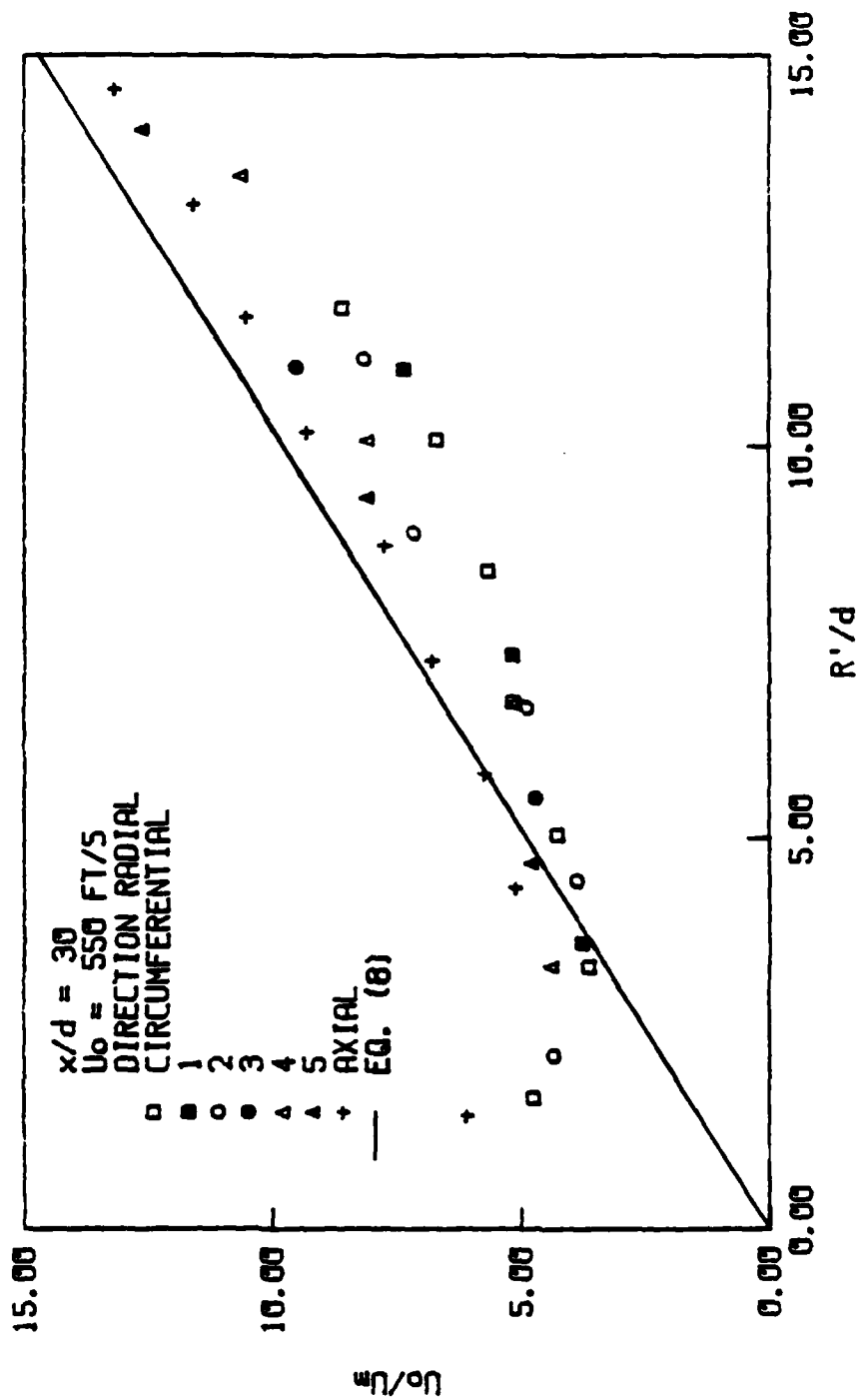


Fig. 100 Velocity scale of the wall jet for $U_0 = 550 \text{ ft/s}$, $x/d = 30$.

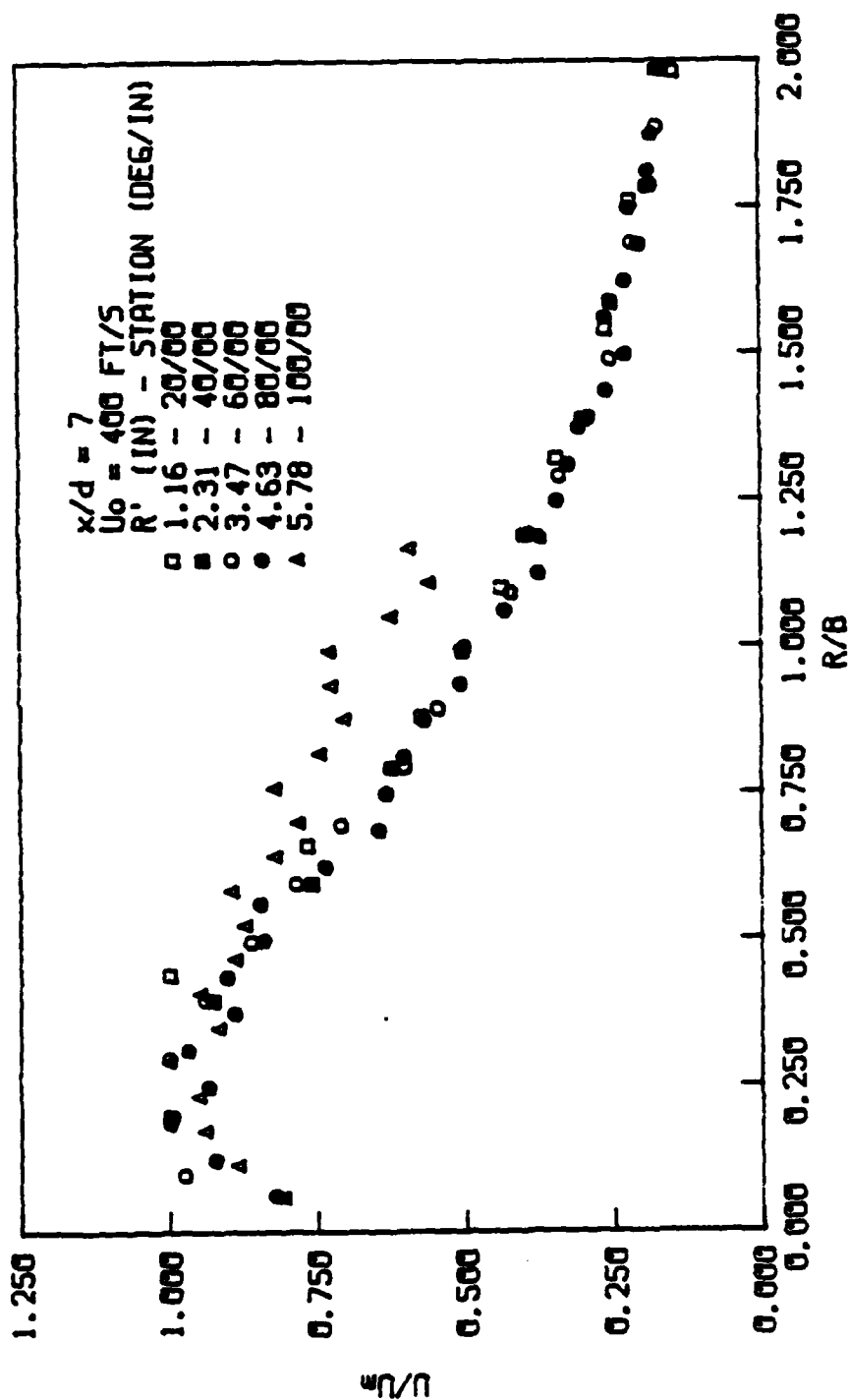


Fig. 101 Nondimensional velocity profiles of the wall jet for $U_0 = 400 \text{ ft/s}$, $x/d = 7$ (circumferential radial).

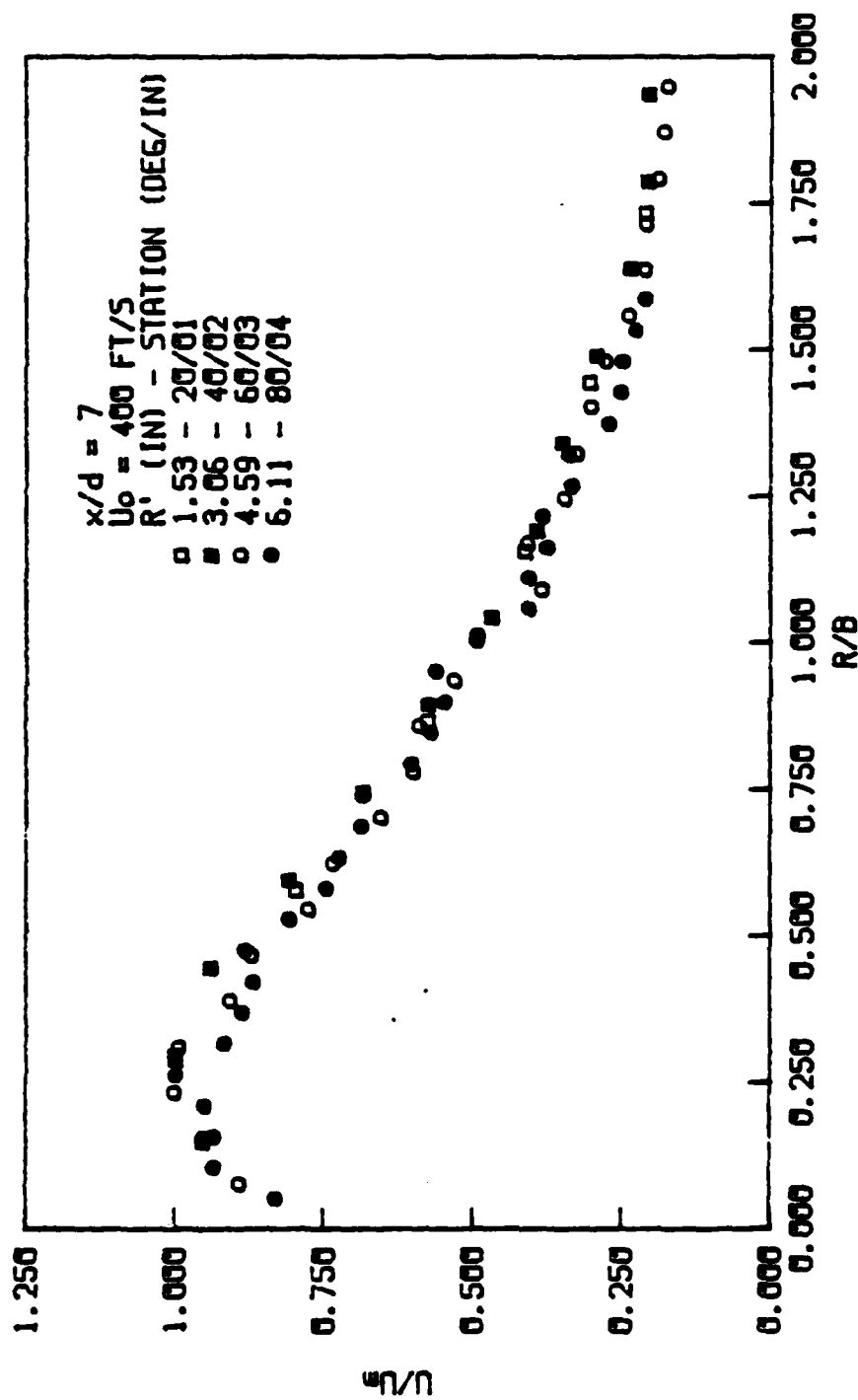


Fig. 102 Nondimensional velocity profiles of the wall jet for $U_o = 400 \text{ ft/s}$, $x/d = 7$ (radial 2).

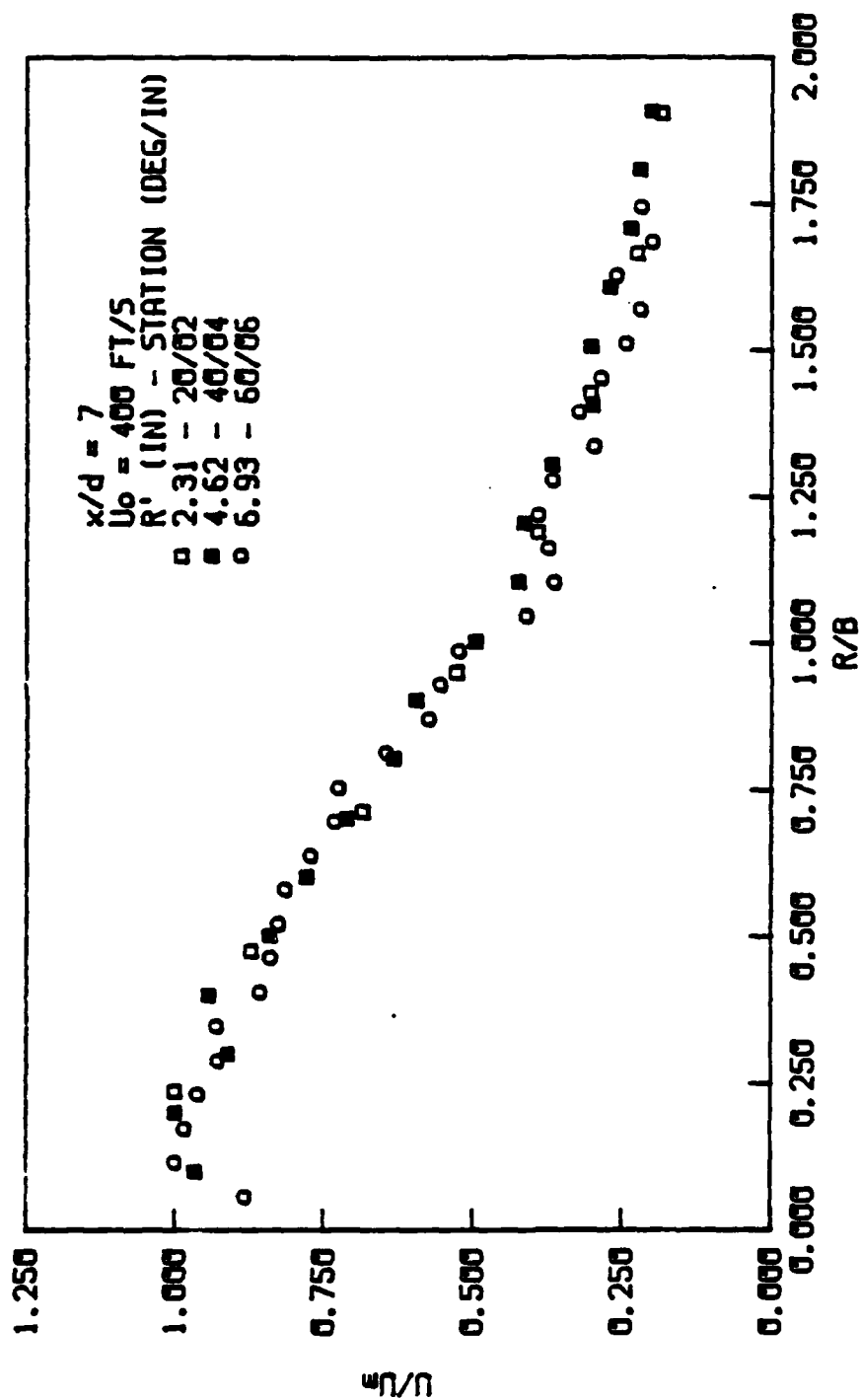


Fig. 103 Nondimensional velocity profiles of the wall jet for $U_0 = 400 \text{ ft/s}$, $x/d = 7$ (radial 4).

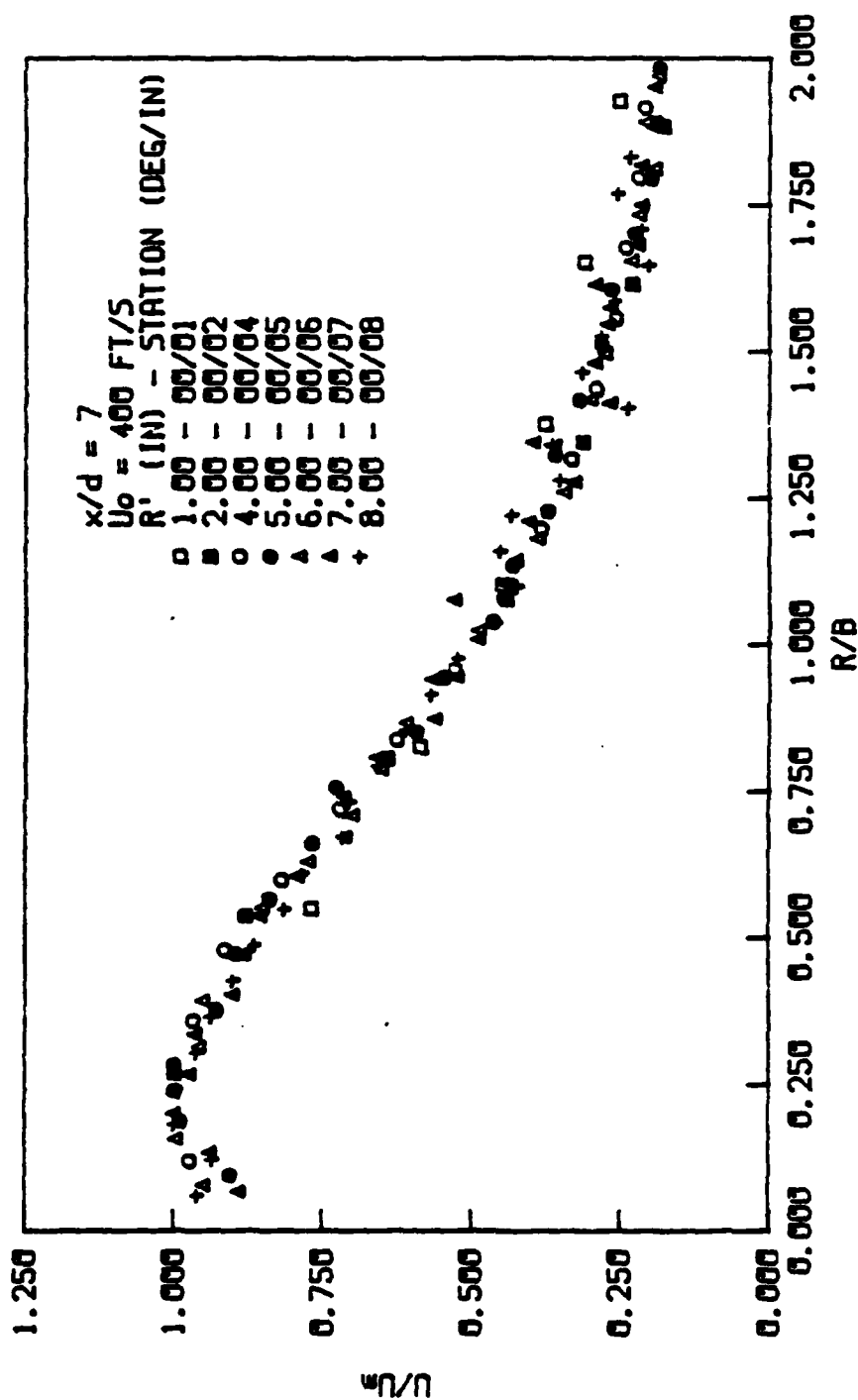


Fig. 104 Nondimensional velocity profiles of the wall jet for $U_0 = 400 \text{ ft/s}$, $x/d = 7$ (axial radial).

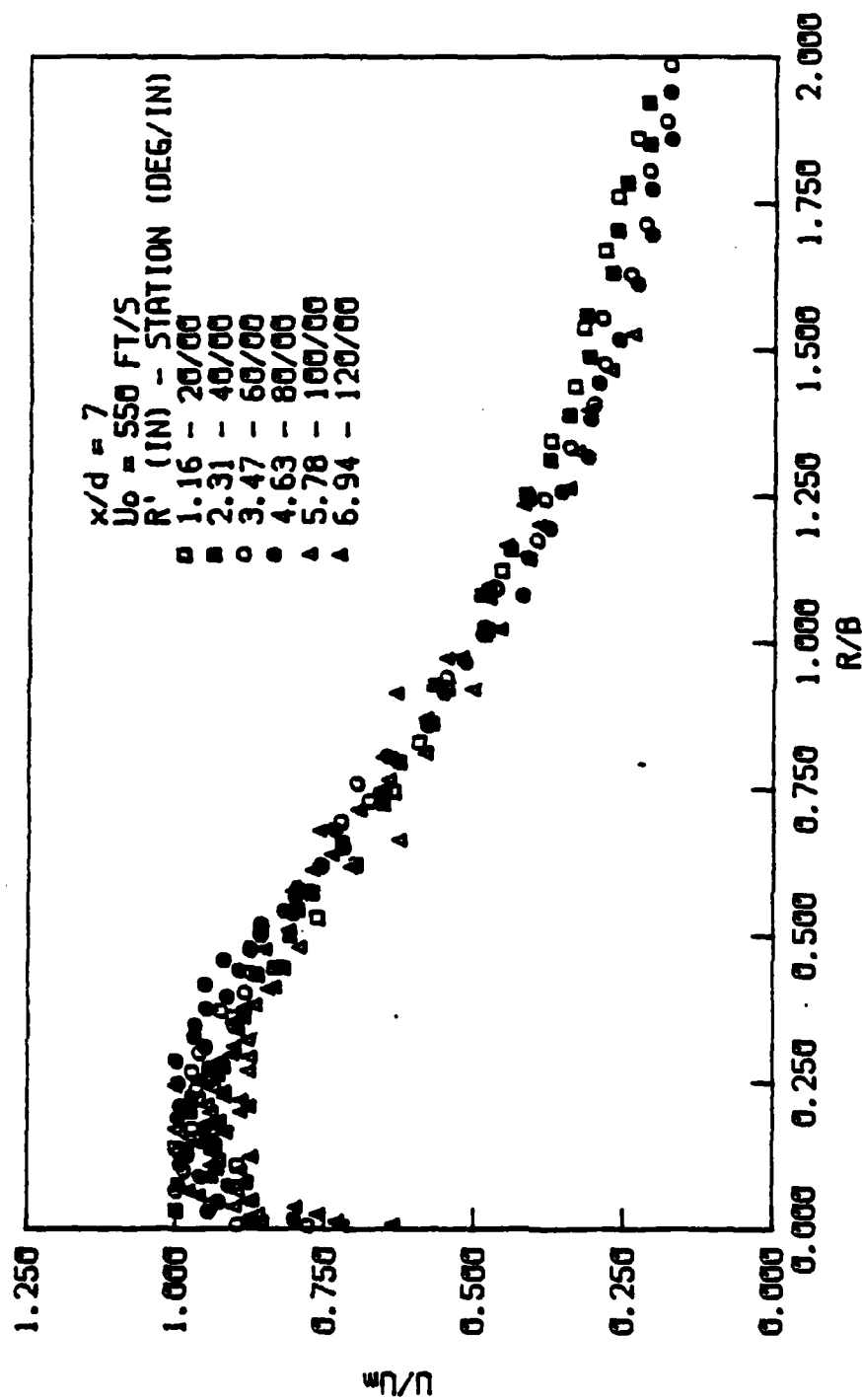


Fig. 105 Nondimensional velocity profiles of the wall jet for $U_0 = 550 \text{ ft/s}$, $x/d = 7$ (circumferential radial).

**THIS
PAGE
IS
MISSING
IN
ORIGINAL
DOCUMENT**

p. 152

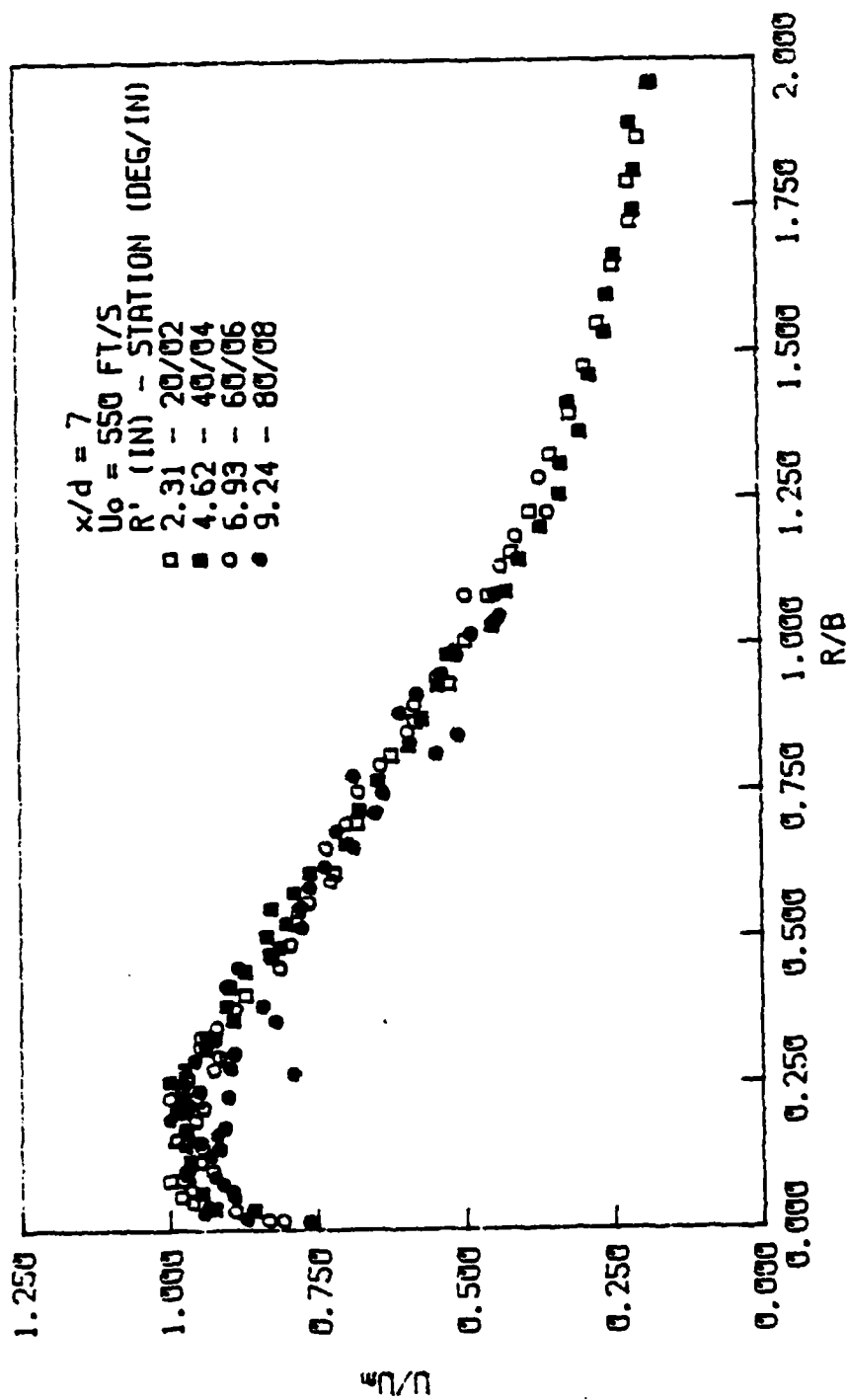


Fig. 107 Nondimensional velocity profiles of the wall jet for $U_0 = 550 \text{ ft/s}$, $x/d = 7$ (radial 4).

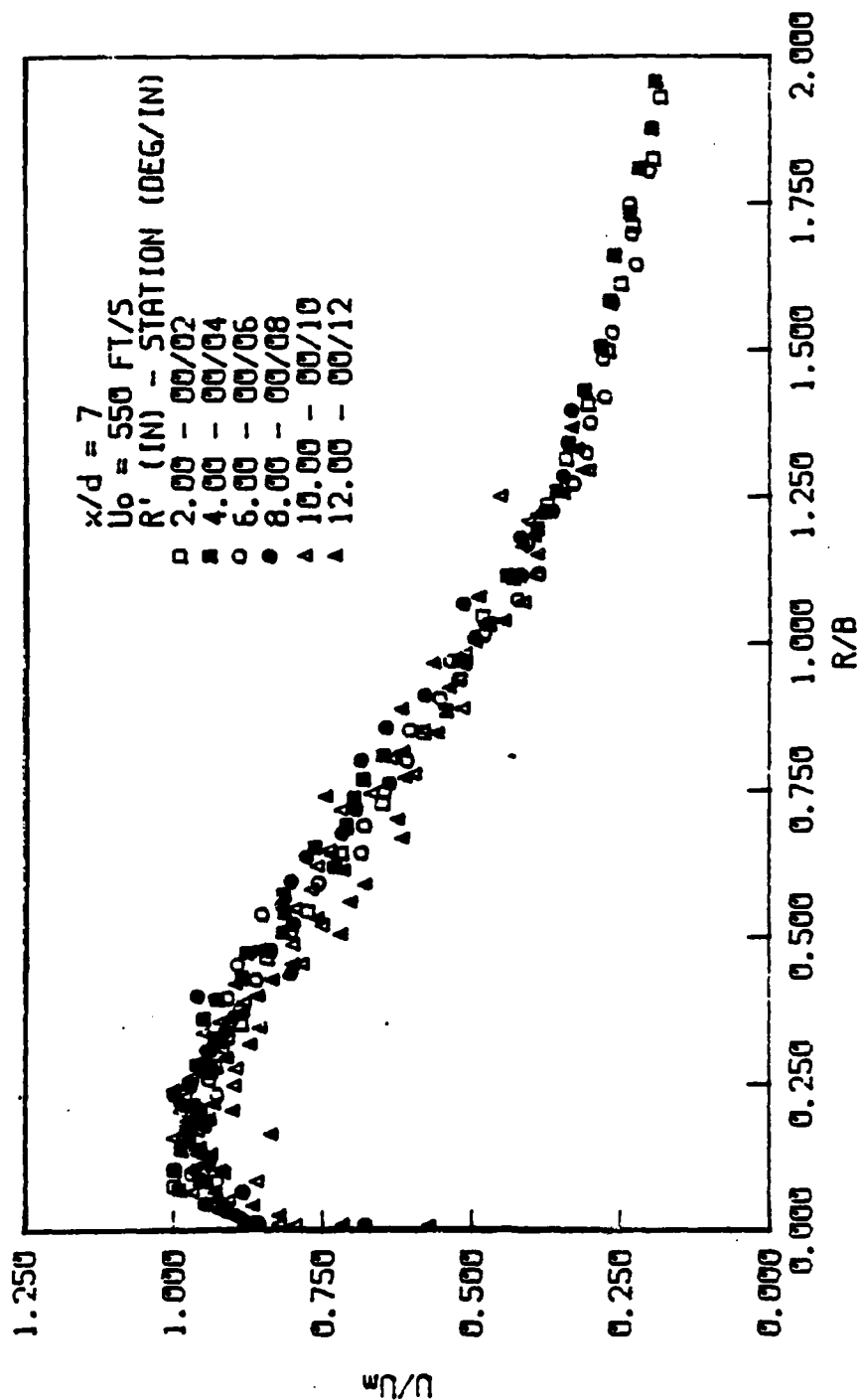


Fig. 108 Nondimensional velocity profiles of the wall jet for $U_o = 550 \text{ ft/s}$, $x/d = 7$ (axial radial).

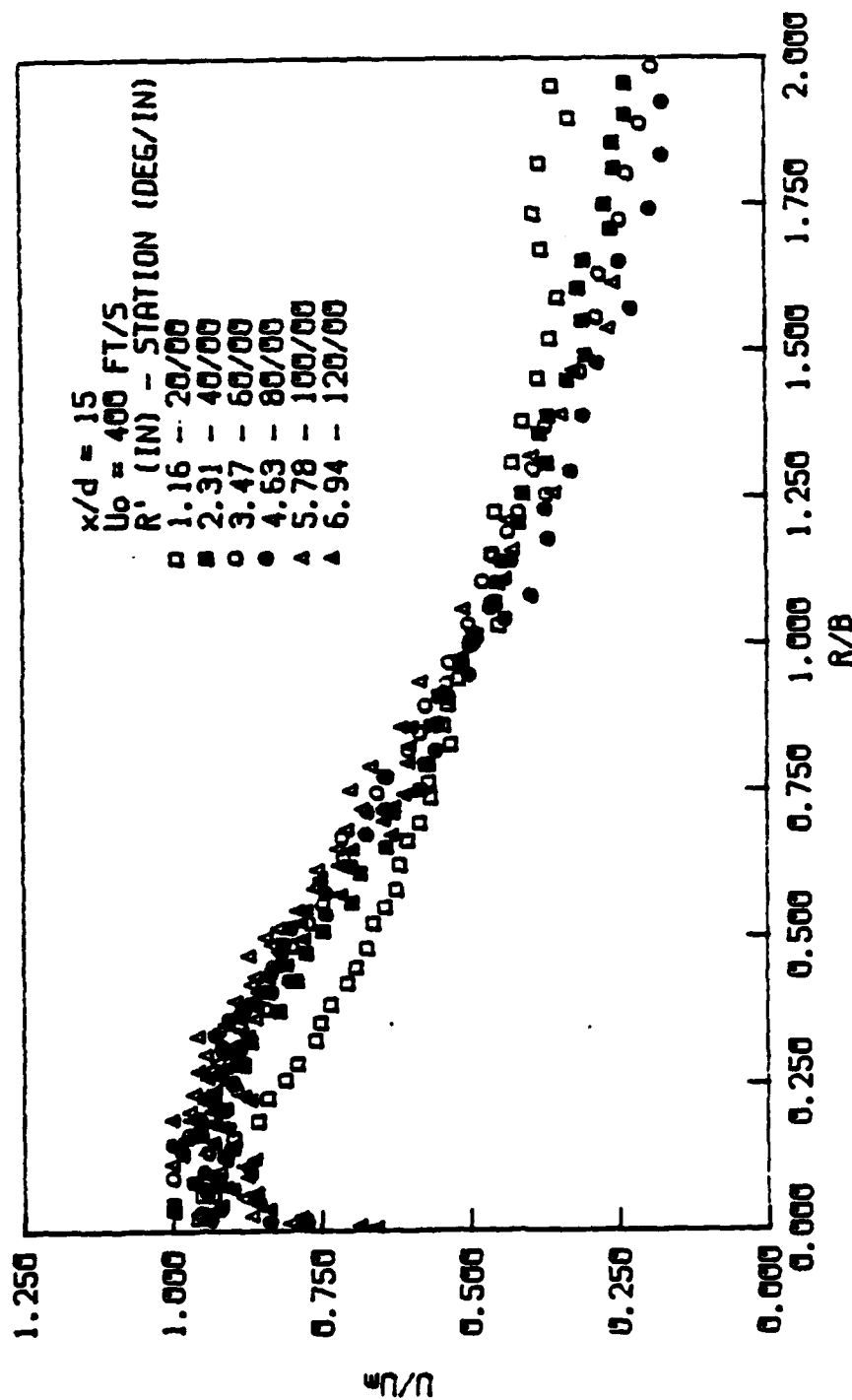


Fig. 109 Nondimensional velocity profiles of the wall jet for $U_o = 400 \text{ ft/s}$, $x/d = 15$ (circumferential radial).

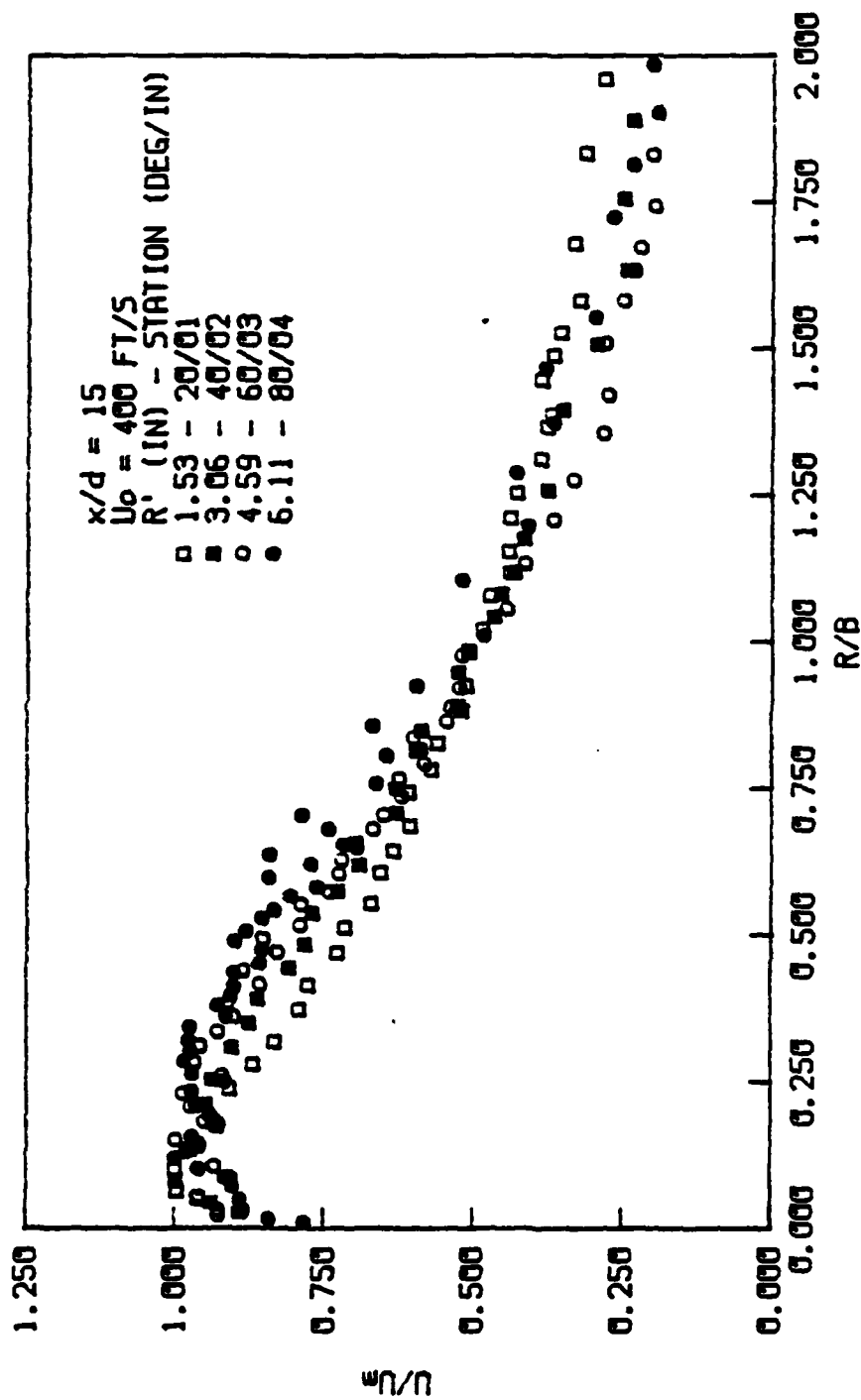


Fig. 110 Nondimensional velocity profiles of the wall jet for $U_0 = 400 \text{ ft/s}$, $x/d = 15$ (radial 2).

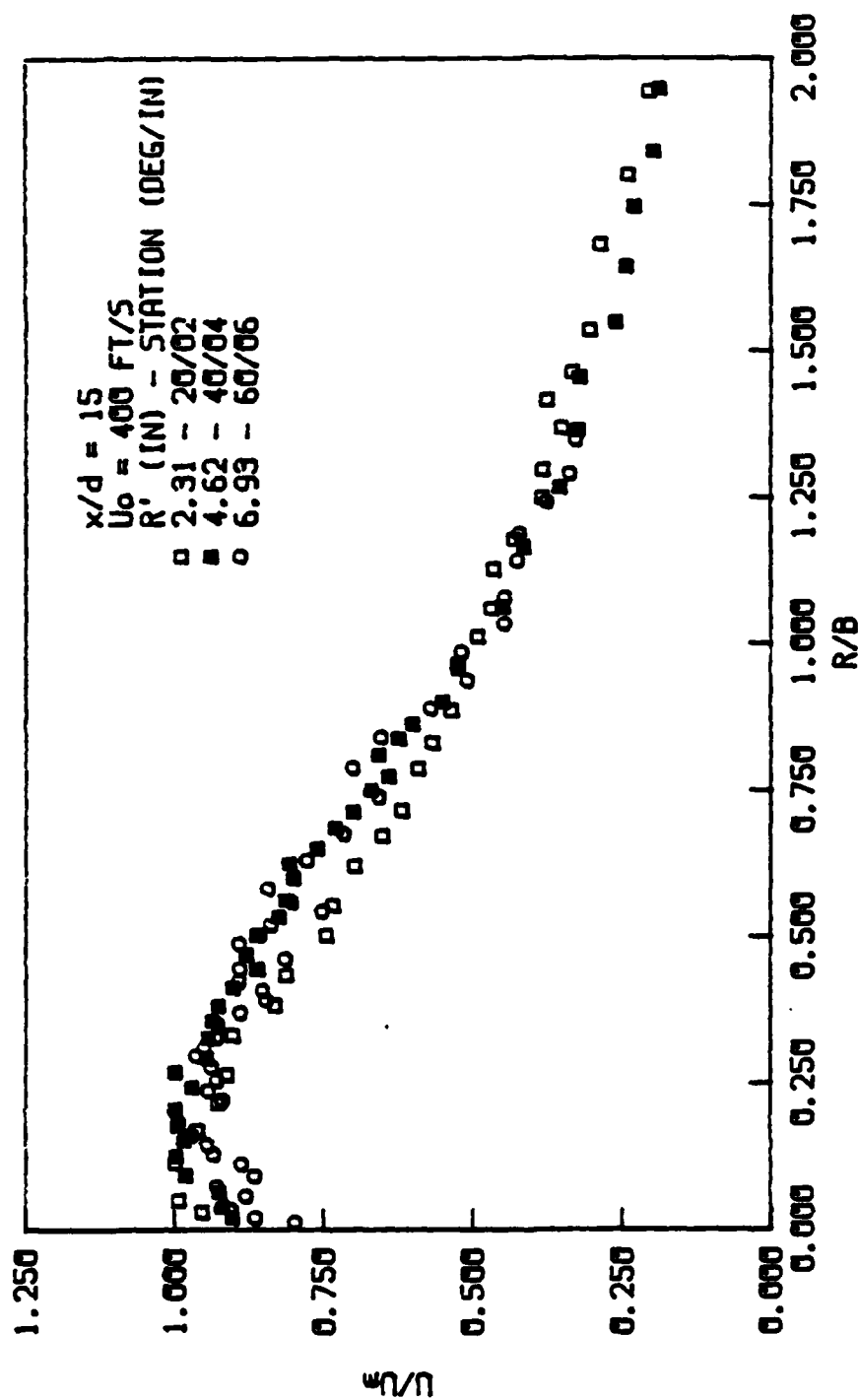


Fig. 111 Nondimensional velocity profiles of the wall jet for $U_0 = 400 \text{ ft/s}$, $x/d = 15$ (radial 4).

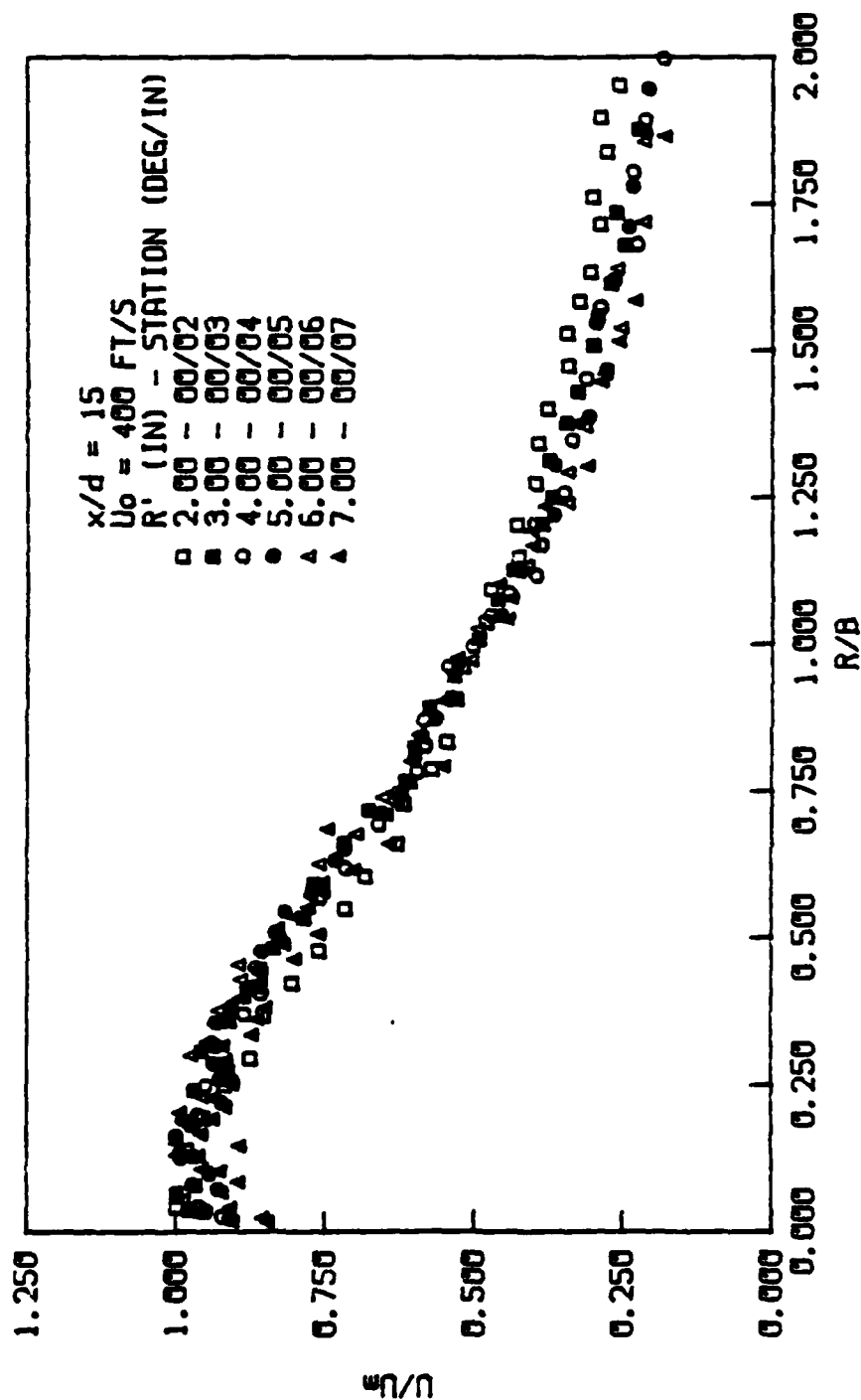


Fig. 112 Nondimensional velocity profiles of the wall jet for $U_0 = 400$ ft/s, $x/d = 15$ (axial radial).

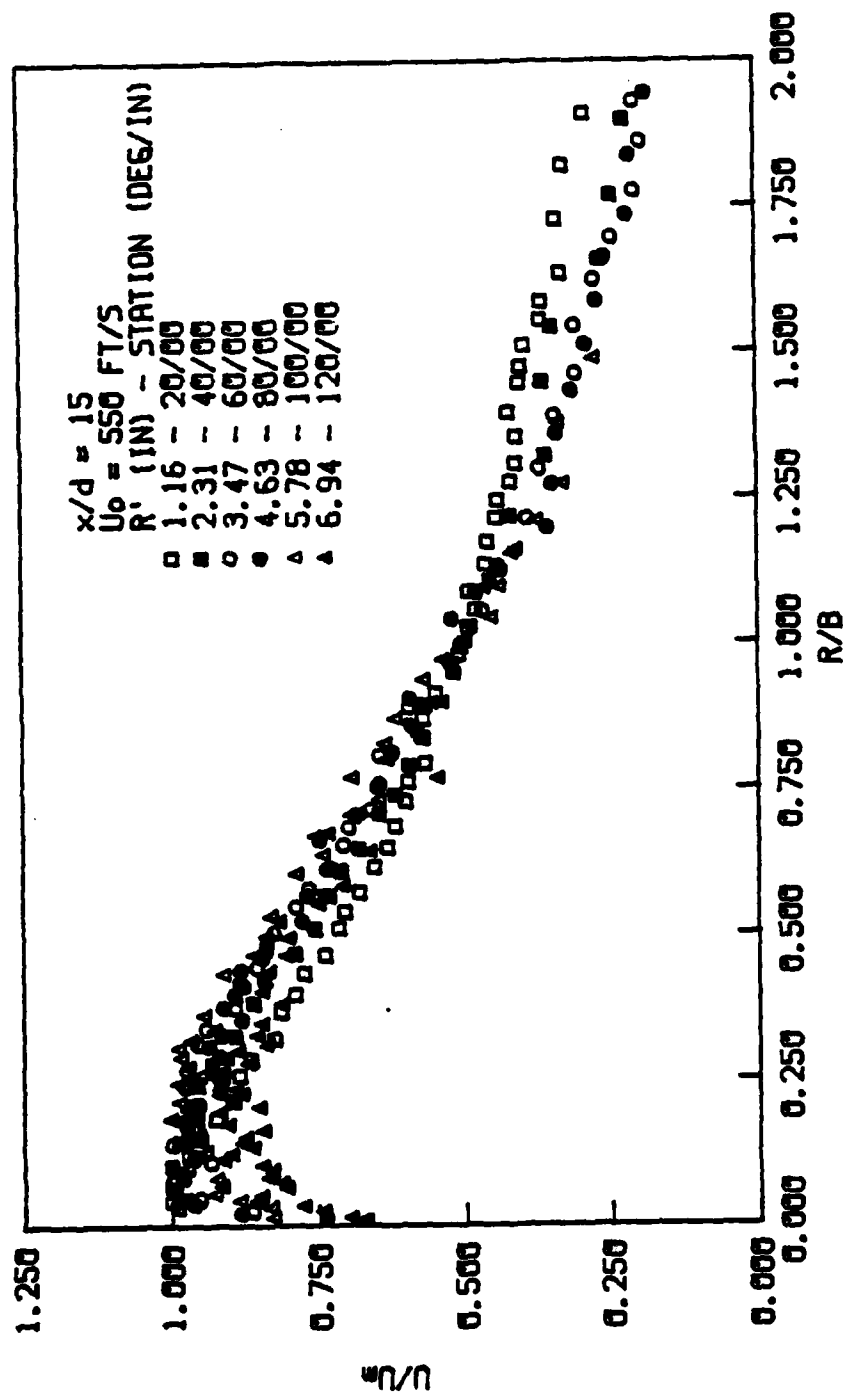


Fig. 113 Nondimensional velocity profiles of the wall jet for $U_0 = 550 \text{ ft/s}$, $x/d = 15$ (circumferential radial).

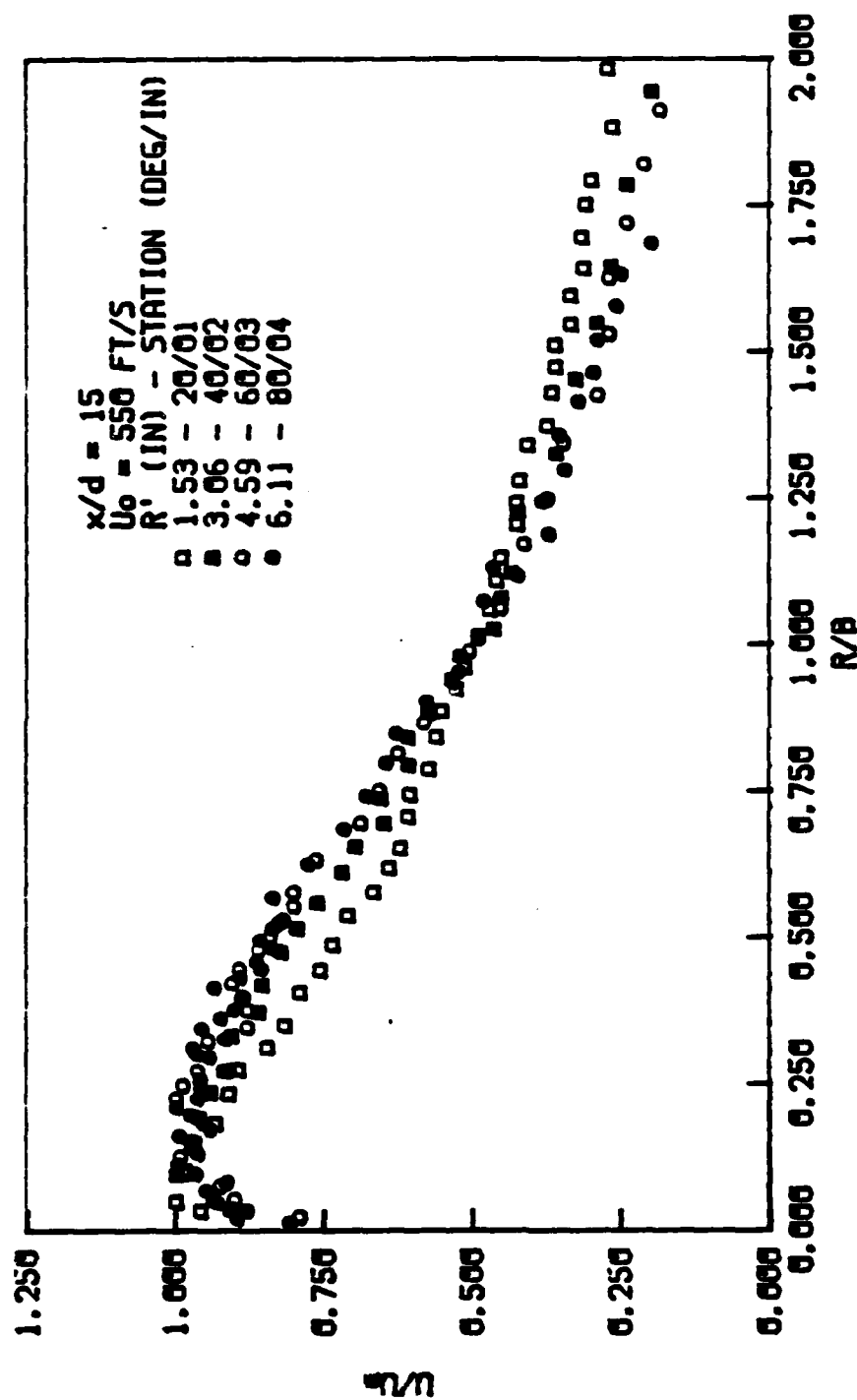


Fig. 114 Nondimensional velocity profiles of the wall jet for $U_0 = 550 \text{ ft/s}$, $x/d = 15$ (radial 2).

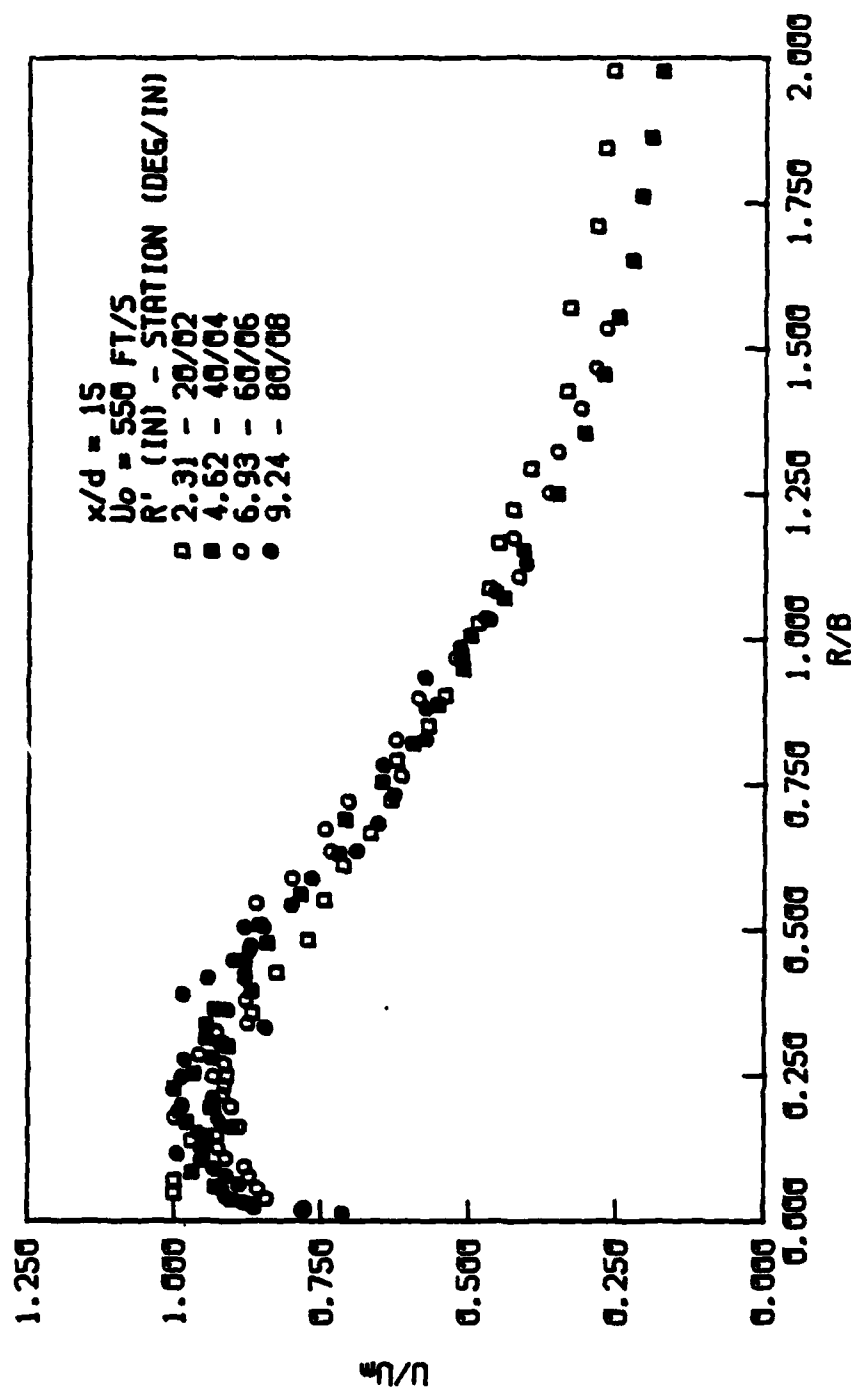


Fig. 115 Nondimensional velocity profiles of the wall jet for $U_0 = 550 \text{ ft/s}$, $x/d = 15$ (radial 4).

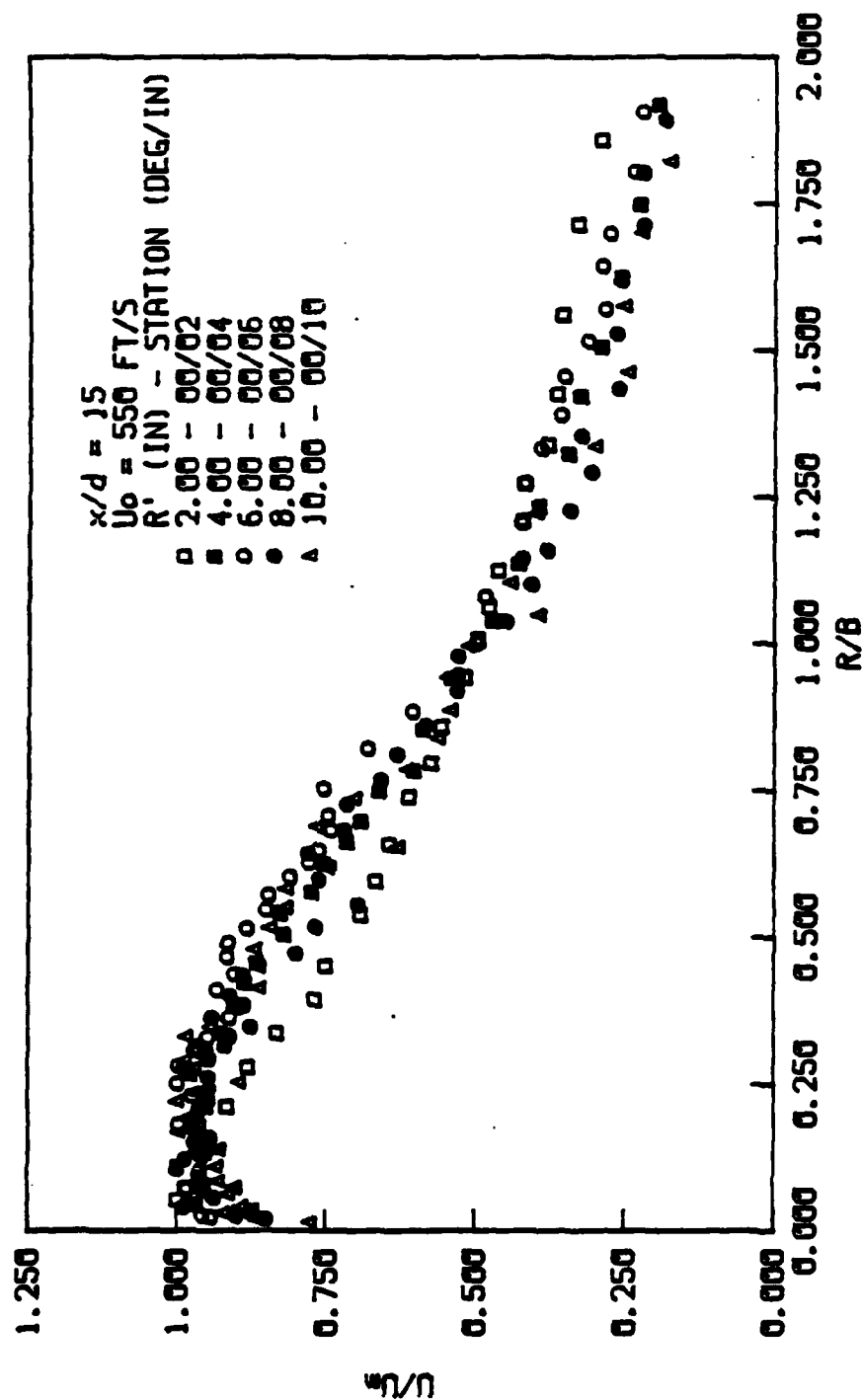


Fig. 116 Nondimensional velocity profiles of the wall jet for $U_0 = 550 \text{ ft/s}$, $x/d = 15$ (axial radial).

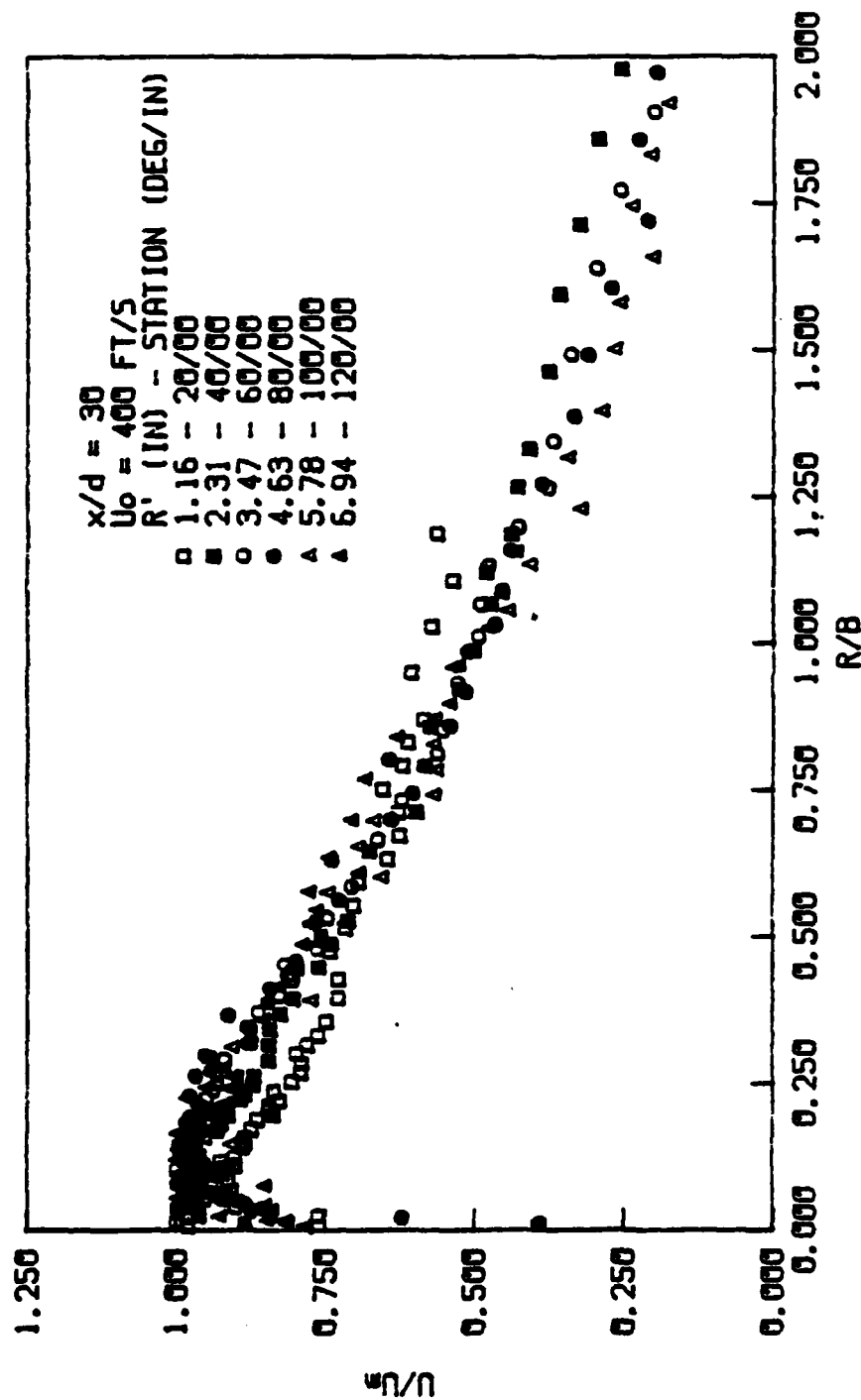


Fig. 117 Nondimensional velocity profiles of the wall jet for $U_0 = 400 \text{ ft/s}$, $x/d = 30$ (circumferential radial).

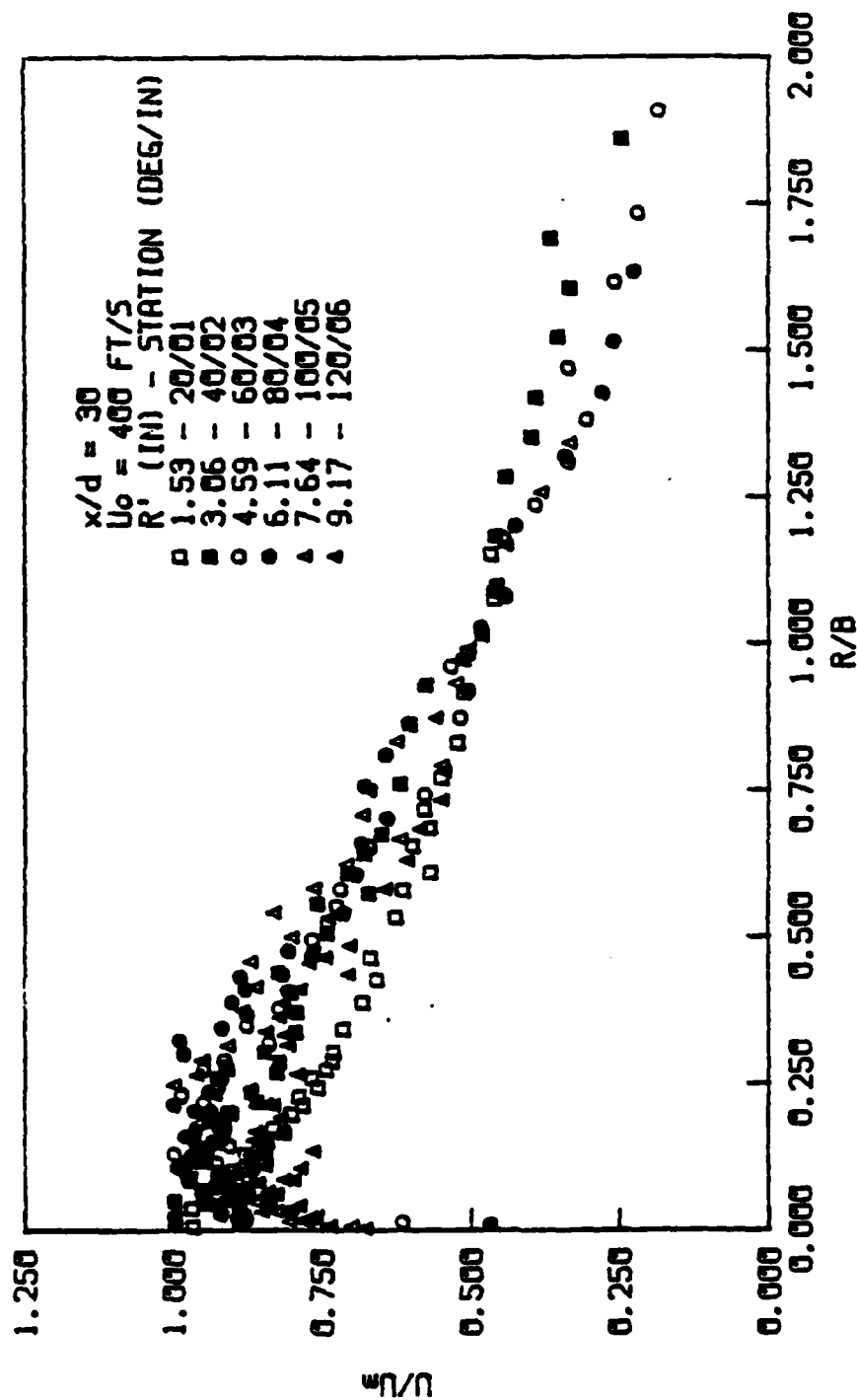


Fig. 118 Nondimensional velocity profiles of the wall jet for $U_0 = 400 \text{ ft/s}$, $x/d = 30$ (radial 2).

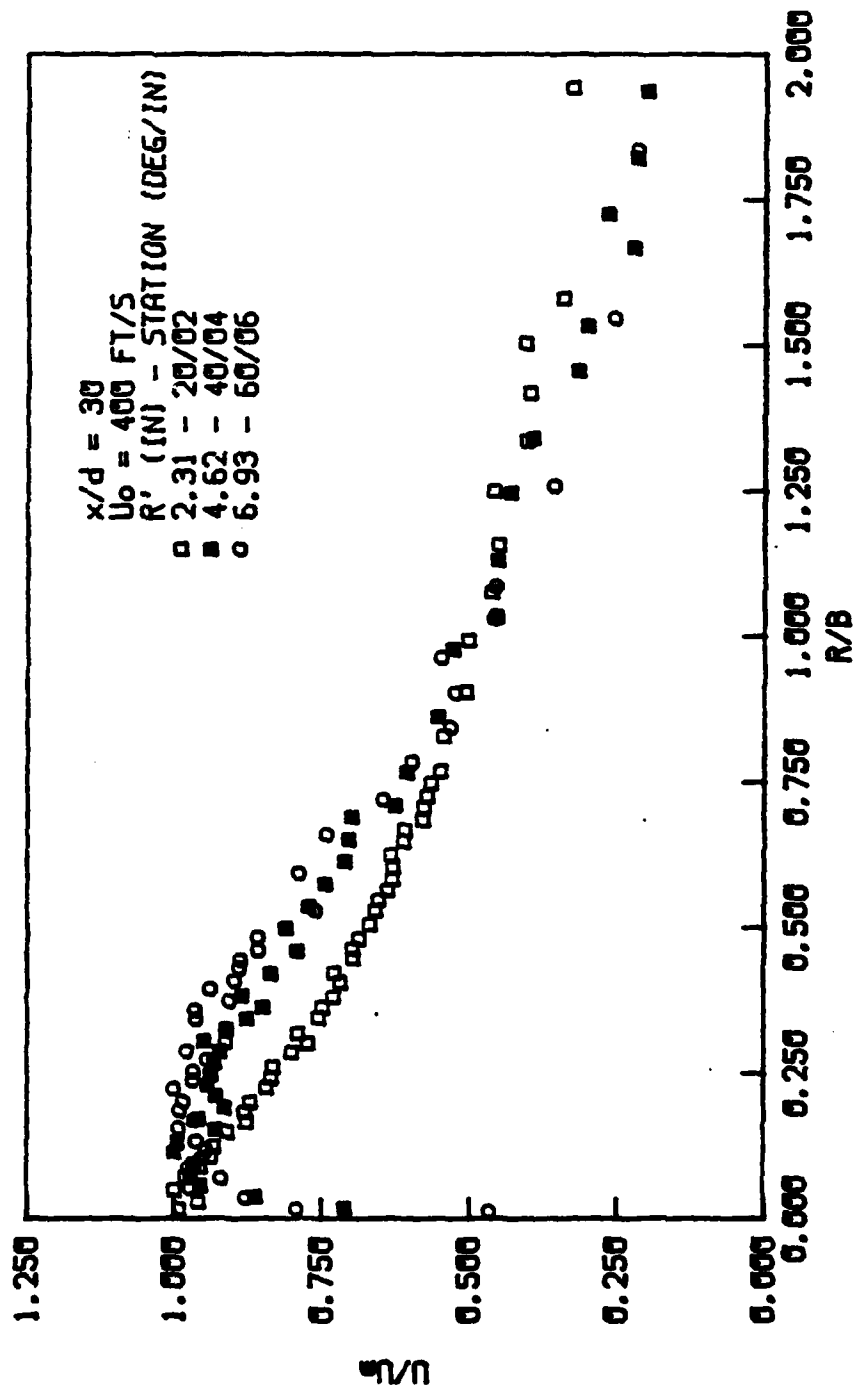


Fig. 119 Nondimensional velocity profiles of the wall jet for $U_0 = 400 \text{ ft/s}$, $x/d = 30$ (radial 4).

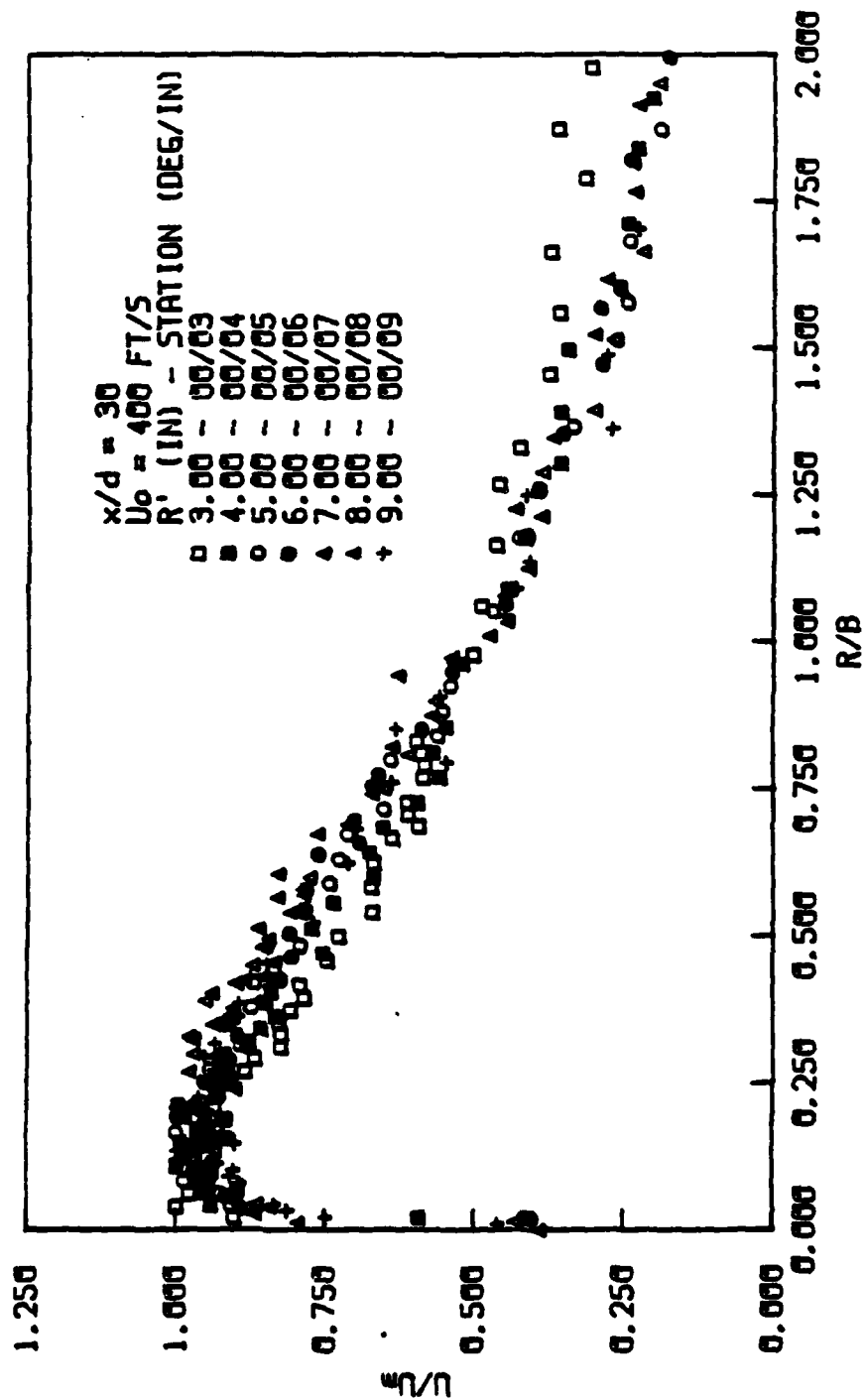


Fig. 120 Nondimensional velocity profiles of the wall jet for $U_0 = 400 \text{ ft/s}$, $x/d = 30$ (axial radial).

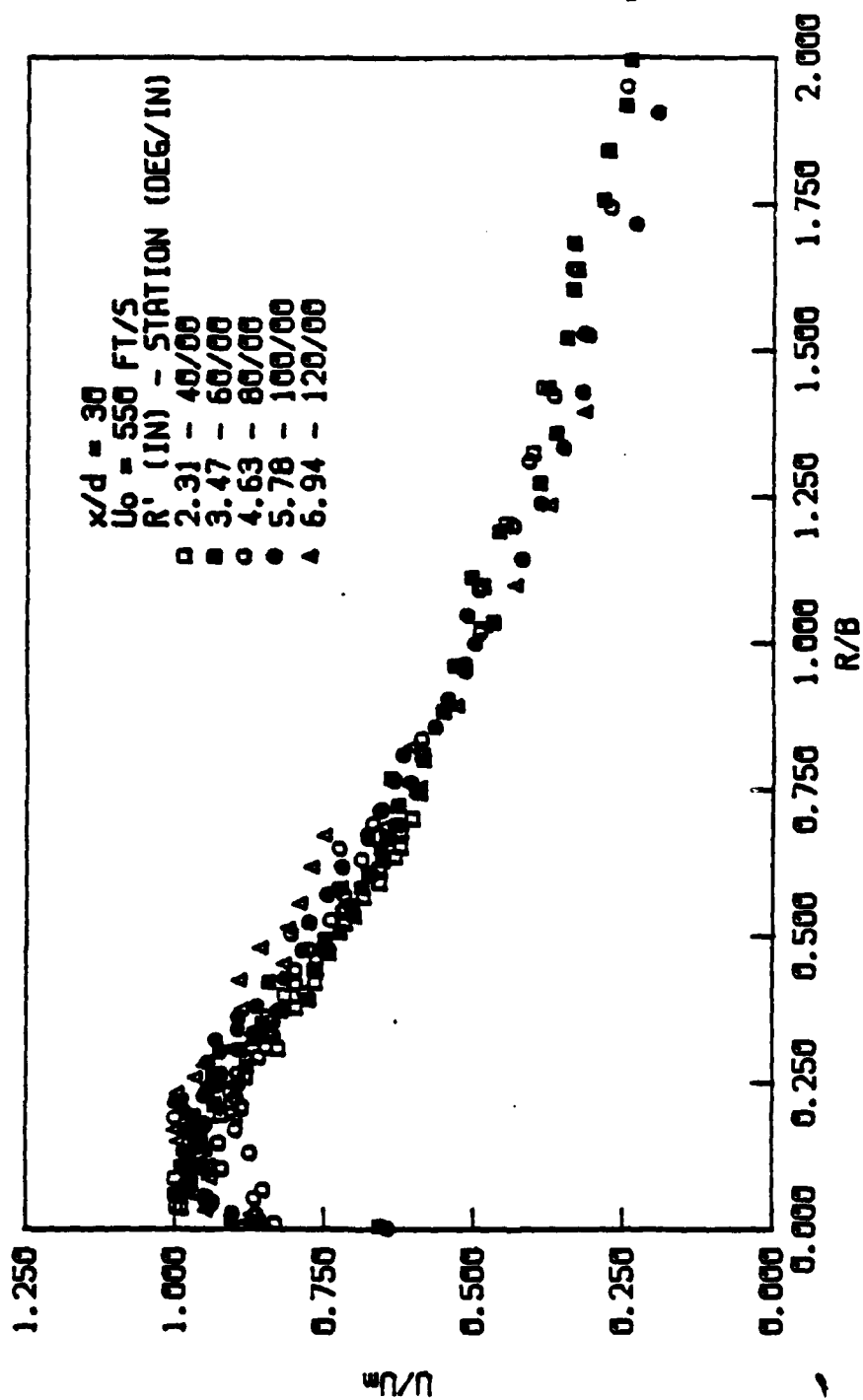


Fig. 121 Nondimensional velocity profiles of the wall jet for $U_0 = 550 \text{ ft/s}$, $x/d = 30$ (circumferential radial).

AD-A145 583

AN EXPERIMENTAL STUDY OF JET IMPINGEMENT ON A CIRCULAR
CYLINDER(U) AIR FORCE INST OF TECH WRIGHT-PATTERSON AFB
OH D W POTTS AUG 84 AFIT/CI/NR-84-50T

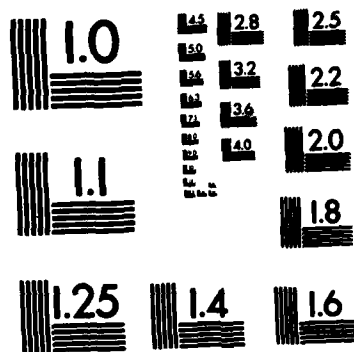
3/3

UNCLASSIFIED

F/G 20/4

NL

END
FILMED
DTIC



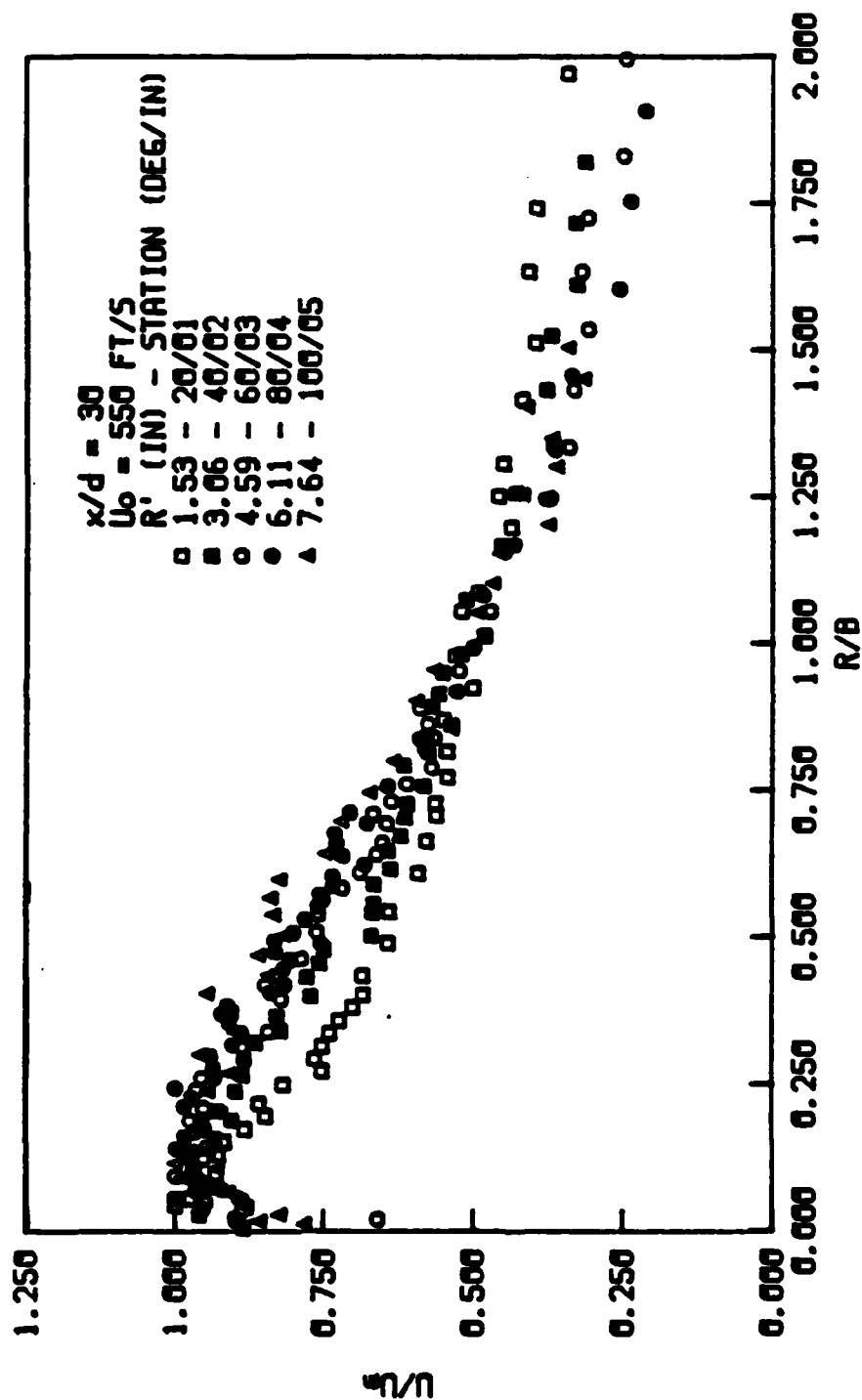


Fig. 122 Nondimensional velocity profiles of the wall jet for $U_0 = 550 \text{ ft/s}$, $x/d = 30$ (radial 2).

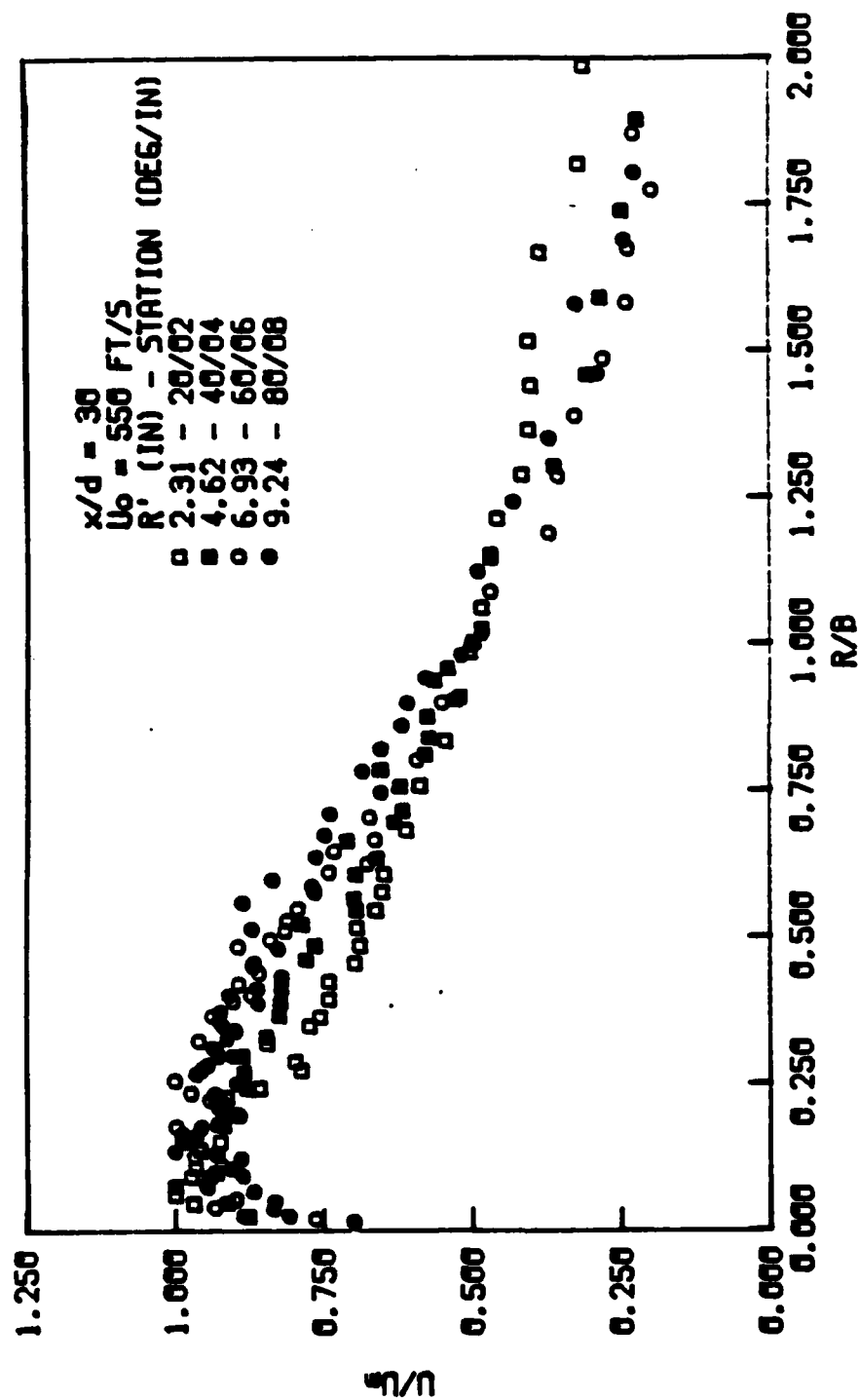


Fig. 123 Nondimensional velocity profiles of the wall jet for $U_0 = 550 \text{ ft/s}$, $x/d = 30$ (radial 4).

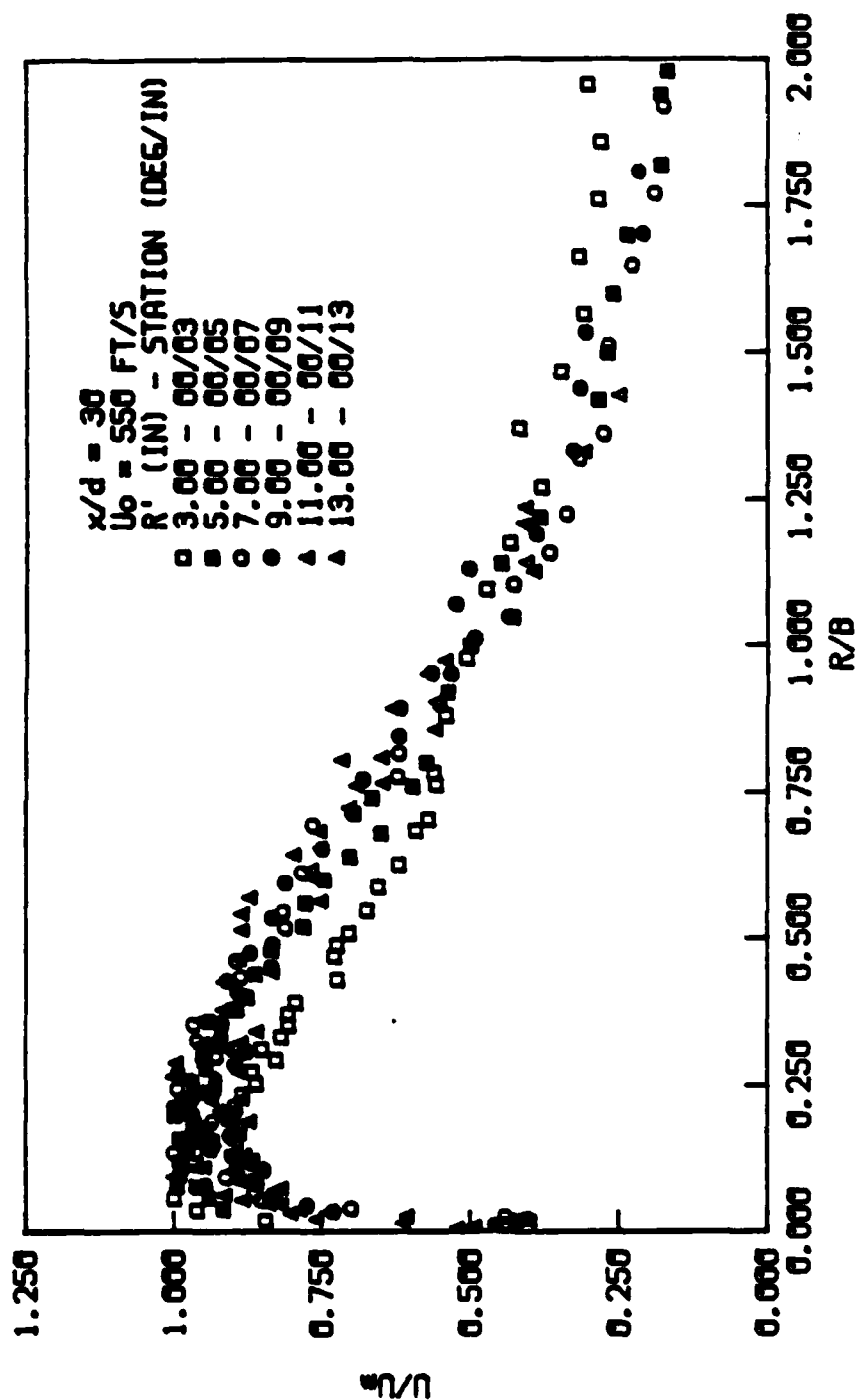


Fig. 124 Nondimensional velocity profiles of the wall jet for $U_o = 550 \text{ ft/s}$, $x/d = 30$ (axial radial).

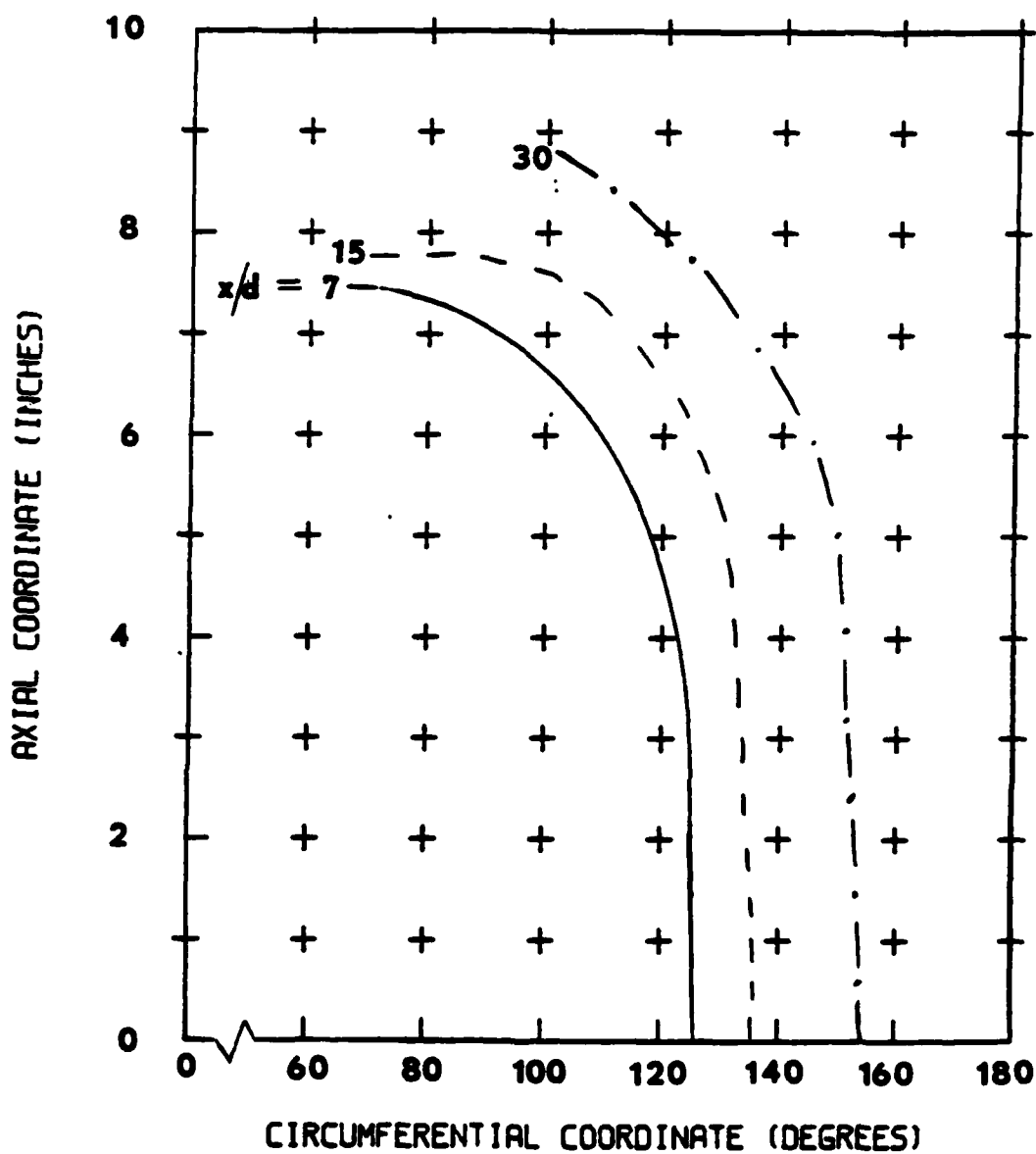


Fig. 125 Possible areas where the wall jet separates from the surface of the cylinder for $U_0 = 400$ ft/s.

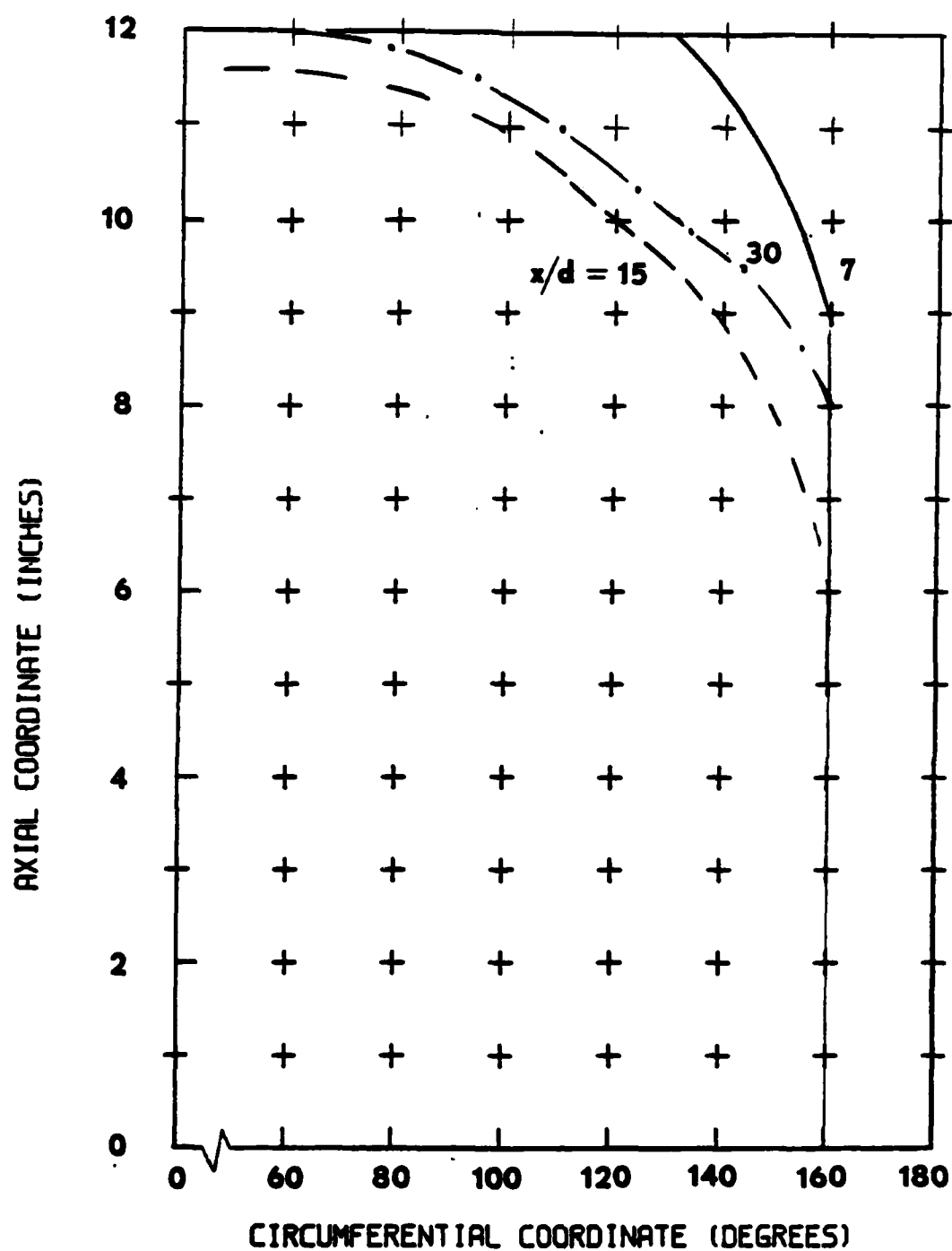


Fig. 126 Possible areas where the wall jet separates from the surface of the cylinder for $U_0 = 550$ ft/s.

VITA

Dennis Wayne Potts was born on October 16, 1953 in Massillon, Ohio. He is the son of Glenn E. and Martha L. Potts. His family lived in Ohio and Michigan before moving to Pinellas Park, Florida in 1960. In May 1971, he graduated from Northeast High School, St. Petersburg, Florida. From August, 1971 until May, 1973 he attended St. Petersburg Junior College. On August 4, 1973 he married the former Miss Eleanor J. Peacock. Dennis enlisted in the Air Force on August 27, 1973 where he served as a weather forecaster with tours at Chanute AFB, Illinois; Fort Hood, Texas; and Andrews AFB, Washington D.C. In April 1978, he received an Associate in Applied Sciences Degree in weather forecasting from the Community College of the Air Force. He attended the University of Maryland from July, 1978 until December, 1979 and in August, 1980 he was assigned to Texas A&M University where he graduated in December, 1982 as an Air Force Institute of Technology distinguished graduate with a Bachelor of Science degree in aerospace engineering. On April 22, 1983, he received a commission as a Second Lieutenant through the USAF Officers Training School. Dennis can be reached through his father-in-law, Lt. Col. Darel E. Peacock, USAF (Ret.) at 5711 Venetian Blvd. NE., St. Petersburg, Florida 33703. Dennis is a member of Tau Beta Pi, Phi Kappa Phi and Sigma Gamma Tau.

**END
FILMED**

DATE:

2-93

DTIC